

Durham E-Theses

Diffraction studies of hydrogen bonding and other intermolecular interactions in organic crystal structures

Broder, Charlotte Kate

How to cite:

Broder, Charlotte Kate (2002) *Diffraction studies of hydrogen bonding and other intermolecular interactions in organic crystal structures*, Durham theses, Durham University. Available at Durham E-Theses Online: <http://etheses.dur.ac.uk/3886/>

Use policy

The full-text may be used and/or reproduced, and given to third parties in any format or medium, without prior permission or charge, for personal research or study, educational, or not-for-profit purposes provided that:

- a full bibliographic reference is made to the original source
- a [link](#) is made to the metadata record in Durham E-Theses
- the full-text is not changed in any way

The full-text must not be sold in any format or medium without the formal permission of the copyright holders.

Please consult the [full Durham E-Theses policy](#) for further details.

Academic Support Office, Durham University, University Office, Old Elvet, Durham DH1 3HP
e-mail: e-theses.admin@dur.ac.uk Tel: +44 0191 334 6107
<http://etheses.dur.ac.uk>

Diffraction Studies of Hydrogen Bonding and Other Intermolecular Interactions in Organic Crystal Structures

Charlotte Kate Broder

The copyright of this thesis rests with the author. No quotation from it should be published in any form, including Electronic and the Internet, without the author's prior written consent. All information derived from this thesis must be acknowledged appropriately.

Thesis submitted in part fulfillment of the requirements for the degree of

**Doctor of Philosophy
at the
University of Durham**

**Department of Chemistry
University of Durham
March 2002**



31 MAY 2002

Diffraction Studies of Hydrogen Bonding and Other Intermolecular Interactions in Organic Crystal Structures

Submitted for the degree of Doctor of Philosophy, February 2002, by Charlotte Broder,
University of Durham

ABSTRACT

In this work three different approaches to the study of intermolecular interactions are shown. The aim is to further the understanding of specific intermolecular interactions with a view to eventually allowing the prediction and design of crystal structures from the initial molecular building blocks: crystal engineering. All three approaches make use of crystal structural information derived from X-ray and/or neutron diffraction studies.

The three approaches are:

- Data base approach. Specifically, the study of occurrence of bi- and tri-furcated hydrogen bonds in the Crystallographic Structural Database, and the analysis of the frequency with which they occur and the geometric restrictions of such interactions.
- Analysis of a series of compounds, where there are small changes in the molecular structure as the series progresses. The influence of these changes in the molecular structure on the crystal structure is considered. The series studied was the 4-amino-4'-hydroxydiphenylalkanes as well as some of the corresponding 4-amino-4'-hydroxydiphenylsulphides and -alkylsulphides.
- Detailed analysis of individual structures to identify the intermolecular interactions that are influencing the structure. The compounds analysed in this part were 2,4,6-*tris*-(4-chlorophenoxy)-1,3,5-triazene co-crystallised with tribromobenzene, triphenylisocyanurate co-crystallised with trinitrobenzene, 4,4'-dinitrotetraphenyl methane, 2,3-dichloro-1,4-diethynyl-1,4-dihydroxy-napthalene and, 4,4-diphenyl-2,5-cyclohexadienone.

DECLARATION

The work described in this thesis was carried out in the Department of Chemistry at the University of Durham between October 1998 and September 2001, under the supervision of Prof. Judith A. K. Howard. The work discussed in appendix A was carried out, in part, at the School of Chemistry, University of Hyderabad, India, in collaboration with Professor G. R. Desiraju and Dr. A. Nangia under the Indo-UK cooperation project. All the work is my own, unless otherwise stated, and has not been submitted previously for a degree at this or any other university.

Charlotte Broder

The copyright of this thesis rests with the author. No quotation from it should be published without prior consent and information derived from it should be acknowledged.

Acknowledgements

My deepest thanks to:

Professor G.R. Desiraju, Dr. A. Nangia, and their students; Venugopal Rao Vangala, J. Ramakoteswara Rao, Praveen K. Thallapally, V. S. Senthil Kumar, Rahul Banerjee, Basavoju Srinivas, for providing me with such interesting crystals!

Judith for all the help and ideas I needed when I needed them and for giving me the freedom to get on with things at my own pace when I didn't!

Everyone at CCDC, especially Dr. Frank Allen and Dr Sam Motherwell and most especially Dr. Greg Shields for all his help with the bi- and tri-furcated hydrogen bond work, for running the searches when my computer couldn't cope and for helping me understand the results!

Dr. Chick Wilson and Dr. Dave Keen for all their help with the SXD experiments and likewise to Dr. Sax Mason and Dr. Trevor Forsyth for all their help with the D19 experiments at the ILL.

All my friends and colleagues from the BCA meetings and schools, the Erice schools and Hercules course. And, to all my friends and colleagues from the University of Hyderabad who made my visit so wonderful, especially Venu, Praveen, Asok, Ram (Snr, & Jr), Vani and Pooja.

Everyone who has worked in the Durham Crystallography Lab both past and present.

My parents and brother and Mike (especially for all the proof reading!) and my friends for all their support.

Contents:

Introduction	18
Chapter 1 : Introduction	19
1.1 Crystal Engineering	19
1.2 Methods of Studying Molecular Interactions	20
1.3 Hydrogen Bonds	21
1.4 π - π Interactions	24
1.5 Halogen – Halogen Interactions.....	25
Chapter 2 : Techniques	26
2.1 Crystallography and Diffraction	26
2.2 From the Diffraction Pattern to the Model.....	27
2.3 Neutron Diffraction.....	30
2.4 Diffractometers and Other Equipment.....	32
2.5 Interpretation of the Results.....	38
2.6 The Cambridge Structural Database	38
2.7 References for Introduction	39
Part 1:	41
Bi-Furcated Hydrogen Bonds	41
Chapter 3 : Furcation in Hydrogen Bonds	42
3.1 Introduction.....	42
3.2 Bi-Furcated Hydrogen Bonds	43
3.3 Experimental.....	44
3.4 Clusters and Unavoidable Bias Within the CSD	46
Chapter 4 : Bi-Furcated Hydrogen Bonds	47
4.1 Frequency of Occurrence	47
Chapter 5 : Case I, the General Case	51
5.1 Differences Between Oxygen and Nitrogen as the Hydrogen Donor in the General Case (Case I)	55
Chapter 6 : Case II, Where Both the Acceptors are Part of the Same Molecule	58
Chapter 7 : Case III, Where One of the Hydrogen Bonds is an Intramolecular Hydrogen Bond and the Other is Intermolecular	64
Chapter 8 : Case IV, Where Both of the Hydrogen Bonds are Intramolecular Hydrogen Bonds	68
Chapter 9 : Conclusions	74
Chapter 10 : Tri-Furcated Hydrogen Bonded Systems.....	76
10.1 Introduction.....	76
10.2 Frequency of Occurrence	77

10.3 Tri-Furcated Hydrogen Bonds	79
10.4 Conclusions.....	83
10.5 References for Part 1.....	84
Part 2:	85
Hydrogen Bonding in Amino-Phenols	85
Chapter 11 : Amino-phenols.....	86
11.1 Hydroxy and Amino Group Complementarily	86
11.2 The Aminophenol Series.....	89
Chapter 12 : 4-Amino-4'-hydroxy-diphenylalkanes.....	91
12.1 Crystal Data and the β -As Structures	91
12.2 The 'Square Motif' Structure of 1a and The 'Stacked Vees' Structure of 3a and 5a	96
Chapter 13 : The Effect of Sulphur, the 4-Amino-4'-hydroxydiphenyl Sulphides and Alkanesulphides	105
13.1 Compounds With One Atom Links, 1a and 1b.....	105
13.2 Compounds With Two Atoms in the Link, 2a, 2b and 2c	110
13.3 Compounds With Three Atoms in the Link, 3a and 3b	115
Chapter 14 : Conclusions.....	120
14.1 Molecular Geometry	120
14.2 Melting Point Comparisons	121
14.3 Conclusions.....	122
14.4 References for Part 2.....	124
Part 3:	125
Interesting Structures	125
Chapter 15 : Introduction.....	126
Chapter 16 : Co-Crystal (6), 2,4,6- <i>tris</i> -(4-chlorophenoxy)-1,3,5-triazine and Tribromobenzene	128
16.1 Introduction.....	128
16.2 Crystal Data	130
16.3 Crystal Structure and Results.....	131
16.4 Conclusions:.....	135
Chapter 17 : Triphenylisocyanurate Co-Crystallised with Trinitrobenzene	137
17.1 Introduction.....	137
17.2 Crystal Data.....	138
17.3 Crystal Structure and Results.....	139
17.4 Conclusions.....	143
Chapter 18 : 4,4'-dinitrotetraphenyl methane.....	144
18.1 Crystal Data	146

18.2 Crystal Structure and Results.....	147
18.3 Conclusions.....	152
Chapter 19 : 2,3-dichloro-1,4-diethynyl-1,4-dihydroxy-napthalene	153
19.1 Introduction.....	153
19.2 Crystal Data	157
19.3 Crystal Structure and Results.....	158
19.4 Conclusions.....	161
Chapter 20 : 4,4-diphenyl-2,5-cyclohexadienone	162
20.1 Introduction.....	162
20.2 Crystal Data	164
20.3 Crystal Structure and Results.....	165
20.4 Conclusions.....	176
20.5 References for Part 3.....	177
Chapter 21 : Conclusions.....	179
Appendix	181
Appendix A: Melting Points of Meta and Para Disubstituted Benzenes.....	182
21.1 Introduction.....	182
21.2 Experimental	183
21.3 Results.....	186
21.4 References for Appendix A.....	192
Appendix B: Publications	193
Appendix C: Cif Files.....	195
Appendix D: Conferences and Courses Attended	286

Figures:

Figure 1.1: Types of hydrogen bond.....	22
Figure 1.2: Schematic of the electron density around a phenyl ring.	24
Figure 1.3: Types of π - π interaction.	24
Figure 1.4: Types of halogen halogen interaction.	25
Figure 2.1: A schematic of a diffraction experiment.	26
Figure 2.2: 2-D representation of molecules in a lattice.	27
Figure 2.3: Schematic of Bragg's law.	28
Figure 2.4: Phase shift caused by an atom (coloured red).	28
Figure 2.5: Schematic of the mathematical conversions used on diffraction data.	29
Figure 2.6: Scattering length for neutron radiation (reproduced from: 'Single Crystal Neutron Diffraction From Molecular Materials', C.C.Wilson ²⁶). Red line indicates corresponding scattering length for X-ray radiation.	31
Figure 2.7: The basic diffractometer set up.	32
Figure 2.8: The Rigaku AFC6S diffractometer.	34
Figure 2.9: The SMART diffractometer.	35
Figure 3.1: The bi-furcation motif.	42
Figure 3.2: Schematic of a bi-furcated hydrogen bond.	43
Figure 3.3: A scheme to define the angles, distances analysed in the bi-furcated systems.	45
Figure 5.1: Scheme to define angles and distances for the case I motif.	51
Figure 6.1: Scheme to define the angles and distances for the case II motif.	58
Figure 6.2: Two examples of case II bi-furcated hydrogen bond structures where the A...A path length is 1, examples have been taken from the CSD, ref codes AMAPTZ ¹³ and VIDYOV ¹⁴ (* indicates atom that is part of a symmetry generated molecule).	59
Figure 6.3: Increasing AHA and decreasing DHA angles with increasing acceptor-acceptor path length.	61
Figure 6.4: a) geometric layout assumed for acceptor repulsion analysis, b) geometry of some of the acceptor-acceptor path length, path 3 = 1 systems.	62
Figure 7.1: Scheme to define the angles and distances for the case III motif.	64
Figure 8.1: Scheme to define the angles and distances for the case IV motif.	68
Figure 8.2: The main contributors to the 4,4,6 and 5,5,8 path length combinations.	72
Figure 10.1: The tri-furcated motif.	76
Figure 10.2: Scheme to define the angles, distances, and intramolecular path lengths for the tri-furcated motif.	77

Figure 11.1: Hydrogen bond acceptor and donor sites of the amino and hydroxy groups.	86
Figure 11.2: Hydrogen bonding motif possible with a 1:1 mixture of hydroxy and amino groups, a) a schematic view, b) in a real crystal, showing the puckering of the sheet.	87
Figure 11.3: The diamond and wurtzite based structures ¹ , built up from layers of β -As sheets. R=Linear linking unit between hydroxy and amino groups (represented by black and white circles).	87
Figure 11.4: The structure of m-aminophenol. Note: the β -As sheet structure is not formed.	88
Figure 11.5: The aminophenol series studied.. Box colour indicates structure type: Red = β -As sheets, Blue = Square motif chains, Yellow = Stacked Vees. See following chapter for description of these structures types.	90
Figure 12.1: The difference in geometry between odd and even alkanes.	93
Figure 12.2: The molecular shapes of p-aminophenol and compounds 0a , 2a and 3a . The boxes are to emphasize the changes in molecular shape and are NOT related to the unit cell.	94
Figure 12.3: The structures of 2a , 3a , 4a and 5a , viewed down the b-axis. Note the similar hydrogen bond chain in each case leading to similar molecular spacing, and similar c-axis length's.	95
Figure 12.4: The square motif of hydrogen bonds forming chains of 1a .	96
Figure 12.5: The 'double faced' hydrogen bond about the phenyl ring A, and the single C-H... π hydrogen bond to the phenyl ring B.	97
Figure 12.6: Hydrogen bonding between adjacent chains.	97
Figure 12.7: Packing of the sheets of 1a molecules in the crystal, hydrogen bonds to the aromatic rings are not shown in this diagram.	98
Figure 12.8: 1a model from neutron data, showing thermal ellipsoids plotted at 50%, including hydrogen atoms.	98
Figure 12.9: The geometry of the H... π hydrogen bonds.	99
Figure 12.10: The N ₁ -H _{1b} ... π interaction viewed in the aromatic ring plane.	100
Figure 12.11: The asymmetric unit of crystals of 3a and 5a .	101
Figure 12.12: O(H)N chain in crystal 3a , and 5a . In the structure 5a molecule 1 is coloured blue and molecule 2 is coloured purple for clarity.	101
Figure 12.13: O(H)N chains in crystal 5a viewed approximately down the molecular axis (i.e. at 90° rotation to previous diagram, the aromatic rings and pentane chain have been removed from the diagram for clarity). Note the hydrogen bond shown by dots is fairly long (O ₁ ...H _{21b} = 2.70(3)Å, O ₁ ...N ₂₁ = 3.461(2)Å).	102
Figure 12.14: N-H... π interactions in crystals 3a and 5a .	103

Figure 12.15: The packing of the sheets in compounds 3a , and 5a	104
Figure 13.1: The square motif of hydrogen bonds forming chains of 1a , and 1b	107
Figure 13.2: The 'double faced' hydrogen bond about the phenyl ring A and the single N-H... π hydrogen bond to the phenyl ring C.	107
Figure 13.3: Hydrogen bonding between adjacent chains in compound 1a and 1b	108
Figure 13.4: Diagram indicating the relationship between adjacent chains in compound 1a , and 1b . Each arrow represents a chain, chains in one sheet are coloured blue, chains in the adjacent sheet are coloured red.....	108
Figure 13.5: The packing of the sheets in compound 1a , and 1b	109
Figure 13.6: The structure of 2a , and 2b , showing the β -As sheet structure in both cases and the additional C -H...S chains in compound 2b	111
Figure 13.7: The molecular geometry of 2a , 2b , and 2c	112
Figure 13.8: N(H)O chains in compound 2c forming sheets.....	113
Figure 13.9: The packing of the sheets of 2c	113
Figure 13.10: The O(H)N chain in compound 3a , 3b and 5a	116
Figure 13.11: The interactions in compounds 3a , 3b and 5a that form in addition to the O(H)N chain.	117
Figure 13.12: The interactions in compound 3b a) O(H)N chains with additional N-H... π interactions, b) chains of N-H...O and bi-furcated (C-H) ₂ ...O hydrogen bonds, c) both of the previous chains forming sheets of hydrogen bonds, viewed from above with part of each molecule removed for clarity.....	118
Figure 13.13: The overall crystal packing of compound 3a , 3b and 5a	119
Figure 15.1: Compounds studied in part 3.....	127
Figure 16.1: Motifs generated by sym-triaryloxytriazines ^{4,1} . * see footnote on previous page.....	129
Figure 16.2: The full structure of compound 6	131
Figure 16.3: 2,4,6-tris-(4-chloro-phenoxy)-1,3,5-triazine and tribromobenzene, model from neutron data with thermal ellipsoids (including hydrogen atoms) plotted at 50% probability.....	131
Figure 16.4: the trigonal based net of triazines containing tribromobenzenes.	132
Figure 16.5: The orientation of the tribromobenzene molecule in the triazine net.	133
Figure 16.6: Side view of 2 layers of tribromobenzene molecules in the triazine nets.	133
Figure 16.7: The structure of 2,4,6-tris-(4-chloro-phenoxy)-1,3,5-triazine, in P6 ₃ /m and P6 ₃ space groups. The space group depends on the identity of the guest solvent molecule.....	134
Figure 17.1: Triphenylisocyanurate with trinitrobenzene and benzene. Model from neutron data, thermal ellipsoids (including hydrogen atoms) plotted at 50% probability.....	137

Figure 17.2: Triphenylisocyanurate trinitrobenzene and benzene hydrogen bonded unit, thermal ellipsoids (including hydrogen atoms) plotted at 50% probability.....	139
Figure 17.3: The π - π interaction a) side view b) top view.....	140
Figure 17.4: Ladder of quadruple π - π interactions.	140
Figure 17.5: Two chains of triphenylisocyanurate with trinitrobenzene and benzene.	141
Figure 17.6: Interaction between two sheets viewed down the π - π interactions. Thermal ellipsoids (including hydrogen atoms) plotted at 50% probability.....	142
Figure 18.1: 4,4'-dinitrotetraphenylmethane, with two water molecules in partially occupied positions. Thermal ellipsoids plotted at 50% probability.....	145
Figure 18.2: The disordered water molecules.....	147
Figure 18.3: Dimers of 4,4'-dinitrophenyl methane a) dimer 1, b) dimer 2.	148
Figure 18.4: Helix of 4,4'-dinitrophenyl methane molecules (helix 1), a) viewed perpendicular to helix axis, b) viewed down axis of helix.	149
Figure 18.5: Helix of 4,4'-dinitrophenyl methane molecules (helix 2), a) viewed perpendicular to helix axis, b) viewed down axis of helix.	149
Figure 18.6: Six-membered rings of 4,4'-dinitrophenyl methane molecules a) ring propagated by C-H...O hydrogen bonds b) ring propagated by C-H... π hydrogen bonds.....	150
Figure 18.7: The packing of 4,4'-dinitrotetraphenyl methane in the three dimensional structure.	151
Figure 19.1: Possible hydrogen bond interactions between two gem-alkynol groups.	153
Figure 19.2: 2,3-dichloro-1,4-diethynyl-1,4-dihydroxy-napthalene, thermal ellipsoids plotted at 50% probability.....	156
Figure 19.3: Ladder built up from gem-alkynol - gem-alkynol interactions (i) and (ii).	158
Figure 19.4: Zig-zag sheets of compound 9 showing the various gem-alkynol interactions and the chlorine - chlorine interaction, a) viewed from above with interactions (i), (ii), and (iii) labelled in grey, b) side view.....	159
Figure 19.5: Zig-zag sheets of compound 9 showing all the various interactions, a) side view, b) looking down on a sheet with interactions within and between sheets shown.....	160
Figure 20.1: 4,4-diphenyl-2,5-cyclohexadienone, form 3 , thermal ellipsoids plotted at 50% probability.....	163
Figure 20.2: Helical chains mediated by O...H-C hydrogen bonds.	166
Figure 20.3: Sheets of C-H... π linked chains, a) top view of sheet, b) side view of sheet.	166
Figure 20.4: Hydrogen bonding within and between two sheets of polymorph 1 , viewed edge on to the sheets.	167

Figure 20.5: Red-red dimer in polymorph 2 structure, the blue-blue dimer is similar.	168
Figure 20.6: Ladder of red-red and blue-blue dimers.	169
Figure 20.7: Yellow-yellow dimers in the polymorph 2 structure.	169
Figure 20.8: All the interactions within one sheet of the polymorph 2 structure. Each type of interaction has been given a different number.	170
Figure 20.9: The C-H... π interactions that occur between sheets, note the double faced C-H... π hydrogen bond across the phenyl ring of the blue coloured molecule.	170
Figure 20.10: The packing of the first type of molecule into sheets in polymorph 3, a) viewed from above and b) viewed from the side.	172
Figure 20.11: The interweaving of two of the sheets shown in Figure 20.10, a) viewed from above and b) viewed from the side.	173
Figure 20.12: Dimers of the cyan coloured molecule.	173
Figure 20.13: The 'double faced' hydrogen bond in polymorph 3.	174
Figure 20.14: The overall structure of polymorph 3.	175
Figure 21.1: Crystals of 4,4'-Dinitrotetraphenylmethane (8) and 4-amino-4'-hydroxybenzylphenyl-sulphide (2b) (left and right of previous page respectively). A 'hedgehog' of needle crystals of thiodianiline and thiodiphenol (on going work), and thin plates of 4-amino-4'-hydroxy-diphenylpropane (3a) (left and right of current page respectively).	180

Graphs:

Graph 5.1: dS (Å) versus dL (Å) for case I all data.	52
Graph 5.2: dL (Å) for all data.	53
Graph 5.3: dS (Å) for all data.	53
Graph 5.4: dL (Å) versus aL (°) for case I all data.	53
Graph 5.5: dS (Å) versus aS (°) for case I all data.	53
Graph 5.6: aL (°) versus aS (°) for case I all data.	54
Graph 5.7: Distance (Å) of hydrogen atom out of donor acceptor plane.	55
Graph 5.8: Sum of aS, aL and A3 angles (°).	55
Graph 5.9: dL (Å) for case I where the hydrogen donor is nitrogen.	56
Graph 5.10: dL (Å) for case I where the hydrogen donor is oxygen.	56
Graph 5.11: dL (Å) versus aL (°) for case I where the hydrogen donor is nitrogen.	56
Graph 5.12: dL (Å) versus aL (°) for case I where the hydrogen donor is oxygen.	56
Graph 5.13: dS (Å) versus aS (°) for case I where the hydrogen donor is nitrogen.	57
Graph 5.14: dS (Å) versus aS (°) for case I where the hydrogen donor is oxygen.	57
Graph 6.1: aL (°) versus aS (°) for case I and II, all data. Data coloured by acceptor-acceptor path lengths.	60
Graph 6.2: dL (Å) versus dS (Å) for case II all data. Data coloured by path lengths. ..	62
Graph 6.3: dL (Å) for all data.	63
Graph 6.4: dS (Å) for all data.	63
Graph 6.5: dL (Å) versus aL (°) for all data.	63
Graph 6.6: dS (Å) versus aS (°) for all data.	63
Graph 7.1: aIntra (°) versus aInter (°) for case III all data. Data colour coded by intra path length.	66
Graph 7.2: dIntra (°) versus aIntra (°) for case III all data, colour coded by intra path length.	67
Graph 7.3: dInter (Å) for all data.	67
Graph 7.4: dIntra (Å) for all data.	67
Graph 8.1: aL (°) versus aS(°) for case IV, all data. Colour coded by path length.	70
Graph 8.2: dL versus dS for case IV, all data. Colour coded by path length.	71
Graph 8.3: dL (Å) for all data.	73
Graph 8.4: dS (Å) for all data.	73
Graph 8.5: dL (Å) versus aL (°) for all data.	73
Graph 8.6: dS (Å) versus aS (°) for all data.	73
Graph 10.1: dL (Å) for all tri-furcated systems.	79
Graph 10.2: dL (Å) versus aL (°) for all tri-furcated systems.	79
Graph 10.3: dM (Å) for all tri-furcated systems.	80

Graph 10.4: dM (Å) versus aM (°) for all tri-furcated systems.	80
Graph 10.5: dS (Å) for all tri-furcated systems.	80
Graph 10.6: dS (Å) versus aS (°) for all tri-furcated systems.....	80
Graph 10.7: dS (Å) vs aS (°) for the cases where there are two intramolecular hydrogen bonds. Data points where the acceptor-acceptor path length is one are coloured red and where the acceptor-acceptor path length is greater than one are coloured blue.	83
Graph 13.1: C-S-S-C torsion angles (°) occurring in CSD ¹³	112
Graph 14.1: Ph-N vector, Ph-O vector angle in relation to the number of atoms in the link. Note: compounds 1b, and 5a have two molecules in the asymmetric unit, and therefore two data points.....	120
Graph 14.2: Ph-N vector, Ph-O vector angle versus the angle between the phenyl plane and the phenol plane.	121
Graph 14.3: Melting points of the crystals.	122

Tables:

Table 4.1: Overall statistics of the furcation of hydrogen bonds in CSD.....	48
Table 4.2: Hydrogen bond frequencies for case I (inter:inter), case II (inter:inter A-A intra), case III (inter:intra) and case IV (intra:intra) for all the data.....	48
Table 4.3: Hydrogen bond frequencies for case I (inter:inter), case II (inter:inter A-A intra), case III (inter:intra) and case IV (intra:intra) for nitrogen as donor atom. ..	48
Table 4.4: Hydrogen bond frequencies for case I (inter:inter), case II (inter:inter A-A intra), case III (inter:intra) and case IV (intra:intra) for oxygen as donor atom.	49
Table 6.1: Number of occurrences of different numbers of bonds in Path 3.....	58
Table 7.1: Number of occurrences of different numbers of bonds in the intramolecular path, Path 1.	65
Table 8.1: Combinations of path lengths found for case IV data.	69
Table 10.1: Frequency of occurrence for the tri-furcated system.....	78
Table 10.2: Distance (Å) versus angle (°) plots for all three hydrogen bonds, for each inter/intramolecular hydrogen bond combinations of tri-furcated cases.	82
Table 12.1: Crystal data for the 4-amino-4'-phenol alkane series.	92
Table 12.2: Hydrogen bond distances in compound 1a	98
Table 12.3: The geometry of the H... π hydrogen bonds.	99
Table 12.4: Hydrogen bond distances in compound 3a	103
Table 12.5: Hydrogen bond distances in compound 5a	103
Table 13.1: Crystal data for the compounds with one atom in the link.	106
Table 13.2: Hydrogen bond distances in compound 1a	109
Table 13.3: Hydrogen bond distances in compound 1b	109
Table 13.4: Crystal data for the compounds with two atoms in the link.	110
Table 13.5: Hydrogen bond distances in compound 2a	111
Table 13.6: Hydrogen bond distances in compound 2b	111
Table 13.7: Hydrogen bond distances in compound 2c	114
Table 13.8: Crystal data for compounds with three atoms in the link, and also compound 5a for comparison.	115
Table 13.9: The hydrogen bond distances in compound 3b	119
Table 16.1: Crystal data for co-crystal 6 , 2,4,6-tris-(4-chlorophenoxy)-1,3,5-triazine and tribromobenzene.	130
Table 16.2: Geometry of the C-H...N hydrogen bond linking adjacent layers.....	134
Table 16.3: Occurrences of 2,4,6-tris-(4-chloro-phenoxy)-1,3,5-triazine with various solvents in the CSD ⁶	135
Table 17.1: Crystal data for co-crystal 7 , triphenylisocyanurate with trinitrobenzene and benzene.	138

Table 17.2: Hydrogen bond distances within the triphenylisocyanurate trinitrobenzene and benzene unit.	139
Table 17.3: π - π and C-H... π interactions in compound 7	142
Table 17.4: C-H...O interactions between two adjacent sheets in compound 7	143
Table 18.1: Crystal data for compound 8 , 4,4'-dinitrotetraphenyl methane.....	146
Table 18.2: Hydrogen bonding interactions in compound 8	151
Table 19.1: Frequencies of occurrence of the four gem-alkynol - gem-alkynol interactions.....	154
Table 19.2: Frequencies of occurrence of the possible combinations of the four gem-alkynol - gem-alkynol interactions.	155
Table 19.3: Crystal data for compound 9 , 2,3-dichloro-1,4-diethynyl-1,4-dihydroxy-napthalene.	157
Table 19.4: Interactions within the 2,3-dichloro-1,4-diethynyl-1,4-dihydroxy-napthalene crystal structure.....	160
Table 20.1: The different polymorphs of compound 10	163
Table 20.2: Crystal data for compound 10 , 4,4-diphenyl-2,5-cyclohexadienone, form 3	164
Table 20.3: Comparison of forms 1 , 2 , and 3 of compound 10	165
Table 20.4: Hydrogen bonds occurring in polymorph 1	167
Table 20.5: Hydrogen bonds occurring in polymorphs 2	171
Table 20.6: Hydrogen bonds occurring in polymorph 3	175

Standards, Abbreviations, and Points of Note:

All hydrogen atom for structures from X-ray data are given at positions derived from X-ray data, i.e. the hydrogen atoms positions have not been 'neutron normalised'. The only exception is in the CSD searches in Part 1 Bi-furcated hydrogen bonds, where the hydrogen atoms have been 'neutron normalised' to prevent inconsistencies between structures from X-ray and from neutron data, and inconsistencies arising from the treatment of the hydrogen atom in the structure models.

Unless otherwise stated, all atomic scale distances have been measured in angstroms (Å) all laboratory scale distances (crystal dimensions etc.) measured in millimetres (mm) and all angles measured in degrees (°).

In diagrams showing thermal ellipsoid plots all thermal ellipsoid have been plotted at 50% probabilities.

CSD = Cambridge Structural Database.

Throughout this work molecules have been referred to as being held together to give the crystal lattice by only very specific directional interactions, this of-course is an over simplification that ignores the very important influences of van der Waals forces, non-bonded interactions, close packing and other effects.

Introduction

Chapter 1 : Introduction

1.1 Crystal Engineering

The study of the structure of molecules is of vital importance to chemistry. It helps with every aspect, from the analysis of reactions and reactions pathways, to the understanding of the physical properties of the compound. After all, of all the various pieces of information available on a particular compound, the molecular structure has to be one of the most fundamental.

In much the same way, in the study of crystalline solids, the crystal structure; the way the molecules pack into a regular periodic lattice, is of fundamental importance if there is to be any hope of understanding fully the physical properties of the crystal. It is with the aim of both understanding and eventually directing and controlling these physical properties that the field of crystal engineering^{1,2} and supramolecular chemistry has developed.

One aspect of crystal engineering is the use of crystal structures to study, analyse, characterise and categorise the various forces and interactions that direct, and control, the way the molecules pack³. The hope is that a full understanding of these forces and interactions will give the ability to design crystals with specific structures and therefore specific physical properties. Unfortunately, other than in a few specific cases, there is still a long way to go before this aim is achieved.

There are many types of inter-molecular forces that are important in directing the formation of a crystal structure. Some interactions can be considered as non-directional forces involving the whole molecule such as shape fitting to achieve a close-packed arrangement of the molecules, electrostatic interactions, and Van der Waals forces. Other interactions such as hydrogen bonds, halogen-halogen interactions and π - π stacking are much more directional interactions and can be considered as non-covalent intermolecular bonds. It is an optimisation of all the various influences that leads to the preferential formation of one crystal structure over another. It is in fact amazing that the optimisation of such a wide range of forces, often acting in opposition to each other, can lead, so consistently, to a single, reproducible, structure. And that each crystal in itself

has a nearly perfectly consistent structure across the whole crystal, no errors, or random defects, just one molecule stacked in a precise orientation to the next. Of course there are exceptions to this, such as are seen in the cases of polymorphs, disordered and twinned crystals, but it is these exceptions that fully emphasise this point.

In this work I have been studying the influences on crystal structure of some of the more directional interactions, mainly of hydrogen bonds of various types, but also π - π stacking and halogen - halogen interactions.

1.2 Methods of Studying Molecular Interactions

Leaving aside any purely theoretical calculation techniques, there are three main methods of studying interactions, the first, and perhaps the most obvious, is to carefully study one structure looking at all the close atom-atom contacts. This is a good way to identify new and novel interactions. Where a detailed structure has been obtained from accurate X-ray, or better, neutron data the structure can be used to 'benchmark' a particular interaction.

Another method is to study a series of compounds where just one aspect of the molecule is changing through the series, thus reducing the variables in the system. For instance a series of compounds with increasing chain length, substituent group size or nature. This method is especially useful from a crystal engineering point of view, indicating stable motifs and areas where the structure prediction might be possible. It can highlight areas where the understanding of intermolecular interactions is not great enough to allow prediction, or where an interaction, or a major effect of the interactions, is not being accounted for in the structure prediction considerations, and more research is needed. This method is also useful in the understanding of the relative degree of influences of the interactions. For instance where there are two possible but mutually (or even just partially) exclusive interactions, which one will be found in the resulting structure? Such as in the case where there could be a close packed structure, or a structure based on a hydrogen bond network, but with a less dense structure containing voids, which structure will be found, or will neither?

The final way is to use a statistical analysis of a large number of crystal structures to discover trends and patterns^{4,5}. This can be very useful in establishing the standard geometry and the geometric limits of an interaction. The Cambridge Structural Database⁶ is a useful source for such a search and provides comprehensive search and

analysis software.

Perhaps slightly paradoxically the last method of statistical analysis is the method used in Part 1, Part 2 covers the analysis of a series of amino-phenols and the first method of detailed analysis of interesting structures is covered in Part 3.

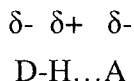
The experimental techniques behind these methods are discussed in detail in Chapter 2.

1.3 Hydrogen Bonds

Classically, hydrogen is considered to have a valence of one, i.e. it can only form one bond. This is logical since a hydrogen atom only has a single electron with which it can form only one normal covalent bond. However, sometimes a hydrogen atom is obviously involved in two bonds (or more), the longer and weaker of which are referred to as a hydrogen bond(s).



A hydrogen bond is an interaction that occurs between an electropositive hydrogen e.g. a hydrogen bound to an electron withdrawing atom or group (oxygen, nitrogen, etc), and an electronegative atom such as oxygen, nitrogen or a halogen. In the example above, there is a covalent bond between atom D (known as the hydrogen donor) and the hydrogen atom, and the electron pair is located between the hydrogen and atom D. If atom D is more electronegative than hydrogen then the electron pair is pulled closer to the atom D leaving the hydrogen nucleus 'exposed'. Any area of electron density occurring nearby, e.g. another electronegative atom (in the case above this is atom A, known as the hydrogen acceptor) which can contribute electron density, for instance from a lone pair of electrons, which will interact with the electropositive hydrogen nucleus^{7,8}.



This is a very simplified explanation of hydrogen bonding, a more detailed explanation can be found in most standard textbooks on the subject, such as those by G. A. Jeffery, J.C.Speakman etc. See ref 9,8.

The first types of hydrogen bond that were identified and accepted as genuine attractive interactions were the types where both the hydrogen donor and acceptor were strongly electronegative atoms such as oxygen or nitrogen, i.e. N-H...O. In terms of hydrogen bond strength these types of hydrogen bonds are strong, usually of the order of -20 to -100 kJ/mol¹⁰. In this work these types of hydrogen bond are referred to as either *strong* or a *conventional* types of hydrogen bond.

Subsequently, other types of hydrogen bonds have been identified and accepted^{11,10}, where the acceptor is some other electronegative atom such as a halogen, or where the acceptor is a more diffuse area of electron density in a group of atoms, for instance, the π bond of alkene group or of a phenyl ring. Alternatively, where the hydrogen donor is not oxygen or nitrogen but some other atom (not even necessarily a very electron withdrawing one) such as carbon.

Various Types of Hydrogen Bond

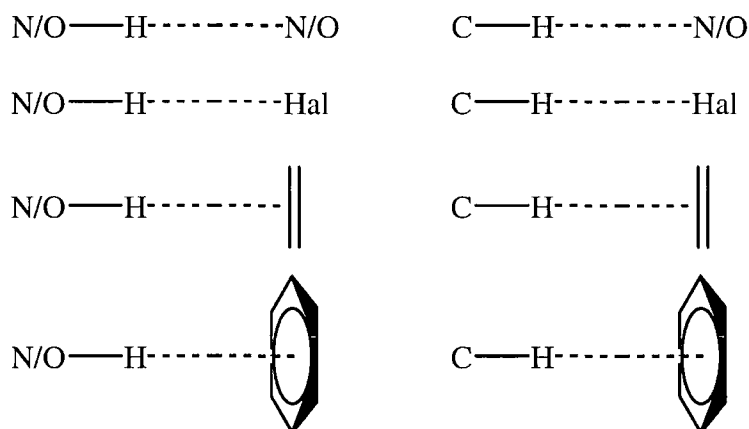


Figure 1.1: Types of hydrogen bond.

Hydrogen bonds are usually identified by analysing the various inter-atomic distances, obtained from diffraction data. The best identification is an H...A distance that is shorter than expected i.e. less than the sum of the Van der Waals radii¹². Unfortunately, unless the X-ray diffraction data are very good, the positions of the hydrogen atoms are only poorly defined, or not found at all, but generated in the calculated positions. Even when the hydrogen atom positions can be identified from X-ray data, the position is not the true position of hydrogen nucleus. X-rays are diffracted by electrons, not the atom nucleus, thus hydrogen, having only one electron and that electron involved in a bond to

the donor atom, will be modelled in a position closer to the donor atom than is the true position of the nucleus.

There are 3 solutions to this problem:

- ⊙ Ideally, a neutron diffraction experiment can be undertaken. Neutrons are diffracted by the atom nucleus and therefore give the true hydrogen position. Also, since the degree of scattering is not dependent on atomic weight, hydrogen atoms scatter well and therefore their positions tend to be well defined in a model based on neutron data. However, neutron experiments can only be run at certain large dedicated facilities, are expensive, and require large crystals with volumes in the order of mm^3 , which can be difficult to grow.
- ⊙ The D...A distance can be considered instead of the H..A distance. D and A are usually well defined since they have more electrons than hydrogen. In a hydrogen bond the D...A distance is less than the sum of the Van der Waals radii of the two atoms.
- ⊙ The hydrogen position can be corrected by moving it along the D-H bond vector to a given standard D-H bond distance, measured from previous neutron experiments of other systems. This, however, will hide any influence that there has been on the hydrogen position by the interaction.

The length of the hydrogen bond gives an indication of the strength of the hydrogen bond; the stronger the interaction, the shorter it is. Hydrogen bonds tend to be linear, and stronger hydrogen bonds tend to be more linear than weak ones. Although the sum of the Van der Waals radii can be a useful boundary when defining an H...A distance as a hydrogen bond it can hardly be taken as the definitive limit. As a hydrogen bond gets weaker it gets longer, but there is no sudden cut off point beyond which there is no interaction, the interaction just becomes weaker until its effect becomes negligible. In a practical sense, the limit to which an H...A distance is considered to be an interaction depends on the question that is being asked.

1.4 π - π Interactions

A phenyl ring can be considered as a more electropositive σ -bonded carbon atom framework sandwiched between two electronegative regions of electron density arising from the π electron density^{13,14}.

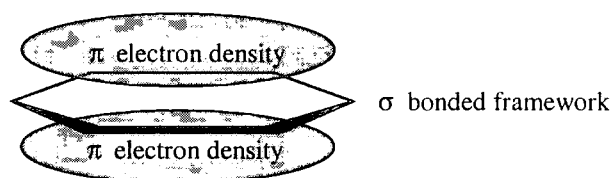
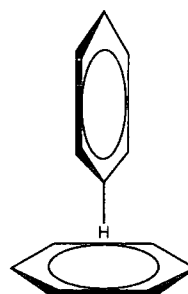


Figure 1.2: Schematic of the electron density around a phenyl ring.

Electrostatic considerations and structural studies suggest that there are 3 ways such groups could pack¹⁴:

- **Face to Edge:** where an electropositive ring substituent e.g. H will interact favourably with the electronegative π density – this is the same as the C-H... π hydrogen bond mentioned previously.



- **Face to Face Stacking:** Eclipsed rings. There is direct overlap between the rings. At very short distances this will tend to be an unfavourable interaction.



- **Face to Face Offset Stacking:** The offset minimises the π ... π repulsion and maximises the σ ... π interaction.



Figure 1.3: Types of π - π interaction.

1.5 Halogen – Halogen Interactions

The nature of halogen...halogen interactions, particularly Cl...Cl interactions, has been the subject of considerable debate over the past decade. Studies by Desiraju & Parthasarathy¹⁵ and Pedireddi *et al.*¹⁶ using the Cambridge Structural Database⁶ indicated the occurrence of two types of interactions, type I and type II. If we denote the larger of the two C-Cl...Cl angles as θ_1 , and the smaller as θ_2 , then Type I interactions have $\theta_1 = \theta_2$ and Type II have $\theta_1 = 180^\circ$ and $\theta_2 = 90^\circ$.

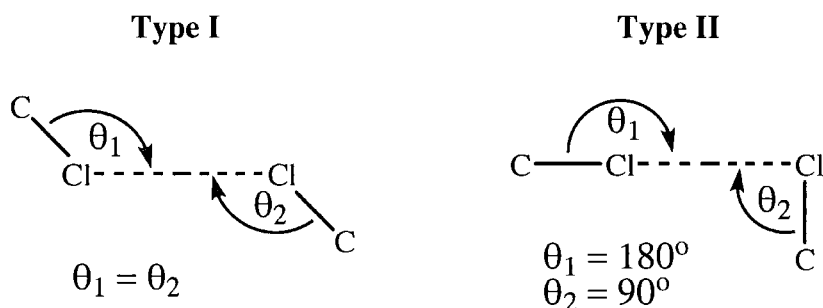


Figure 1.4: Types of halogen halogen interaction.

The vast majority of Type I examples arise from interactions across a crystallographic centre of symmetry, however situations having a linear C-Cl...Cl-C system, $\theta_1 = \theta_2 = 180^\circ$, are seldom observed. Type II interactions were deemed to arise due to the polarisability of the halogen, which increases from Cl through Br to I. Calculations of interaction energies using intermolecular perturbation theory¹⁷ have been carried out for Cl...Cl by Price *et al.*¹⁸ and for C-Cl...O interactions by Lommerse *et al.*¹⁹ In broad terms, all of these authors agree that carbon-bound halogens in a sufficiently electron-withdrawing environment, will present an anisotropic charge distribution, δ^+ forward of the halogen along the C-halogen bond vector ($\theta_1 = 180^\circ$), and δ^- perpendicular to the bond vector ($\theta_2 = 90^\circ$). In these cases, stabilising interaction energies of up to about 10 kJ mol^{-1} can be attained for linear C-Cl...O interactions, about one-half to one-third of the interaction energy for a strong hydrogen bond¹⁹. These authors also found evidence that the interactions become stronger for the more readily polarisable halogens, Br and I.

Chapter 2 : Techniques

2.1 Crystallography and Diffraction

Crystallography is a technique for the study of molecular structure, at an atomic scale, of phases of matter that exhibit long range order, i.e. crystalline solids. Within a crystal the atoms, and the molecules that they constitute, have a regular repetitive arrangement in the crystal lattice. When an X-ray or neutron beam is directed onto a crystal, it is diffracted by the atoms giving rise to a diffraction pattern that can be analysed to allow the identification of the structure that created it.

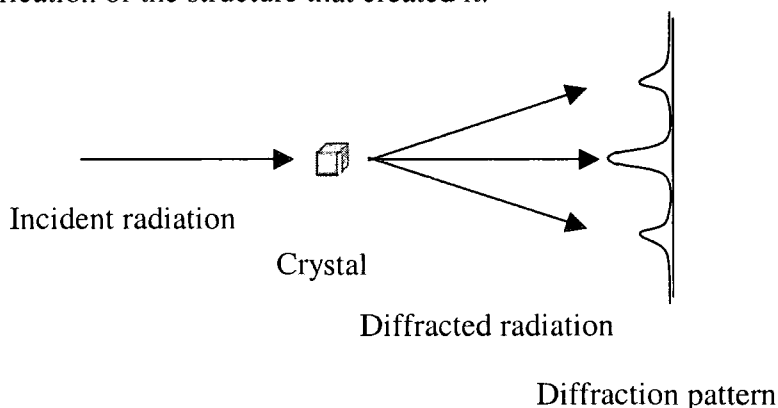


Figure 2.1: A schematic of a diffraction experiment.

The definition of diffraction is 'the interaction of electromagnetic radiation with an object in space'. When a beam of radiation is passed through a grating where the size of the holes is of the same order of magnitude as the wavelength, the beam is split. The difference in path length of the parts of the beam from the different holes in the grating to a point further on in space lead to constructive and destructive interference, which in turn leads to a pattern of intensities – the diffraction pattern.

From an observed diffraction pattern it is possible to calculate information on the grating that caused it. The regular arrangement of atoms in a crystal is, in effect, a 3-D diffraction grating. The atomic spacing, i.e. the size of the holes in the grating is of the

same order of magnitude as the wavelength of X-rays and neutron radiation. This is why these forms of radiation are used to study the diffraction patterns of crystals.

2.2 From the Diffraction Pattern to the Model

The information contained in a diffraction pattern can be considered as consisting of two parts; the arrangement of the diffraction peaks in space, and the intensities of these peaks. While neither part is independent of the other, when analysed they give information on different aspects of the crystal structure; the arrangement of the peaks gives information on the unit cell of the crystal, while the intensity of the peaks can give information on the atomic positions within the unit cell.

The Unit Cell

A simple description of diffraction can be reached by considering the crystal in terms of the crystal lattice. The crystal lattice is a theoretical construction that consists of a framework of identical repeat units, each repeat unit contains an identical arrangement of atoms and molecules. The smallest repeat unit of the lattice, the building block from which the rest of the lattice is made up, is referred to as the unit cell.

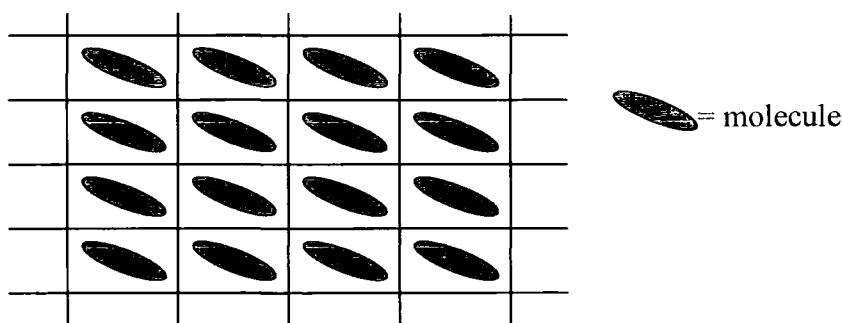


Figure 2.2: 2-D representation of molecules in a lattice.

In 1913 W. L. Bragg derived a law for diffraction by considering the X-ray or neutron beam to be reflecting off the lattice planes²⁰:

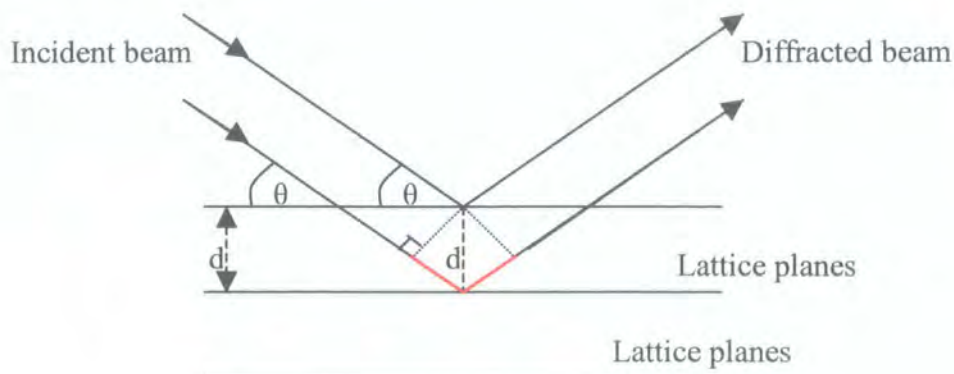


Figure 2.3: Schematic of Bragg's law.

Constructive interference, which gives rise to the diffraction peaks, will be seen only when the path length difference (shown in red) is equal to a whole number of wavelengths (λ), at which point it can be shown that:

$$n\lambda = 2d \sin\theta \quad (\text{Bragg's Law})$$

Where d is the spacing between the lattice planes. From the d -spacings the size and shape of the unit cell can be found.

The Atomic Positions

Diffraction peaks arise from the constructive interference of the electromagnetic waves. The position of the atoms in the unit cell can cause the wave to undergo a phase shift, which in turn effects the degree of interference between the waves, and therefore the peak intensity.

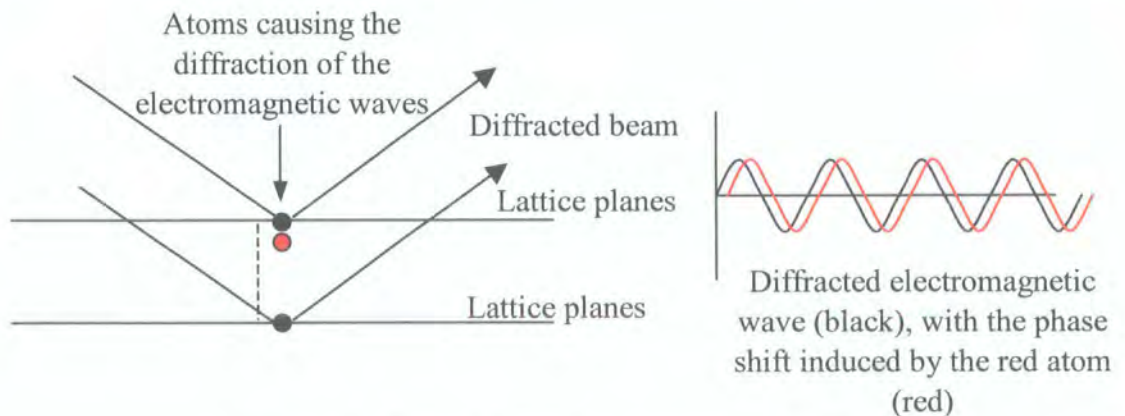


Figure 2.4: Phase shift caused by an atom (coloured red).

The intensity of each peak is proportional to the sum of the waves diffracted from different parts of the crystal. The information on the atomic positions is contained in the phases of each of these waves. The de-convolution of the peak intensity into the individual waves, and the phases of these component waves, is a major difficulty known as the 'phase problem'.

The data obtained from a diffraction experiment (after indexing and integration) is in the form of a list of peaks described in terms of the hkl values of the lattice plane that has diffracted the radiation, and the intensity of that peak ($I(hkl)$). The measured intensity $I(hkl)$ can be converted to $|F(hkl)|^2$ (the relative structure factor). $F(hkl)$ can be converted by Fourier transform²¹ to the $\rho(xyz)$ (electron density – real space). But, although $F(hkl)$ can be converted to $|F(hkl)|^2$, $|F(hkl)|^2$ cannot be converted to $F(hkl)$ since $\sqrt{F(hkl)^2} = +F$ or $-F$. This is another way of describing the phase problem.

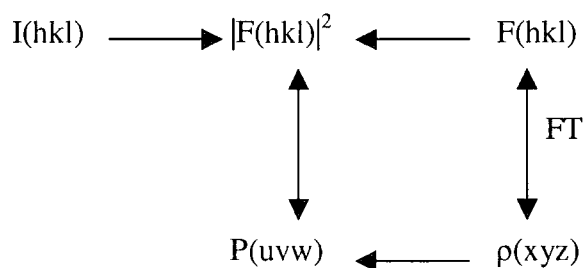


Figure 2.5: Schematic of the mathematical conversions used on diffraction data.

Because of these problems it is not possible to work directly back from the data, to the structure that it was generated from. Instead a very approximate solution – the *initial* or *trial* solution – is obtained, then the structure is solved by an iterative refinement process. The procedure is to take the initial estimate of the electron density distribution (the initial or trial model), convert $\rho(xyz)$ to $F(hkl)$ by Fourier transform procedures, convert $F(hkl)$ to $|F(hkl)|^2$ (the 'calculated' structure factors $|F_{calc}|^2$ or $|F_c|^2$) and compare with the experimentally derived $|F(hkl)|^2$'s (the 'observed' structure factors $|F_{obs}|^2$ or $|F_o|^2$). A small adaptation is then made to the model and the $|F_{calc}|^2$ re-compare $|F_{obs}|^2$ to see if the fit is improved. If the model has improved, the new model is taken as a starting point, adapted and re-compared. If the model has not improved then the new model is discarded and a different adaptation of the original model is tried, this process continues until the model can no longer be improved – the refinement has converged.

The initial trial structure is usually found from one of two methods, either Patterson methods, or from direct methods. The Patterson method uses the Patterson function $P(uvw)$ to calculate the vector relationship between all the atoms, since these inter-atomic vectors can be calculated from $|F(hkl)|^2$ the phase problem is not encountered. In a many atom system this leads to a very complicated solution that is difficult to interpret. But, if there are just a very small number of heavy elements in the system, the vector relationships of these can be pulled out from the sea of vectors arising from the lighter elements. The positions of these heavy elements can be identified, and, since most of the diffraction is due to these heavy elements this provides a good model to start the iterative refinement process. This method is not much use for structures containing only light elements or many elements of similar mass, and for that reason it has not been used to solve the mainly organic structures studied here.

Direct methods is a much more computationally intensive method. A vast quantity of possible phase combinations are calculated and used to generate electron density maps. Given certain assumptions, such as the peaks of electron density must be discrete and the electron density cannot be negative, etc., most of the phase combinations can be discarded. The best resulting solution is then used as a starting point for the refinement of the structure. This method works very well provided there are not too many atoms in the structure. For structures containing more than 100 non-hydrogen atoms direct methods may not work, although, with increasing computational power larger and larger structures are being solved.

For reasons of clarity and conciseness, many of the more detailed aspects of structural determination have been omitted from the above discussion. There are many books on the subject, see ref. 22-25 for further information.

2.3 Neutron Diffraction

Much of the above discussion has been based on X-ray diffraction techniques. Apart from the obvious difference in radiation type, neutron diffraction is very similar, but there are a few important differences between the two techniques, these are mainly due to differences in scattering properties between the types of radiation. X-rays are scattered by electrons, this means that the scattering power of an element is directly proportional to its atomic number. Neutrons are scattered by the atomic nucleus, and, although there is a very slight overall increase in scattering power with atomic number,

it is not as dramatic as in the case of X-rays and is hidden by the large fluctuations from element to element and even isotope to isotope.

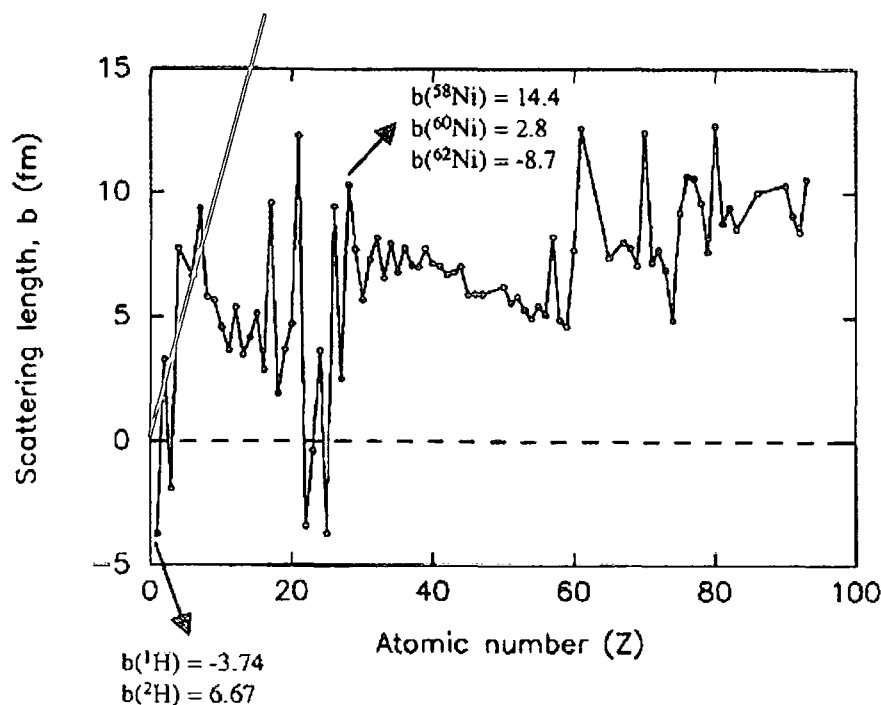


Figure 2.6: Scattering length for neutron radiation (reproduced from: 'Single Crystal Neutron Diffraction From Molecular Materials', C.C.Wilson²⁶). Red line indicates corresponding scattering length for X-ray radiation.

The fact that the X-ray scattering power of an element is directly proportional to its atomic weight is an important factor in the solving of structures using Patterson methods, and this means that, except in very simple cases, Patterson methods cannot be used to solve neutron data. Direct methods also cannot be used to solve neutron data, since, one of the basic criteria for the selecting or discarding of a phase combination is that the scattering (in X-ray data directly related to the electron density) is always going to be positive. As can be seen from the graph above (Figure 2.6) in neutron diffraction not only is there the possibility for negative scattering, but one of the more common and important elements, hydrogen, scatters negatively. Having said this it is still sometimes possible to solve neutron data directly using direct methods, however the normal procedure is to use a model obtained from X-ray data as the initial model and then refine this structure against the neutron data.

As was mentioned in section 1.3 (hydrogen bonds), a consequence of the fact that, in X-ray diffraction, the scattering power of an element is proportional to the number of electrons, is that hydrogen atoms are very hard to identify since they have only one electron from which to scatter the X-rays. Because of this, it is standard practice, except

for very good data sets, to constrain the hydrogen atoms to standard geometrically calculated positions rather than to allow free refinement. Even where the position of the hydrogen can be identified from the X-ray data, the electron density is shifted into the H-X bond away from the hydrogen nucleus. Thus, hydrogen atoms identified from X-ray data, appear displaced along the H-X bond vector, closer to the X atom than is the true position of the hydrogen nucleus, and this gives very inaccurate bond length. One of the prime advantages of neutron diffraction is that hydrogen scatters to nearly the same magnitude as, for instance, carbon. However, the hydrogen scattering factor is negative so the hydrogen atoms appear as a hole, rather than a peak, in the electron density map. This makes the hydrogen atoms easy to identify in the scattering density map. Also the neutrons 'see' the atomic nucleus, not the electrons, this means that the hydrogen positions found from neutron data are the 'true' hydrogen nuclear positions. There are other advantages of neutron diffraction experiment, see ref. 26,24.

2.4 Diffractometers and Other Equipment

The diffraction pattern is recorded using a diffractometer. A standard X-ray diffractometer consists of:

- An X-ray generator with a beam collimator and monochromator.
- A goniometer head on which the crystal is mounted and which allows the crystal to be positioned accurately.
- 2 to 4 circles (depending on the individual diffractometer set up and geometry) these allow the crystal to be rotated bringing different parts of the diffraction pattern onto the detector.
- A beam stop to absorb the direct beam.
- A detector to measure the diffraction peaks, there are two main types of detector – point detector and area detectors.

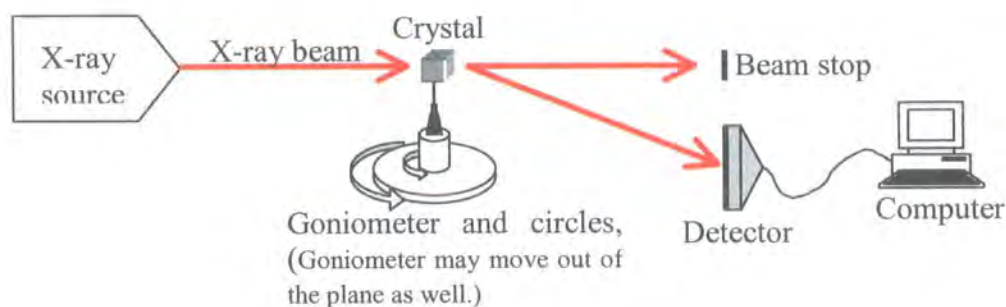


Figure 2.7: The basic diffractometer set up.

Detectors

There are 2 main types of detector in common use in the laboratory, the point detector and the area detector:

Point detectors simply record the diffracted radiation at a single point. They measure each reflection individually. They can give very accurate data but they are relatively slow, this can give problems if the crystal is sensitive to X-rays and begins to decay during the experiment. Also, each reflections position in laboratory space must be known so it can be found and recorded, so, before the data collection can begin, the position of each expected reflection must be calculated, this requires accurate cell measurement at the start of the experiment. If the cell is not identified correctly, for instance in the case of pseudo symmetry, then not all the data needed to solve the structure will be collected.

An area detector is, effectively, a sophisticated electronic substitute for the photographic paper used in the original diffraction experiments. The positions and intensities of a large number of peaks can be measured simultaneously, greatly reducing the data collection time. The whole of diffraction space can be covered and data collected regardless of whether a diffraction peak is expected at that point or not, so if the cell was identified wrongly, the data are available to correct the error, and other effects such as diffuse scattering can be spotted easily. The area detector reduces the amount of movement of the crystal needed to bring every spot onto the detector. In effect the χ – circle is not required.

For the experiments discussed in this work three very different types of diffractometer have been used:

The RIGAKU AFC6S

The RIGAKU 4 circle diffractometer²⁷ has a point detector. The crystal can be rotated to almost any given orientation by movement of three different angles:

- ϕ - rotates the crystal on the goniometer head,
- χ - rotates the goniometer head about a vertical circle,
- ω - rotates the χ circle with respect to the X-ray beam,

which together with 2θ , the circle that carries the detector and allows the detector to move relative to the incident X-ray beam, give the four circles of the machine's name.

The use of the four circle geometry means that any diffraction peak can be brought to lie on the point detector and hence recorded. At the start of the experiment the detector scans through a zig-zag pattern and records the first ten peaks found randomly. The recorded angles of these peaks are used to determine the unit cell, this is then checked against the next ten peaks found. This information is enough to allow the orientation matrix to be determined and therefore the positions of the rest of the peaks calculated, the crystal and detector can then be driven to the correct orientation to allow individual measurement of each peak in the main data collection.

The Rigaku diffractometer used in the experiments discussed here has an X-ray tube with a copper target providing X-rays with a mean wavelength of 1.54178\AA . Copper radiation has the advantage of being relatively intense, but also has disadvantages such as strong absorption by the heavier elements.

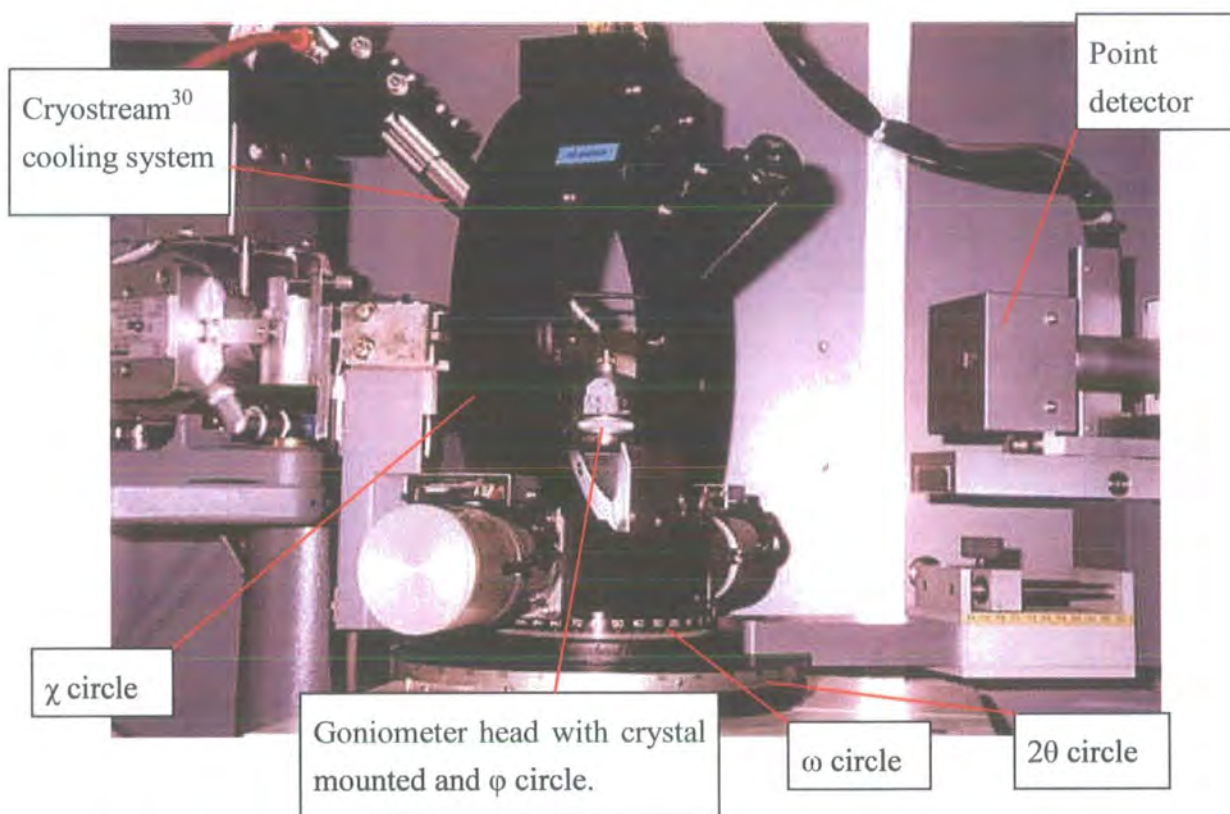


Figure 2.8: The Rigaku AFC6S diffractometer.

The SMART

The SMART-1000 (Siemens SMART Version 4.050 (Siemens Analytical X-ray Instruments, 1995))²⁸ is a newer machine than the Rigaku and has an 'area detector'.

The Smart diffractometer used in the experiments discussed here has an X-ray tube with a molybdenum target providing X-rays with a mean wavelength of 0.71073\AA . Molybdenum radiation is better for the heavier elements since it does not have the absorption problems of Cu radiation, and the shorter wavelength can give rise to higher resolution data.

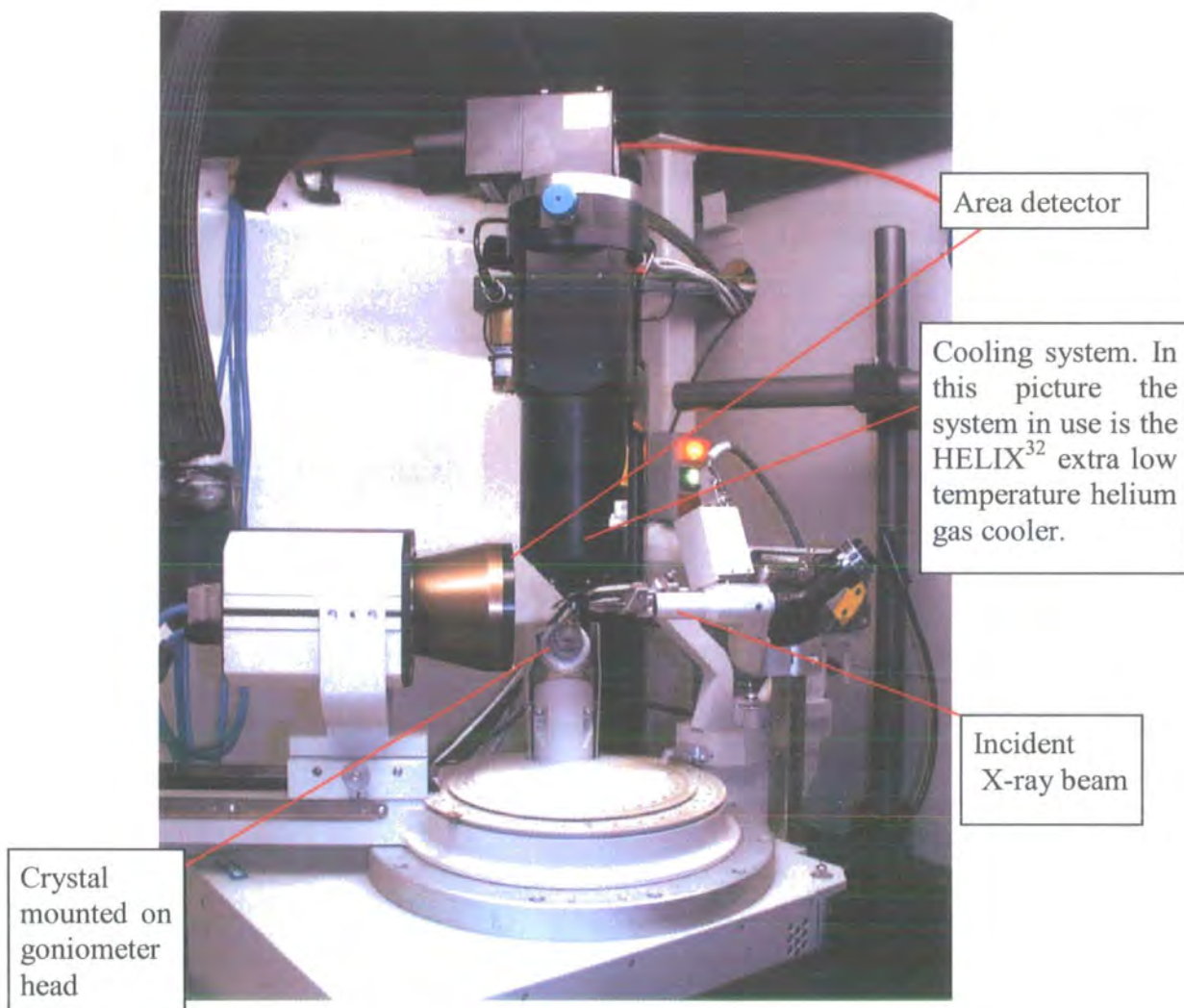


Figure 2.9: The SMART diffractometer.

SXD – Single Crystal Neutron Diffractometer

For the neutron diffraction experiments the diffractometer used was SXD at ISIS²⁹. SXD has a geometry that is similar to that of the SMART-CCD and has 3 large area detectors (currently being upgraded to 11 slightly smaller detectors to give full coverage of reciprocal space) around the crystal allowing many data to be collected simultaneously. Unlike all the other machines described above that rely on a beam of monochromatic radiation, SXD is a time of flight machine. The crystal is subjected to a pulse of white radiation (i.e. a wide range of wave lengths) the arrival time of each

neutron at the detector is directly related to its wavelength. This adds an extra dimension to the data, each peak is defined in terms of position, intensity and wavelength as usual, except the wavelength is now a variable giving access to more of reciprocal space in each frame of data recorded. All SXD experiments were carried out in collaboration with Dr C.C.Wilson and Dr D.Keen.

Set-up of the experiments

The crystals for X-ray experiments were either mounted on a glass fibre or a hair using either 'Araldite' epoxy resin, or a drop of oil (standard motor oil) frozen solid in the cold gas stream, to hold the crystal firmly in place.

A suitable crystal was chosen: a suitable crystal is a single crystal, one that is not twinned, cracked or split. This can be checked by rotating the crystal while viewing, using a microscope, under two, crossed, polarising filters; the crystal should undergo sharp uniform extinction. In many cases it is possible to solve data from a twinned crystal, but the results are rarely as good as would be obtained from a single crystal.

The X-ray beam used was collimated to approximately 0.8mm in diameter on both machines. The crystal had to be in the very centre of the beam where the X-ray intensity was expected to be uniform, therefore a crystal of less than 0.5 mm in any dimension was used. If the crystal was too big, it was cut to size using a very sharp razor blade.

For a neutron experiment the crystal needs to be much larger, in the order of several mm³. Obtaining crystals of this size is often the limiting factor in a neutron experiment. The crystals were mounted by attaching them using a small strip of aluminium tape onto the tip of an aluminium pin.

If possible the crystal should be approximately equal size in all directions, particularly since the incident X-ray beam undergoes absorption by the crystal, which depends on the path length in the crystal. This absorption reduces the intensities recorded such that:²²⁻²⁵

$$I = I_0 e^{-\mu t}$$

where: I = intensity of the X-rays recorded

I_0 = intensity of incident beam

μ = linear absorption coefficient dependent
on the crystal

t = path length of beam through crystal

The error due to absorption can be modelled and the data adjusted to correct for the effects of X-ray or neutron absorption.

The Cooling systems

Cooling the crystal often leads to improved results since when the atoms are vibrating less, the atomic positions can be better defined and give rise to higher intensity data. The cooling system on both X-ray diffractometers was the Oxford Cryosystem Cold N₂ gas cooler³⁰. This uses a stream of cold nitrogen gas flowing over the crystal to cool it. Using a nitrogen cryostream the crystal can be cooled down to temperatures as low as 90K, however good temperature stability is rarely achieved below 100K.

The cooling system on the neutron diffractometer was a Displex system³¹. This uses a closed cycle refrigerating system to cool, by conduction, the metal pin on which the crystal is mounted, which means that the crystal is also cooled down to the same temperature. The pin and crystal are enclosed inside a metal can, under a vacuum. This can means that centering the crystal can be a problem, and flash cooling is not possible, however the Displex can cool crystals down to temperatures as low as 9K.

The HELIX cryosystem³² is an attempt to combine the ease of use of the cryostream with the greater temperature range of the Displex. The HELIX uses a Displex like refrigerating system to cool a stream of helium gas which then, like the cryostream system flows over the crystal to cool it. The HELIX can reach temperatures as low as 25K.

In all the experiments described here the data were integrated using the SAINT+ NT program³³, the data prepared using the XPREP program³⁴ the initial trial structure was determined using the SHELXS-97 (Sheldrick, 1990)³⁴ and the refinement carried out using the SHELXL-97 (Sheldrick, 1997)³⁴, the molecular graphics were generated using SHELXTL (Sheldrick, 1998)³⁴.

2.5 Interpretation of the Results

It is very important to remember that the final structural solution is still only a model. The accuracy of the model is given by the R1 and wR2 values, which give an indication of how similar the structure factors calculated from the model (F_c) are to the experimentally derived structure factors (F_o), more precisely:

$$R1 = \Sigma | |F_o| - |F_c| | / \Sigma |F_o|$$

and

$$wR2 = \{ \Sigma [w(F_o^2 - F_c^2)^2] / \Sigma [w(F_o^2)^2] \}^{1/2}$$

It is always important to think about how these values are obtained. For a compound where most of the X-ray diffraction is arising from a heavy metal atom, which is well defined in the model, good R1 and wR2 values may be obtained despite the fact the lighter atoms are only poorly defined. The use of restraints and constraints can help to force the model to take a more chemically and physically logical form, usually with very little effect on the accuracy of fit to the experimental data. However, care must always be taken not to force the model to take some preconceived form that is not accounted for in the data.

2.6 The Cambridge Structural Database

Of all the various databases of structural information available, the Cambridge Structural Database⁶ is the most suitable for wide ranging searches of intra and intermolecular geometry.

The database aims to contain information from of every published structure, the information is usually obtained from the CIF³⁵ file. The current release has well over 245,000 entries. For each entry various levels of information are available, from publication data, text such as chemical name and formula, cell size, experimental information, to 2-D structural diagrams and, wherever available, the 3-D crystallographic model.

A search can be carried out using the 'Quest' search program which allows a search or combination of searches to be carried out on any or all of these levels. For searches involving numerical output such as intra and inter-atomic distances and angles etc. the statistical program 'Vista' can be used to analyse the data and generate graphics. Very complicated analyses may require the data to be exported to other packages such as the SPSS program Sigmaplot³⁶.

2.7 References for Introduction

- 1) C.B.Aakeroy. *Acta Cryst.*, 1997, **B53**, 569-586.
- 2) D.Braga, F.Grepioni, A.G.Orpen. *Crystal Engineering: From Molecules and Crystals to Materials*. Netherlands: Kluwer Academic Publications, 1999.
- 3) C.B.Aakeroy, K.R.Seddon, *Chem. Soc. Rev.*, 1993, 397-407.
- 4) F.H.Allen, O.Kennard. R.Taylor. *Acc. Chem. Res.*, 1983, **16**, 146-153.
- 5) A.Nangia. *Cryst. Eng. Comm.*, 2002, **17**, 1-18.
- 6) F.H.Allen, O.Kennard. *Chem. Des. Autom. News*, 1993, **8**, 30-37.
- 7) W.C.Hamilton, J.A.Ibers. *Hydrogen Bonding in Solids*. New York: W.A.Benjamin, Inc., 1968.
- 8) J.C.Speakman. *The Hydrogen Bond and Other Intermolecular Forces*. London: The Chemical Society, 1975.
- 9) G.A.Jeffrey. *An Introduction to Hydrogen Bonding*. New York: Oxford University Press, 1997.
- 10) G.R.Desiraju, T.Steiner, *The Weak Hydrogen Bond in Structural Chemistry and Biology*. New York, Oxford: Oxford University Press, 1999.
- 11) I.Alkorta, I.Rozas, J.Elguero. *Chem. Soc. Rev.*, 1998, **27**, 163-170.
- 12) J.Emsley. *Chem. Soc. Rev.*, 1980, **9**, 91-93.
- 13) C.A.Hunter, J.K.M.Sanders, *J. Am. Chem. Soc.*, 1990, **112**, 5525-5534.
- 14) C.A.Hunter, K.R.Lawson, J.Perkins, C.J.Urch. *J. Chem. Soc., Perkin Trans. 2*, 2001, 651-669.
- 15) G.R.Desiraju, R.Parthasarathy. *J. Am. Chem. Soc.*, 1989, **111**, 8725-8726.
- 16) V.R.Pedireddi, D.S.Reddy, B.S.Goud, D.C.Craig, A.D.Rae, G.R.Desiraju. *J. Chem. Soc. Perkin Trans., 2*, 1994, 2353-2360.
- 17) I.C.Hayes, A.J.Stone. *Mol. Phys.*, 1984, **53**, 83-105.
- 18) S.L.Price, A.J.Stone, J.Lucas, R.S.Rowland, A.E.Thornley. *J. Am. Chem. Soc.*, 1994, **116**, 4910-4918.
- 19) J.P.M.Lommerse, A.J.Stone, R.Taylor, F.H.Allen, *J. Am. Chem. Soc.*, 1996, **118**, 3108-3116.
- 20) W.L.Bragg. *Proc. Camb. Phil. Soc.*, 1913, **17**, 43-57.
- 21) a) H.Lipsom, C.A.Taylor. *Fourier Transforms and X-Ray Diffraction*. London: G.Bell and Sons Ltd. 1958. b) Notes from: The Seventh BCA Intensive Teaching School in X-Ray Structure Analysis. University of Durham. April 7th –15th, 1999.

- 22) J. P. Glusker, K. N. Trueblood. *Crystal Structure Analysis, A Primer*. New York, Oxford: Oxford University Press. 1985.
- 23) J. P. Glusker, M. Lewis, M. Rossi. *Crystal Structure Analysis for Chemists and Biologists*. New York, Wienheim, Cambridge: VCH Publishers. 1994.
- 24) HERCULES course notes: J.Baruchel, J.L.Hodeau, M.S.Lehmann, J.R.Regnard, C.Schlenker eds. *Neutron and Synchrotron Radiation for Condensed Matter Studies, vol. I and II*. France: Les Editions De Physique, Berlin: Springer-Verlag, 1993.
- 25) C. Giacovazzo, ed. *Fundamentals of Crystallography*. New York, Oxford: International Union of Crystallography, Oxford University Press, 1992.
- 26) C.C.Wilson. *Single Crystal Neutron Diffraction From Molecular Materials*. Singapore: World Scientific. 2000.
- 27) a) MSC/AFC. Molecular Structure Corporation (1991). b) Molecular Structure Corporation (1991). MSC/AFC Diffractometer Control Software. (1991). MSC, 3200 Research Forest Drive, Woodlands, TX77381, U.S.A.
- 28) SMART-1000 CCD, Bruker AXS, Madison, Wisconsin, U.S.A.
- 29) ISIS Facility, Rutherford Appleton Laboratories, Chilton, Oxon, OX11 0QX.
- 30) Cryostream Cooler, Oxford Cryosystems Ltd, Oxford, UK.
- 31) J.M.Archer, M.S.Lehmann, *J. Appl. Cryst.*, 1986, **19**, 456-458.
- 32) Oxford HeliX. Oxford Cryosystems Ltd, Oxford, U.K.
- 33) SAINTPLUS Version 6.02. Bruker AXS., Madison, Wisconsin, U.S.A.
- 34) G.M. Sheldrick, (1997). SHELXS-97, SHELXL 97. Program for the Refinement of Crystal Structures. University of Göttingen, Germany. G. M. Sheldrick, (1998). SHELXTL Version 5.1. Bruker AXS., Madison, Wisconsin, U.S.A.
- 35) S.R.Hall, F.H.Allen, I.D.Brown. *Acta Cryst. (A)*, 1991, **A47**, 655-685.
- 36) SigmaPlot 2000, SPSS Inc, Chicago, U.S.A.

Part 1:

Bi-Furcated Hydrogen Bonds

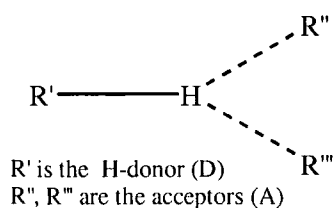
Chapter 3 : Furcation in Hydrogen Bonds

3.1 Introduction

An n-furcated hydrogen bond is one where the hydrogen donor or acceptor is simultaneously involved in more than one hydrogen bond. Such systems are sometimes referred to as 'multi-centred hydrogen bonds' or even 'chelated hydrogen bonds'. Bi-furcated hydrogen bond motifs are found in both small molecule crystal structures, and in protein structures^{1,2}, and can be seen to play an important role in both. It has been suggested that in certain types of structure such as carbohydrates, nucleosides and nucleotides, where the number of hydrogen bond acceptors exceeds the number of hydrogen bond donors, up to a quarter of all the hydrogen bonds are bi-furcated¹.

Although there are well documented examples of individual cases of crystal structures in which such systems appear^{3,4,5}, and even some detailed analysis of specific types of bi-furcated hydrogen bond motifs^{6,7,8}, there is very little systematic knowledge about these systems.

Bi-furcation of the donor:



Bi-furcation of the acceptor:

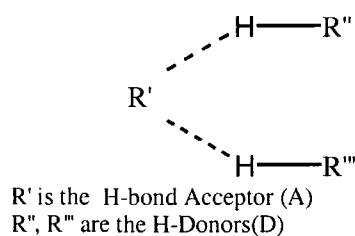


Figure 3.1: The bi-furcation motif.

3.2 Bi-Furcated Hydrogen Bonds

Here a survey of n-furcated donor systems found in the Cambridge Structural Database⁹ has been carried out and a detailed study made of bi-furcation of hydrogen donor systems where the donor is oxygen or nitrogen. The aim being to try and establish some of the parameters of the system, from simple frequency of occurrence information, to detailed geometric parameters.

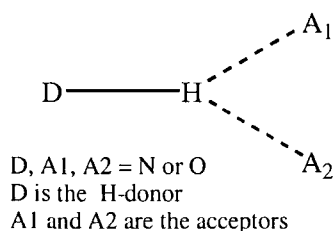


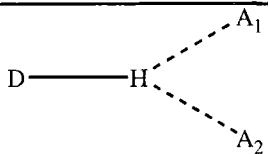
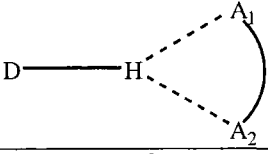
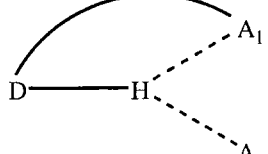
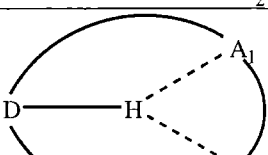
Figure 3.2: Schematic of a bi-furcated hydrogen bond.

There are many interesting questions that could be asked when trying to establish patterns and parameters within the data. The main questions that are considered here are; what are the effects of the different H-donor atoms (i.e. oxygen and nitrogen) on the frequency of occurrence and the system geometry, and does whether the hydrogen bonds are intra or inter molecular have an effect on the frequency of occurrence and on the system geometry.

For the first question the data can be considered in 3 different groups:

- a) All the data, i.e. where the H-donor atom is either nitrogen or oxygen.
- b) Where the H-donor atom is nitrogen.
- c) Where the H-donor atom oxygen.

To answer the second question the data must be classified into the following systems depending on whether the various relationship between the hydrogen donor, D, and the acceptor molecules, A₁ and A₂, are intra molecular or inter molecular:

Case I)	D-A ₁ =Inter, D-A ₂ =Inter and A ₁ -A ₂ =Inter (hydrogen bonds occur between 3 molecules).	
Case II)	D-A ₁ =Inter, D-A ₂ =Inter and A ₁ -A ₂ =Intra (hydrogen bonds occur within and between 2 molecules)	
Case III)	D-A ₁ =Intra, D-A ₂ =Inter (hydrogen bonds occur within and between 2 molecules)	
Case IV)	D-A ₁ =Intra, D-A ₂ =Intra (both hydrogen bonds occur within 1 molecule)	

Case I, where the donor and both acceptors are all from different molecules, can be considered as the most general case, since, as far as is possible, there are no pre-imposed geometric restraints. Case IV is the most restrained case, and it might be expected that the occurrences and geometry of this case will be very dependent on the particular molecule type.

3.3 Experimental

Hydrogen bonded systems with a bi-furcated donor were studied. To simplify the analysis, all systems where the n-furcation is greater than two, i.e. tri-furcated, tetra-furcated, etc. have been removed from the data sets.

In all cases, the October 1999 release of the Cambridge Structural Database⁹ (207506 entries) was searched.

The search routine was carried out using the program Quest3D, using non-bonded contact criteria of H...A distance limit of 2.6Å, this is the same limit used in a study on bi-furcated hydrogen bonds of the type where one bond is intramolecular, that was carried out as part of a wider study of intramolecular hydrogen bonded motifs by Bilton *et al.*¹⁰. This limit was chosen after careful examination of histograms of intra and inter N/O-H...N/O hydrogen bond distances^{10,11,9}. When this limit was extended the results

obtained did not alter. Graphs were produced using the CSD program Vista and the SPSS program SigmaPlot¹².

Only organic structures with an R factor $\leq 7.5\%$, that exhibit no disorder, are not polymers, that are error free at 0.05\AA level, have 3-D coordinates, and have chem/cryst connectivities which match, were accepted. All hydrogen atom positions were recalculated to give neutron-normalized positions.

For the analysis, the two hydrogen bonds were distinguished from each other by length and separated into a shorter (S) and a longer (L) bond. Thus the bonds lengths are tabulated as dL and dS and the corresponding angles as aL and aS. The distance and the angle between the two acceptor molecules, A_1 and A_2 , are designated d3 and A3 respectively. DP is the perpendicular distance of the hydrogen atom out of the donor/acceptor plane. In the cases where the hydrogen bonds are intramolecular or the A_1 and A_2 are part of the same molecule, the number of covalent bonds between the intramolecular link is given by the path length:

- Path1 is the number of covalent bonds between the hydrogen and A_1 the acceptor of the longer hydrogen bond.
- Path2 is the number of covalent bonds between the hydrogen and A_2 the acceptor of the shorter hydrogen bond.
- Path3 is the number of covalent bonds between A_1 and A_2 the two acceptor atoms.

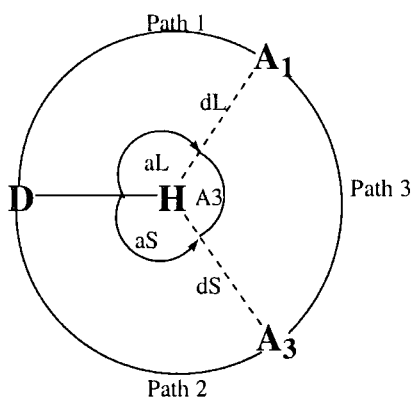


Figure 3.3: A scheme to define the angles, distances analysed in the bi-furcated systems.

3.4 Clusters and Unavoidable Bias Within the CSD

In the following cases (especially in case IV) peaks and clusters in the data are often seen superimposed on the distribution seen for the general case. Closer analysis often revealed these clusters to be groups of chemically similar molecules. Certainly, the parts of the molecules related to the bi-furcated moiety were often identical within a data cluster. This is an example of the kind of bias that can occur even within as large a data set as is found in the CSD; where a family of molecules is of particular interest, or is especially easy to crystallise, and therefore extensively studied, many occurrences may be found within the database. Alternatively, a family of compounds that is very hard to make or crystallise may have relatively few entries in the database. It is worth remembering that the CSD is not a database of all possible compounds but only those deemed worthy of study or where study has been possible. Thus bias will occur within the data and needs to be allowed for.

Chapter 4 : Bi-Furcated Hydrogen Bonds

4.1 Frequency of Occurrence

A simple way to establish an idea of how important an interaction is, as well as to get a general feel for the factors that influence the interaction, is to look at the simple statistics of how often the interaction occurred i.e. the frequency of occurrence. For instance:

Is the donor atom more likely to be oxygen or nitrogen and in what type of situations is one type of donor found more commonly than the other?

Given that one intra molecular hydrogen bond is found, what is the frequency with which a second intra molecular hydrogen bond is found from the same hydrogen donor?

The frequencies of occurrence for the different types of bi-furcated hydrogen bonds are given in the tables below. The data is given as the number of occurrences of each type (in terms of donor atom and intra- and intermolecular hydrogen bonds) of bi-furcated hydrogen bonds, and what percentage this is of the total number of hydrogen bonds of this type found in the database (i.e. the total number of mono and bi-furcated hydrogen bonds. Tri-furcated systems and above have been excluded). This percentage gives a better indication of what is the likelihood of a bi-furcated bond forming, given that one hydrogen bond at least is found.

In the tables below there is one slightly strange artefact of the analysis method used, this is that the percentage of hydrogen bonds which fit the case III motif (i.e. one intra- and one intermolecular hydrogen bond) varies depending on whether they are considered in relation to the total number of intra- or the total number of intermolecular hydrogen bonds. That is to say, the probability of an intramolecular hydrogen bond being found given that an intermolecular hydrogen bond has been found is different to the probability of an intermolecular hydrogen bond being found given that an intramolecular hydrogen bond has been found.

The results for these questions are given in the following tables:

Donor atom = Nitrogen or Oxygen Acceptor atoms = Nitrogen or Oxygen	
Total no of mono-, and above, furcated hydrogen bonds	74505
Total no of bi-, and above, furcated hydrogen bonds	12857
Total no of tri-, and above, furcated hydrogen bonds	1097

Table 4.1: Overall statistics of the furcation of hydrogen bonds in CSD.

Donor atom = Nitrogen or Oxygen Acceptor atoms = Nitrogen or Oxygen				
Total no of hydrogen bonds (mono- or bi-furcated)	Intra = 12190		Inter = 48258	
Hydrogen bond A Hydrogen bond B	Intra		Inter	
Intra	1260	10.3%	4503	9.3%
Inter (acceptors on same molecule)	~		2218	4.6%
Inter (acceptors on different molecule)	4503	36.9%	958	2.0%

Table 4.2: Hydrogen bond frequencies for case I (inter:inter), case II (inter:inter A-A intra), case III (inter:intra) and case IV (intra:intra) for all the data.

Donor atom = Nitrogen Acceptor atoms = Nitrogen or Oxygen				
Total no of hydrogen bonds (mono- or bi-furcated)	Intra = 6652		Inter = 22087	
Hydrogen bond A Hydrogen bond B	Intra		Inter	
Intra	972	14.6%	2274	10.3%
Inter (acceptors on same molecule)	~		1147	5.2%
Inter (acceptors on different molecule)	2274	34.2%	590	2.7%

Table 4.3: Hydrogen bond frequencies for case I (inter:inter), case II (inter:inter A-A intra), case III (inter:intra) and case IV (intra:intra) for nitrogen as donor atom.

Donor atom = Oxygen				
Acceptor atoms = Nitrogen or Oxygen				
Total no of hydrogen bonds (mono- or bi-furcated)	Intra = 5538		Inter = 26171	
Hydrogen bond A Hydrogen bond B	Intra		Inter	
Intra	288	5.2%	2229	8.5%
Inter (acceptors on same molecule)	~		1071	4.1%
Inter (acceptors on different molecule)	2229	40.2%	368	1.4%

Table 4.4: Hydrogen bond frequencies for case I (inter:inter), case II (inter:inter A-A intra), case III (inter:intra) and case IV (intra:intra) for oxygen as donor atom.

The first important fact to note is that, overall, n-furcation is more common than might be expected given the rarity with which such interactions are identified and discussed in the literature. As can be seen from Table 4.1 around 20% of all hydrogen bonds are furcated*.

It can be seen that nearly the same trends are followed by both the nitrogen and the oxygen donors. In all cases where there is at least one inter hydrogen bond case III (the inter:intra case) is the most common, then case II (inter:inter, acceptor on the same molecule), then case I (inter:inter, acceptors on different molecules).

The notable difference between the nitrogen and oxygen cases occurs in the frequency of occurrence of case IV (the intra:intra case), there are many more examples of intra:intra bi-furcated hydrogen bonds when nitrogen is the hydrogen donor than when oxygen is the hydrogen donor. As will be seen later in Chapter 8, a large proportion of the intra:intra bi-furcated hydrogen bonded systems occur within peptide chains where the donor atom is nitrogen. This accounts for the greater proportion of donor N than donor O in the [intra:intra] case.

So in answer to the first question asked at the beginning of the chapter (namely is the donor atom more likely to be oxygen or nitrogen and in what type of situations is one

* Note: In the general statistics a simple count of bonds has been carried out, i.e. all bi-furcated systems contribute two hydrogen bonds each to the count of 'Total number of mono-, and above, furcated H-bonds'. Similarly all trifurcated systems contribute three bonds to the count of 'Total number of mono- and above, furcated H-bonds', and two bi-furcated motif counts to the 'Total number of bi- and above, furcated H-bonds'.

type of donor found more commonly than the other.) it can be seen that the identity of the hydrogen donor atom (within the bounds of this data set) has very little influence on the frequency of occurrence. Bi-furcated hydrogen bonds are almost equally likely for systems with an oxygen donor as for those with a nitrogen donor atom.

Chapter 5 : Case I, the General Case

Case I, where the donor (D) and both acceptors (A_1 , A_2) are from different molecules, can be taken to be the most general case, since, as far as is possible, there are no pre-imposed geometric restraints such as would be found in an intramolecular case where two or more of the H-donor/acceptors are constrained by their positions within the same molecule.

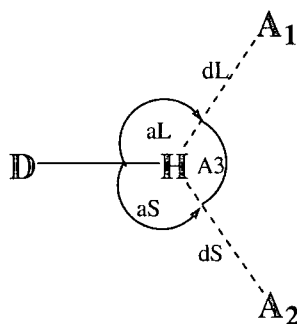
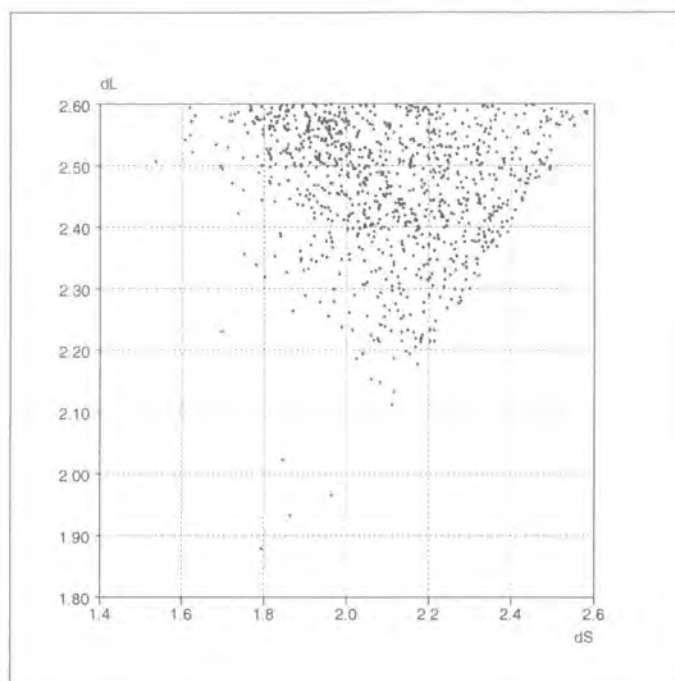


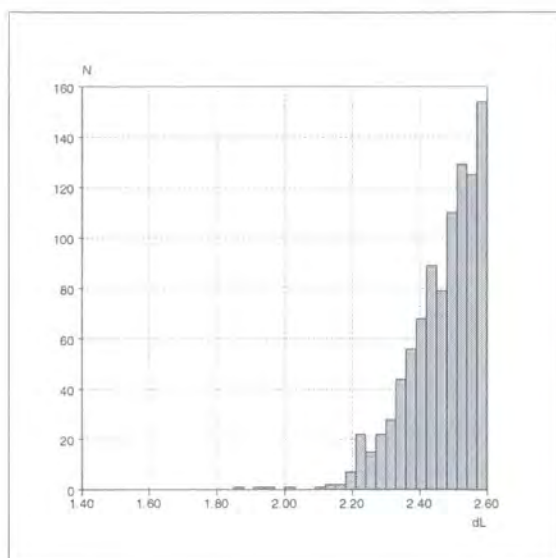
Figure 5.1: Scheme to define angles and distances for the case I motif.

Interestingly, there are very few symmetrically bi-furcated hydrogen bonds. Instead, the system tends to consist of one shorter and more linear bond (S) and another longer bond with an angle tending to 120° (L). In Graph 5.1 and later in Graph 5.6 symmetric bonds would lie on the diagonal line described by the equation $x=y$. By definition dS is shorter than dL so all the data points in Graph 5.1 must lie on or above the $x=y$ line.

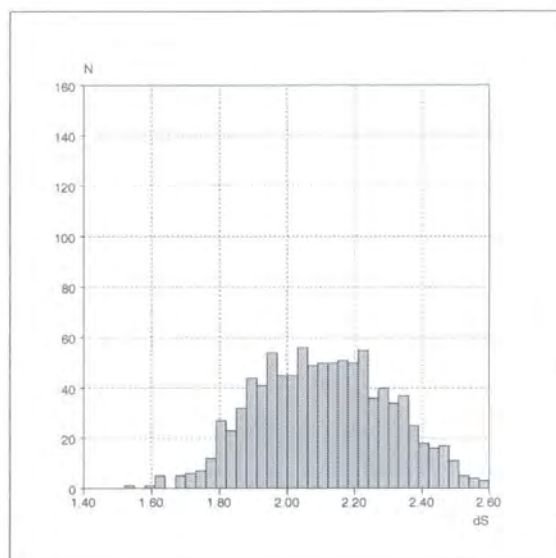


Graph 5.1: dS (\AA) versus dL (\AA) for case I all data.

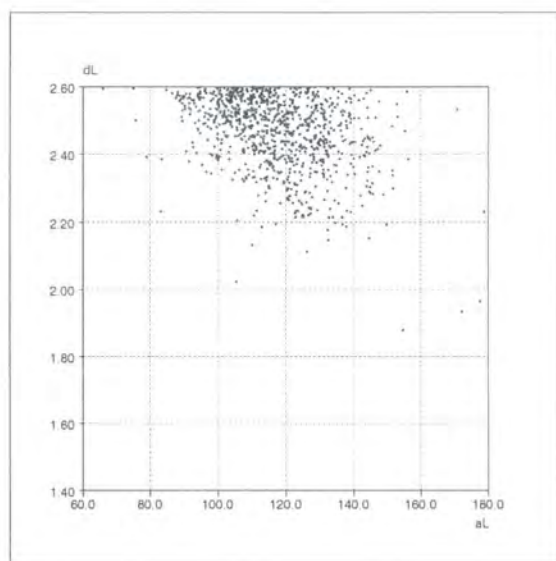
In most cases the bonds can be considered as a primary interaction (S) that exhibits all the usual patterns associated with a hydrogen bond, with the shorter/stronger bonds tending towards linearity, and the longer bonds being less linear. The familiar patterns can be seen in Graph 5.5. The secondary interaction (L) is still a hydrogen bond in its own right but loses out to the primary interaction in terms of geometry, the usual pattern is no longer seen in the distance versus angle plot, the length/angle correlations is much less evident and it can be seen that the limit of 2.6\AA is an arbitrary cut off point of this interaction. See Graph 5.4 for geometry of L and Graph 5.1 and Graph 5.6 for relationship between S and L.



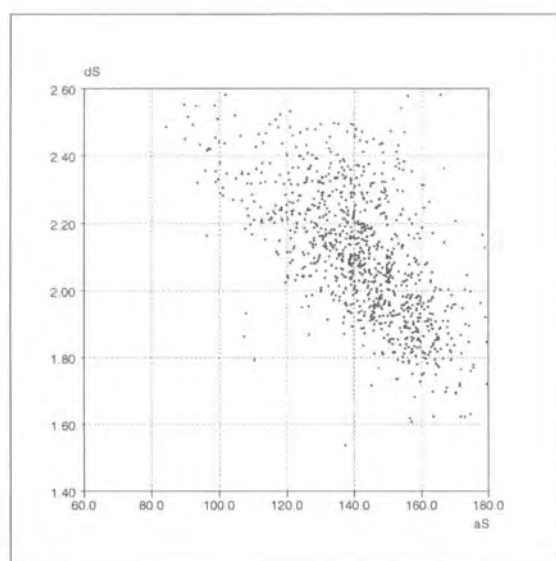
Graph 5.2: dL (Å) for all data.



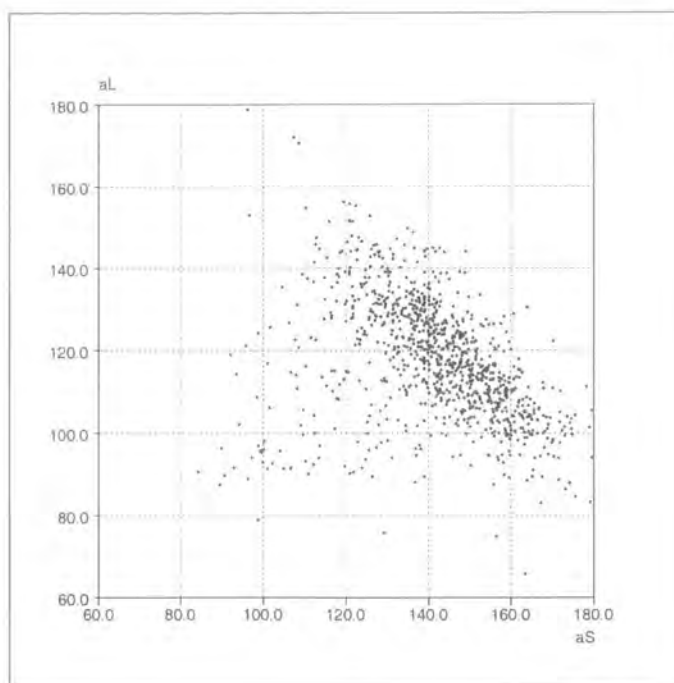
Graph 5.3: dS (Å) for all data.



Graph 5.4: dL (Å) versus aL (°) for case I all data.



Graph 5.5: dS (Å) versus aS (°) for case I all data.



Graph 5.6: aL ($^{\circ}$) versus aS ($^{\circ}$) for case I all data.

In Graph 5.6 it can be seen that there is a correlation between the angles aS and aL , with a large angle aS generally corresponding to a small angle aL and vice versa. This can be attributed to acceptor-acceptor repulsion, i.e. there is a minimum distance (and therefore angle) between the acceptors. It is worth noting from construction in Figure 5.1 that for a planar system:

$$aS + aL + A3 = 360$$

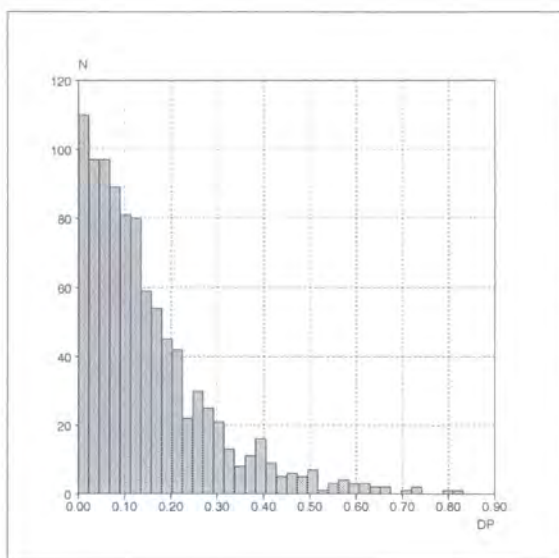
so

$$aS + aL = 360 - A3$$

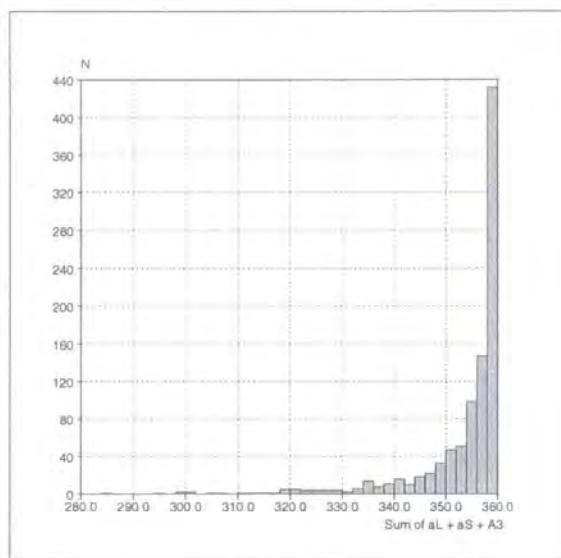
where $A3$ is the angle between the acceptors.

This point is further confirmed by the fact that there are no data points where $aS + aL > 295^{\circ}$ i.e. $A3 < 65^{\circ}$ (in fact the majority of the data lie below the $aS + aL = 275^{\circ}$) this corresponds to an acceptor-acceptor distance in a planar system of about 2.47\AA . Most systems are clustered around an optimum acceptor-acceptor angle ($A3$) of about 100° however some systems show much larger acceptor-acceptor angles.

All these hydrogen bond systems tend to be fairly planar though not necessarily completely flat, a plot of DP – the distance of the hydrogen from the donor acceptor plane (defined by D, A_1, A_2) is shown in Graph 5.7 and the sum of all the angles (assumed to sum to 360° in analysis above) in Graph 5.8.



Graph 5.7: Distance (Å) of hydrogen atom out of donor acceptor plane.

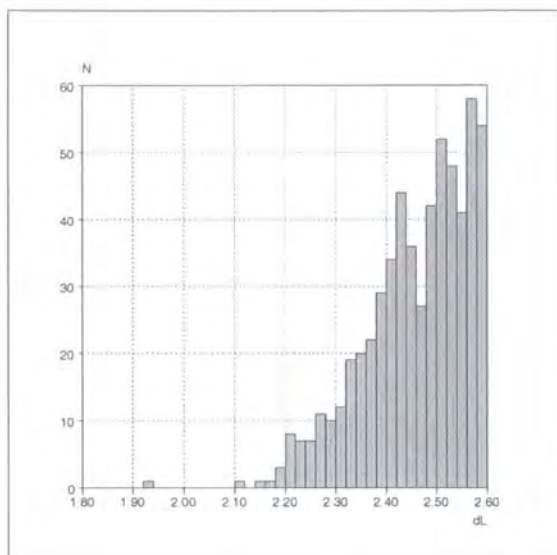


Graph 5.8: Sum of aS , aL and $A3$ angles ($^{\circ}$).

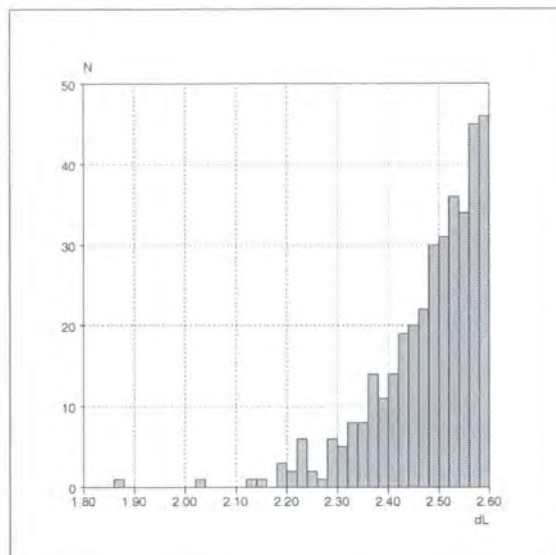
5.1 Differences Between Oxygen and Nitrogen as the Hydrogen Donor in the General Case (Case I)

There are some differences between the picture seen where oxygen is the hydrogen donor atom (D) and where nitrogen is the donor atom (D). As well as there being overall fewer occurrences of the case where $D=O$ there also tends to be a greater divergence within this data, indicating weaker correlations between dS and aS and aL and dL hydrogen bonds.

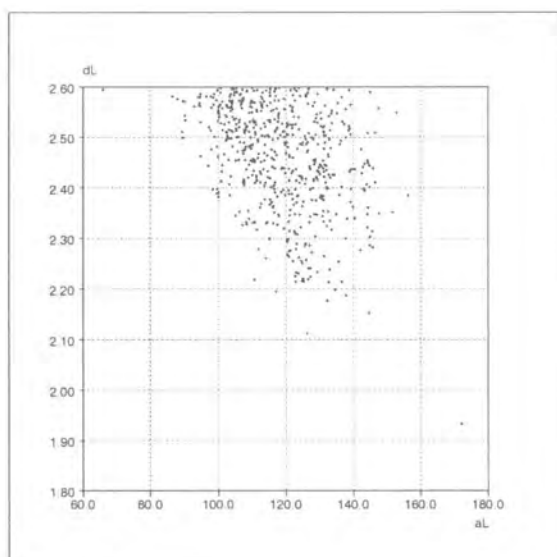
There are also slight differences in the data for the longer hydrogen bond dL (See Graph 5.9 and Graph 5.10 for the histograms of dL for $D=N$ and $D=O$ respectively). In the case where $D=O$ the graph shows a steady increase of frequency with length until the data cut off point (2.6\AA). In the case where $D=N$ the increase starts more sharply then appears to be steadying off. The apparent peak at 2.43\AA is a function of the bin size used rather than any real feature of the data.



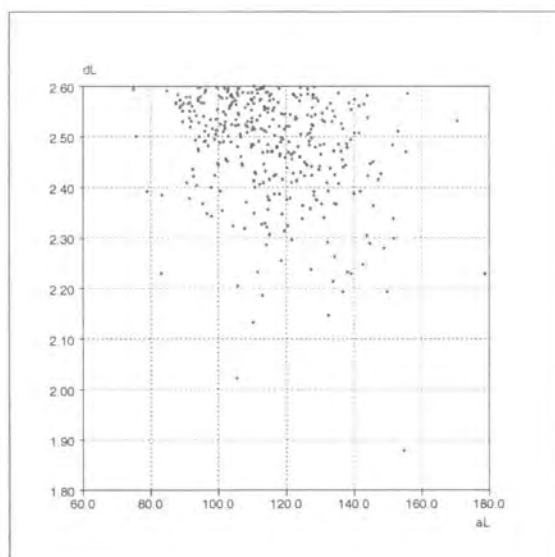
Graph 5.9: dL (Å) for case I where the hydrogen donor is nitrogen.



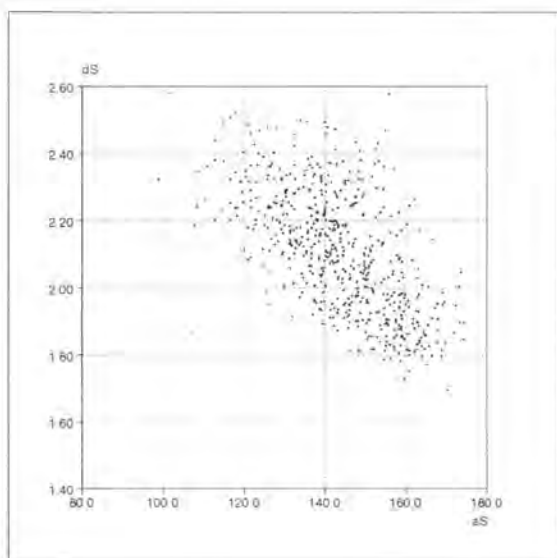
Graph 5.10: dL (Å) for case I where the hydrogen donor is oxygen.



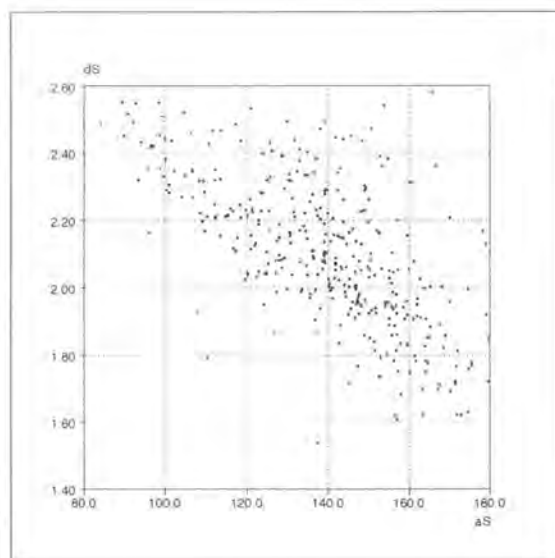
Graph 5.11: dL (Å) versus aL (°) for case I where the hydrogen donor is nitrogen.



Graph 5.12: dL (Å) versus aL (°) for case I where the hydrogen donor is oxygen.



Graph 5.13: dS (Å) versus aS ($^\circ$) for case I where the hydrogen donor is nitrogen.



Graph 5.14: dS (Å) versus aS ($^\circ$) for case I where the hydrogen donor is oxygen.

Once we start considering cases which diverge from the very general case I, i.e. cases where only one or two molecules are involved in the system and there are either intra hydrogen bonds or both acceptors come from the same molecule, then we immediately have another parameter to consider; that of path length between the donor and acceptor moieties ($D...A$) or acceptor-acceptor moieties (A_1-A_2). All, or nearly all of the variations from the distribution patterns seen for the general case I (above) are directly related to path length, since this provides an intramolecular constraint on the hydrogen bond geometry.

Chapter 6 : Case II, Where Both the Acceptors are Part of the Same Molecule

When considering the case where both acceptors are part of the same molecule (case II) there is an extra parameter that needs to be considered; the acceptor-acceptor path length, path 3. This parameter will be seen to have a very important impact on the system geometry.

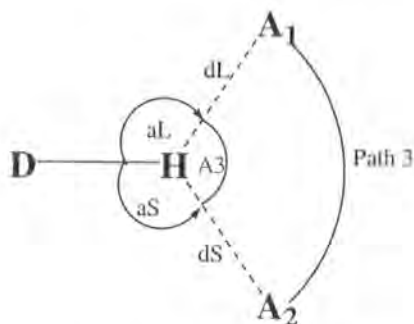


Figure 6.1: Scheme to define the angles and distances for the case II motif.

A---A Path Length (Path 3) as no. of Covalent Bonds	Frequency
1	208
2	783
3	904
4	254
5	55
6	8
7	2
8	2
9	0
10	2

Table 6.1: Number of occurrences of different numbers of bonds in Path 3.

There are very few examples with a long acceptor-acceptor path length, only 3% of all occurrences of case II have a path length greater than 4 bonds.

Can an acceptor-acceptor path length of 1 bond really count as a bi-furcated system? Probably not, the second acceptor position is far more constrained by the molecular geometry than it is ever going to be effected by the potential hydrogen bond. For instance, a short hydrogen bond to a nitrogen of a N=N group could easily bring the second nitrogen into close enough contact to the hydrogen donor to be categorized as a hydrogen bond by the criteria used in this study. However, for consistency, the data for path lengths of 1 has been included in this analysis.

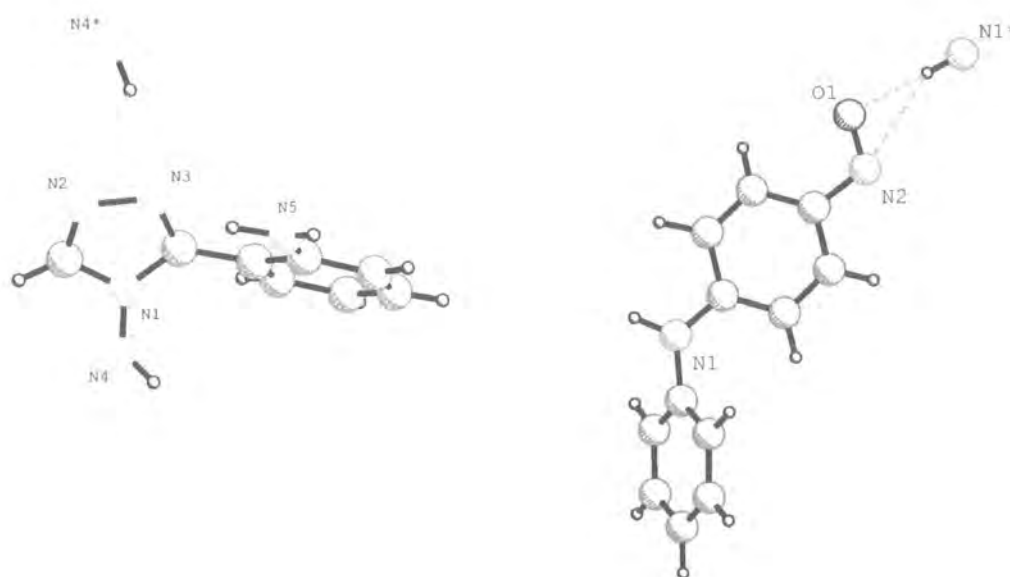
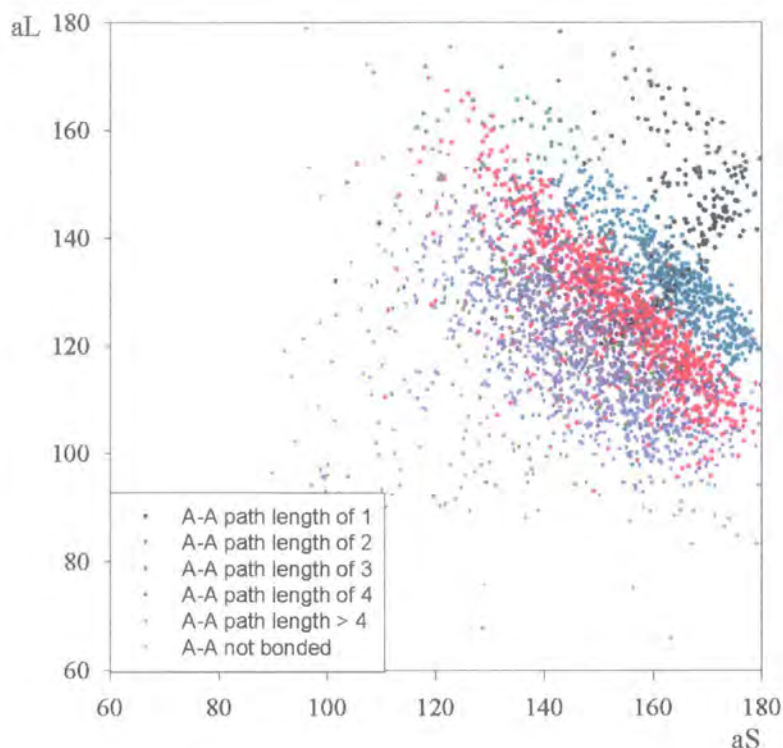


Figure 6.2: Two examples of case II bi-furcated hydrogen bond structures where the A...A path length is 1, examples have been taken from the CSD, ref codes AMAPTZ¹³ and VIDYOV¹⁴ (* indicates atom that is part of a symmetry generated molecule).



Graph 6.1: aL ($^{\circ}$) versus aS ($^{\circ}$) for case I and II, all data. Data coloured by acceptor-acceptor path lengths.

As in case I there is still a distinct preference for a non-symmetric geometry, this result has been studied in detail by Allen *et al.*⁶ and Gorbitz and Etter⁸, for the 'path length of 2' systems where the A-A moiety is the NO_2 group and the carboxylate group respectively.

In Graph 6.1 it can be seen that there is a strong correlation between the aL vs aS distribution and the acceptor-acceptor path length, as the path length decreases, the angles (both dS and dL) tend more towards 180° . This is logical; in case I it was seen that there is a preferred AHA angle ($A3$) corresponding to a preferred acceptor-acceptor distance. In this case (II) the acceptor-acceptor distance is restrained by the intramolecular path length between the acceptors. As the path length increases the distance between the acceptors increases, the hydrogen moves into the gap between the acceptors and the sum of aS and aL decreases (see Figure 6.3). Once the acceptor-acceptor path length becomes greater than 4, the angular distribution occupies the same region of the graph as the examples of case I (blue-grey in Graph 6.1) where the acceptor-acceptor path length could be considered as infinite.

For each A---A path length data set there is a cut off line at $aS + aL = 360 - x$, where x is a set constant value for each different path length and equal to the minimum possible

value of A_3 (i.e. the closest possible approach of the A_1 to A_2) given the path length restraints of the system.

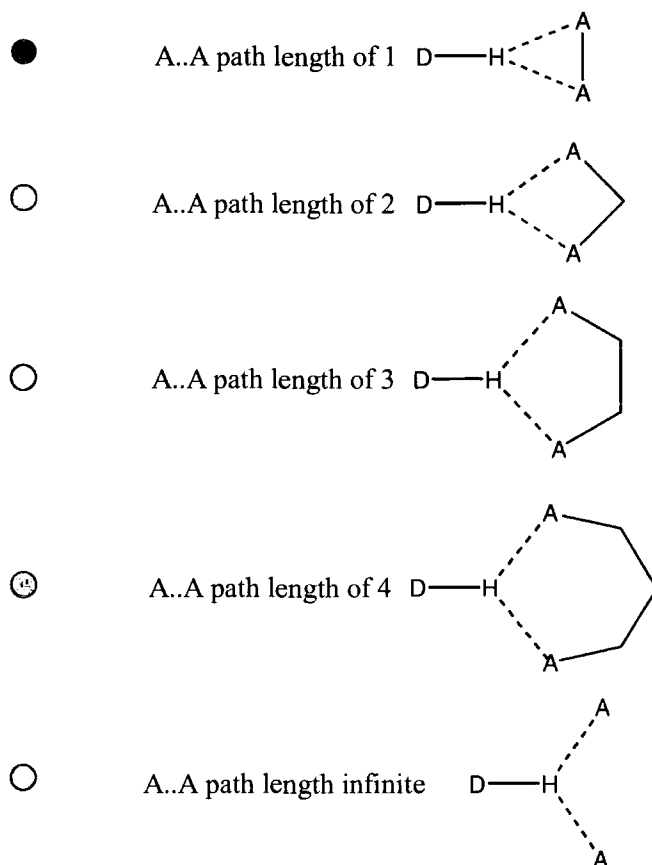


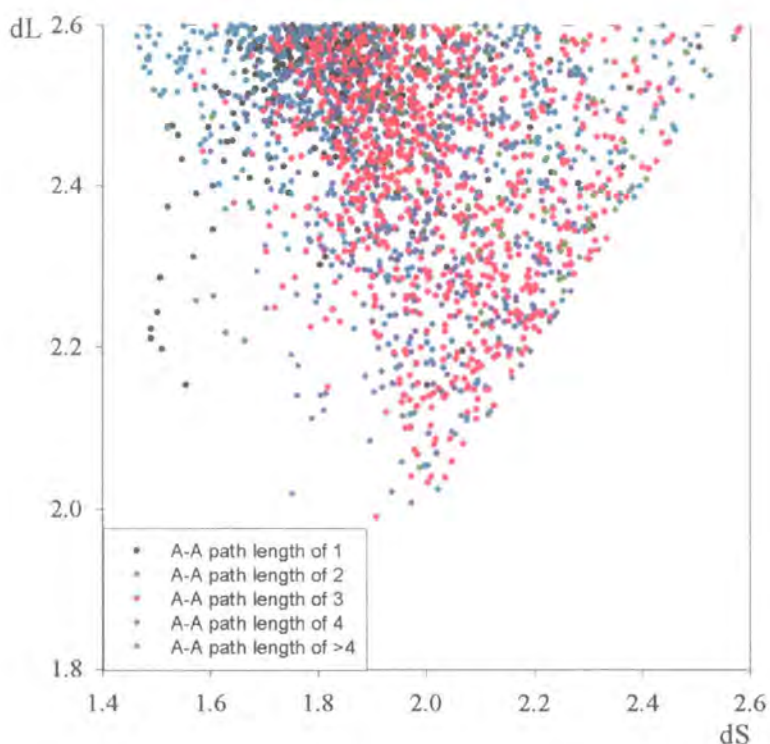
Figure 6.3: Increasing AHA and decreasing DHA angles with increasing acceptor-acceptor path length.

Only path lengths of 1 don't fit this analysis, some lie in the expected position where the sum of aS and aL equals $180-A_3$ (where A_3 is the AHA angle). Others lie on a line with a gradient in the opposite direction cutting through the rest of the data. These data points have a sum of $aS + aL$ that gives an range of A_3 values all much larger than should be possible for acceptors constrained to be one bond length apart. One basic assumption of the acceptor repulsion analysis is that the acceptors lie on either side of the hydrogen, so if aS is measured clockwise from the D-H bond, aL is measured anti-clockwise (or vice versa), see Figure 6.4:a). However for an A---A path length of one, the two acceptors are bound so close together that it is possible for them both to attack the hydrogen from the same side (see Figure 6.4:b)) this means that for the acceptor repulsion analysis equations to work, one of the angles, a must be taken to be $360-a'$ (where a and a' is either aS or aL).



Figure 6.4: a) geometric layout assumed for acceptor repulsion analysis, b) geometry of some of the acceptor-acceptor path length, path 3 = 1 systems.

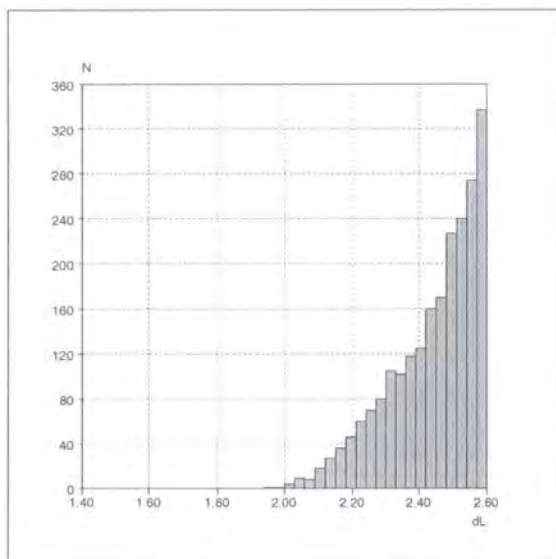
This correlation with the path length is only seen for angular distribution not for the length distribution.



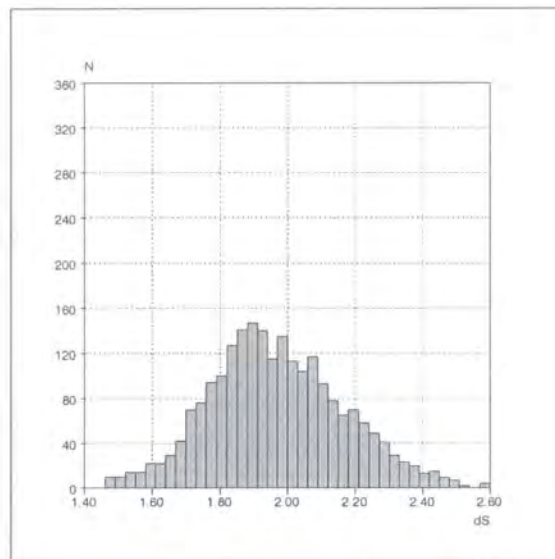
Graph 6.2: dL (Å) versus dS (Å) for case II all data. Data coloured by path lengths.

The general shape of the histograms of dL and dS (Graph 6.3 and Graph 6.4) remains unchanged from case I (Graph 5.2 and Graph 5.3). For dL the frequency increases as dL tends to 2.6Å , however, the increase is less steep than for case I resulting in a shorter mean dL . In dS as well, the mean is shifted giving shorter average bond lengths for case II. This inclination towards shorter bond lengths for case II is probably simply a result of a reduction in the steric hindrance effects when trying to fit 2 molecules

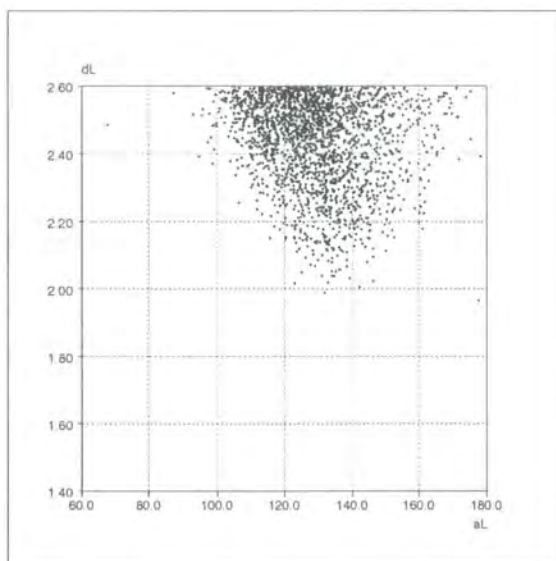
together instead of 3, allowing more favourable dL and dS angles and stronger hydrogen bonds.



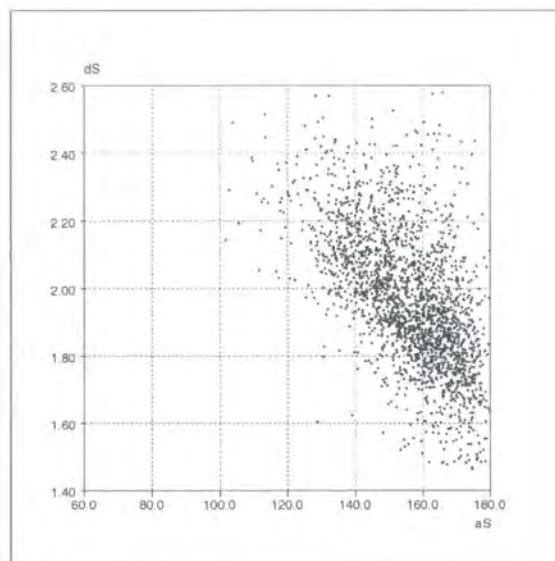
Graph 6.3: dL (Å) for all data.



Graph 6.4: dS (Å) for all data.



Graph 6.5: dL (Å) versus aL (°) for all data.



Graph 6.6: dS (Å) versus aS (°) for all data.

The separation of the data for case II into D=N and D=O does not reveal any major changes resulting from the identity of the H-donor.

Chapter 7 : Case III, Where One of the Hydrogen Bonds is an Intramolecular Hydrogen Bond and the Other is Intermolecular

There are two ways to analyse this data, either by defining the hydrogen bonds in terms of length, i.e. d_L and d_S as has been done for the previous cases, or in terms of intra and intermolecular hydrogen bonds. The latter method gives the clearest analysis and is used here. In fact, in over three quarters of the hits the intra hydrogen bond is the longer one, i.e. d_L .

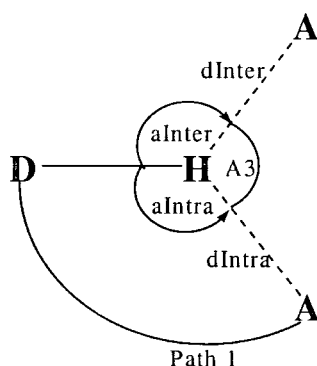


Figure 7.1: Scheme to define the angles and distances for the case III motif.

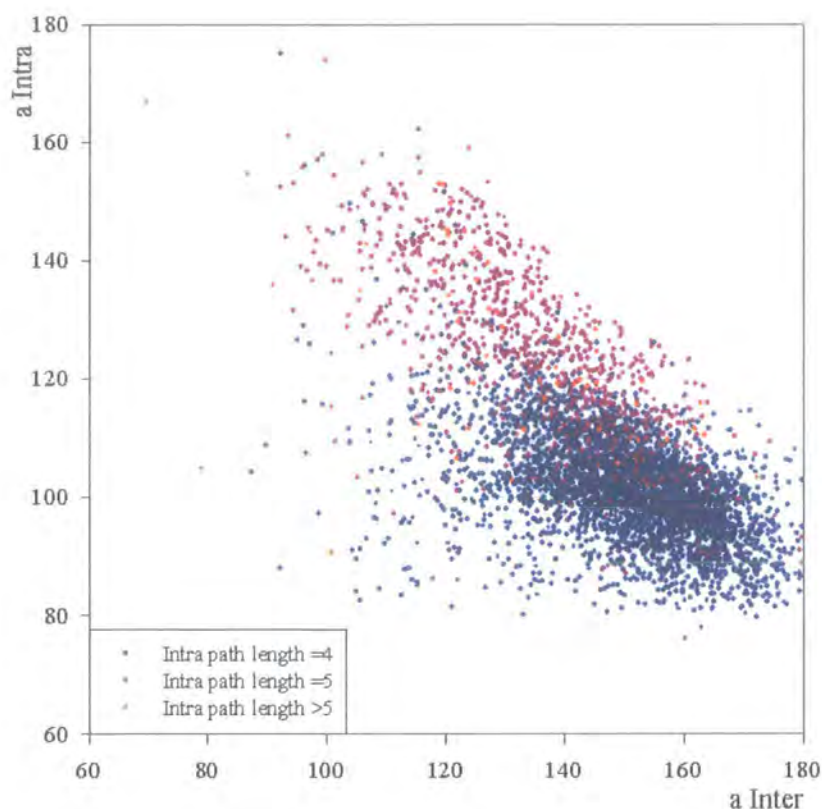
The number of bonds in path 1 and the corresponding frequency of hits is given in Table 7.1. An intramolecular bond path length of 4 is by far the most common motif for this case, perhaps because the geometry of this motif puts the hydrogen and acceptor in close contact resulting in a stable 5 membered ring. A path length of 5 gives a 6 membered ring. There are very few cases with a intra bond path length of greater than 5 (less than 2% of all examples of this type of system) presumably the steric bulk of systems with a path length greater than 5 tends to restrict the approach of a second acceptor.

Path length	No. where dL=Intra	No. where dS=Intra	Total cases per path length
4	3142	514	3656
5	271	517	788
6	23	20	43
7	2	9	11
8	2	1	3
9-12	0	0	0
13	1	0	1
14	0	1	1

Table 7.1: Number of occurrences of different numbers of bonds in the intramolecular path, Path 1.

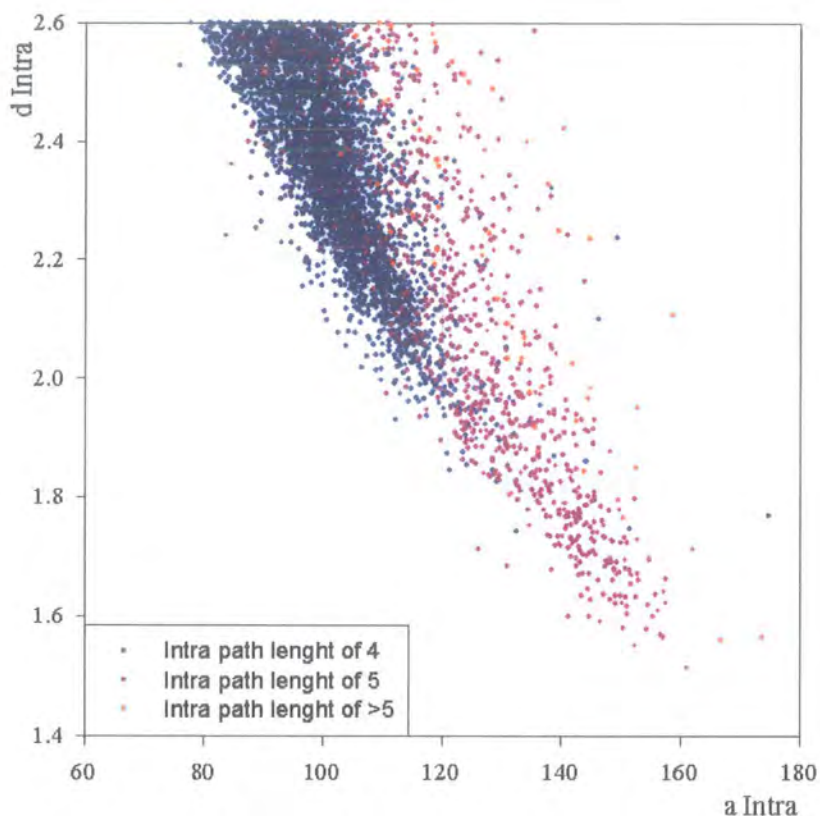
A path length of 4 gives a system where the possible hydrogen bond length and angles for the intra hydrogen bond are restricted to a narrow range (intramolecular hydrogen bond angles of between 80° and 120°). It must be pointed out, however, that a system such as this is sensitive to the D-H vector direction, that is to say that the practise of generating the hydrogen in a geometrically sensible, but possibly not physically accurate, position may have a strong influence on both the angle and distance. What is interesting to note is that the hydrogen bond length and angles for the intermolecular hydrogen bond are also restricted to an only slightly broader range.

As has been seen previously, there is a limit to the size of the AHA angle (A3). In this case A3 is always greater than 70° , in fact there are so few data points with A3 between 70° and 80° that this limit could be taken as 80° , i.e. the sum of aS and aL or aIntra and aInter must be less than 290° (for $A3 > 70^\circ$) or 280° (for $A3 > 80^\circ$), no data is seen above this line (see Graph 7.1). This is a closer A---A distance i.e. smaller AHA angle than is seen for case I and fits the data limits for path lengths of 3 or 4 for case II. Once again this can be attributed to the fact that two molecules can fit together more easily than three.

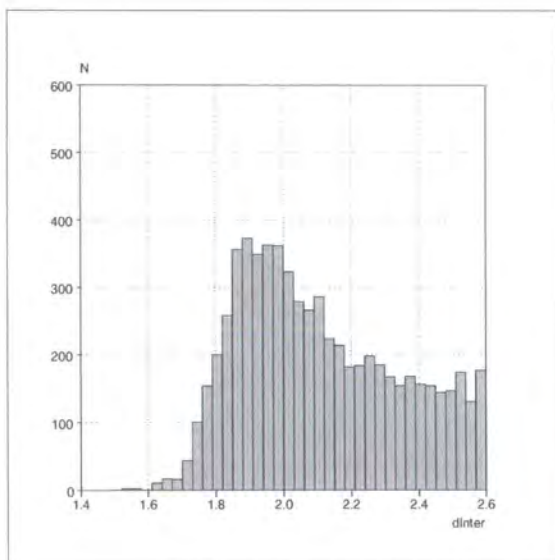


Graph 7.1: a_{Intra} ($^{\circ}$) versus a_{Inter} ($^{\circ}$) for case III all data. Data colour coded by intra path length.

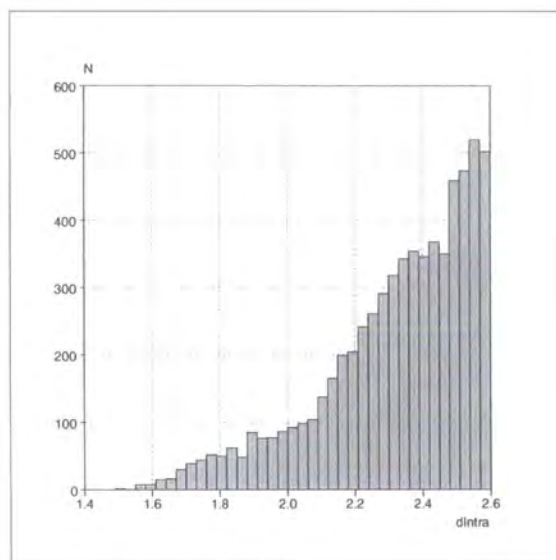
There is a strong correlation between the intramolecular bond length and the intramolecular bond angle for an intramolecular path length of 4, as the angle increases the bond length decreases (Graph 7.2). This trend continues for the examples with an intramolecular path length of greater than 4, with the increased path length allowing the acceptor to reach greater angles and correspondingly shorter distances. In general the intramolecular hydrogen bond is the longer bond when the path length is equal to 4 and the shorter bond for path length greater than 4 (see Table 7.1).



Graph 7.2: d_{Intra} ($^{\circ}$) versus a_{Intra} ($^{\circ}$) for case III all data, colour coded by intra path length.



Graph 7.3: d_{Inter} (\AA) for all data.



Graph 7.4: d_{Intra} (\AA) for all data.

Chapter 8 : Case IV, Where Both of the Hydrogen Bonds are Intramolecular Hydrogen Bonds

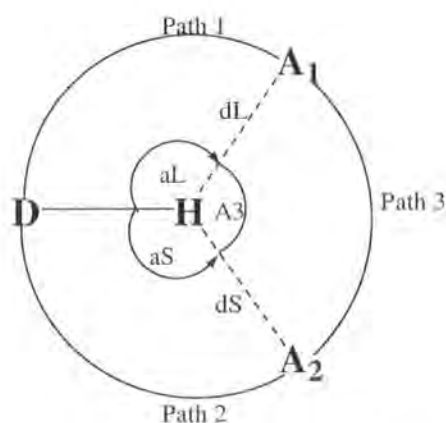


Figure 8.1: Scheme to define the angles and distances for the case IV motif.

Of the 1260 occurrences of this type of bond nearly two thirds can be attributed to just five path length combinations:

H---A path lengths of 4 bonds and 4 bonds and an A---A path of 6 bonds (103 occurrences),

H---A paths of 4 and 5 bonds and an A---A path of 1 bond (147 occurrences),

H---A paths of 4 and 5 bonds and an A---A path of 7 bonds (135 occurrences),

H---A paths of 5 and 5 bonds and an A---A path of 8 bonds (131 occurrences),

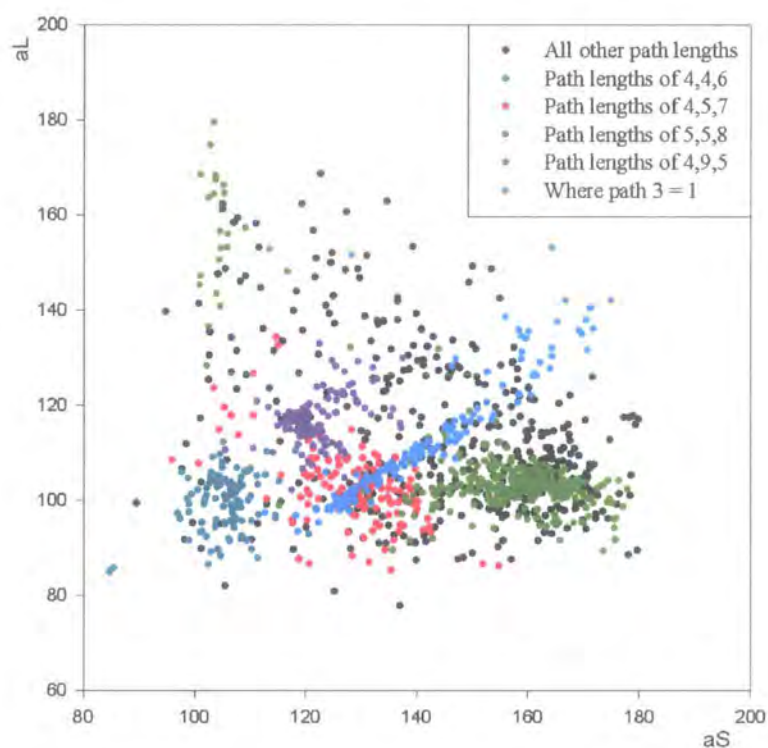
H---A paths of 4 and 9 bonds and an A---A path of 5 bonds (302 occurrences).

These are outlined in red in the following table of all the path length combinations found for case IV data.

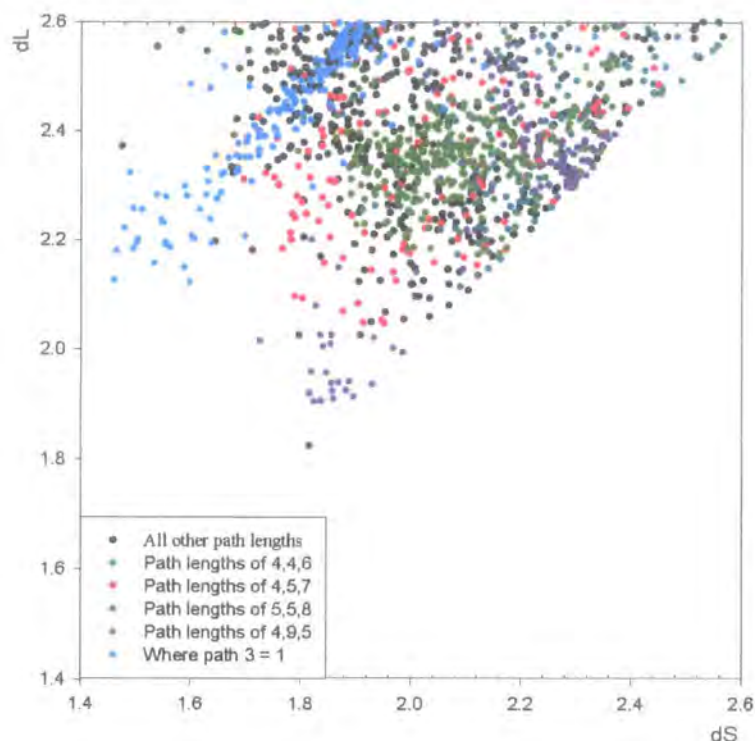
Path 1	Path 2	Path 3	No.	Path 1	Path 2	Path 3	No.	Path 1	Path 2	Path 3	No.
4	4	2	3	5	6	9	5	4	12	8	19
4	4	3	1	6	5	9	4	12	4	8	1
4	4	4	9	5	6	1	21	12	4	14	2
4	4	5	1	6	5	1	1	8	6	2	2
4	4	6	103	5	6	5	2	6	8	2	1
4	5	1	147	6	5	5	1	7	7	2	1
4	5	2	2	6	5	2	1	7	7	10	1
4	5	3	6	6	5	8	1	5	10	5	2
5	4	3	1	4	8	4	37	4	13	9	1
4	5	4	1	8	4	4	2	4	13	10	1
5	4	4	1	4	8	5	2	4	13	11	1
4	5	5	5	8	4	5	2	13	4	9	1
5	4	5	3	4	8	8	1	6	9	3	5
5	4	6	1	8	4	8	1	9	6	3	10
4	5	7	121	4	8	10	2	5	11	6	2
5	4	7	14	5	7	2	3	4	14	12	1
4	6	2	44	7	5	2	4	4	14	14	2
6	4	2	3	5	7	3	1	6	10	4	1
4	6	3	2	7	5	3	1	12	5	13	1
4	6	5	1	7	5	10	1	9	7	3	1
4	6	6	1	6	6	1	1	4	16	14	1
4	6	7	1	6	6	2	2	4	16	16	1
6	4	7	2	4	9	5	277	4	16	18	2
4	6	8	17	9	4	5	25	10	7	3	1
6	4	8	2	4	9	11	1	7	10	3	2
5	5	2	10	4	10	6	5	14	5	9	1
5	5	3	2	10	4	6	1	5	14	11	1
5	5	4	3	10	4	10	1	4	18	6	1
5	5	6	3	5	8	3	21	7	11	6	1
5	5	7	2	8	5	3	17	11	7	6	1
5	5	8	131	6	7	7	2	4	21	23	1
4	7	3	52	7	6	7	1	8	11	3	1
7	4	3	10	4	11	7	7	13	14	1	1
4	7	7	4	11	4	13	1	19	20	2	1
4	7	8	1	5	9	4	3				
4	7	9	4	9	5	4	14				

Table 8.1: Combinations of path lengths found for case IV data.

Looking at the geometries of these 5 groups of hits, it is clear that the hydrogen bond angle, Graph 8.1 (and to a lesser extent length, Graph 8.2) are closely dependent on the path length, i.e. the hits are tightly clustered by path length combination.



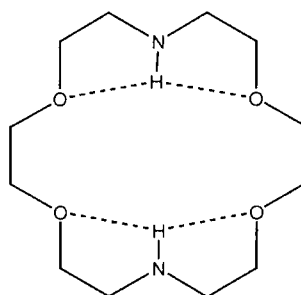
Graph 8.1: aL ($^{\circ}$) versus aS ($^{\circ}$) for case IV, all data. Colour coded by path length.



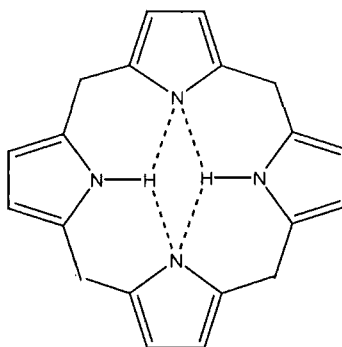
Graph 8.2: dL versus dS for case IV, all data. Colour coded by path length.

Once again there is the problem of whether an A---A path length of 1 really counts as a bi-furcated hydrogen bond or just a feature arising from the molecular geometry. There are a couple of points to note about these systems; firstly the path length combination when $\text{path3} = 1$ is nearly always 4,5,1, and secondly, there is a strong correlation between the various angles and distances, this is because in such a system there is very little freedom of movement.

Some of the frequently occurring path length combinations can be seen to arise from a specific class of compounds, for instance, most of the occurrences of the path length combination of 4,9,5, are for peptide chains. Equally, most of the occurrences of the path length combination of 4,4,6, are either also peptide chains or aza-crown ethers, and most of the occurrences of the path length combination of 5,5,8, occur in porphyrin derivatives.



Aza-crown ether showing the 4,4,6 path length combination



Porphyrin showing the 5,5,8 path length combination

Figure 8.2: The main contributors to the 4,4,6 and 5,5,8 path length combinations.

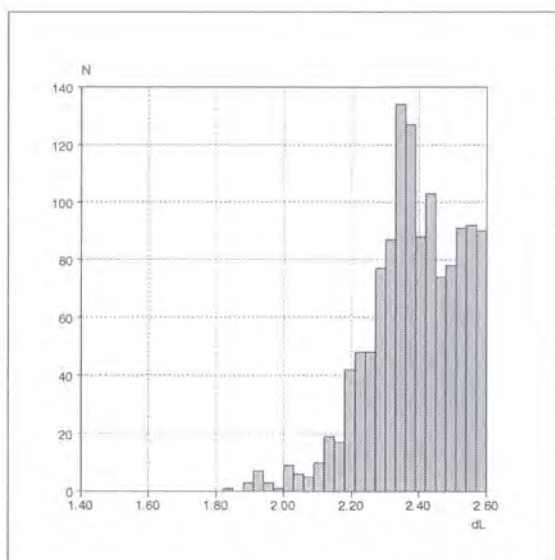
The fact that so many of these cases can be attributed to so few, and to such specific, molecular types, is a drastic example of the cluster and bias within the CSD discussed in section 3.4.

In systems such as the aza-crown ether and the porphyrin shown above it is clear that the molecular geometry is controlling the bi-furcated hydrogen bond formation not the hydrogen bonds influencing the molecular geometry.

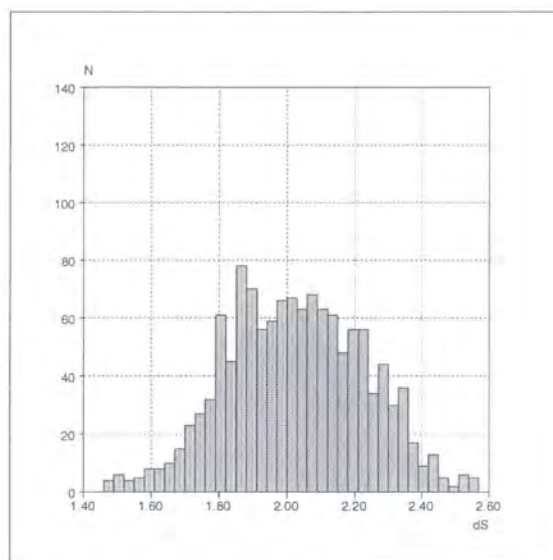
There is a tendency for the shorter hydrogen bond to have a longer path length than the longer hydrogen bond i.e. $\text{path1} < \text{path2}$. In 847 cases the path length of the shorter hydrogen bond is greater than the path length of the longer hydrogen bond, in 275 the path lengths are equal and in only 138 cases does the longer path length correspond to the longer bond. In systems where the path lengths are equal, the two hydrogen bonds tend towards a more symmetrical system, in terms of both length and angles.

Given these clusters dependence on molecular geometry influences rather than on hydrogen bond geometry influences, it is reasonable to expect that the plots of hydrogen bond distances and angles for each bond show the same cluster effects and to be more

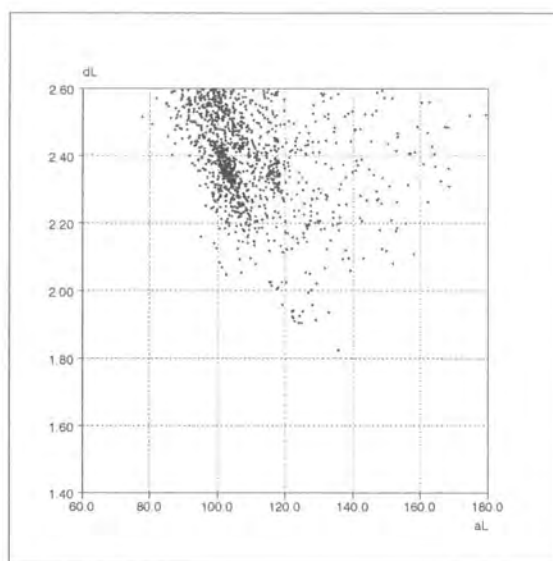
informative about the geometric restraints of the specific molecular types that generate the clusters than any overall information about the expected geometry of a case IV system.



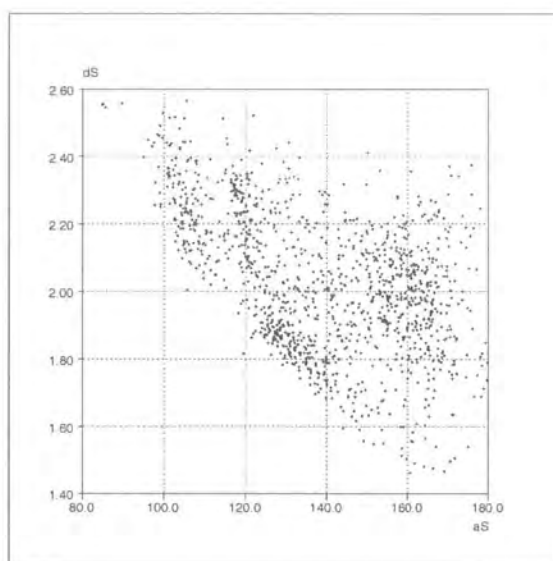
Graph 8.3: dL (Å) for all data.



Graph 8.4: dS (Å) for all data.



Graph 8.5: dL (Å) versus aL (°) for all data.



Graph 8.6: dS (Å) versus aS (°) for all data.

Chapter 9 : Conclusions

In the introduction two main questions were posed: 1) what are the effects of the different hydrogen donor atoms (i.e. oxygen and nitrogen) on the frequency of occurrence and the system geometry, and 2) what sort of effect does whether the hydrogen bonds are intra or inter molecular have on the frequency of occurrence and the system geometry.

In answer to the first question, there is very little difference in the influence of the two hydrogen bond donors (N and O) in such systems. Oxygen is found as the donor atom slightly less frequently than nitrogen, though this could be a feature of the relative occurrence of oxygen and nitrogen as possible donors in the database.

In answer to the second question, when two or more of the system components (D-H, A₁ and A₂) are intramolecular, the effect of intramolecular geometric constraints comes into play, affecting the range of possible acceptor-acceptor distances or restricting the hydrogen bond angles. The motif geometry can be traced back to the geometric restrictions placed on the system by the specific intramolecular hydrogen bond path length or the acceptor-acceptor path length. It is interesting to note that most of the interactions involve short path lengths of 4 or 5 bonds for intramolecular hydrogen bonds and 1 to 4 bonds for acceptor-acceptor path lengths, this is probably due to the difficulty of bending a molecule round to get longer path lengths and then fitting the steric bulk of the molecule around the hydrogen bond motif. There are very few examples of either intramolecular or acceptor-acceptor path lengths of greater than 10.

The largest influence on the bi-furcated H-donor hydrogen bond system seems to be acceptor-acceptor repulsion. The preferred geometry of the system, given no other constraints, is to have one short fairly linear bond and the second acceptor coming in as close as possible to the first, allowing for acceptor-acceptor repulsions keeping the acceptors at an optimum distance and giving an AHA angle, A₃, of about 100° in a planar system. Because of the constraints imposed by the position of first short and linear hydrogen bond, the second hydrogen bond is both non-linear (often about 120°) and longer.

Perhaps the most interesting fact to come out of this study is the degree of bias that can sometimes be seen in the database. This bias is most important in situations like that seen in case IV where the constraints of a highly specific and limiting search fragment fits one or some of the most well studied system in chemistry (peptide chains, porphyrin and aza-crown ether fragments among others). Add to this the fact that by the very nature of the system a specific motif is likely to be restricted to only a limited range of possible angles and distances, the result is the very dramatic clustering of certain structure types seen in case IV.

Chapter 10 : Tri-Furcated Hydrogen Bonded Systems

10.1 Introduction

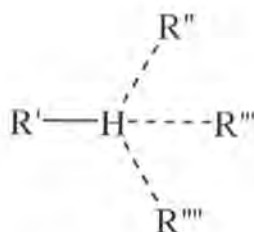


Figure 10.1: The tri-furcated motif

Tri-furcated hydrogen bonds are a much rarer occurrence than bi-furcated hydrogen bonds, and are rarely identified or commented on during crystal structure analysis or other studies, however some studies have been carried out^{1,15,16} including some novel 'non-conventional' tri-furcated hydrogen bonds^{17,18}.

Tri-furcated hydrogen bonded systems are much more complicated to analyse. Not only are there more parameters to consider but the relationships between the various distances, angles and intramolecular path lengths of the three hydrogen bonds are hard to illustrate using only the two dimensions of a standard graph, and the spread of the data points is such that '3D graphs' are hard to interpret.

The data were obtained in the same way and with the same restraints as for the bi-furcated system, see Section 3.3 Experimental.

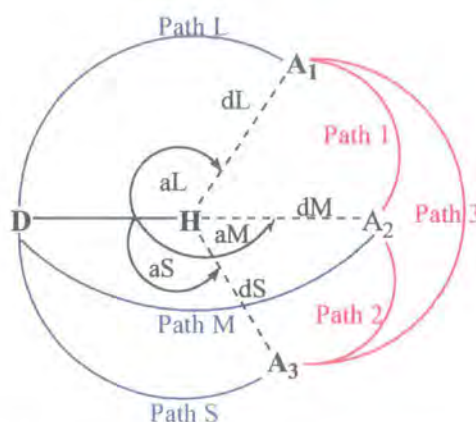


Figure 10.2: Scheme to define the angles, distances, and intramolecular path lengths for the tri-furcated motif.

In a similar manner to the bi-furcated system, the three hydrogen bonds of the tri-furcated system have been distinguished from each other in terms of length, with the longer bond designated L, the mid-length bond M, and the shortest bond S. The corresponding intramolecular hydrogen bond path lengths are labelled Path L, Path M, and Path S, and the acceptor-acceptor path lengths defined as Path 1 between the longest and middle length bonds, Path 2 between the middle length and shortest bonds, and Path 3 between the longest and shortest hydrogen bonds, see Figure 10.2.

10.2 Frequency of Occurrence

Instead of the four cases seen in the bi-furcated system there are now seven cases: case I, two forms of case II, three forms of case III, and case IV. A full description of these cases is given in the table below along with the number of hits for each case.

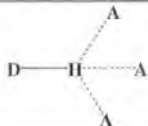
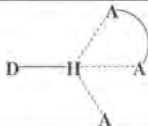
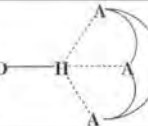
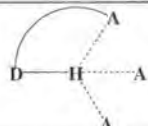
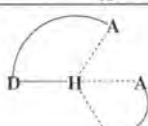
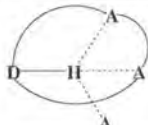
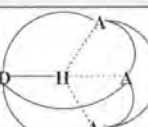
Donor Atom:			N or O	N	O
Inter Inter Inter			307	227	80
Case I	Inter, Inter, Inter. (acceptors from different molecules), 4 molecules		34	24	10
Case II a	Inter, Inter, Inter. (2 acceptors from same molecule), 3 molecules		69	58	11
Case II b	Inter, Inter, Inter. (all acceptors from same molecule), 2 molecules		204	145	59
Inter Inter Intra			225	152	73
Case III a	Inter, Inter, Intra. (acceptors from different molecules), 3 molecules		99	80	19
Case III b	Inter, Inter, Intra (one bond intra other two acceptors from same molecule), 2 molecules		126	72	54
Inter Intra Intra			225	192	63
Case III c	Inter, Intra, Intra. (two bond intra other acceptor from different molecule), 2 molecules		225	192	63
Intra Intra Intra			86	80	6
Case IV	Intra, Intra, Intra. 1 molecule		86	80	6
Total :			873	651	222

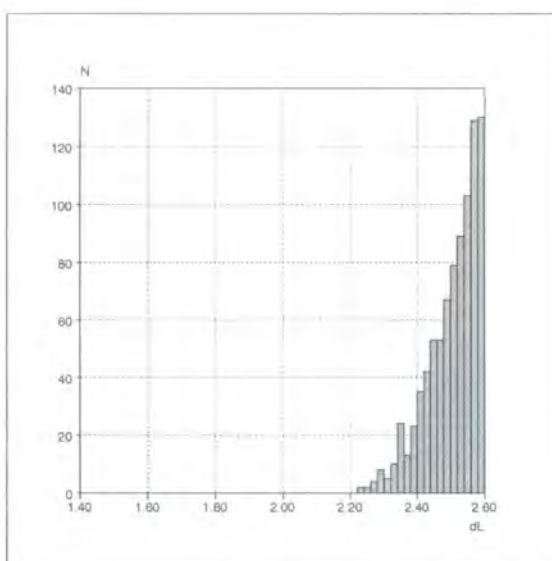
Table 10.1: Frequency of occurrence for the tri-furcated system.

It can be seen from Table 10.1 that there are far fewer examples of this type of motif than the bi-furcated motif. This makes the case-by-case type of analysis carried out in the previous chapters difficult, as, at least in some of the cases, there are too few data to achieve statistically meaningful results. For example, the very general case, case I, where there are no intramolecular links to influence and constrain the geometry, has only 34 occurrences. This is not unexpected, given the difficulty of squeezing four

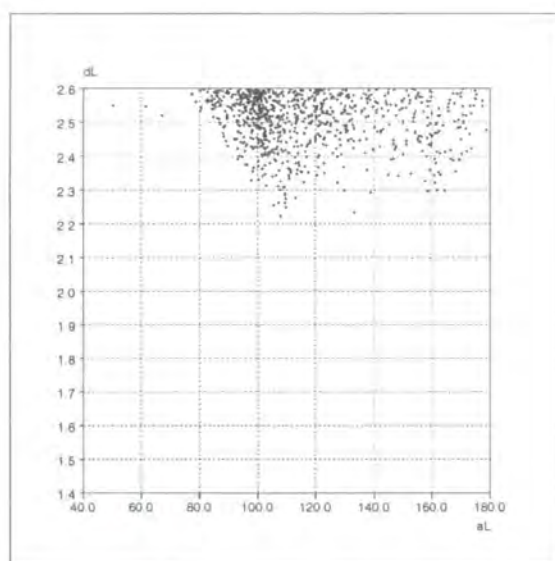
molecules together to form the motif, however it does make it impossible to draw any reliable conclusions about the system geometry. With the number of entries in the Cambridge Structural Database⁹ increasing at a very fast rate it makes sense to only carry out a very preliminary study here with a view to running a more detailed analysis when the size of the dataset has increased.

Nitrogen is almost twice as likely as oxygen to be the hydrogen donor atom. This is different from the bi-furcated situation, where nitrogen was only slightly more likely than oxygen to be the donor atom. As in the bi-furcated system, case III is the form most commonly found, then case II, then either case IV or I. The exact order of cases IV and I depending on the donor atom; case IV is the more common of the two if nitrogen is the donor atom and it appears that case I is more common than case IV if oxygen is the donor (though the lack of data makes this last observation very unreliable).

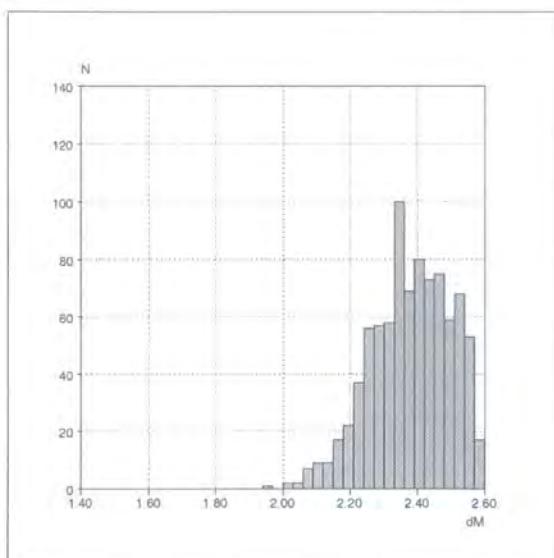
10.3 Tri-Furcated Hydrogen Bonds



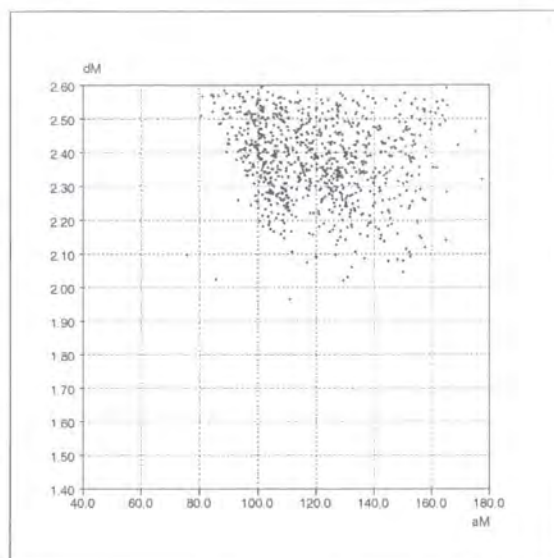
Graph 10.1: dL (Å) for all tri-furcated systems.



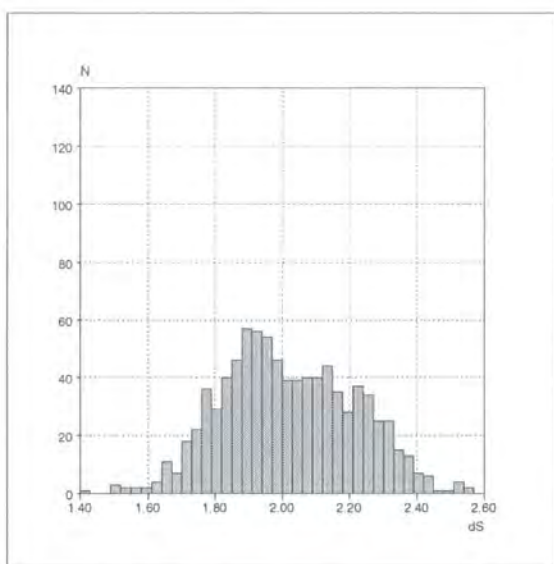
Graph 10.2: dL (Å) versus aL (°) for all tri-furcated systems.



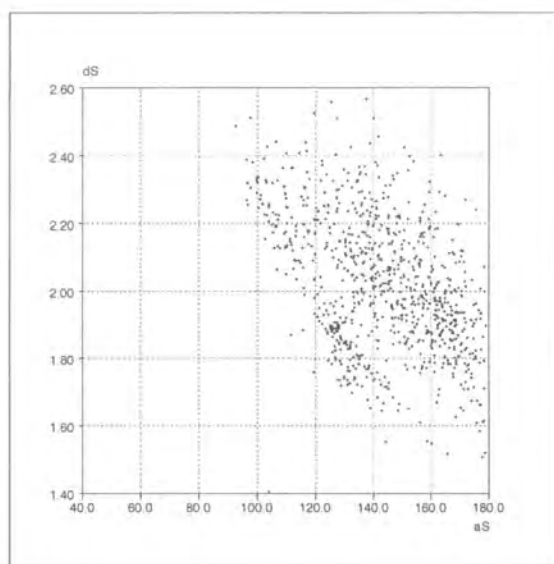
Graph 10.3: dM (Å) for all tri-furcated systems.



Graph 10.4: dM (Å) versus aM (°) for all tri-furcated systems.



Graph 10.5: dS (Å) for all tri-furcated systems.

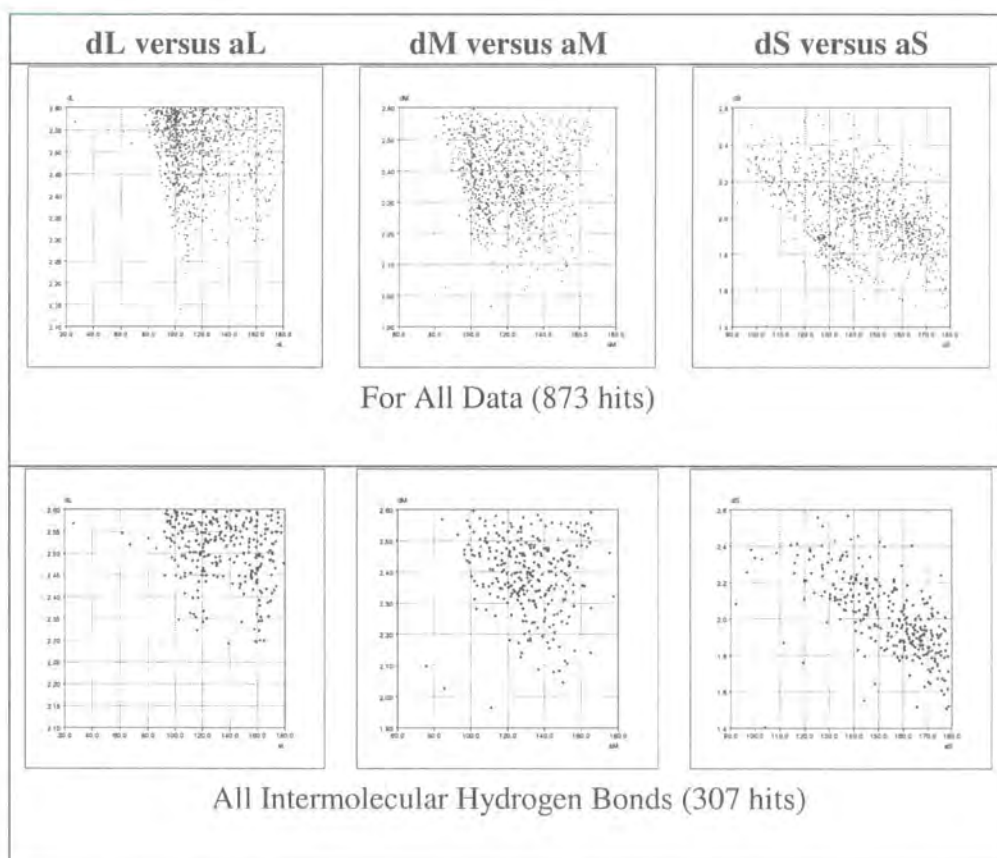


Graph 10.6: dS (Å) versus aS (°) for all tri-furcated systems.

As in the bi-furcated system the graphs corresponding to the longest bond show none of the characteristics expected for a set of normal hydrogen bonds. In the histogram of dL there is a steady increase till the cut off point of 2.6Å and the scattergram of dL versus aL shows a tendency towards an angle of 100° regardless of the bond length. The plots for the mid and shortest bonds are much closer to those expected for hydrogen bonds with the bond length frequency (N) forming a peak with a maximum at about 2.4Å for dM and 1.9Å for dS . Similarly the scattergrams in both cases show a tendency for the

bonds to become more linear as the bond length decreased. In going from the longest hydrogen bond to the middle hydrogen bond to the shortest hydrogen bond the graphs become closer to what would be expected for a hydrogen bond plot.

These graphs, especially Graph 10.6, dS versus aS show a lot of structure, in the same way that the graph of case IV for bi-furcated systems showed structure arising from clusters of similar molecules (see Graph 8.1). In the table below (Table 10.2) the data are separated into cases distinguished by the number of bonds that are intramolecular rather than intermolecular. The first row shows the plots generated by all the data together i.e. the same plots as Graph 10.2, Graph 10.4, and Graph 10.6 above. The following rows show plots generated from just one combination of inter- and intramolecular hydrogen bonds. In other words the plots on the first row are the sum, or superposition of all the other plots in that column. As with the bi-furcated system, the situation where all the hydrogen bonds are intermolecular is the most general case. However, in the all inter-graphs below it must be remembered that the data includes some case II type systems where the acceptors are from the same molecule.



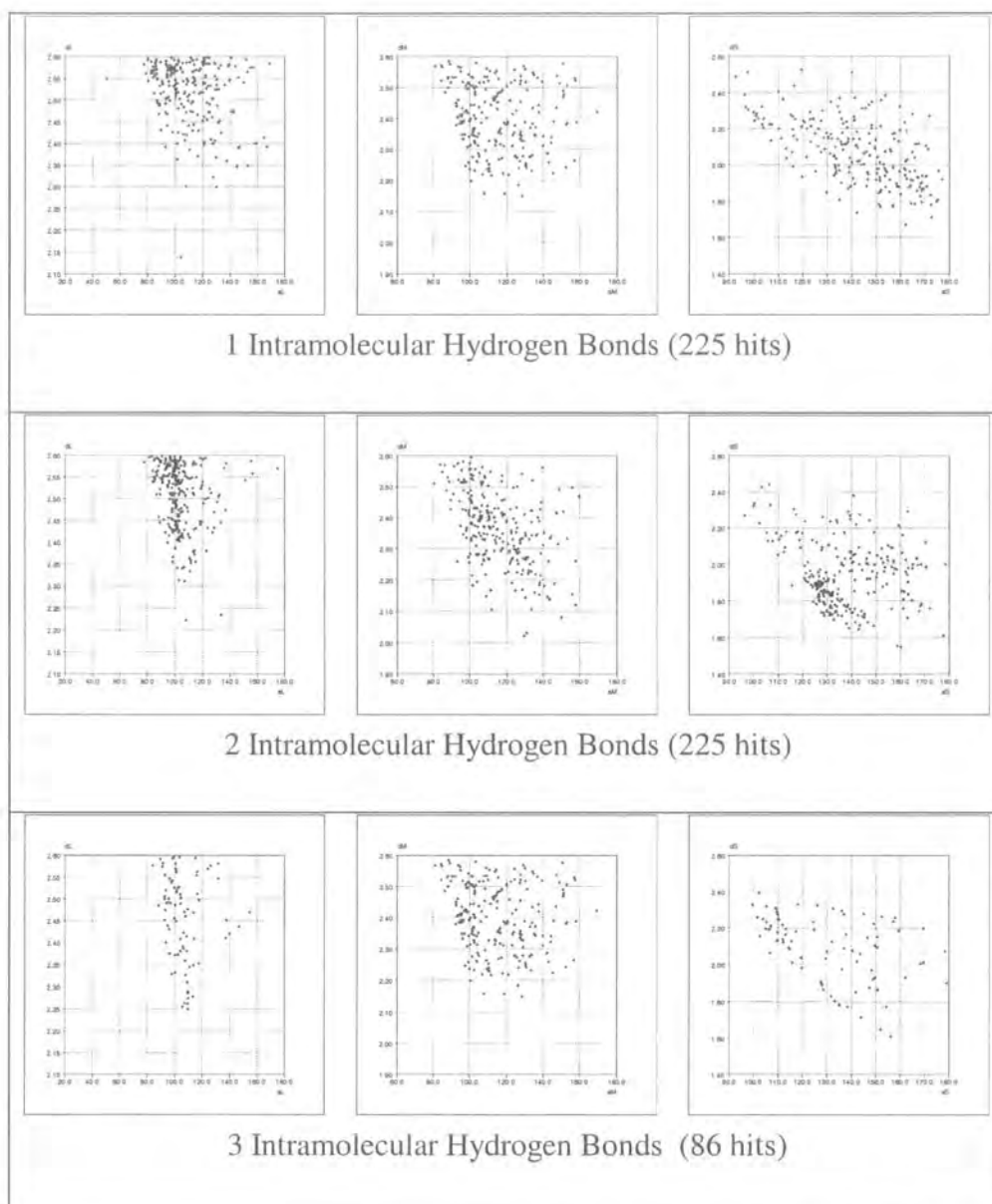
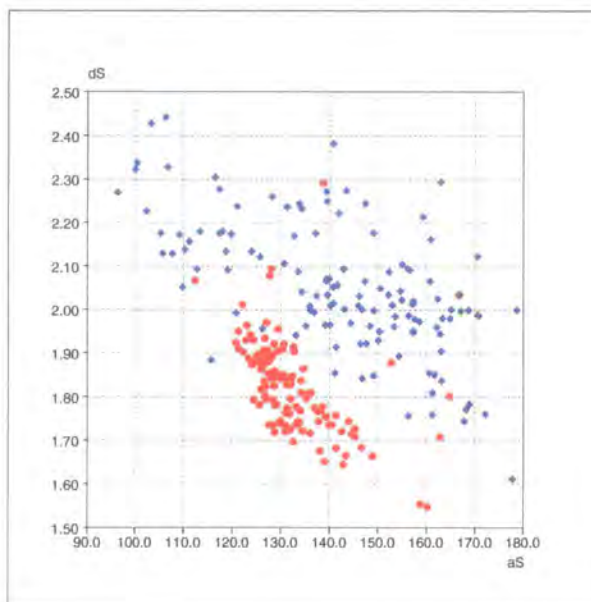


Table 10.2: Distance (Å) versus angle (°) plots for all three hydrogen bonds, for each inter/intramolecular hydrogen bond combinations of tri-furcated cases.

As might be expected from the bi-furcated system analysis, the degree to which the data points fall into clusters rather than a single distribution increases as the number of intramolecular bonds increases, and therefore, as the geometric constraints due to path length increases.

Closer analysis shows that the data clusters can be attributed to acceptor-acceptor path length, and especially to path lengths of 1. Out of the four inter/intramolecular combinations shown in Table 10.2 the clusters can be seen to be arising mainly from the system where there are two intramolecular hydrogen bonds (case IIIc). A plot of dS vs

aS for this case is shown in Graph 10.7 below with data points corresponding to systems where the acceptor-acceptor path length is one (data points coloured red) and where the acceptor-acceptor path length is greater than one (coloured blue).



Graph 10.7: dS (Å) vs aS (°) for the cases where there are two intramolecular hydrogen bonds. Data points where the acceptor-acceptor path length is one are coloured red and where the acceptor-acceptor path length is greater than one are coloured blue.

10.4 Conclusions

From this very brief analysis it can be seen that the tri-furcated system shows much of the same patterns and influences as the bi-furcated system. The constraints imposed on the system by the internal molecular geometry i.e. by the intramolecular and acceptor-acceptor path lengths, throws greater constraints on the system than the influence of the hydrogen bonds.

There are far fewer examples of tri-furcated systems than bi-furcated systems in the database, as it is a much less common system.

Tri-furcated systems are much more likely for cases where the hydrogen donor is nitrogen than where the hydrogen donor is oxygen.

10.5 References for Part 1

- 1) G.A.Jeffrey, *An Introduction to Hydrogen Bonding*, New York: Oxford University Press, 1997.
- 2) C.B.Aakeroy, K.R.Seddon, *Chem. Soc. Rev.*, 1993, 397-407.
- 3) G.A.Jeffery, W.Saenger. *Hydrogen Bonding in Biological Structures*, Berlin: Springer-Verlag. 1991, ch. 8, pp 136-146.
- 4) J.Yang, S.H.Gellman. *J. Am. Chem. Soc.*, 1998, **120**, 9090-9091.
- 5) L.van Meervelt, M.Goethals, N.Leroux, Th.Zeegers-Huyskens. *J. Phys. Org. Chem.*, 1997, **10**, 680-686.
- 6) F.H.Allen, C.A.Baalham, J.P.M.Lommerse, P.R.Raithby, E.Sparr. *Acta Cryst.*, 1997, **B53**, 1017-1024.
- 7) I.Rozas, I.Alkorta, J.Elguero. *J. Phys. Chem. A*, 1998, **102**, 9925-9932.
- 8) C.H.Gorbitz, M.C.Etter. *J.Chem. Soc. Perkin Trans. 2*, 1992, 131-135.
- 9) F.H.Allen, O.Kennard. *Chem. Des. Autom. News*, 1993, **8**, 30-37.
- 10) C.Bilton, F.H.Allen, G.P.Shields, J.A.K.Howard. *Acta Cryst.*, 2000, **B56**, 849-856.
- 11) F.H.Allen, W.D.S.Motherwell, P.R.Raithby, P.G.Shields, R.Taylor. *New J. Chem.*, 1999, 25-34.
- 12) SigmaPlot 2000, SigmaPlot 2000, SPSS Inc, Chicago, U.S.A.
- 13) C.H.Stam, H.C.van der Plas, *Acta Cryst.*, 1976, **B32** 1288-1290.
- 14) N.N.Dhaneshwar, S.N.Naik. S.S.Tavale. *Acta. Cryst.*, 1991, **C47** 217-218.
- 15) P.Prince, S.F.Watkins, F.R.Fronczek, R.D.Gandour, B.D.White, G.W.Gokel. *Acta Cryst.*, 1991, **C47**, 893-895.
- 16) Th.Steiner, W.Saenger. *Acta. Cryst.*, 1992, **B48**, 819-827.
- 17) L.R.Nassimbeni, A.L.Rodgers. *Inorg. Neuc. Chem. Lett.*, 1975, **11**, 757-759.
- 18) D.A.Braden, G.L.Gard, T.J.R.Weakley, *Inorg. Chem.*, 1996, **35**, 1912-1914.

Part 2:

Hydrogen Bonding in Amino-Phenols

Chapter 11 : Amino-phenols

11.1 Hydroxy and Amino Group Complementarity

Two of the most important groups in hydrogen bond studies are the alcohol and amino groups. These two groups make an interesting pair to study since, in terms of hydrogen bond donors and acceptors, they are perfectly complementary; the hydroxy group has two lone pairs of electrons to act as hydrogen bond acceptors and one hydrogen atom, so one possibility for a hydrogen bond donor. In contrast the amino has only one lone pair, but two hydrogen atoms.

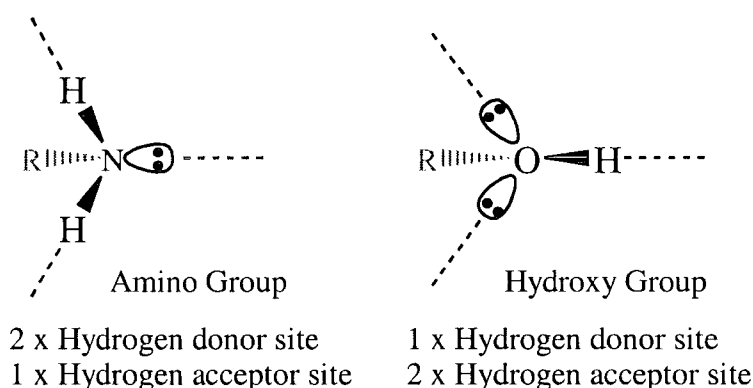


Figure 11.1: Hydrogen bond acceptor and donor sites of the amino and hydroxy groups.

While neither of these groups can fulfil their full hydrogen bond valence alone, the complementary nature of these two groups means that a 1:1 mixture of hydroxy and amino groups in a crystal system gives the potential for the use of all the donor and acceptor sites, resulting in a fully saturated system. A comprehensive study of this complementary nature for molecular recognition has been made by Ermer and Eling¹.

When a fully saturated system occurs both groups are involved in three hydrogen bonds (as both donors and acceptors) as well as one covalent bond to the rest of the molecule. In ideal cases this can lead to an infinite net of hydrogen bonds, a hexagonal based sheet such as shown in Figure 11.2 below. This motif, when considered in three dimensions with the tetragonal geometry of the hydroxy and amino groups taken into account, is

analogous to the β -sheet structure of 'grey' arsenic and is referred to as a β -As sheet or 'super arsenic' sheets¹.

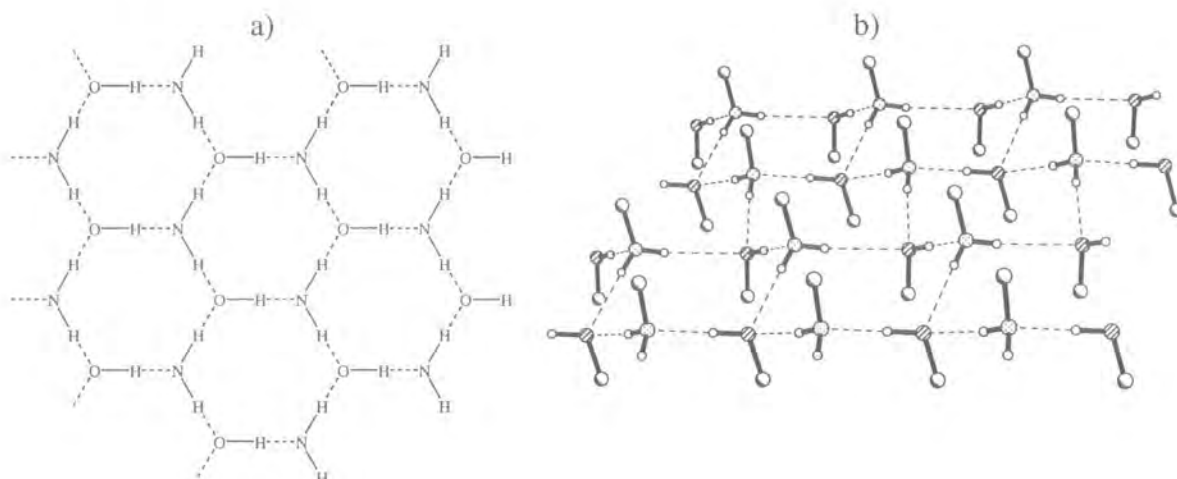


Figure 11.2: Hydrogen bonding motif possible with a 1:1 mixture of hydroxy and amino groups, a) a schematic view, b) in a real crystal, showing the puckering of the sheet.

In systems where the hydroxy and amino groups occur on the same molecule linked by a linear linker, for instance a benzene ring in *p*-aminophenol, the whole structure can be considered analogous to structures such as diamond and wurtzite: instead of a structure built up of tetrahedral units joined by covalent bonds, the hydroxy and amino groups act as the tetrahedral units, three of the covalent bonds are replaced by three hydrogen bonds, and the last covalent bond is replaced by the rest of the molecule - the linear linker described above.

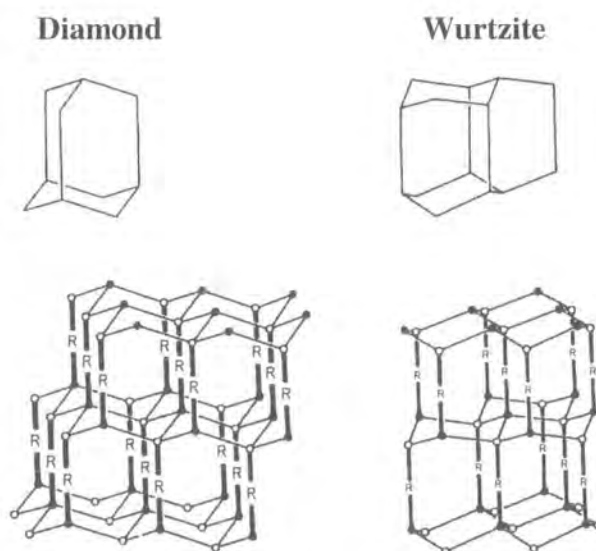


Figure 11.3: The diamond and wurtzite based structures¹, built up from layers of β -As sheets. R=Linear linking unit between hydroxy and amino groups (represented by black and white circles).

It has long been known that O-H...O bonds are shorter and stronger than O-H...N bonds and N-H...O bonds, which in turn are shorter and stronger than N-H...N bonds². Ermer and Eling¹ noted that in all the β -As sheet structures they studied O(H)N bonds formed in preference to a combination of strong O-H...O and weak N-H...N hydrogen bonds. This can be understood as a tendency to avoid weak N-H...N bonds and a preference for hydrogen bonds of at least approximately similar lengths and strengths, within a structure.

This is not the only motif seen for crystals containing a 1:1 combination of hydroxy and amino groups: co-crystals of simple chiral compounds such as 1,2-diaminohexane and hexane-1,2-diol have been found to form helical structures^{3,4} known as 'superminols'⁵. These structures do not utilise the full hydrogen bond potential of the groups, but still utilise self recognition to form very stable and beautiful single and triple helical structures.

One of the simplest group of compounds to fulfil the criteria of a 1:1 ratio of hydroxy and amino groups are the aminophenols. A study^{6,7} of the structures of *ortho*- *meta*- and *para*-aminophenol showed that while the linear *p*-aminophenol exhibits a β -As sheet structure analogous to the wurtzite type lattice, the *o*- and *m*-aminophenol each have a distinctly different structure involving N-H... π hydrogen bonds rather than N-H...O and the oxygen acts as a strong hydrogen bond acceptor only once rather than twice per atom.



Figure 11.4: The structure of *m*-aminophenol. Note: the β -As sheet structure is not formed.

These structural differences can be attributed to an optimisation of a herringbone interaction of the aromatic rings^{6,7}. An alternative explanation is that the angle between

the amino and phenol groups prevents the formation of parallel β -As sheets (more details of this explanation are presented on pages 92-93.).

11.2 The Aminophenol Series

With the aim of further improving the understanding of when and why the β -As sheet structures are formed, the following series of compounds were synthesised* and the structures analysed. The series consists of 4-amino-4'-hydroxydiphenylalkane where alkane chains of up to five CH_2 groups were studied, see scheme below, the structural details are given in chapter 2. In addition, for the compounds with chain lengths of one, two, and three atoms, the corresponding sulphide derivatives were also synthesised and analysed, (also see scheme below, structural details are given in chapter 3). Attempts to obtain good structural data for 4-amino-4'-hydroxydiphenylsulphide failed due to unsolvable twinning of the crystal, however a co-crystal of methylenedianiline and thiodiphenol did give suitable data for a structural analysis and this had been included in the analysis instead.

* All the synthetic work was carried out by Mr. Venugopal Vangala, University of Hyderabad, India.

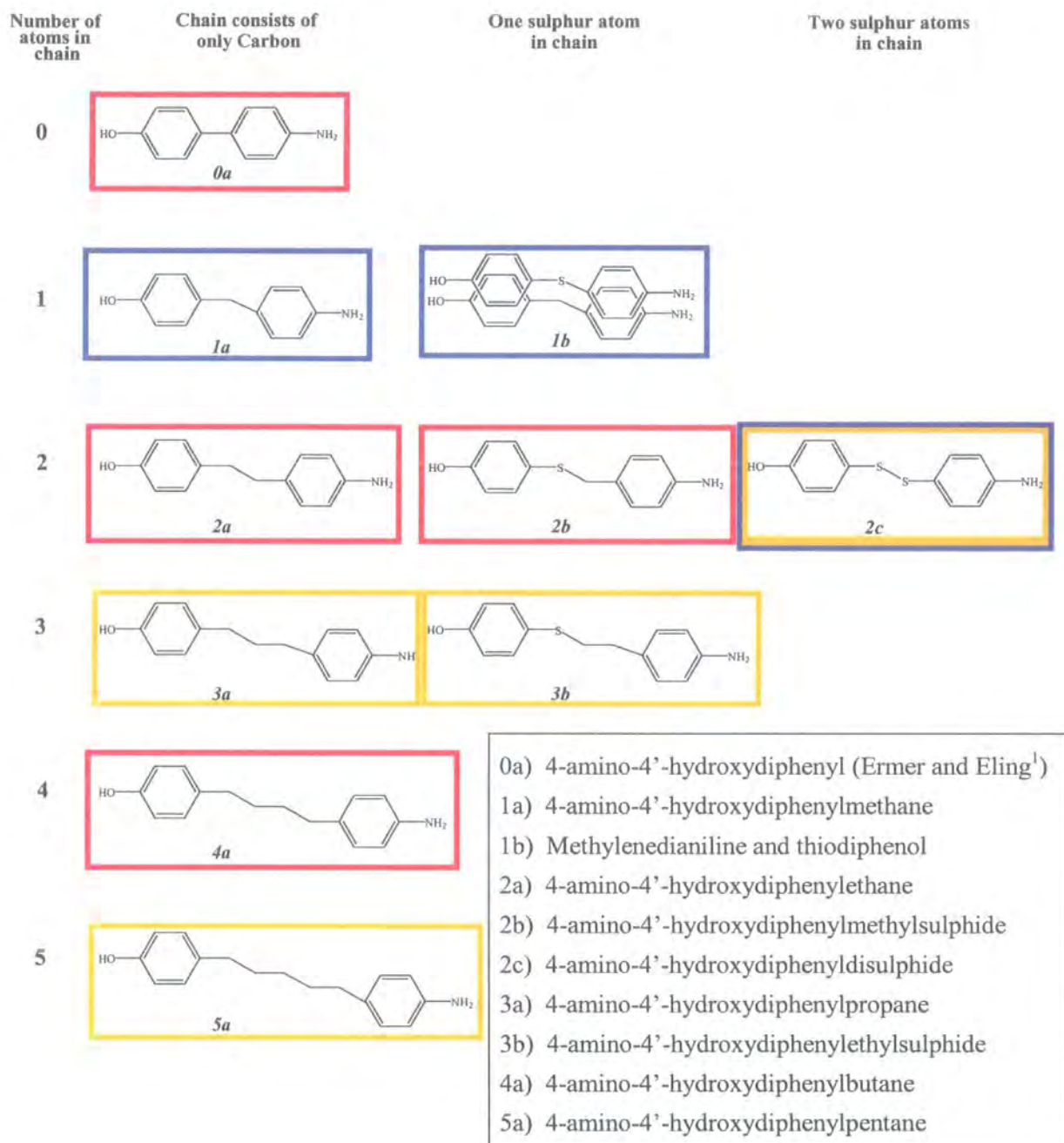


Figure 11.5: The aminophenol series studied.. Box colour indicates structure type: Red = β -As sheets, Blue = Square motif chains, Yellow = Stacked Vees. See following chapter for description of these structures types.

Chapter 12 : 4-Amino-4'-hydroxy-diphenylalkanes

12.1 Crystal Data and the β -As Structures

All the X-ray experiments were carried out on a Bruker Smart 1000⁸, using Mo radiation ($\lambda = 0.71073 \text{ \AA}$). The neutron study was performed at the ISIS facility, Rutherford laboratories, Oxford, on the time of flight instrument, SXD^{9,10}. Since the crystals were smaller than is usually required for a neutron single crystal experiment, the new technique of a multi-crystal experiment¹¹ was used. An array of four small crystals was mounted in the neutron beam and diffraction carried out on the four crystals simultaneously. In the data processing stage, the intensities recorded for all four crystals were extracted and used.

Crystal Data

Code	1a-(Neutron)	2a	3a	4a	5a
Link	(CH ₂)	2(CH ₂)	3(CH ₂)	4(CH ₂)	5(CH ₂)
Structure type	Square motif chains	β -As sheet	Stacked VeEs	β -As sheet	Stacked VeEs
Instrument	SXD at ISIS (Neutron) ^{9,10}	Smart-CCD ⁸	Smart-CCD ⁸	Smart-CCD ⁸	Smart-CCD ⁸
Formula weight	199.00	213.27	227.30	241.32	255.35
Temp /K	12(2)	100(2)	100(2)	105(2)	100(2)
Crystal system	Monoclinic	Monoclinic	Orthorhombic	Monoclinic	Monoclinic
Space group	P2 ₁ /n	Pc	Pca2 ₁	Pc	Pc
Colour	Brown	Colourless	Colourless	Brown	Colourless
Habit	Block	Plate	Plate	Cone	Block
Size /mm	1.5x1.5x1.3 Multi-crystal ¹¹	.50x.35x.10	.52x.25x.07	.40x.20x.20	.60x.55x.30
a / \AA	5.9180(3)	13.682(3)	23.9370(7)	15.788(2)	14.9554(9)
b / \AA	19.213(1)	5.262(1)	6.2160(2)	5.2088(6)	11.2370(8)

c / Å	9.6510(4)	8.192(2)	8.3970(3)	8.3399(8)	8.6841(6)
α ($= \gamma$) / °	90	90	90	90	90
β / °	101.250(4)	107.28(3)	90	100.912(5)	90.893(3)
Z	4	2	4	2	4
μ / mm ⁻¹	1.870 (at 1 Å)	0.079	0.075	0.074	0.071
Abs. corr. type	empirical	None	None	None	Psi-scan
R(int)	0.064	0.0322	0.0374	0.0546	0.0215
Data/restraints/parameters	2365/0/189	2509/2/205	3440/1/223	2816/2/176	5476/2/367
GooF	4.966	1.034	1.016	1.026	1.033
Flack parameter	—	-0.7(13)	0.4(15)	0.1(19)	-0.2(11)
R1	0.0881	0.0405	0.0421	0.0429	0.0355
wR2	0.1761	0.1087	0.0935	0.0960	0.0885
Angle between C-N and C-O vectors. /°	117.1	175.5	119.05	174.2	129.4 125.1
Angle between phenyl phenol plane. /°	91.53	2.25	55.94	1.95	81.37 69.99

Table 12.1: Crystal data for the 4-amino-4'-phenol alkane series.

The first thing to notice from the table above is that it is the compounds with an even number of carbon atoms in the alkane chain that form structures with β -As sheets. One of the main differences between alkane chains with even and alkane chains with odd numbers of carbon atoms is that 'even' chains can form a linear link between the end groups where as the 'odd' chains can not. One of the geometric requisites for a structure of the wurtzite or diamond type is that the β -As sheets must be parallel. To achieve this the link between the hydroxy and amino group must be approximately linear. The angle between the C-NH₂ and the C-OH vectors has been measured (see Table 12.1 above), in the β -As sheet structures **2a** and **4a** this angle is approximately 180°, in the other structures (**1a**, **3a**, and **5a**) the angle is closer to 120° (see Figure 12.1).

This dependence of the β -As sheets structures on a linear link between the hydroxy and amino group could also account for the structural differences between the *o*- *m*- and *p*-aminophenols discussed in the previous chapter.

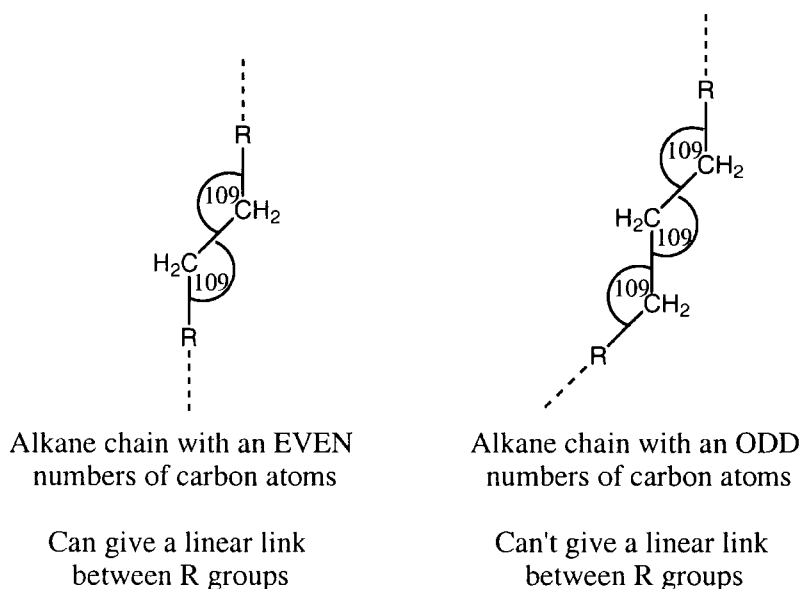


Figure 12.1: The difference in geometry between odd and even alkanes.

The next point of interest from the table is that compounds **3a** and **5a** have similar structure motifs, while **1a** has a completely different structure. As will be seen in Section 12.2, all three structures rely on N-H... π hydrogen bonds to supplement the N-H...O and O-H...N hydrogen bonds.

The two β -As sheet structures **2a** and **4a** exhibit a structure analogous to the diamond type lattice. Both have the same space group Pc. However, this is a different space group to either *p*-aminophenol or 4-amino-4'-hydroxydiphenyl, compound **0a**, (Orthorhombic Pna2₁ 8.184(1) 5.262(1) 12.951(2), and Orthorhombic Pna2₁ 8.096(1) 5.396(1) 21.217(2) respectively, both data sets recorded at room temperature¹). This difference might arise from the different molecular shapes, as both *p*-aminophenol and **0a** have a straight link unit and **2a** and **4a** have a slanted link unit, as shown in Figure 12.2.

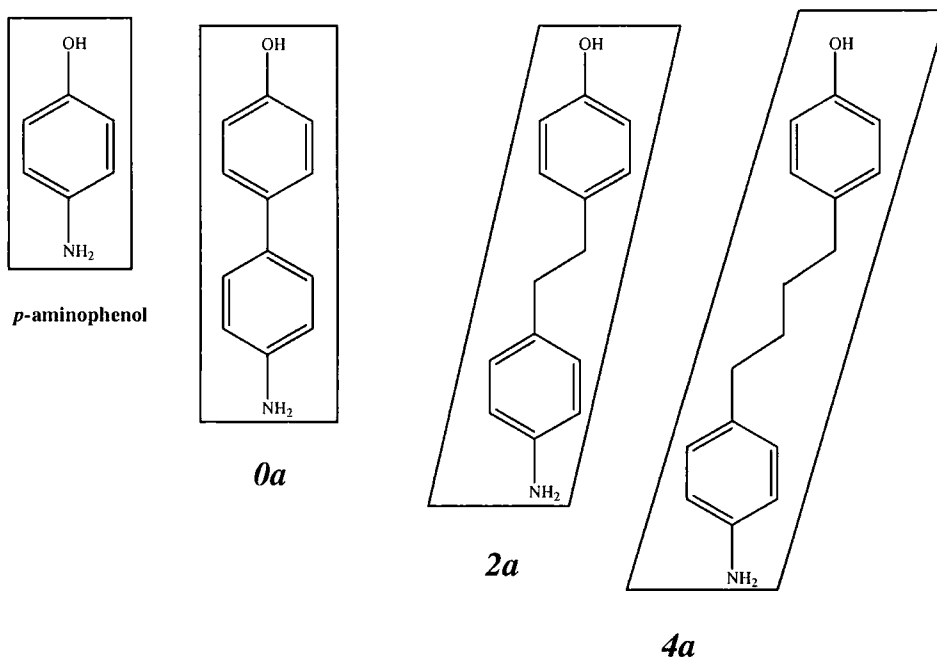


Figure 12.2: The molecular shapes of *p*-aminophenol and compounds **0a**, **2a** and **3a**. The boxes are to emphasize the changes in molecular shape and are NOT related to the unit cell.

All four of these compounds have similar *b* and *c* axes dimensions, this is logical as the β -As sheet runs in the *b*-*c* plane. The length of the *a* axis increases from *p*-aminophenol through to **4a** as the length of the link unit increases.

An interesting point is that all the compounds apart from **1a** exhibit a similar length *c* axis ranging from 8.1 to 8.6 Å. In each of these compounds the molecular spacing (and therefore the cell dimensions) is governed by a O(H)N hydrogen bonded chain, see Figure 12.3.

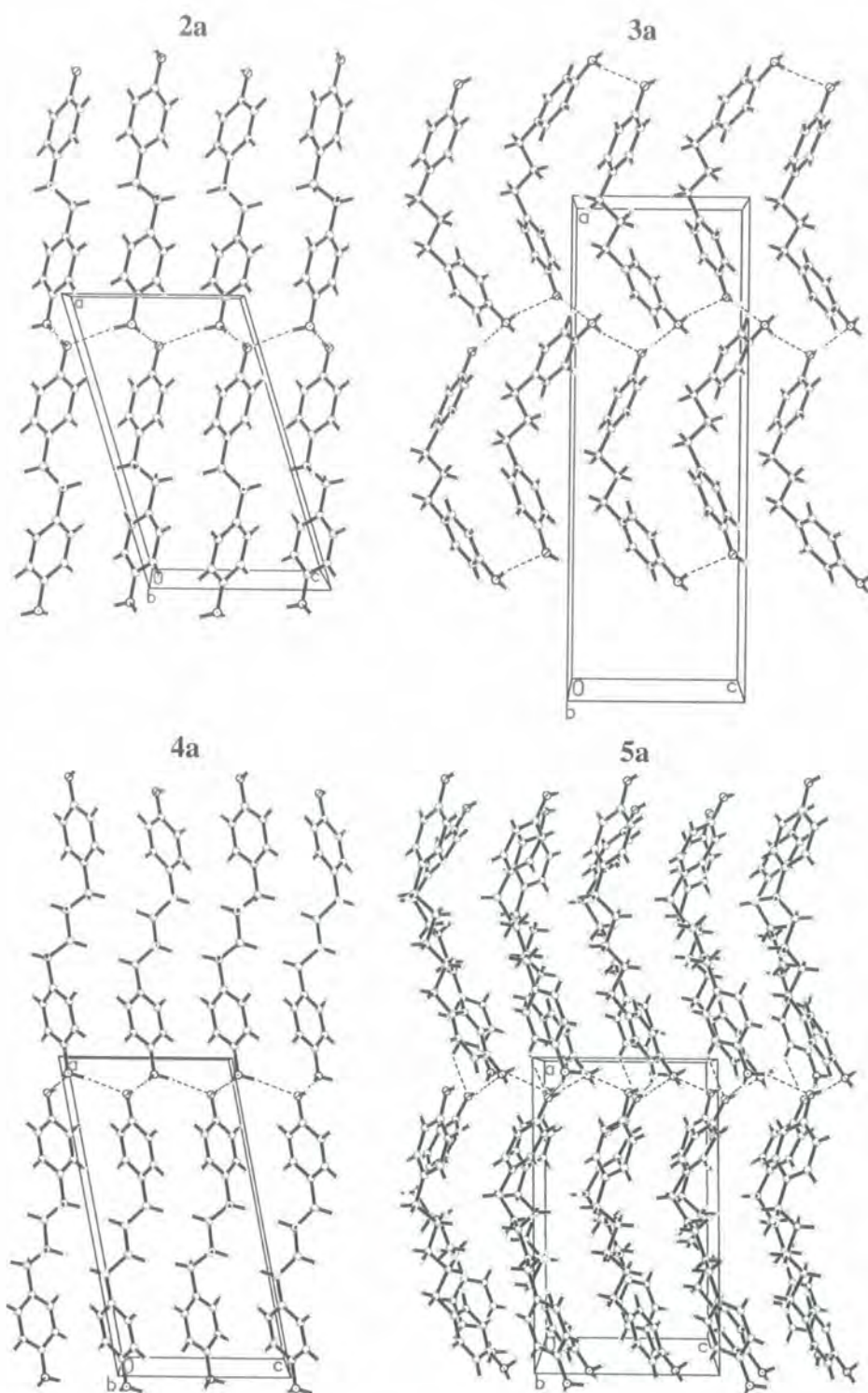


Figure 12.3: The structures of **2a**, **3a**, **4a** and **5a**, viewed down the *b*-axis. Note the similar hydrogen bond chain in each case leading to similar molecular spacing, and similar *c*-axis length's.

12.2 The 'Square Motif' Structure of 1a and The 'Stacked Vees' Structure of 3a and 5a

The β -As sheet structure of compounds **2a** and **4a** has been discussed in 11.1, but the structure of compounds **1a**, **3a** and **5a**, needs some description:

The 'Square Motif' Structure of 1a

In this structure only two of the three possible strong N(H)O hydrogen bonds are formed. The motif formed by these strong hydrogen bonds is a square, linking the molecules into chains.

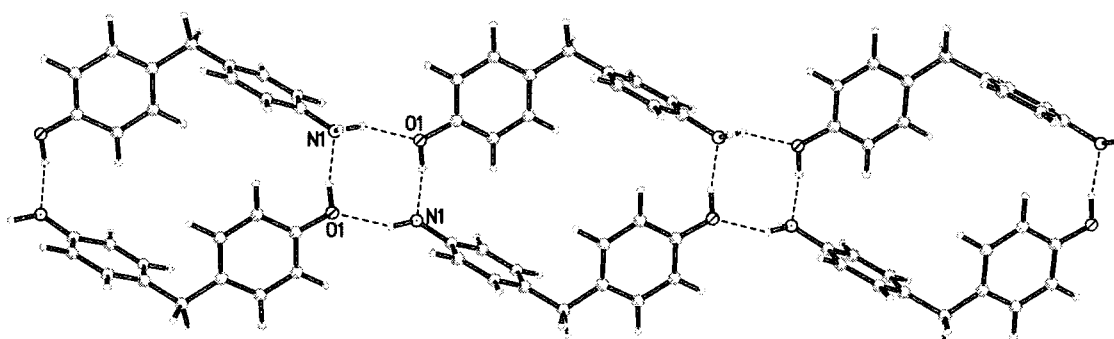


Figure 12.4: The square motif of hydrogen bonds forming chains of **1a**.

The N-H hydrogen donor not used in the above square motif is involved in a hydrogen bond to the π -electrons of the phenyl ring A (the phenyl ring of the hydroxyphenyl group). A C-H from an adjacent phenyl ring B (the phenyl ring of the aminophenyl group) is also involved in a hydrogen bond to these same π -electrons, but to the opposite face of the phenyl ring A, making a 'double faced' hydrogen bond. The phenyl ring B also acts as a hydrogen bond acceptor for a single C-H hydrogen.

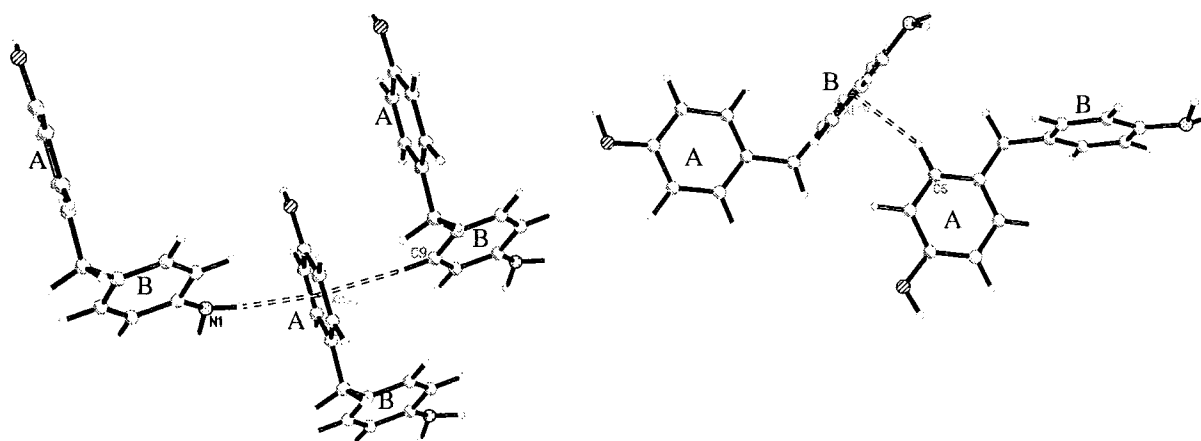


Figure 12.5: The 'double faced' hydrogen bond about the phenyl ring A, and the single C-H... π hydrogen bond to the phenyl ring B.

The 'double faced' hydrogen bonds around the phenyl ring A are important in holding adjacent chains together to form sheets.

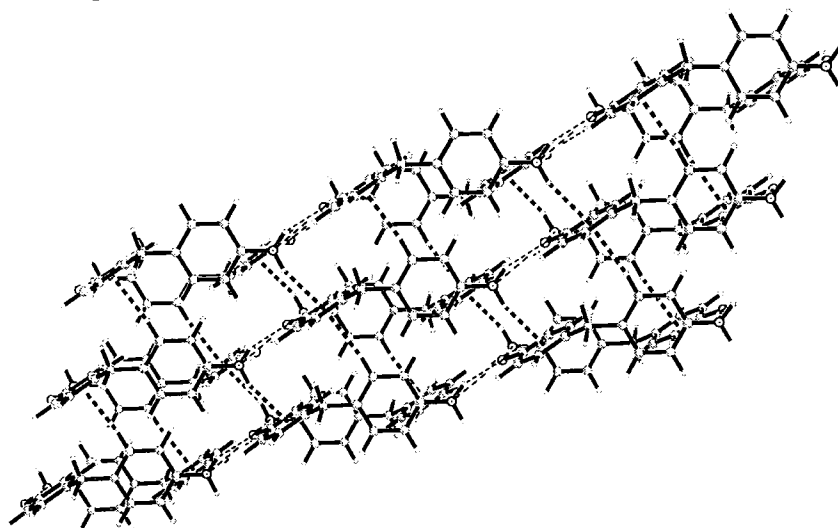


Figure 12.6: Hydrogen bonding between adjacent chains.

Adjacent sheets are then bound together by the single C-H... π bond to the phenyl ring B.

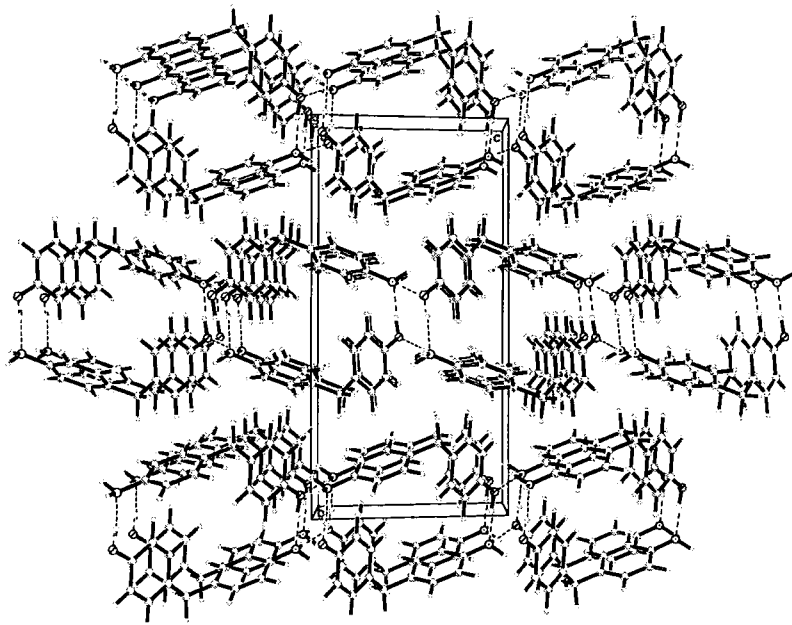


Figure 12.7: Packing of the sheets of **1a** molecules in the crystal, hydrogen bonds to the aromatic rings are not shown in this diagram.

This structure was determined by neutron diffraction on SXD at ISIS, so accurate hydrogen positions have been obtained and the geometry of the hydrogen bonds to the π -electrons in the aromatic rings can be studied in more detail.

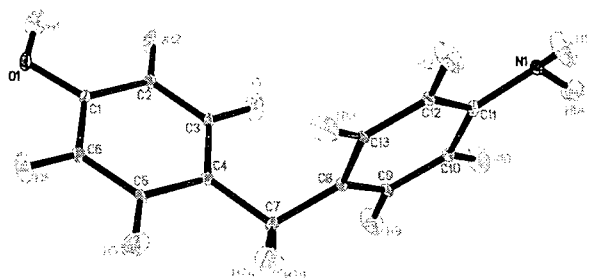


Figure 12.8: **1a** model from neutron data, showing thermal ellipsoids plotted at 50%, including hydrogen atoms.

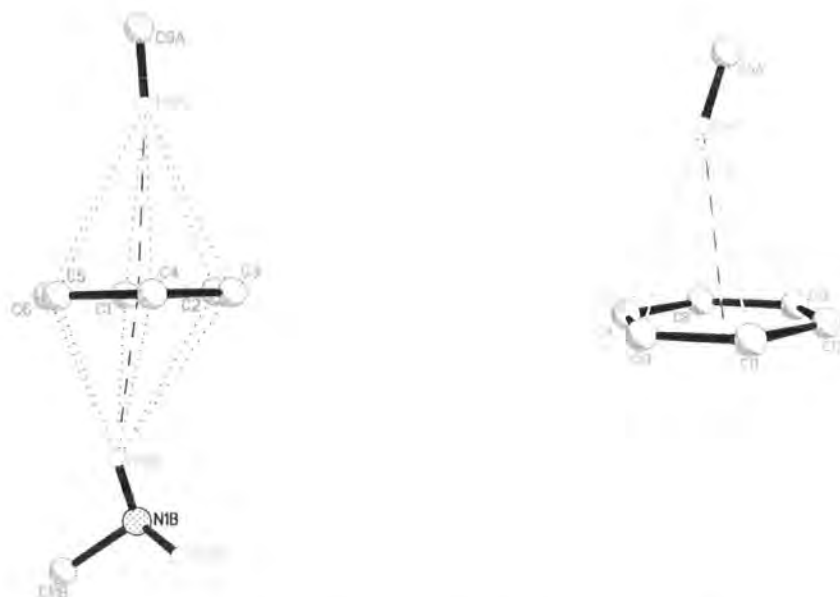
	Distance D...A /Å	Distance H...A/Å	Angle DHA /°
N ₁ -H _{1a} ...O ₁	2.723(6)	1.77(1)	167.9(9)
O ₁ -H ₁ ...N ₁	2.908(4)	1.989(9)	150.1(9)
N ₁ -H _{1b} ... π	3.33	2.40	156
C ₉ -H ₉ ... π	3.73	2.66	173
C ₅ -H ₅ ... π	3.54	2.58	148

Table 12.2: Hydrogen bond distances in compound **1a**.

	Dist. H...A / Å	Ang. DHA / °
H_{1b}...π	2.40	156
H _{1b} ...C ₁	2.56(1)	137(1)
H _{1b} ...C ₂	2.81(1)	127(1)
H _{1b} ...C ₃	2.98(1)	131.8(8)
H _{1b} ...C ₄	2.97(1)	147.1(7)
H _{1b} ...C ₅	2.74(1)	169(1)
H _{1b} ...C ₆	2.53(1)	159.9(9)

	Dist. H...A / Å	Ang. DHA / °
H₉...π	2.66	173
H ₉ ...C ₁	3.042(9)	148.1(7)
H ₉ ...C ₂	2.95(1)	154(1)
H ₉ ...C ₃	2.922(9)	158.8(7)
H ₉ ...C ₄	2.983(9)	155.2(9)
H ₉ ...C ₅	3.04(1)	150(1)
H ₉ ...C ₆	3.069(9)	146.3(7)

	Dist. H...A / Å	Ang. DHA / °
H₅...π	2.58	148
H ₅ ...C ₈	2.94(1)	127.1(7)
H ₅ ...C ₉	2.83(1)	148.8(8)
H ₅ ...C ₁₀	2.82(1)	176.6(8)
H ₅ ...C ₁₁	2.92(1)	151.6(9)
H ₅ ...C ₁₂	3.01(1)	129.7(8)
H ₅ ...C ₁₃	3.02(1)	120.7(7)

Table 12.3: The geometry of the H... π hydrogen bonds.Figure 12.9: The geometry of the H... π hydrogen bonds.

It can be seen from the tables and diagrams above, that in each case the hydrogen is closer to the aromatic ring centroid (π) than to any of the ring atoms or bonds. However while the C_9-H_9 vector points directly towards the ring centre, the N_1-H_{1b} vector points towards the C_5-C_6 bond and the C_5-H_5 vector points towards the C_{10} atom. In addition the hydrogen of the $N_1-H_{1b} \dots \pi$ interaction is definitely not located over the centre of the ring:



Figure 12.10: The $N_1-H_{1b} \dots \pi$ interaction viewed in the aromatic ring plane.

The ‘Stacked Vees’ Structure of **3a** and **5a**

Despite having different crystal symmetry (Orthorhombic $Pca2_1$, for **3a**, and Monoclinic Pc for **5a**) the packing of these structures appears remarkably similar at first glance. However, along with this similarity there are notable differences between the structures in terms of molecular geometry, molecular interactions, and overall packing.

Both compounds have four molecules in the unit cell ($z=4$) but the differences in crystal symmetry means that while **3a** has only one molecule in the asymmetric unit, **5a** has two independent molecules.

The two independent molecules of **5a** have quite different geometries (see Figure 12.11). The geometry of molecule 2 ($C_{21}-C_{37}$) is similar to that of **3a** however the geometry of molecule 1 (C_1-C_{17}) is quite different - the pentane chain is twisted at C_7 . The interesting point is that one might expect that compound **5a** could easily have taken the same crystal structure as **3a**, if molecule 1 was the same as molecule 2 the symmetry would increase. Even as it is the β angle of **5a**’s monoclinic cell is very nearly 90° , why include the twisted pentane chain geometry, when the more elegant higher symmetry structure is (at least apparently) so easily within reach? If such questions could be fully answered and understood the field of crystal engineering would be far more advanced than it is now.

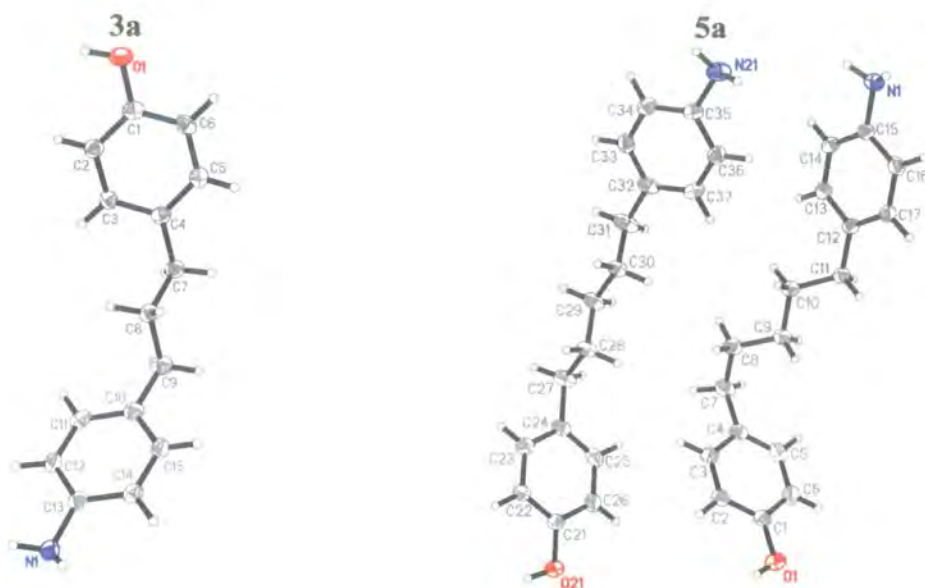


Figure 12.11: The asymmetric unit of crystals of **3a** and **5a**.

In compound **3a** the main intermolecular interaction is a simple chain of O(H)N hydrogen bonds. The chain is formed at both ends of the molecule, thus forming sheets of molecules:

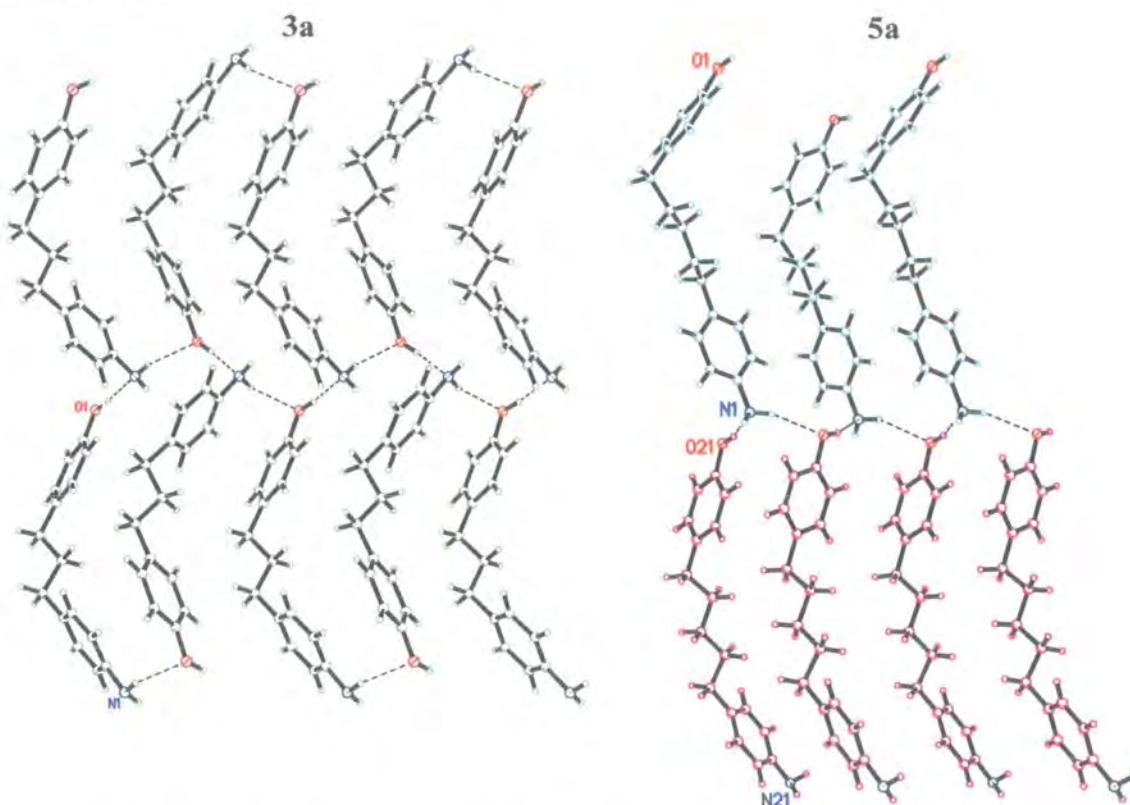


Figure 12.12: O(H)N chain in crystal **3a**, and **5a**. In the structure **5a** molecule 1 is coloured blue and molecule 2 is coloured purple for clarity.



In compound **5a** the picture is more complicated, an O(H)N chain can also be seen (see Figure 12.12) but the molecules don't have the simple alignment seen for **3a**. Looking at the row of molecules going across the page, in **3a** the molecular orientation alternates, in **5a** one row is molecule 1, all in the same orientation, the next row is molecule 2, all in opposite orientation.

Viewing the chain in **5a** from above, it can be seen that the structural pattern is much more complicated, there are various O(H)N hydrogen bonds running in approximately perpendicular directions, to form sheets.

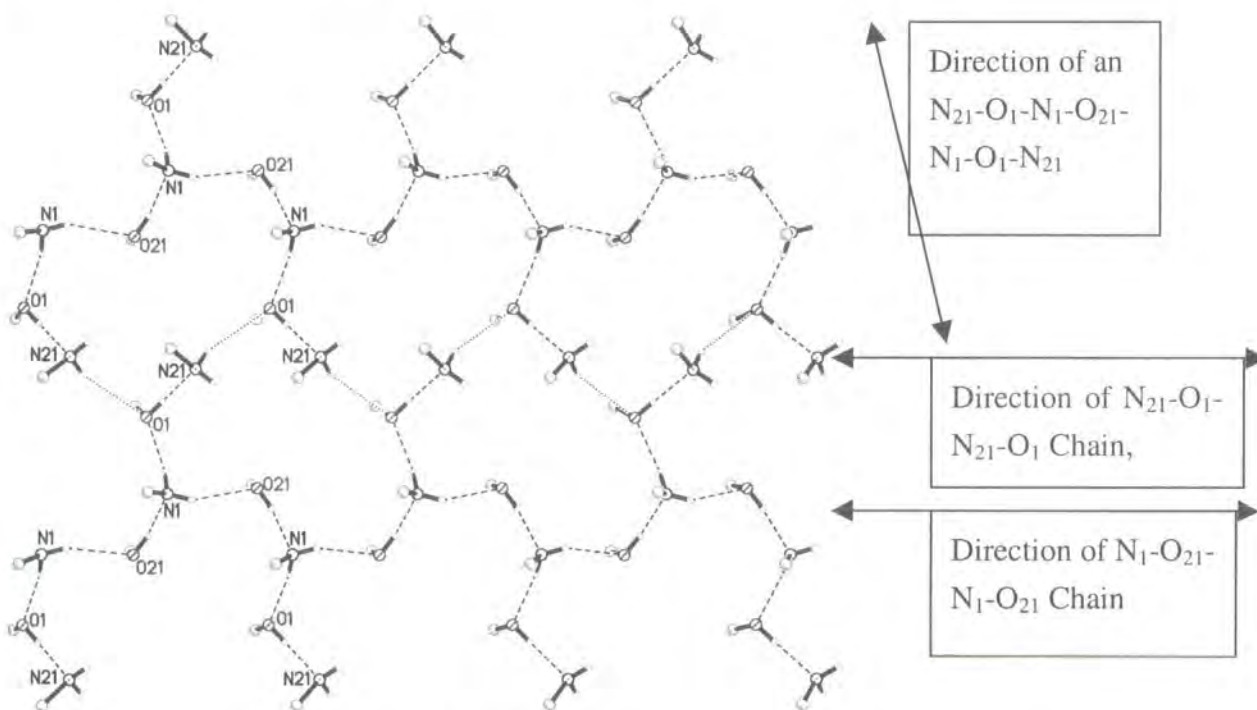


Figure 12.13: O(H)N chains in crystal **5a** viewed approximately down the molecular axis (i.e. at 90° rotation to previous diagram, the aromatic rings and pentane chain have been removed from the diagram for clarity). Note the hydrogen bond shown by dots is fairly long ($O_1 \dots H_{21b} = 2.70(3)\text{\AA}$, $O_1 \dots N_{21} = 3.461(2)\text{\AA}$).

As well as the O(H)N interactions shown above, compound **5a** also exhibits N-H... π bonds and also a bi-furcated hydrogen bond (at the acceptor) (C-H)₂...O interaction. In compound **3a** the N-H not involved in the O(H)N chain is also involved in a N-H... π interaction with a phenyl ring. These interactions are shown in Figure 12.14, the N-H... π interaction in **3a** acts to reinforce the O(H)N chain. As well as this, there is a C-H... π interaction with a phenyl ring, of a neighbouring sheets (see Figure 12.15). Table 12.4 and Table 12.5 give a full list of hydrogen bonds in compound **3a** and **5a** respectively.

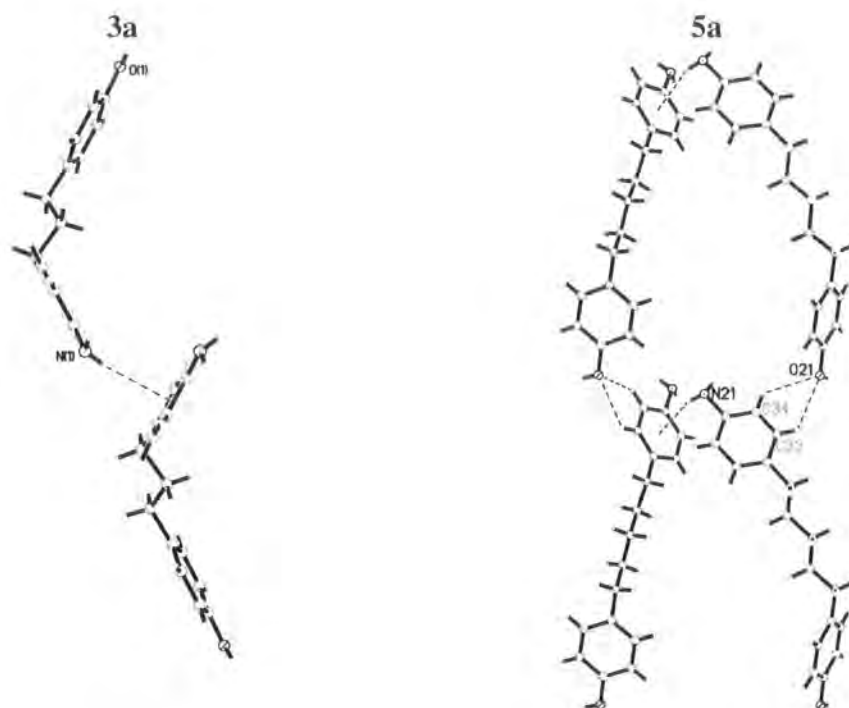


Figure 12.14: N-H... π interactions in crystals **3a** and **5a**.

	Distance D...A / Å	Distance H...A / Å	Angle DHA / °
O ₁ -H ₁ ...N ₁	2.776(2)	1.87(2)	173(2)
N ₁ -H _{1b} ...O ₁	3.205(2)	2.37(2)	115(2)
N ₁ -H _{1a} ... π	3.355	2.54	162
C ₇ -H _{7a} ... π	3.732	2.97	136

Table 12.4: Hydrogen bond distances in compound **3a**.

	Distance D...A / Å	Distance H...A / Å	Angle DHA / °
O ₂₁ -H ₂₁ ...N ₁	2.758 (2)	1.89 (3)	164 (3)
N ₁ -H _{1a} ...O ₂₁	3.181 (2)	2.38 (3)	148 (2)
N ₁ -H _{1b} ...O ₁	3.067 (2)	2.17 (3)	163 (2)
N ₂₁ -H _{21b} ...O ₁	3.461 (2)	2.70 (3)	149 (2)
O ₁ -H ₁ ...N ₂₁	2.788 (2)	1.95 (3)	170 (3)
N ₂₁ -H _{21a} ... π	3.54	2.7	155
O ₂₁ ...H ₃₃ -C ₃₃	3.312 (2)	2.70	123
O ₂₁ ...H ₃₄ -C ₃₄	3.298 (2)	2.68	123

Table 12.5: Hydrogen bond distances in compound **5a**.

From the distances and angles listed above it can be seen that, overall, the compound **5a** has shorter and more linear interactions than compound **3a**. So while the structure of **3a** appears to be the simpler and more logical structure (and certainly in terms of analysis is the easier structure to understand!) it is the structure of **5a** that is the more stable structure. Perhaps compound **3a** would take a structure closer to that of **5a** if it could, but it has less flexibility due to having a shorter alkane chain.

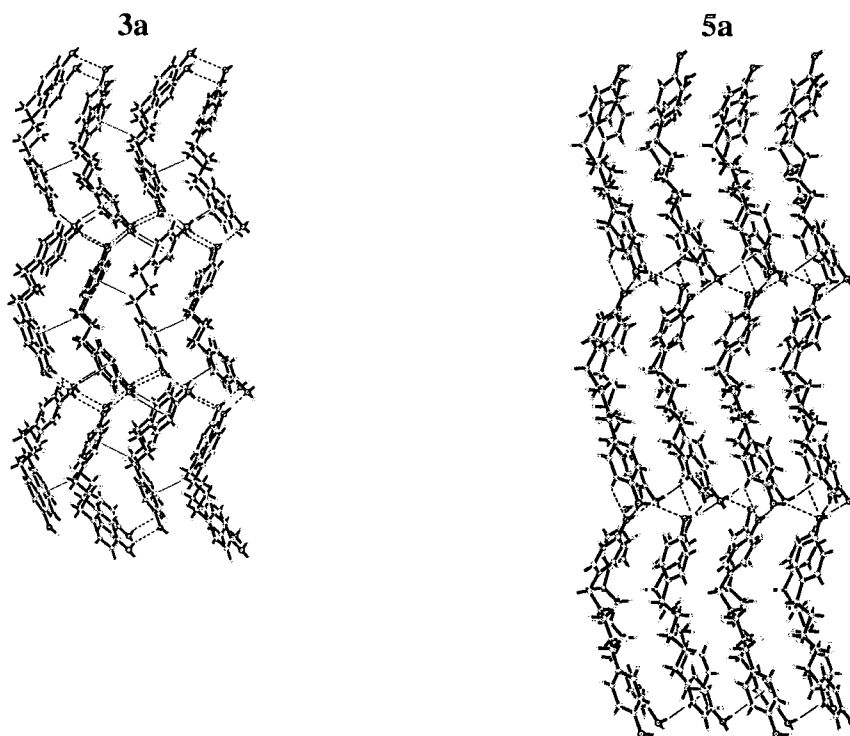


Figure 12.15: The packing of the sheets in compounds 3a, and 5a.

It can be seen from this in depth structural analysis that although at first sight the structural packing of these 2 compounds is remarkably similar and utilise very similar types of hydrogen bond interactions, they are in fact quite different in the way the interactions are used.

Chapter 13 : The Effect of Sulphur, the 4-Amino-4'-hydroxydiphenyl Sulphides and Alkanesulphides

Compounds **1b**, **2b**, **2c**, and **3b** are all sulphur derivatives of the 4-amino-4'-hydroxydiphenylalkanes, discussed in the previous chapter.

The exchange of a CH₂ group for a sulphur atom might be expected to have very little effect on the structure. The sulphur atom is slightly smaller than a CH₂ group and the angle at the sulphur is roughly 103°* compared to 109° for the -CH₂- group there is also a difference between the C-C and C-S bond lengths¹², but these differences in geometry are not great. In none of the alkane structures studied above do any of the CH₂ linker groups appear to be directly involved in structural determining interactions. But, as will be seen, the effect of sulphur is not straightforward.

13.1 Compounds With One Atom Links, 1a and 1b

Because of difficulties in obtaining diffraction quality crystals of 4-amino-4'-hydroxydiphenylsulphide (crystals appeared to be twined but the twin relationship could not be resolved). A co-crystal of methylenedianiline and thiodiphenol (**1b**) was grown and studied instead.

* Average C-S-C angle taken from CSD search¹³, April 2001 release (233,218 entries), search of only organics molecules, no disorder, no polymers, and Rfactor ≤ 10%.

Crystal Data

Code	1a -(Neutron)	1b
Link	(CH ₂)	(CH ₂):S 1:1
Structure type	Square motif chains	Square motif chains
Instrument	SXD at ISIS (Neutron) ^{9,10}	Smart-CCD ⁸
Formula weight	199.00	416.52
Temp /K	12(2)	100(2)
Crystal system	Monoclinic	Monoclinic
Space group	P2 ₁ /n	P2 ₁ /n
Colour	Brown	Colourless
Habit	Block	Block
Size /mm	1.5x1.5x1.3 Multi-crystal ¹¹	.50x.15x.05
a /Å	5.9180(3)	11.255(1)
b /Å	19.213(1)	10.1129(9)
c /Å	9.6510(4)	19.998(2)
α (= γ) / °	90	90
β /°	101.250(4)	103.654(5)
Z	4	4
μ /mm ⁻¹	1.870 (at 1 Å)	0.17
Abs. corr. type	empirical	Psi-scan
R(int)	0.064	0.1065
Data/restraints/ parameters	2365/0/189	5052/0/295
GooF	4.966	0.987
R1	0.0881	0.0571
wR2	0.1761	0.1162
Angle between C-N and C-O vectors. /°	117.1	107.9 115.2
Angle between phenyl phenol plane. /°	91.53	90.38 107.36

Table 13.1: Crystal data for the compounds with one atom in the link.

Compound **1a** had been seen to have a 'square motif' chain structure, compound **1b** has a structure based on a nearly identical motif. The main differences arise from having two different molecules involved in the chain (methylenedianiline and thiodiphenol) so there are two independent square motifs. One of these motifs shows an additional C-H...O interaction.

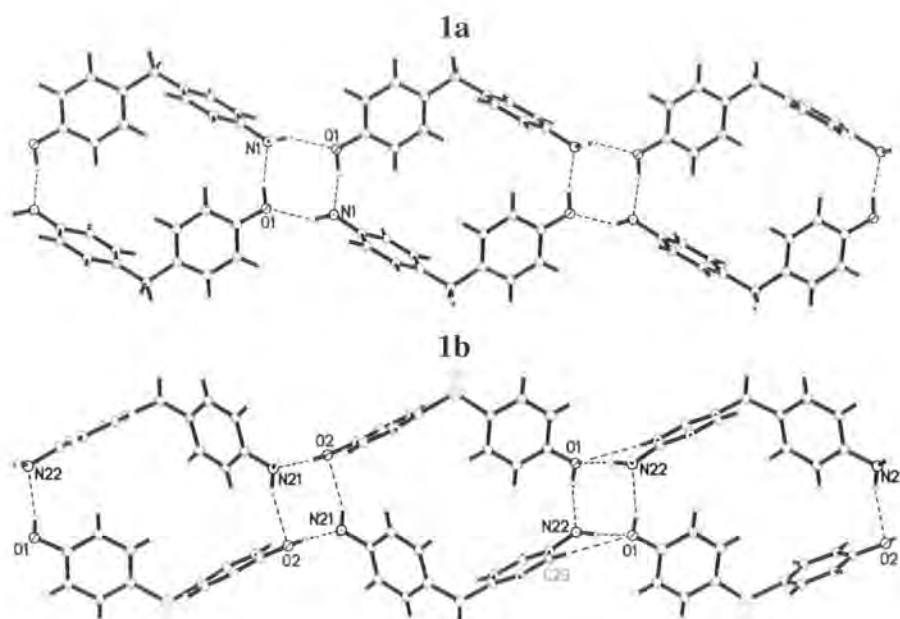


Figure 13.1: The square motif of hydrogen bonds forming chains of **1a**, and **1b**.

In compound **1a** the chains were bound into sheets by 'double faced' hydrogen bonds about the phenyl ring A (see Figure 12.5). In compound **1b** 'double faced' N-H... π ...H-C hydrogen bonds and single N-H... π hydrogen bonds are also seen. All of these π hydrogen bonds are involved in binding the chains into sheets.

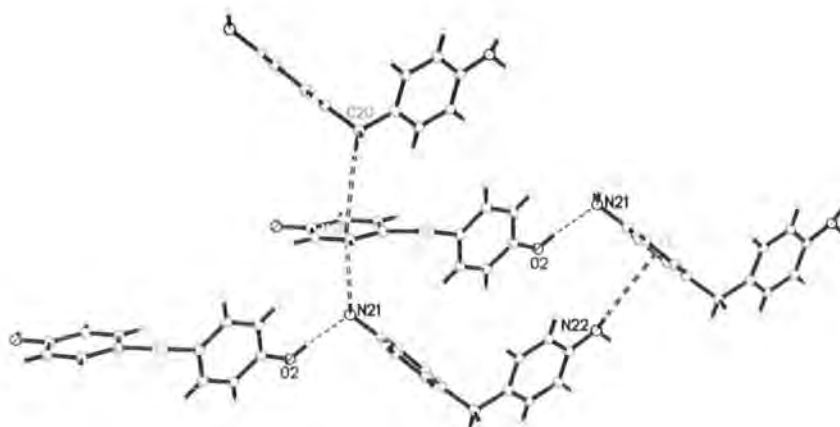


Figure 13.2: The 'double faced' hydrogen bond about the phenyl ring A and the single N-H... π hydrogen bond to the phenyl ring C.

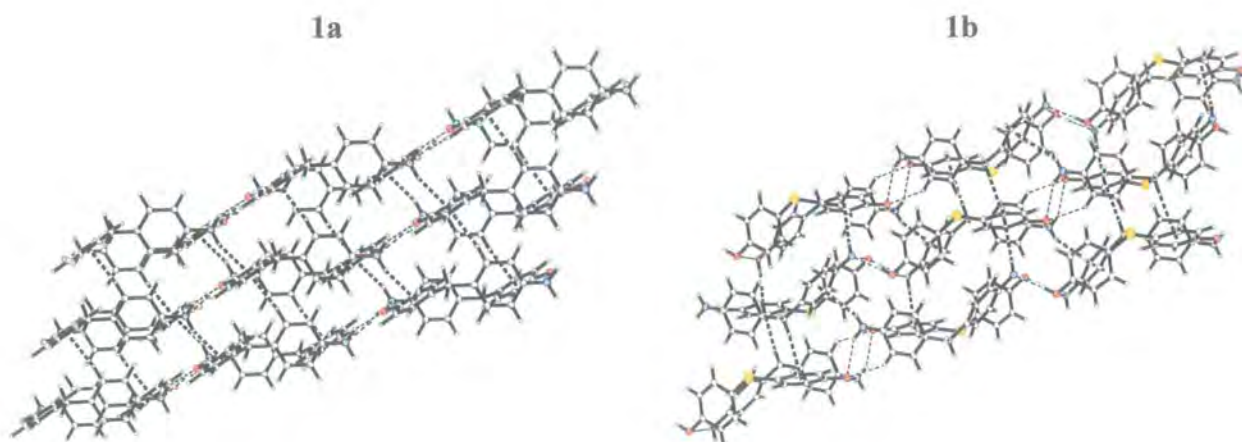


Figure 13.3: Hydrogen bonding between adjacent chains in compound **1a** and **1b**.

As can be seen from the diagram above, despite the fact that the binding between adjacent chains involves very similar interactions in both structures, visually the packing looks quite different. However, it is in the way that the sheets stack that gives the most major difference between the two structures. In compound **1a** the chains in adjacent sheets run in parallel directions, in compound **1b** the chains in one sheet run at an angle of approximately 55° to the chains in the adjacent sheets.

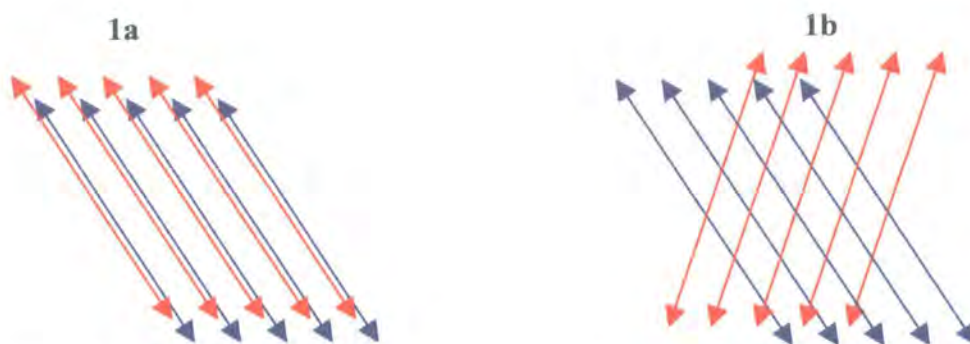
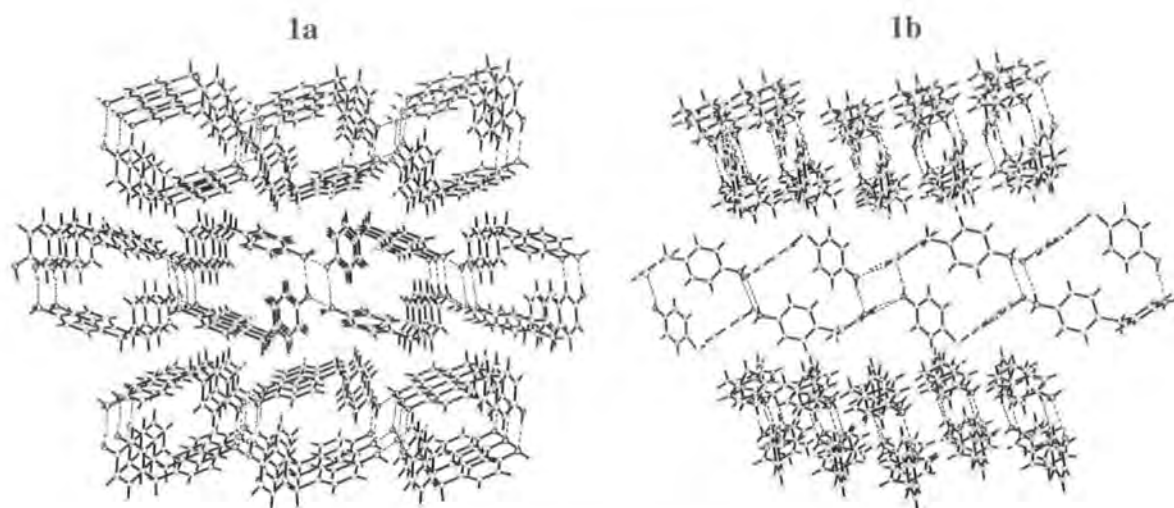


Figure 13.4: Diagram indicating the relationship between adjacent chains in compound **1a**, and **1b**. Each arrow represents a chain, chains in one sheet are coloured blue, chains in the adjacent sheet are coloured red.

Figure 13.5: The packing of the sheets in compound **1a**, and **1b**.

	Distance D...A /Å	Distance H...A /Å	Angle DHA /°
N ₁ -H _{1a} ...O ₁	2.723(6)	1.77(1)	167.9(9)
O ₁ -H ₁ ...N ₁	2.908(4)	1.989(9)	150.1(9)
N ₁ -H _{1b} ...π	3.33	2.40	156
C ₉ -H ₉ ...π	3.73	2.66	173
C ₅ -H ₅ ...π	3.54	2.58	148

Table 13.2: Hydrogen bond distances in compound **1a**.

	Distance D...A /Å	Distance H...A /Å	Angle DHA /°
N ₂₁ -H _{21b} ...O ₂	3.167(4)	2.26(3)	159(2)
N ₂₂ -H _{22b} ...O ₁	3.167(4)	2.36(3)	152(3)
O ₁ -H _{1a} ...N ₂₂	2.798(3)	1.99(3)	162(3)
O ₂ -H _{2a} ...N ₂₁	2.760(3)	1.88(4)	175(4)
C ₂₉ -H ₂₉ ...O ₁	3.372(3)	2.56	143
N ₂₁ -H _{21a} ...π _a	3.340	2.65	137
C ₂₀ -H _{20a} ...π _a	3.745	2.82	156
N ₂₂ -H _{22a} ...π _b	3.739	3.08	136

Table 13.3: Hydrogen bond distances in compound **1b**.

13.2 Compounds With Two Atoms in the Link, 2a, 2b and 2c

Crystal Data

Code	2a	2b	2c
Link	2(CH ₂)	CH ₂ S	S ₂
Structure type	β-As sheet	β-As sheet	Combination structure
Instrument	Smart-CCD ⁸	Rigaku AFC6S ¹⁴	Smart-CCD ⁸
Formula weight	213.27	231.30	249.34
Temp /K	100(2)	100(2)	100(2)
Crystal system	Monoclinic	Monoclinic	Monoclinic
Space group	Pc	Pc	P2 ₁ /c
Colour	Colourless	Pale Brown	Yellow
Habit	Plate	Prism	Block
Size /mm	.50x.35x.10	.45x.15x.05	.55x.50x.10
a /Å	13.682(3)	13.844(3)	10.432(1)
b /Å	5.262(1)	5.163(1)	8.118(1)
c /Å	8.192(2)	8.249(2)	14.791(2)
α (= γ) / °	90	90	90
β / °	107.28(3)	107.22(3)	109.633(6)
Z	2	2	4
μ /mm ⁻¹	0.079	0.235	0.428
Abs. corr. type	None	None	Psi-scan
R(int)	0.0322	0.0449	0.0278
Data/restraints/parameters	2509/2/205	1935/2/158	2926/0/157
GooF	1.034	1.095	1.078
Flack parameter	-0.7(13)	0.02(3)	-
R1	0.0405	0.0435	0.0348
wR2	0.1087	0.1170	0.0836
Angle between C-N and C-O vectors. /°	175.5	174.0	88.25
Angle between phenyl phenol plane. /°	2.25	4.69	94.14

Table 13.4: Crystal data for the compounds with two atoms in the link.

The exchange of one of the CH₂ groups for a sulphur atom results in very little change in crystal structure, the only major change is the presence of a C-H...S interaction that will increase the overall stability of the β -As sheet structure.

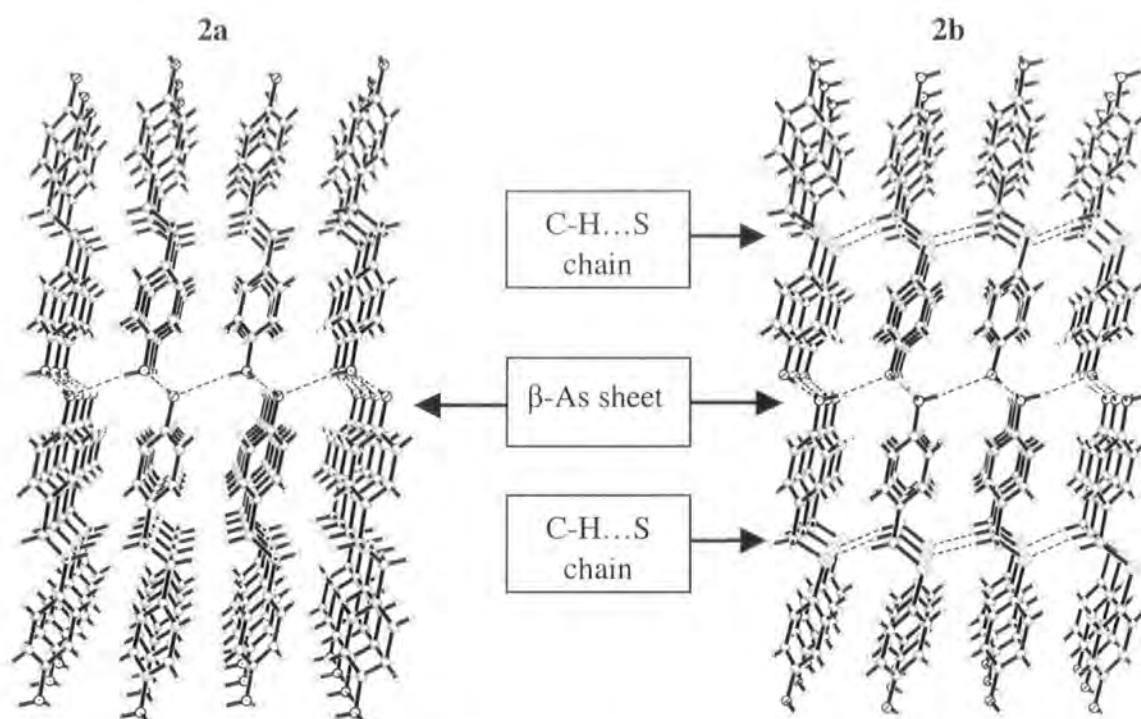


Figure 13.6: The structure of **2a**, and **2b**, showing the β -As sheet structure in both cases and the additional C-H...S chains in compound **2b**.

	Distance D...A / Å	Distance H...A / Å	Angle DHA / °
N ₁ -H _{1a} ...O ₁	3.312(2)	2.34(3)	177(3)
N ₁ -H _{1b} ...O ₁	3.130(2)	2.23(3)	170(2)
O ₁ -H ₁ ...N ₁	2.815(2)	2.02(3)	173(3)

Table 13.5: Hydrogen bond distances in compound **2a**.

	Distance D...A / Å	Distance H...A / Å	Angle DHA / °
N ₁ -H _{1a} ...O ₁	3.299(5)	2.45(6)	170(4)
N ₁ -H _{1b} ...O ₁	3.148(5)	2.24(5)	172(4)
O ₁ -H ₁ ...N ₁	2.785(4)	1.81(7)	178(6)
C ₇ -H _{7a} ...S ₁	3.849(4)	2.94	153.2

Table 13.6: Hydrogen bond distances in compound **2b**.

The exchange of both CH_2 groups for sulphur atoms, however, results in a completely different structure type. Even the molecular geometry of compound **2c** is completely different to that of **2a** and **2b**: the $\text{Ph-CH}_2\text{-CH}_2\text{-Ph}$ torsion angle in **2a** is $176.5(2)^\circ$, the $\text{Ph-CH}_2\text{-S-Ph}$ torsion angle in **2b** is $179.5(3)^\circ$, whereas the Ph-S-S-Ph torsion angle in **2c** is $83.3(1)^\circ$.

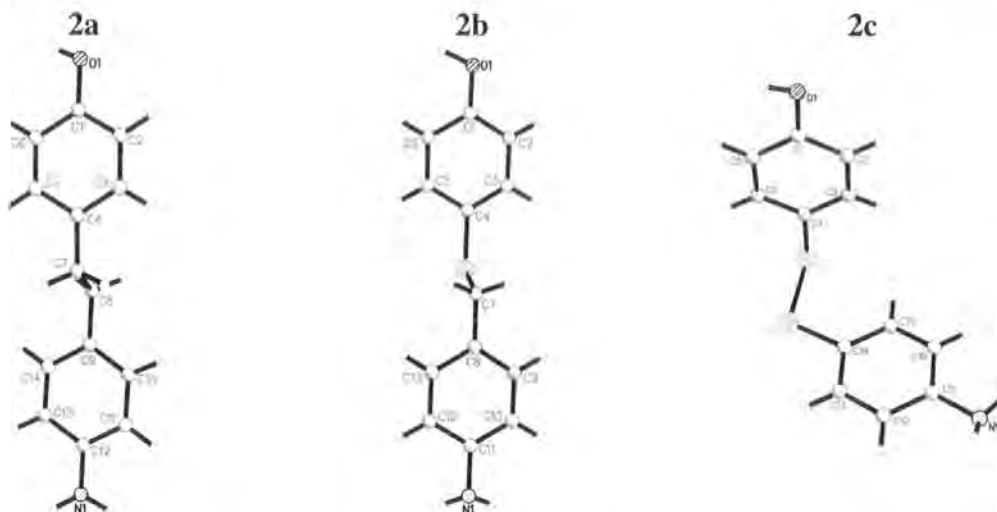
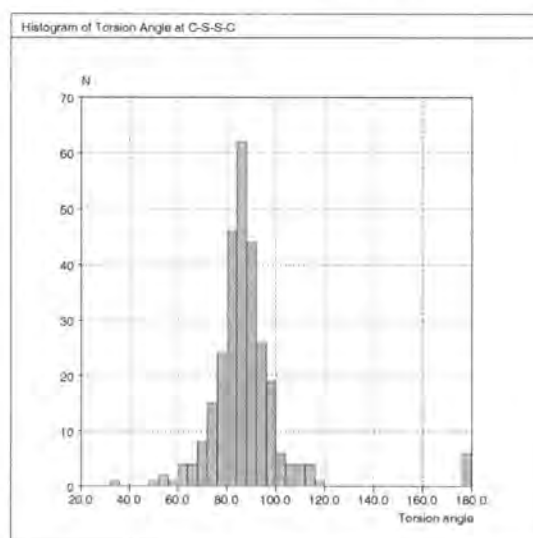


Figure 13.7: The molecular geometry of **2a**, **2b**, and **2c**.

This sudden change in molecular geometry may seem unexpected but a quick survey of the CSD^{13*} reveals that torsion angles of approximately 90° are average for -C-S-S-C- systems, whereas torsion angles of around 180° (or 0°) are extremely rare.



Graph 13.1: C-S-S-C torsion angles ($^\circ$) occurring in CSD¹³.

* C-S-S-C torsion angle search using April 2001 release (233,218 entries) of the CSD¹³, search of only organics molecules, no disorder, no polymers, and $R_{\text{factor}} \leq 10\%$.

The structure of **2c** is complicated and does not really fall into any of the structure types seen so far, however the structure does exhibit the inevitable O-H...N-H chains, forming into sheets and these sheets bear a passing resemblance to a twisted version of those seen in compound **3a** (see Figure 12.12).

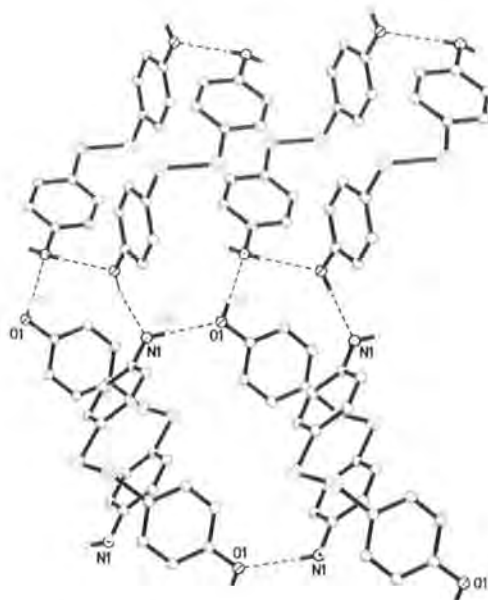


Figure 13.8: N(H)O chains in compound **2c** forming sheets.

A side view down a stack of these sheets shows a structure with a possible similarity to the square motif of **1a** (see Figure 12.7), but the motifs and interactions behind this structure are quite different.

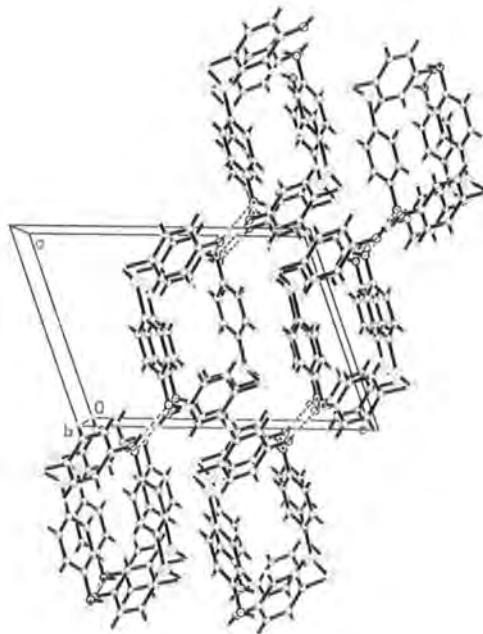


Figure 13.9: The packing of the sheets of **2c**.

This structure is unusual for this series in the lack of hydrogen interactions. Aside from the N(H)O hydrogen bond chain there is only a single C-H...S hydrogen bond. Other than these interactions, any possible contacts are both long and far from linear.

	Distance D...A /Å	Distance H...A /Å	Angle DHA /°
N ₁ -H _{1b} ...O ₁	3.031(2)	2.25(2)	163(2)
O ₁ -H ₁ ...N ₁	2.763(2)	1.92(2)	177(2)
C ₁₆ -H _{16a} ...S ₁	3.685(2)	2.97	133

Table 13.7: Hydrogen bond distances in compound 2c.

13.3 Compounds With Three Atoms in the Link, 3a and 3b

Crystal Data

Code	3a	3b	5a
Link	3(CH ₂)	2(CH ₂)S	5(CH ₂)
Structure type	Stacked Vees	Stacked Vees	Stacked Vees
Instrument	Smart-CCD ⁸	Smart-CCD ⁸	Smart-CCD ⁸
Formula weight	227.30	245.33	255.35
Temp /K	100(2)	100(2)	100(2)
Crystal system	Orthorhombic	Monoclinic	Monoclinic
Space group	Pca2 ₁	Pc	Pc
Colour	Colourless	Colourless	Colourless
Habit	Plate	Block	Block
Size /mm	.52x.25x.07	.35x.25x.20	.60x.55x.30
a /Å	23.9370(7)	12.6341(9)	14.9554(9)
b /Å	6.2160(2)	5.8636(4)	11.2370(8)
c /Å	8.3970(3)	8.5671(5)	8.6841(6)
α (= γ) / °	90	90	90
β / °	90	90.351(3)	90.893(3)
Z	4	2	4
μ /mm ⁻¹	0.075	0.238	0.071
Abs. corr. type	None	Psi-scan	Psi-scan
R(int)	0.0374	0.0256	0.0215
Data/restraints/ parameters	3440/1/223	3138/2/166	5476/2/367
GooF	1.016	1.055	1.033
Flack parameter	0.4(15)	0.04(6)	-0.2(11)
R1	0.0421	0.0322	0.0355
wR2	0.0935	0.0822	0.0885
Angle between C-N and C-O vectors. /°	119.5	112.6	129.4 125.1
Angle between phenyl phenol plane. /°	55.94	76.09	81.37 69.99

Table 13.8: Crystal data for compounds with three atoms in the link, and also compound 5a for comparison.

Structurally compound **3b** seems to share characteristics with both variations on the 'stacked vees' structure, structures **3a** and **5a**. Just like compound **3b** there is just one molecule in the asymmetric unit. The same simple O(H)N chains are seen in all three cases. However, in **3a** horizontally adjacent molecules have alternating orientations, whereas in **3b**, and **5a** the molecular orientation is the same in adjacent molecules.

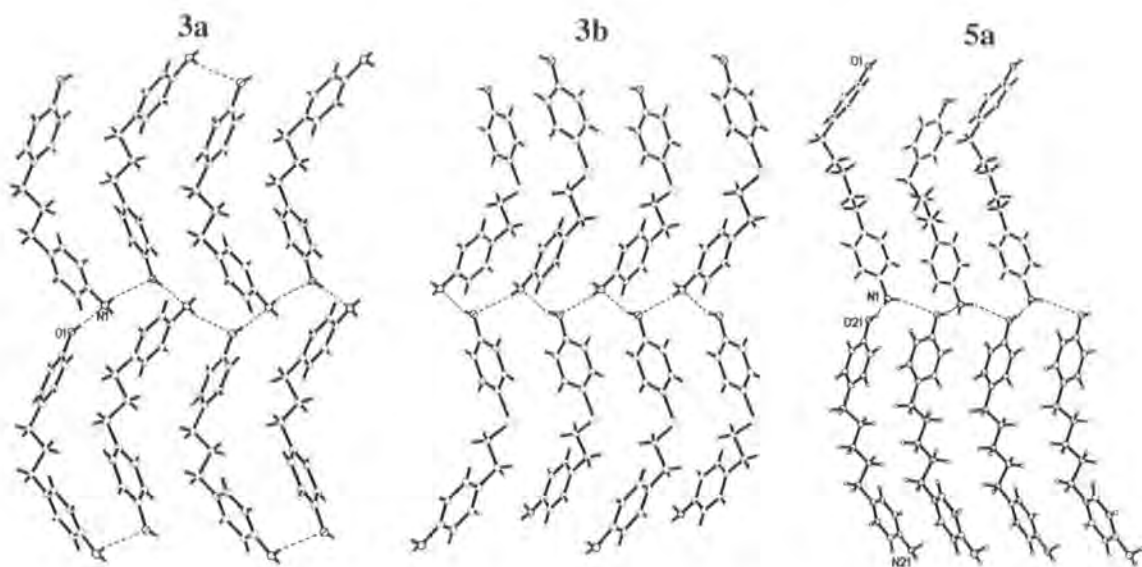


Figure 13.10: The O(H)N chain in compound **3a**, **3b** and **5a**.

As well as the O(H)N chains, all three compounds utilise other interactions to increase the structural stability (Figure 13.11). Compound **3a** has only N-H... π hydrogen bonds whereas **3b**, and **5a** exhibit both N-H... π and bi-furcated (C-H)₂...O hydrogen bonds. The geometry of these interactions in **3b**, and **5a** is remarkably similar.

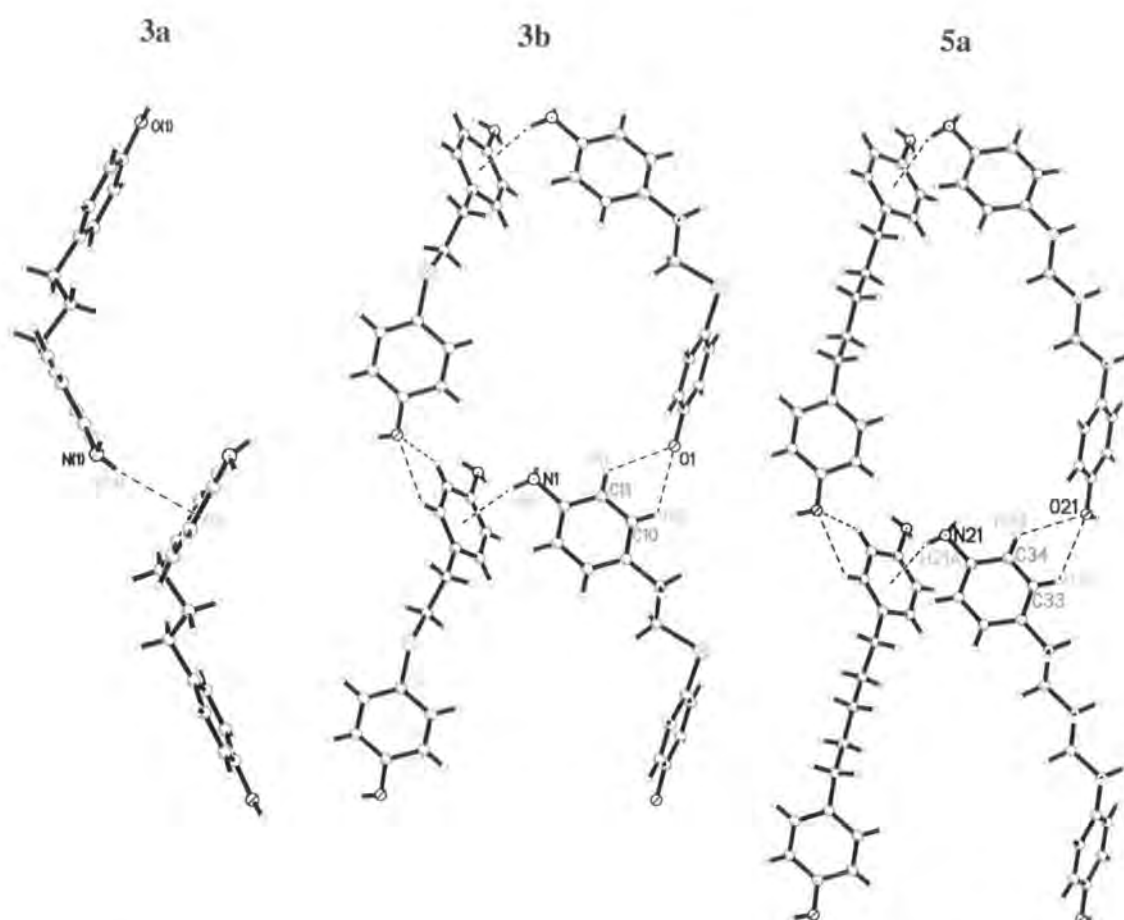


Figure 13.11: The interactions in compounds **3a**, **3b** and **5a** that form in addition to the $O(H)N$ chain.

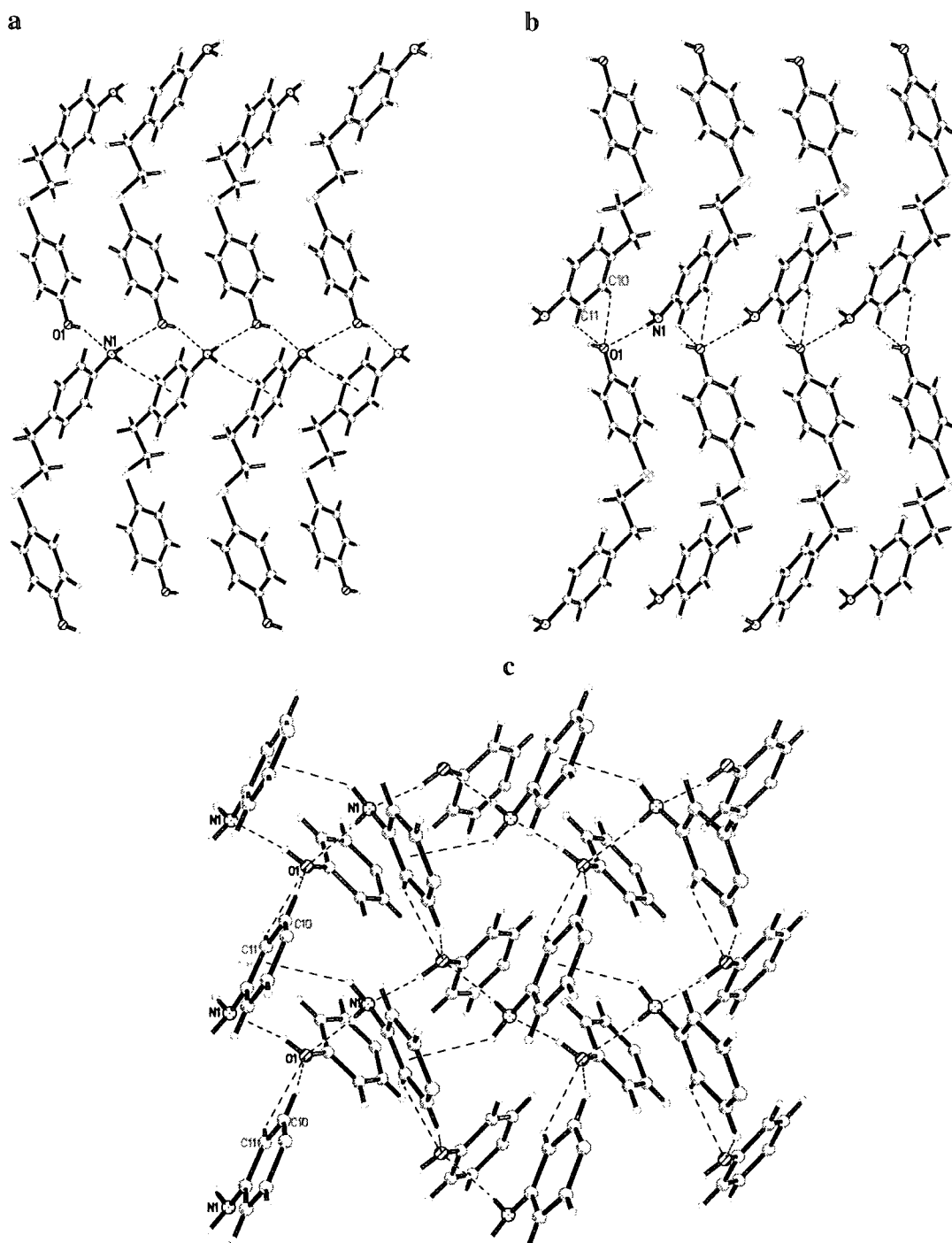


Figure 13.12: The interactions in compound **3b** a) O(H)N chains with additional N-H... π interactions, b) chains of N-H...O and bi-furcated (C-H)₂...O hydrogen bonds, c) both of the previous chains forming sheets of hydrogen bonds, viewed from above with part of each molecule removed for clarity.

This all begs the question of why, if the similarities are so great, are there three forms of this structure? If **3b** and **5a** form structures that are so similar and based on nearly

identical interactions why does **3b** need only one molecule in the asymmetric unit but **5a** two independent molecules? Is it all due to which molecular geometries are possible; how much the linker chain can twist?

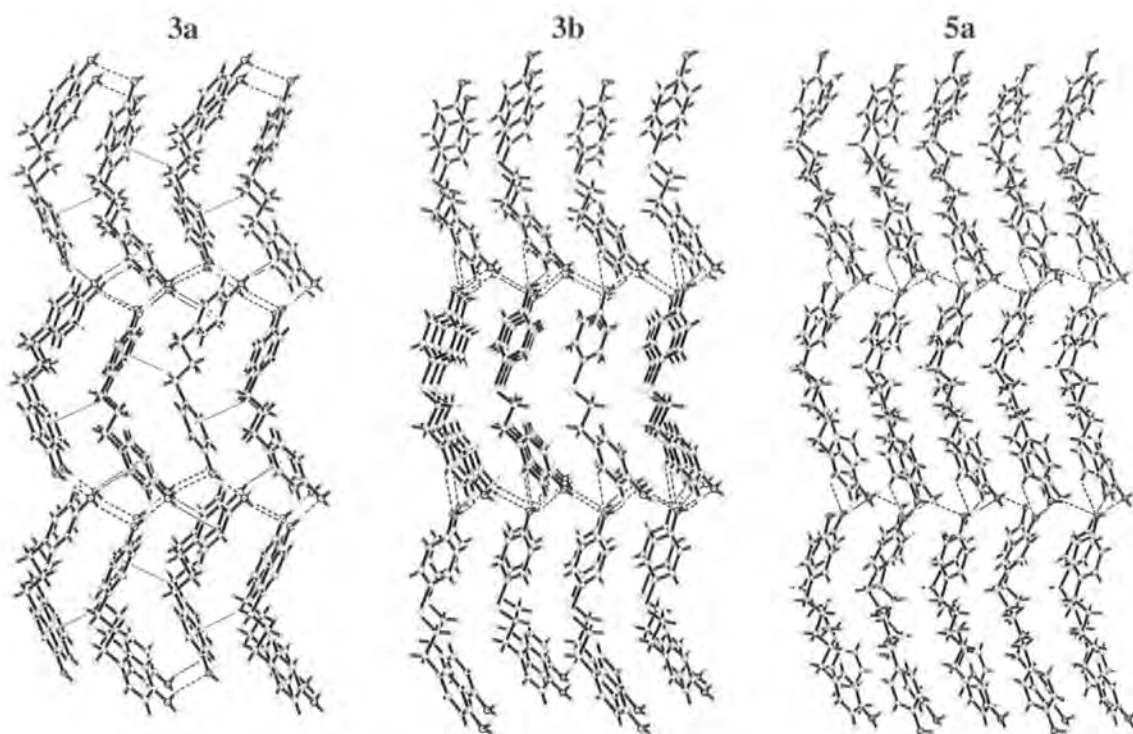


Figure 13.13: The overall crystal packing of compound **3a**, **3b** and **5a**.

	Distance D...A / Å	Distance H...A / Å	Angle DHA / °
N ₁ -H _{1a} ...O ₁	3.114(2)	2.29(3)	174(2)
O ₁ -H ₁ ...N ₁	2.754(2)	1.98(3)	152(3)
O ₁ ...H ₁₀ -C ₁₀	3.199(2)	2.58	123
O ₁ ...H ₁₁ -C ₁₁	3.912(2)	2.58	123
C ₁₆ -H _{16a} ...π	3.382	2.61	175

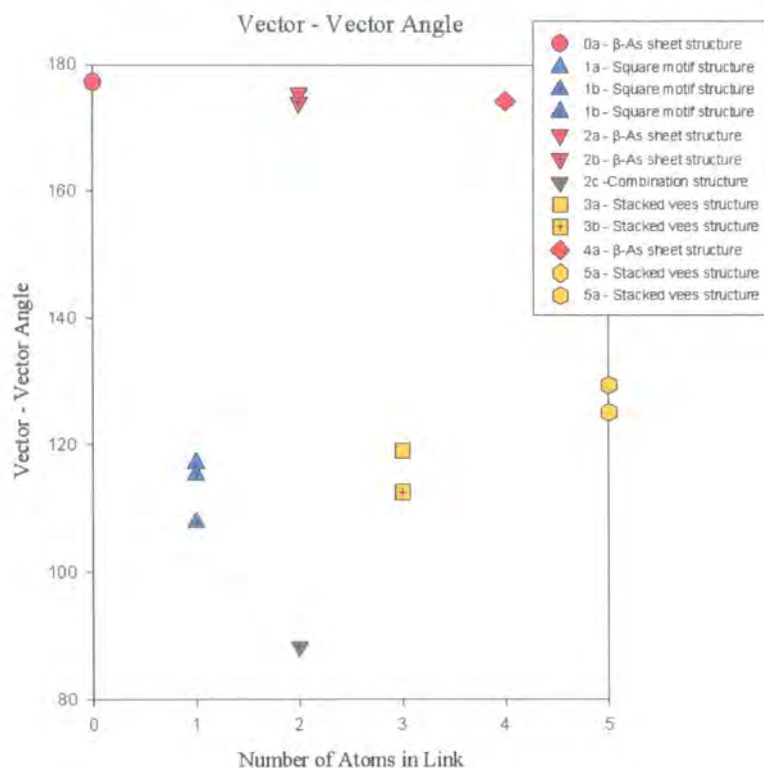
Table 13.9: The hydrogen bond distances in compound **3b**.

Chapter 14 : Conclusions

14.1 Molecular Geometry

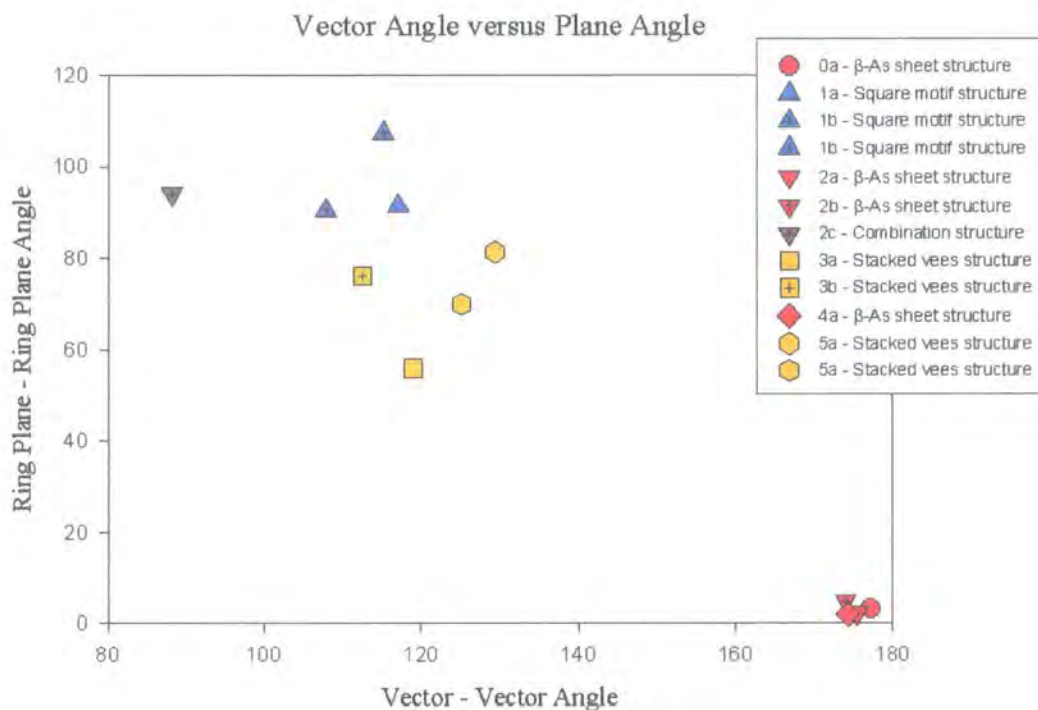
The close correlation between the number of atoms in the alkane or sulphur-alkane chain and the structure is clearly illustrated by the graph below: The red data points correspond to β -As sheet structures, blue data points to 'square motif' structures, yellow to 'stacked vees' structures and grey to the structure of **2c** that does not fall into any of the other structure categories.

Other than compound **2c**, all the compounds with an even number of atoms in the link have a β -As sheet structure whereas compounds with one atom in the link form 'square motif' structures, and compounds with three or five atoms in the link form 'stacked vees' structures. The exchange of a CH_2 group for a sulphur atom (data points marked by a cross) has no effect on the structure type.



Graph 14.1: Ph-N vector, Ph-O vector angle in relation to the number of atoms in the link. Note: compounds **1b**, and **5a** have two molecules in the asymmetric unit, and therefore two data points.

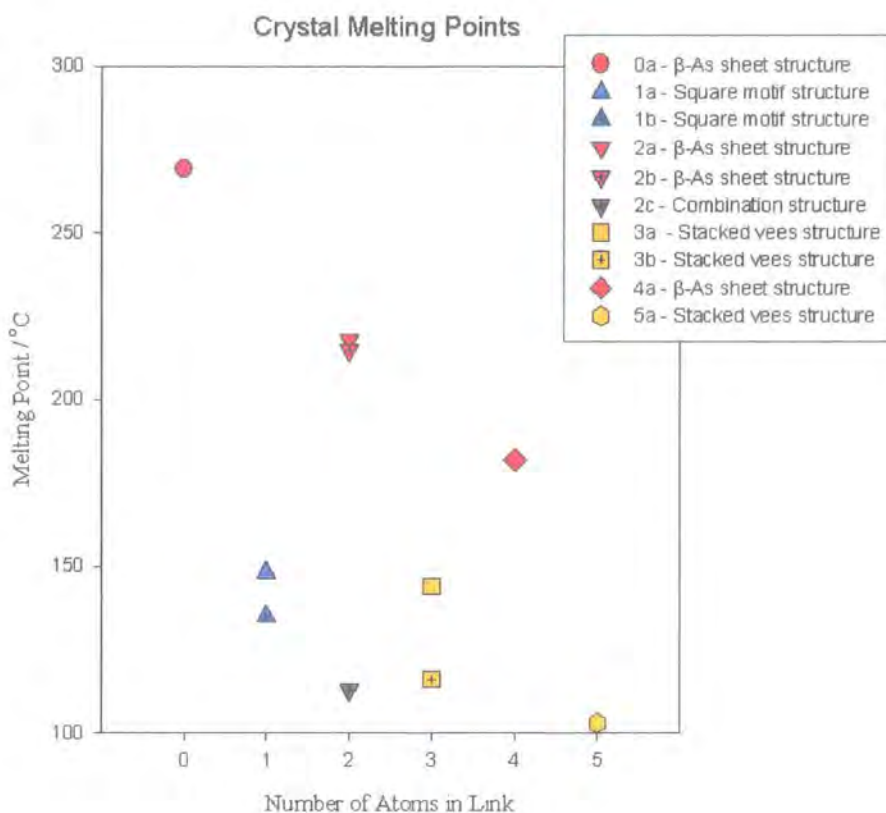
It is the Ph-N vector, Ph-O vector angle that truly distinguishes the β -As sheet structures from the other types. When the angle between the phenyl plane and the phenol plane is considered as well, the compounds separate into 3 distinct clusters based on structural type. Among this small data set these two parameters are sufficient to distinguish the structure types.



Graph 14.2: Ph-N vector, Ph-O vector angle versus the angle between the phenyl plane and the phenol plane.

14.2 Melting Point Comparisons

The graph of the crystal melting points for the compounds is very interesting. Firstly the β -As sheet structures melt at a higher temperature than the other structural types, indicating that the sheet structure, that instinctively seems so stable, is more stable than the other structures. As the number of atoms in the link increases, the melting point decreases. This is unexpected as melting points generally increase with increasing molecular weight, but in this case there are a constant number of hydrogen bonds regardless of molecular weight, so as the molecule gets bigger the relative effect of the hydrogen bonds decreases, and as the link gets longer it has more freedom of movement, which could help destabilise the structure.



Graph 14.3: Melting points of the crystals.

14.3 Conclusions

This series highlights some of the difficulties of structure prediction: the subtle complexities of a crystal structure, seen clearly in the various stacked vees structure, the large changes in overall structure, despite the same initial motif seen in the square motif structures: the way that exchanging a CH_2 group for an sulphur atom can have no structural effect, but repeating the procedure on a second CH_2 group results in a complete structural change, as seen in the 2 atom linker mini-series **2a-c**.

It will be interesting to study the structures of more compounds in this series. At this point in the series trends are starting to appear and predictions are perhaps possible and further questions raised:

- Do the 6 and 8 atom linker molecules form the β -As sheet structure as predicted from the results above, or is the alkane chain too long and the resulting molecule too flexible to be stabilised by the β -As sheet?

- At what point is the alkane chain too long to form a stable β -As sheet structure, and can the structure be stabilised by the addition of sulphur atoms into the alkane chain allowing the formation of C-H...S cross links?
- Will the addition of further sulphur atoms into the 3 atom linker series cause a change from the 'stacked vees' structure? And is the order of the atoms in the linker important i.e does -S-CH₂-S- linker molecule have an analogous structure to the 'stacked vees' structure of the -S-CH₂-CH₂- linker (**3a** and **3b**), whereas the -S-S-CH₂- linker molecule contain a 90° torsion angle about the S-S group preventing the 'stacked vees' structure forming, or is the effect of the -S-CH₂-S- and the -S-S-CH₂- linker the same?

14.4 References for Part 2

- 1) O.Ermer and A.Eling. *J. Chem. Soc. Perkin Trans. 2*, 1994, 925-944.
- 2) F.H.Allen, W.D.S.Motherwell, P.R.Raithby, G.P.Shields, R.Taylor. *New J. Chem.*, 1999, 25-34.
- 3) S.Hanessian, A.Gomtsyan, M.Simard, S.Roelens. *J. Am. Chem. Soc.*, 1994, **116**, 4495-4496.
- 4) S.Hanessian, M.Simard, S.Roelens. *J. Am. Chem. Soc.* 1995, **117**, 7630-7645.
- 5) S.Hanessian, R.Saladino, R.Margarita, M.Simard. *Chem. Eur. J.*, 1999, **5**, 2169-2183.
- 6) F.H.Allen, V.J.Hoy, J.A.K.Howard, V.R.Thalladi, G.R.Desiraju, C.C.Wilson, G.J.McIntyre. *J. Am. Chem. Soc.*, 1997, **119**, 3477-3480.
- 7) V.J.Hoy, *Weak Intermolecular Interactions in Organic Systems : a Concerted Study Involving X-ray and Neutron Diffraction and Database Analysis*, Ph.D thesis, University of Durham, 1996.
- 8) SMART-1000 CCD, Bruker AXS, Madison, Wisconsin, U.S.A.
- 9) C.C.Wilson. in *Neutron Scattering Data Analysis*, ed. M.W.Johnson, pp.145-163, IoP Conference Series, **107**, Bristol: Adam Hilger, 1990.
- 10) C.C.Wilson. *J. Mol. Struct.*, 1997, **405**, 207-217.
- 11) C.C.Wilson. *J. Appl. Cryst.*, 1997, **30**, 184-189.
- 12) F.H.Allen, O.Kennard, D.G.Watson, L.Brammer, A.G.Orpen, R.Taylor, *J. Chem. Soc. Perkin Trans. 2*, 1987, S1-S19.
- 13) F.H.Allen, O.Kennard. *Chem. Des. Autom. News*, 1993, **8**, 30-37.
- 14) a) MSC/AFC. Molecular Structure Corporation (1991). b) Molecular Structure Corporation (1991). MSC/AFC Diffractometer Control Software. (1991). MSC, 3200 Research Forest Drive, Woodlands, TX77381, U.S.A.

Part 3:

Interesting Structures

Chapter 15 : Introduction

In this final section the structures of a number of compounds (**6-10** in Figure 15.1 overleaf) have been analysed in detail. The aim is to identify and understand which interactions and molecular features are influencing the structure, and especially to look for any unusual or novel interactions that may often be overlooked in wider studies.

Compounds **6** and **7** produced crystals of a suitable quality and size for neutron diffraction experiments to be carried out, so accurate hydrogen positions can be obtained, and the various hydrogen bond interactions benchmarked.

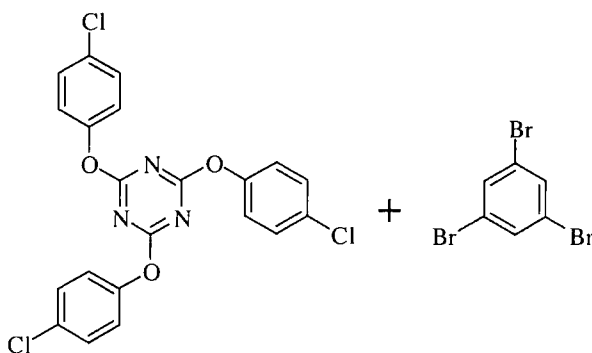
Compound **10** is especially interesting since it can be crystallised in at least five different polymorphs. Ongoing work is being undertaken to obtain, identify and characterise further polymorphs.

All of these compounds have been made as part of wider series for studies into different aspects of crystal engineering, nanotubes and host-guest matching (**6** and **7**)^{1,2}, polymorphism (**10**)³, second harmonic generation (**6**⁴ and **8**), and interplay of a weak and a strong hydrogen bonding group (**9**)⁵, however each one is interesting in its own right and worthy of individual study such as has been carried out here.

Often the structures of these compounds are better understood when taken in a wider context, so while the crystal structure of only one compound is considered in detail in each case, comparisons are drawn to other related compounds taken from literature and the CSD⁶. This helps the understanding of which features of the structural motif are robust enough to be structure determining, the relative influence of various substituents in determining the motif, and the effect of different solvents, guest molecules and co-crystallants on the structure.

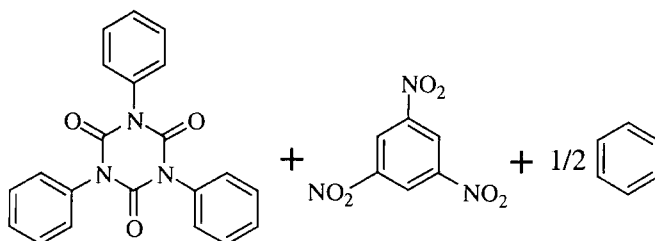
Chapter 16:

- 6) 2,4,6-*tris*-(4-chlorophenoxy)-1,3,5-triazene and tribromobenzene.



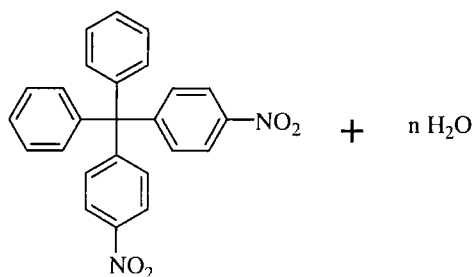
Chapter 17:

- 7) Triphenylisocyanurate co-crystallised with trinitrobenzene.



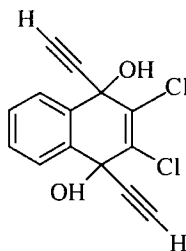
Chapter 18:

- 8) 4,4'-dinitrotetraphenyl methane.



Chapter 19:

- 9) 2,3-dichloro-1,4-diethynyl-1,4-dihydroxy-naphthalene.



Chapter 20:

- 10) 4,4-diphenyl-2,5-cyclohexadienone.

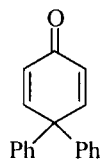


Figure 15.1: Compounds studied in part 3.

Chapter 16 : Co-Crystal (6), 2,4,6-*tris*-(4-chlorophenoxy)-1,3,5-triazine and Tribromobenzene

16.1 Introduction

A selection of *sym*-triaryloxytriazines have been investigated as part of a study to develop crystal engineering strategies, especially strategies to obtain non-linear optical materials^{4,17}. It can be seen that *sym*-triaryloxytriazines can form at least three* different motifs depending on the nature of the substituents R_1 , R_2 and R_3 (see Figure 16.1).

Motif **1** and **2** depend on the triazine dimers known as Piedfort units⁸. When these units form stacks, with each unit in the stack in a parallel orientation, and the stacks aligning to give a close packed arrangement, the resulting motif (motif **1**) can exhibit non-linear optical properties. However, when substituents are added in a meta position of the phenoxy rings the steric bulk of the groups discourages the parallel stacking in favour of anti-parallel stacking giving motif **2**.

Motif **3** is rather different to motifs **1** and **2**, the Piedfort unit no longer forms the basis of the motif, and the crystal structure has a much more open network that is stabilised by the incorporation of 'guest' molecules of the solvent from which the crystal was grown. It would appear that the important factor in the generation of this motif is the presence of a halogen atom in the ortho position (R_1) allowing the formation of a three-fold halogen-halogen interaction, and also the lack of any bulky groups in the meta positions, i.e. R_2 and R_3 are both hydrogen. This would suggest that halogen-halogen interactions play an important role in this motif.

The trigonal symmetry of triazine molecule is carried over into the crystal structure motif in all three cases (**1–3**) resulting in the structures based on trigonal or hexagonal crystal systems.

* Three motifs are found for small substituent groups (R) such as H, CH₃, Cl, Br. More motifs are found with bulkier and more flexible groups, see structures in the CSD⁶ for details.

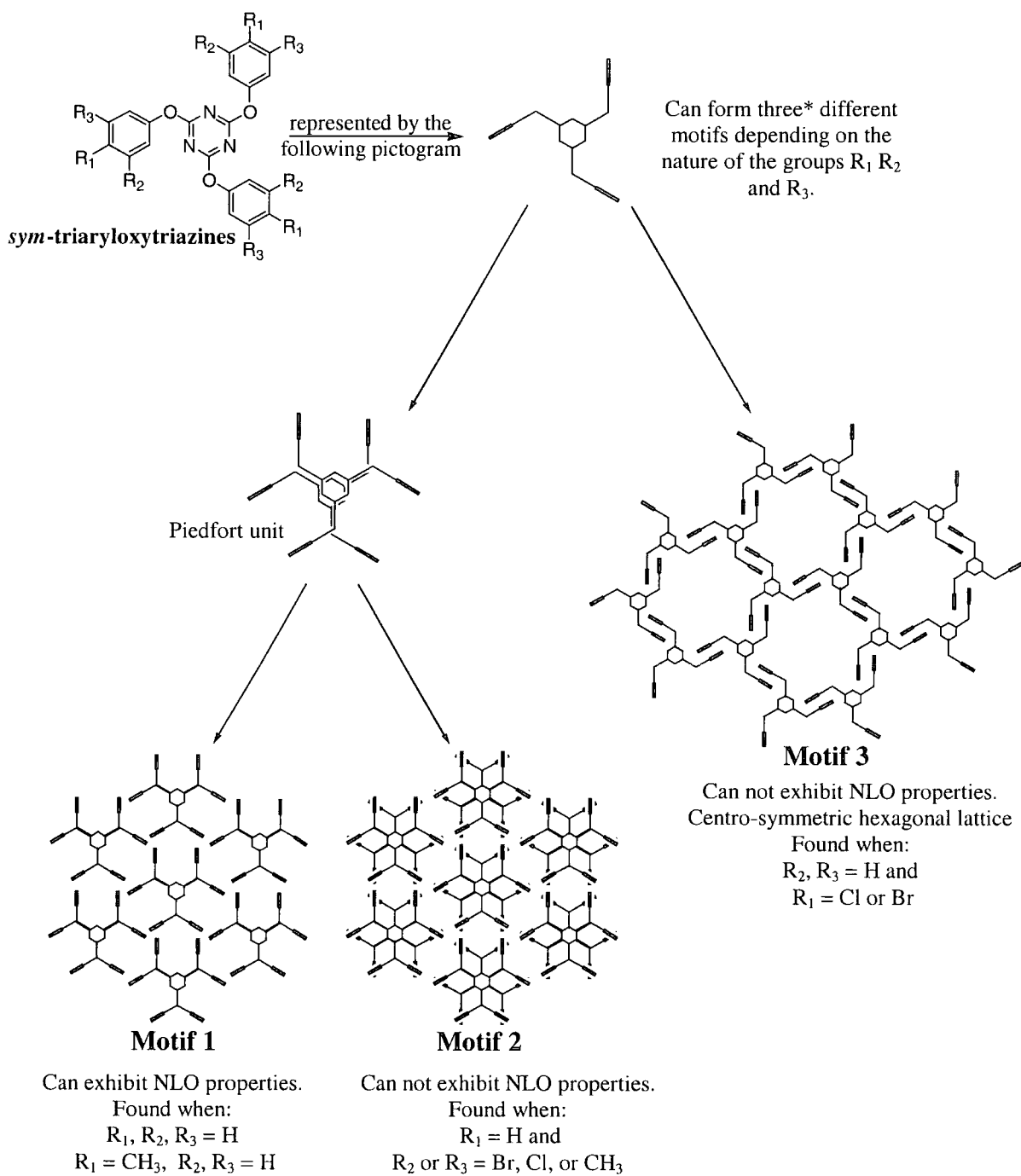


Figure 16.1: Motifs generated by *sym*-triaryloxytriazines^{4,1}. * see footnote on previous page.

16.2 Crystal Data

Code	6_X	6_N
Radiation type	X-ray	Neutron
Instrument	Smart-CCD ⁹	SXD at ISIS ^{10,11}
Instrument type	Area detector	Time of flight
Wavelength / Å	0.71073	0.5-5.0
Formula	C ₂₁ H ₁₂ Cl ₃ N ₃ O ₃ / C ₆ H ₃ Br ₃	C ₂₁ H ₁₂ Cl ₃ N ₃ O ₃ / C ₆ H ₃ Br ₃
Formula weight	775.50	775.50
Temp / K	150(2)	100(5)
Crystal system	Hexagonal	Hexagonal
Space group	P6 ₃	P6 ₃
Colour	Colourless	Colourless
Habit	Block	Block
Size / mm	0.35x0.27x0.27	6.0x1.5x1.0
a(=b) / Å	15.250(2)	15.166(6)
c / Å	6.814(1)	6.743(2)
α(=β) / °	90	90
γ / °	120	120
Z	2	2
Mu / mm ⁻¹	4.737	10.80 (at 1 Å)
Absorb. correction. type	multiscan	empirical
R(int)	0.0523	0.071
Data/restraints/parameters	17004 / 1 / 122	30681 / 1 / 163
GooF	1.037	1.230
R1	0.0276	0.0834
wR2	0.0623	0.2121

Table 16.1: Crystal data for co-crystal **6**, 2,4,6-tris-(4-chlorophenoxy)-1,3,5-triazine and tribromobenzene.

16.3 Crystal Structure and Results

The overall structure of compound **6** is aesthetically very pleasing; the triazine molecules form a two dimensional hexagonal based network with open channels or nanotubes running in the third dimension. These channels are filled with the solvent tribromobenzene.

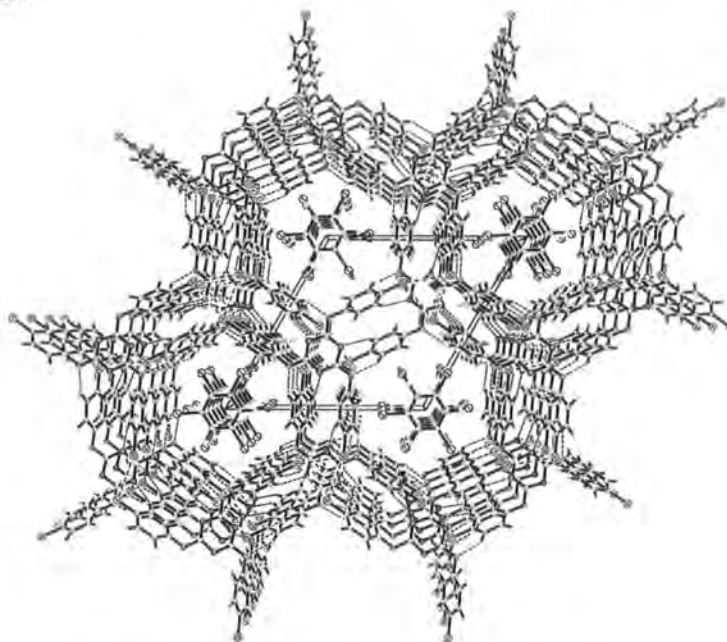


Figure 16.2: The full structure of compound **6**.

The crystal takes a hexagonal system with one third of the triazine and one third of the tribromobenzene molecule in the independent unit. The molecular structure and atom naming system are given below:

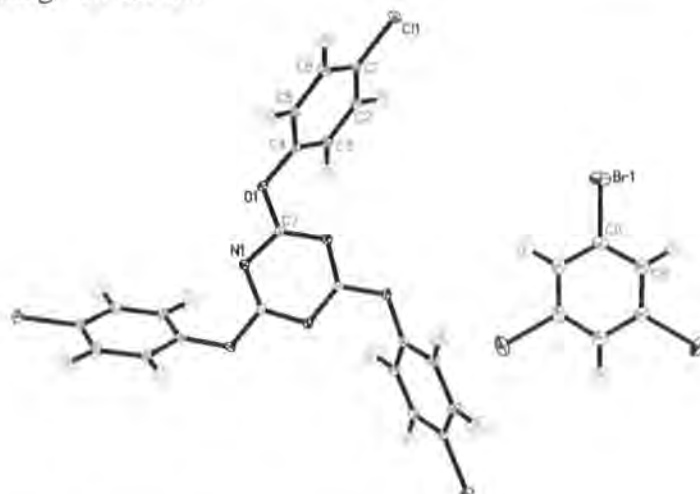


Figure 16.3: 2,4,6-tris-(4-chloro-phenoxy)-1,3,5-triazine and tribromobenzene, model from neutron data with thermal ellipsoids (including hydrogen atoms) plotted at 50% probability.

The structure is built up of a simple trigonal based net with adjacent layers of the structure inverted with relation to each other to give the overall hexagonal structure seen above.

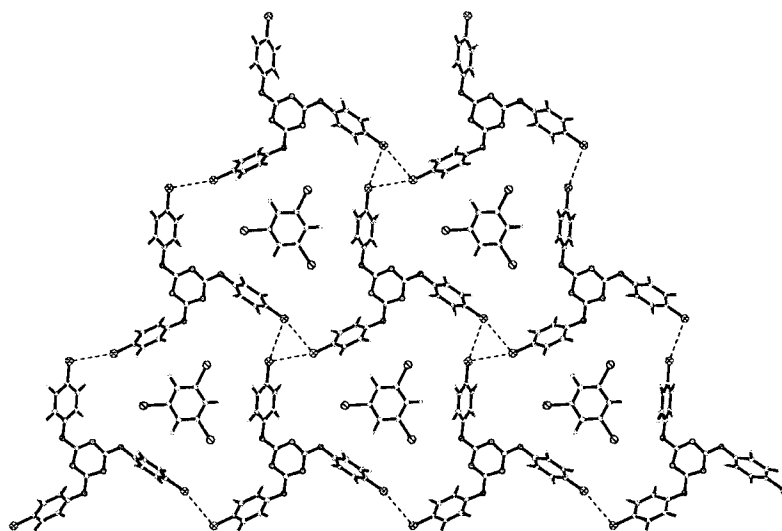


Figure 16.4: the trigonal based net of triazines containing tribromobenzenes.

This trigonal net is built up of three-fold Cl-Cl interactions, with a short Cl...Cl distance of 3.441(3)Å and C-Cl...Cl angles of 165.0(1)° and 105.0(1)°. As discussed in the introduction, the occurrence of close Cl-Cl contacts has been widely studied. Studies^{12,13} using the CSD⁶, indicate that there are two types of C-Cl...Cl-C interactions, type I where the two C-Cl...Cl angles are equal and the more common type, type II, where one of the C-Cl...Cl angles approximately equals 90° and the other 180°. The interaction seen here is of the type II kind. It has been proposed that Type II interactions are due to the polarisability of the halogen. Carbon-bound halogens in a sufficiently electron-withdrawing environment will present an anisotropic charge distribution, δ^+ forward of the halogen along the C-halogen bond vector, giving rise to the C-Cl...Cl bond angle of 180°, and δ^- perpendicular to the bond vector, giving rise to the C-Cl...Cl bond angle of 90°.

The motif **3** structure is dependent on the presence of these Cl-Cl interactions, or rather of halogen-halogen interactions; exchange of the Cl group for a nearly identically sized methyl group (isomorphous replacement) results in a completely different structure, namely that of motif **1**. However, exchange of the chlorine atoms for bromine atoms, which can also exhibit halogen-halogen interactions, results in no change of structure⁴.

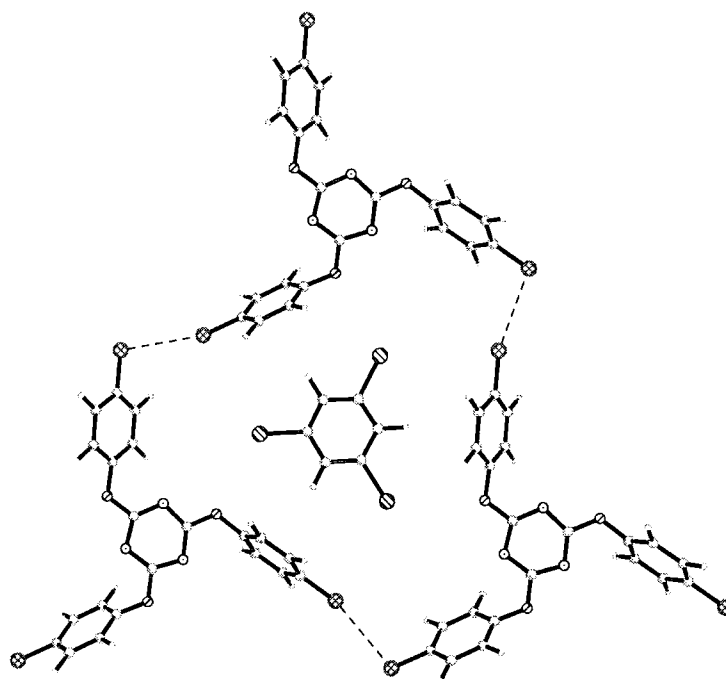


Figure 16.5: The orientation of the tribromobenzene molecule in the triazine net.

It can be seen that the tribromobenzene fits very precisely into the holes created by the triazine net. Each hydrogen is directed towards a phenyl ring, and each bromine fits into a hollow in the ring circumference. A side view (Figure 16.6) shows that the tribromobenzene molecules do not lie in the same plane as the triazine net but about 1 Å below this plane, thus, none of the hydrogen or bromine atoms of the tribromobenzene point directly at the phenyl ring centroids, but instead at a C-C aromatic bond of the ring instead.

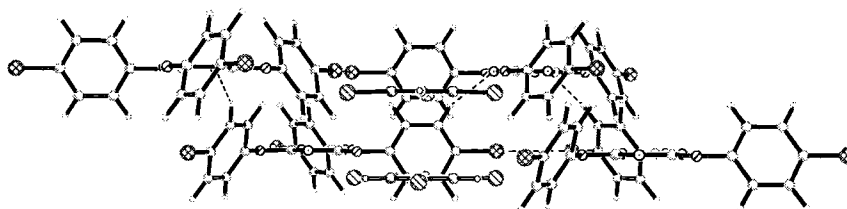


Figure 16.6: Side view of 2 layers of tribromobenzene molecules in the triazine nets.

In addition to the Cl...Cl interactions linking molecules within a net there are C-H...N hydrogen bonds linking adjacent nets, these can be seen in Figure 16.6 above.

Model from:	C-H / Å	H...N / Å	C...N / Å	CHN / °
X-ray data	0.981 (hydrogen atom positions generated)	2.84	2.974(3)	86
Neutron data	1.083(8) (hydrogen atom positions calculated from data)	2.83(1)	2.959(3)	86.3(6)

Table 16.2: Geometry of the C-H...N hydrogen bond linking adjacent layers.

The side view (Figure 16.6) also shows clearly the degree of tilt in the triazines phenyl rings. This tilts the phenyl rings towards the hydrogen atoms and away from the bromine atoms. This tilting of the phenyl rings that breaks the mirror symmetry that can be seen when 2,4,6-tris-(4-chloro-phenoxy)-1,3,5-triazine is co-crystallised with some other solvents. A search of the CSD⁶ produces five hits for 2,4,6-tris-(4-chloro-phenoxy)-1,3,5-triazine with various solvents, these are listed in Table 16.3 below. It can be seen that the crystals form in one of two possible space groups, $P6_3/m$ or, as in compound **6**, $P6_3$. The influence of the mirror plane parallel to the view plane can be seen clearly in the tilt of the phenyl rings.

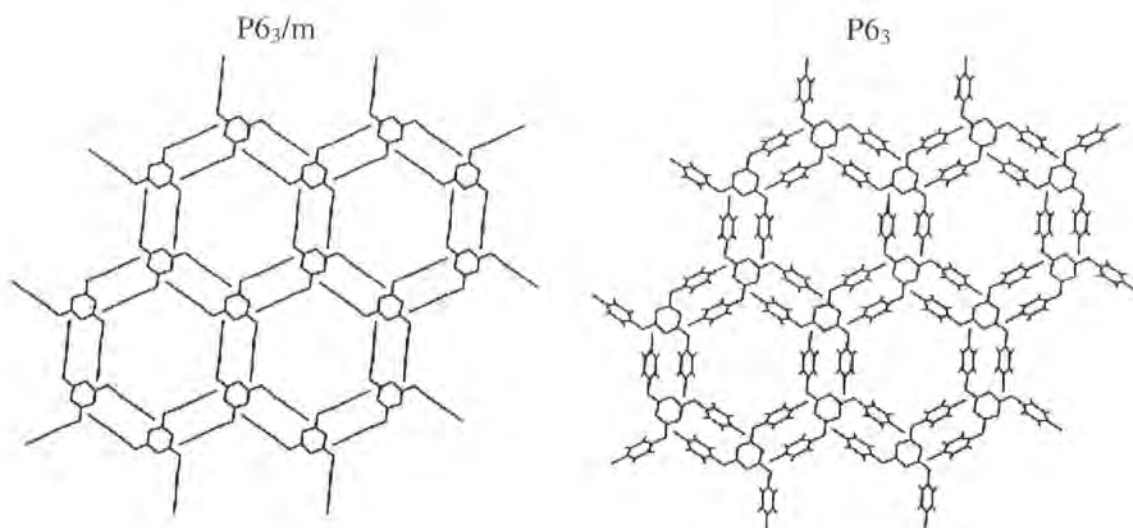


Figure 16.7: The structure of 2,4,6-tris-(4-chloro-phenoxy)-1,3,5-triazine, in $P6_3/m$ and $P6_3$ space groups. The space group depends on the identity of the guest solvent molecule.

Solvent	Space group	Temperature of data collection /K	Disorder	CDS refcode
Chloroform, dichloromethane, Ethylacetate, benzene, toluene	P6 ₃ /m	295	Solvent disordered	VALQEE01 ¹
Hexachlorobenzene	P6 ₃ /m	295	Solvent disordered	VEWDIK ¹⁴
Hexamethylbenzene	P6 ₃ /m	295	Solvent and Phenyl rings disordered	VEWFUY ¹⁴
1,3,5-trinitrobenzene	P6 ₃ /m	295	No disorder	VEWJIQ ¹⁴
Hexamethylphosphoramide	P6 ₃ /m	295	Solvent and Phenyl rings disordered	VEWNEQ ¹⁴
1,3,5-tribromobenzene	P6 ₃	150 / 100	No disorder	XEHMAY ¹⁵ XEHMAY01 ¹⁵

Table 16.3: Occurrences of 2,4,6-tris-(4-chloro-phenoxy)-1,3,5-triazine with various solvents in the CSD⁶.

It might seem that only the very precise fit of the TBB molecule is enough to break the mirror symmetry¹⁶. However the presence of disorder in the same phenyl rings where the presence or absence of the mirror symmetry makes itself felt, might suggest that space group has been incorrectly identified in these cases. Data collection at a lower temperature might resolve the disorder and/or help establish if the true space group has been identified.

16.4 Conclusions:

This is a wonderful example of crystal engineering, with the overall structural motif being determined by the substituent identity (R₁₋₃), and within motif **3** the degree of order and stability being controlled by the fit between the triazene channels and guest solvent molecule. It is also worth noting that in all three motifs the internal trigonal symmetry of the triazine molecule is carried over into the crystal structure, resulting in a trigonal or hexagonal habit.

It is also a clear example of the strong structural determining influence that can be played by halogen-halogen interactions, especially by the strong three-fold Cl-Cl interactions. It is whether or not there is the possibility for these halogen-halogen contacts to occur, that controls whether motif **3** can form.

Motif **3** is seen to be a very robust motif, occurring regardless of halogen identity, or guest solvent identity. Unfortunately the motif is not robust enough to allow the solvent to be removed from the channels without structural degradation¹. And finally, from a purely aesthetic point of view, motif **3** is a very visually pleasing motif.

Chapter 17 : Triphenylisocyanurate Co-Crystallised with Trinitrobenzene

17.1 Introduction

Continuing on from the work on triazines in the previous chapter, the related triazine compound triphenylisocyanurate has been studied. In this case the trigonal symmetry of the molecules is not carried over into the crystal structure, nor is it part of an easily understood pattern of structural motifs. However the structure does exhibit a number of interesting π - π and C-H... π interactions, which have been studied here using neutron diffraction.

The triphenylisocyanurate has been co-crystallised with trinitrobenzene and benzene - the solvent from which the crystals were grown². The molecules crystallise in the ratio of 2:2:1, i.e. there is half a benzene molecule to each triphenylisocyanurate and trinitrobenzene molecule.

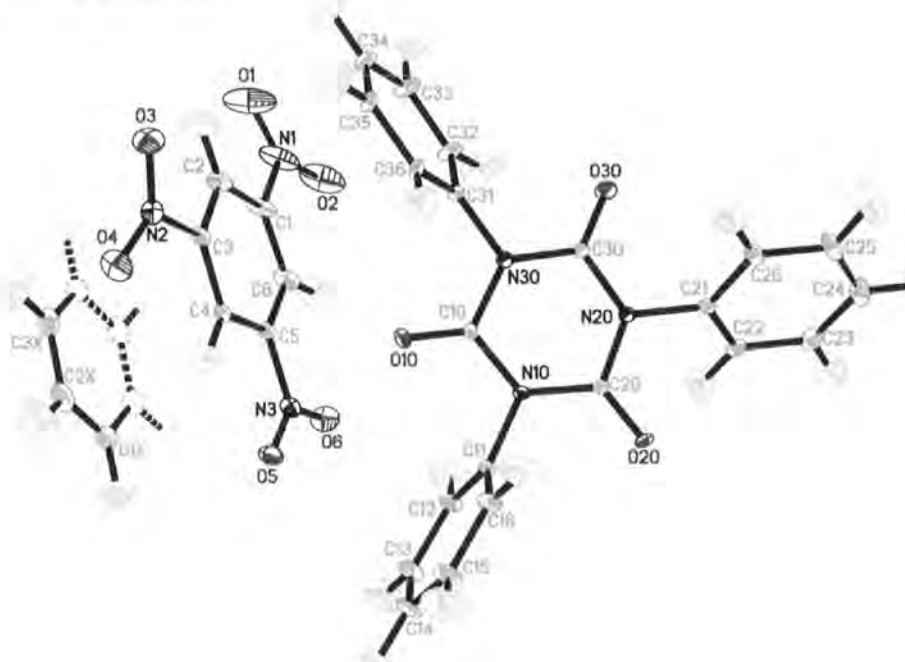


Figure 17.1: Triphenylisocyanurate with trinitrobenzene and benzene. Model from neutron data, thermal ellipsoids (including hydrogen atoms) plotted at 50% probability.

17.2 Crystal Data

Code	7 _X	7 _N
Radiation type	X-ray	Neutron
Instrument	Smart-CCD ⁹	SXD at ISIS ^{10,11}
Instrument type	Area detector	Time of flight
Wavelength / Å	0.71073	0.5-5.0
Formula	C ₂₁ H ₁₅ N ₃ O ₃ / C ₆ H ₃ N ₃ O ₃ / C ₃ H ₃	C ₂₁ H ₁₅ N ₃ O ₃ / C ₆ H ₃ N ₃ O ₆ / C ₃ H ₃
Formula weight	609.53	609.53
Temp / K	100(2)	25(1)
Crystal system	Triclinic	Triclinic
Space group	P-1	P-1
Colour	Colourless	Colourless
Habit	Block	Irregular prism
Size / mm	1.2x0.6x0.25	2.0x2.0.x1.0
a / Å	11.3825(3)	11.320(4)
b / Å	11.5495(3)	11.558(5)
c / Å	12.5513(3)	12.455(5)
α / °	69.866(1)	70.48(2)
β / °	63.497(1)	63.43(3)
γ / °	86.397(1)	86.93(3)
Z	2	2
Mu / mm ⁻¹	0.111	1.230 (at 1 Åmm ⁻¹)
Absorption correction type	none	empirical
R(int)	0.0327	0.066
Data/restraints/ parameters	7227 / 0 / 406	6069 / 0 / 595
GooF	1.034	1.057
R1	0.0392	0.0799
WR2	0.1001	0.2013

Table 17.1: Crystal data for co-crystal 7, triphenylisocyanurate with trinitrobenzene and benzene.

17.3 Crystal Structure and Results

Two triphenylisocyanurate molecules form discrete hydrogen bonded units with two trinitrobenzene molecules about a centre of inversion. Each unit involves three C-H...O interactions, details given in Table 17.2. A single molecule of the solvate benzene fits into the centre of the unit in such a way that it is sandwiched between the phenyl rings of the two trinitrobenzene molecules in a double π - π interaction.

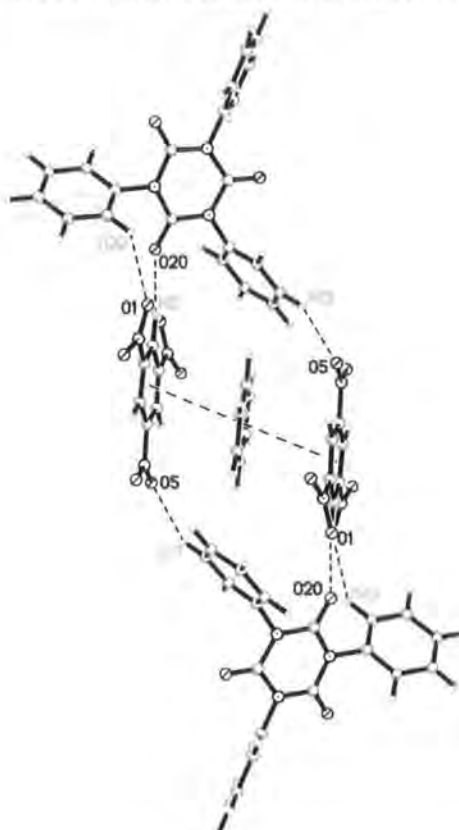


Figure 17.2: Triphenylisocyanurate trinitrobenzene and benzene hydrogen bonded unit, thermal ellipsoids (including hydrogen atoms) plotted at 50% probability.

Hydrogen bond	C-H / Å	O...H / Å	O...C / Å	OHC / °
O ₅ ...H ₁₃ -C ₁₃	1.082(10)	2.519(9)	3.520(5)	153.5(9)
O ₂₀ ...H ₂ -C ₂	1.076(9)	2.303(9)	3.372(4)	172.2(7)
O ₁ ...H ₂₂ -C ₂₂	1.081(8)	2.520(10)	3.349(6)	132.7(7)

Table 17.2: Hydrogen bond distances within the triphenylisocyanurate trinitrobenzene and benzene unit.

The distance between the two adjacent ring centroids of the π - π interaction is 3.538\AA , the benzene molecule sits on the inversion centre hence the two π - π interactions are identical and the angle between the interactions is 180° .

The planes of the phenyl rings are not normal to the π - π interaction, but tilted by approximately 17° . Looking straight down the interaction it can be seen that the inversion centre relates the two trinitrobenzene molecules so that one nitro group on one molecule eclipses the hydrogen on another. The benzene is staggered in relation to the trinitrobenzene molecules.

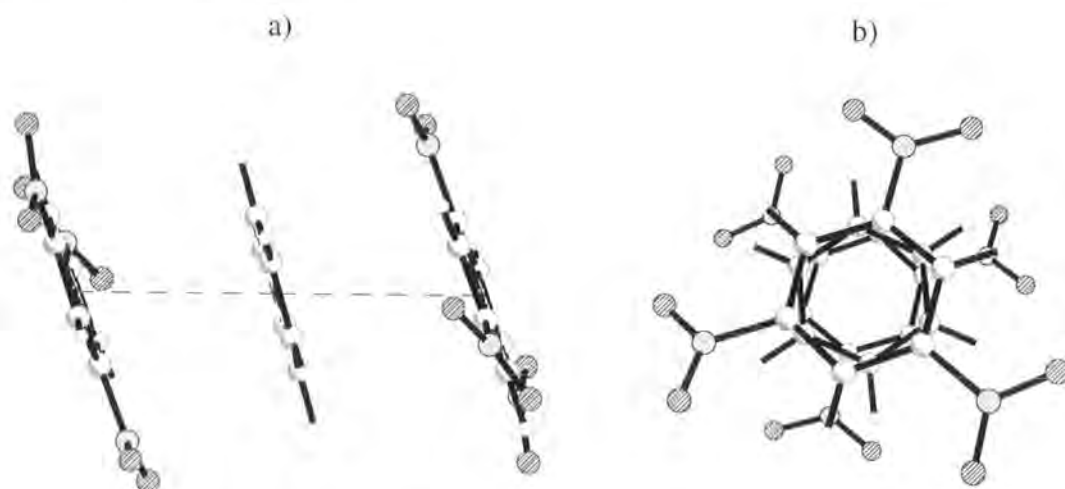


Figure 17.3: The π - π interaction a) side view b) top view.

These hydrogen bonded units (shown in Figure 17.2) arrange to form ribbons in such a way that each of the double π - π interactions, shown above, interacts with two further phenyl ring from both adjacent units thus giving a quadruple π - π interaction.

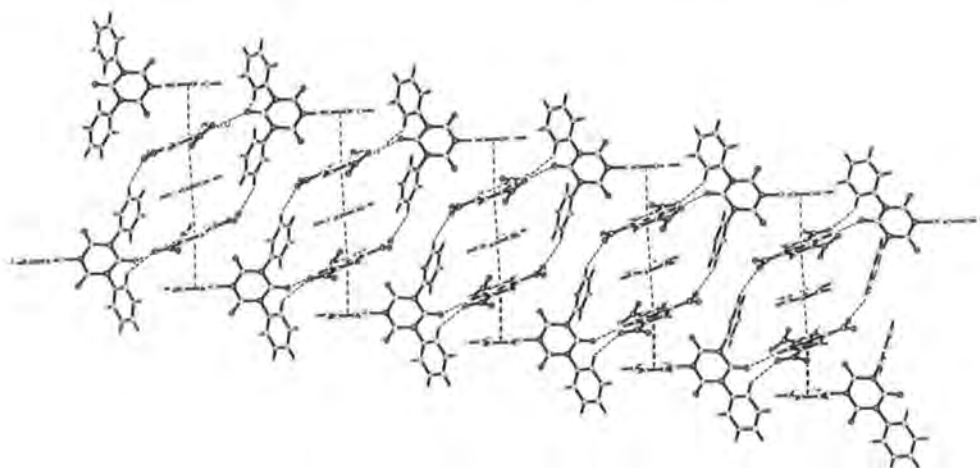


Figure 17.4: Ladder of quadruple π - π interactions.

These ribbons lie side by side in such a way that a C-H... π hydrogen bond (c in Figure 17.5) can form to each of the end phenyl rings in the quadruple π - π interactions stack. These interactions hold the ribbons together to form sheets.

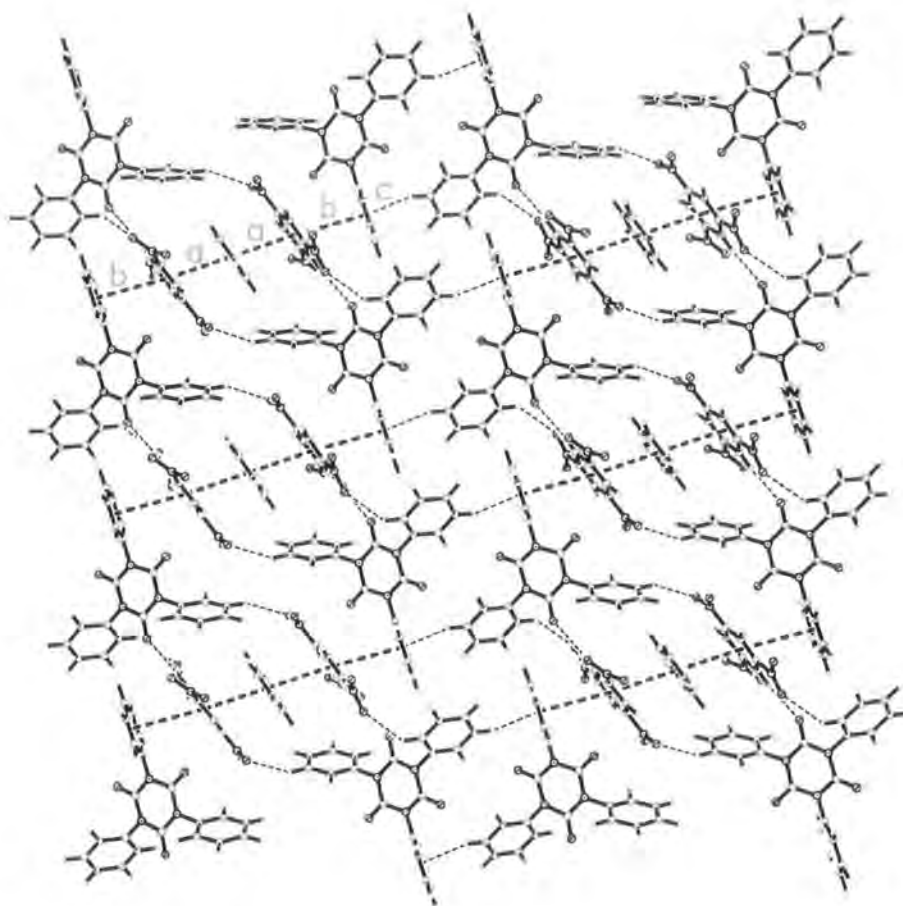


Figure 17.5: Two chains of triphenylisocyanurate with trinitrobenzene and benzene.

The π - π interaction between triphenylisocyanurate and trinitrobenzene, (b in Figure 17.5) is longer than the interaction between trinitrobenzene and benzene (interaction a). Overall the quadruple π - π interaction is fairly linear. All of the phenyl ring planes are tilted with respect to the normal of the π - π interaction, and with respect to each other, i.e. the ring planes are not parallel. The distances and angles are given in the Table 17.3 below:

π - π interactions:				
Ring centroid - ring centroid distance between benzene and trinitrobenzene - distance a			3.538Å	
Ring centroid - ring centroid distance between trinitrobenzene and triphenylisocyanurate - distance b			3.875Å	
Angle between π - π interaction a, and π - π interaction a			180°	
Angle between π - π interaction a, and π - π interaction b			177°	
Angle between trinitrobenzene phenyl ring plane and Benzene ring plane			5.1(2)°	
Angle between triphenylisocyanurate phenyl ring plane and trinitrobenzene phenyl ring plane			21.1(1)°	
Angle between triphenylisocyanurate phenyl ring plane and Benzene ring plane			16.1(1)°	
C-H... π interaction – c :				
Hydrogen bond	C-H / Å	H... π / Å	C... π / Å	CH π /°
C ₂₅ -H ₂₅ ... π	1.075(10)	2.54	3.54	155

Table 17.3: π - π and C-H... π interactions in compound 7.

There are further C-H...O interactions between adjacent sheets, these are shown in the Figure 17.6.

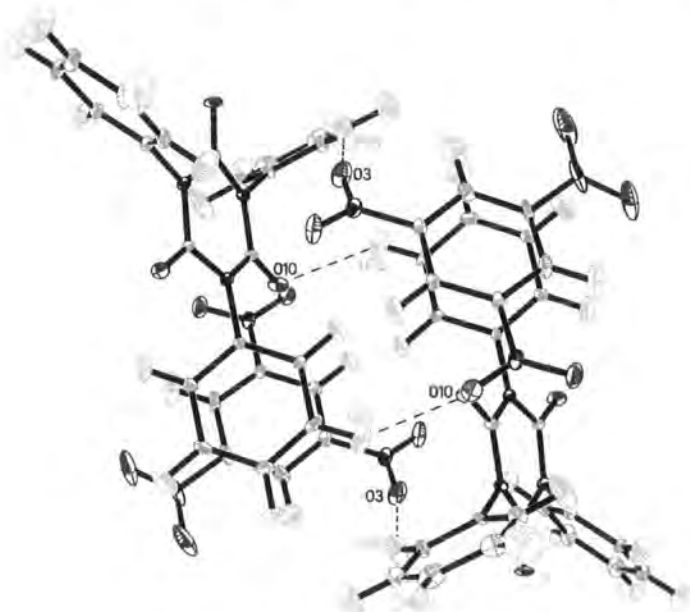


Figure 17.6: Interaction between two sheets viewed down the π - π interactions. Thermal ellipsoids (including hydrogen atoms) plotted at 50% probability.

C-H...O interactions:				
Hydrogen bond	C-H / Å	H... π / Å	C... π / Å	CH π /°
C ₁₆ -H ₁₆ ...O ₃	1.087(8)	2.471(9)	3.381(5)	141.5(7)
C ₃₅ -H ₃₅ ...O ₁₀	1.077(8)	2.444(9)	3.319(5)	136.6(6)

Table 17.4: C-H...O interactions between two adjacent sheets in compound 7.

These inter-sheet C-H...O interactions lie within the same range in terms of length and directionality as those C-H...O interactions found within the triphenylisocyanurate, trinitrobenzene and benzene hydrogen bonded unit.

17.4 Conclusions

Compound 7 exhibits a number of interesting interactions. The triphenylisocyanurate, trinitrobenzene and benzene molecules lack any conventional N-H or O-H donors while having nitro and carbonyl hydrogen bond acceptor groups. As a result the phenyl hydrogen atoms are utilised as hydrogen bond donors and the structure relies on a large number of C-H...O hydrogen bonds to form the three dimensional structure.

The benzene solvate is required as an integral part of the structure. It has been shown that if thiophene is used instead of benzene as the solvent then the crystals formed are isostructural². It would be interesting to investigate if crystals could be grown from any other solvents and what structural changes result.

Chapter 18 : 4,4'-dinitrotetraphenyl methane

Compound 8, 4,4'-dinitrotetraphenyl methane, has been found to exhibit non-linear optical properties*. It is well accepted that non-linear optical crystals must have a non-centro symmetric symmetry, however 4,4'-dinitrotetraphenyl methane appears to crystallise in the centro-symmetric space group R-3. Closer analysis of the structure reveals that there are molecules of water sitting on, and disordered across, the three-fold axis. This water breaks the R-3 symmetry, presumably generating a supercell that will fit the requirements for nonlinear optical properties. It is not unprecedented, in 1997 König et al¹⁷ described the structure of a nonlinear optical host-guest material where the host molecules have a structure best described by the centro-symmetric space group Cmc₂m, it is only the relative orientation of the chains of guest molecules that breaks this symmetry resulting in the polar space group Cma2₁. Since the molecule of interest fits the R-3 symmetry, and it is only the solvent water that breaks the symmetry, the structure has been solved and modelled in the R-3 space group with the water molecules described as disordered. Analysing the structure in terms of a space group in which the water disorder is resolved should not alter the relative positions of the 4,4'-dinitrotetraphenyl methane molecules.

In an attempt to freeze out any kinetic component of the disorder and obtain the best data possible, the crystal was slow cooled and the data were collected at very low temperature (30°K) using the HELIX cryostream. The HELIX is a cryostream that uses a stream of cooled helium gas rather than nitrogen gas to cool the crystal, thus it is able to obtain far lower temperatures than a standard nitrogen based cryostream.

From this data a reasonable model of the R-3 disordered structure was obtained. However, to identify the supercell and fully solve the disorder better data are required, either from a more intense X-ray source or a neutron source where the hydrogen atoms will scatter better and thus the solvent will have a greater influence on the data.

* Non-linear optical measurements carried out at the University of Hyderabad, India

4,4'-dinitrotetraphenyl methane has an excess of hydrogen bond donors in the form of the two nitro groups, while the only possible hydrogen bond donors are the phenyl hydrogen atoms. In the analysis of the hydrogen bonding interactions and motifs any interactions with the disordered solvent have been ignored.

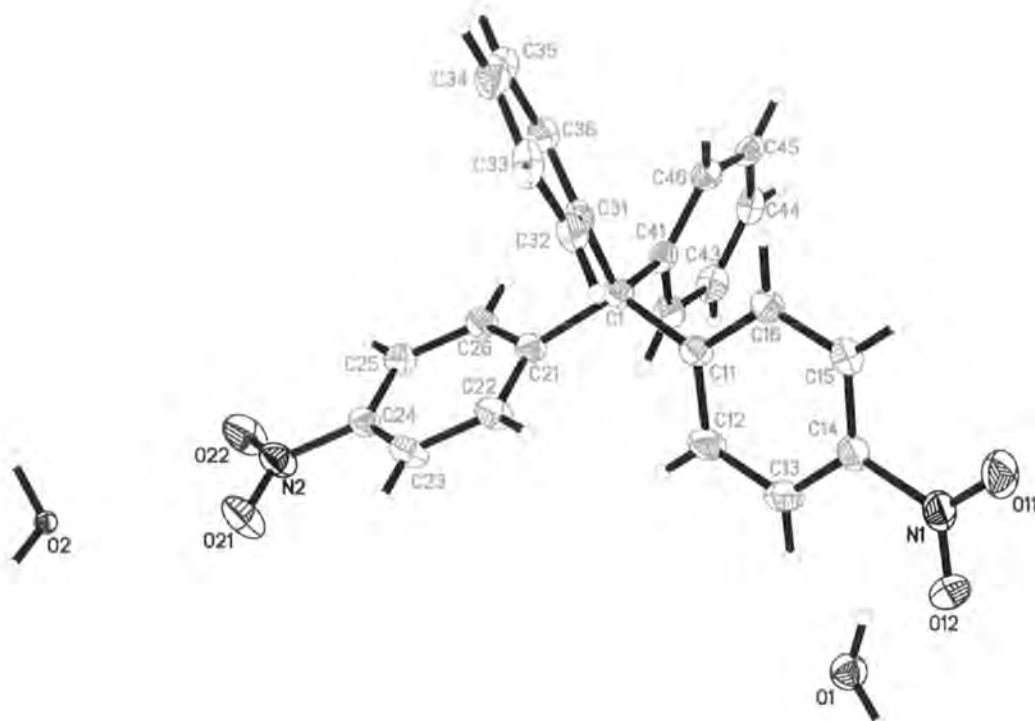


Figure 18.1: 4,4'-dinitrotetraphenylmethane, with two water molecules in partially occupied positions. Thermal ellipsoids plotted at 50% probability.

18.1 Crystal Data

Code	8
Radiation type	X-ray
Instrument	Smart-CCD ⁹
Instrument type	Area detector
Wavelength / Å	0.71073
Formula	C ₂₅ H ₁₈ N ₂ O ₄ + 0.54 H ₂ O
Formula weight	420.18
Temp / K	30(2)
Crystal system	Rhombohedral
Space group	R-3
Colour	Yellow
Habit	Block
Size / mm	0.30x0.26x0.20
a = b / Å	20.759(3)
c / Å	7.5606(5)
$\alpha = \beta$ / °	90
γ / °	120
Z	18
Mu / mm ⁻¹	0.093
Absorption correction type	None
R(int)	0.0604
Data/restraints/parameters	4654 / 6 / 300
GooF	1.044
R1	0.0618
wR2	0.1397

Table 18.1: Crystal data for compound 8, 4,4'-dinitrotetraphenyl methane.

18.2 Crystal Structure and Results

The disorder of the water is very interesting, the fact the disorder lies on the three-fold rotational axis makes the identification of the separate molecules from the peaks of electron density in the Fourier map more difficult than usual. The program SQUEEZE¹⁸ (part of the PLATON¹⁹ suit of programs) was run on a refined model without the water being include in the structure, and used to calculate that in each cell there were six large voids of roughly 112 Å³, and with 14 electrons of un-modelled electron density per void. Given that the value of Z is 18 there is one third of a void per asymmetric unit. With part of the water molecule lying directly on the rotational axis, each orientation of the water molecule can only have a maximum occupancy of one third and in fact has an occupancy of slightly less than that. Given this, it is amazing that the hydrogen atoms appeared at all in the Fourier map, and their positions should be viewed as uncertain. The model below is the best that could be achieved with the data available.

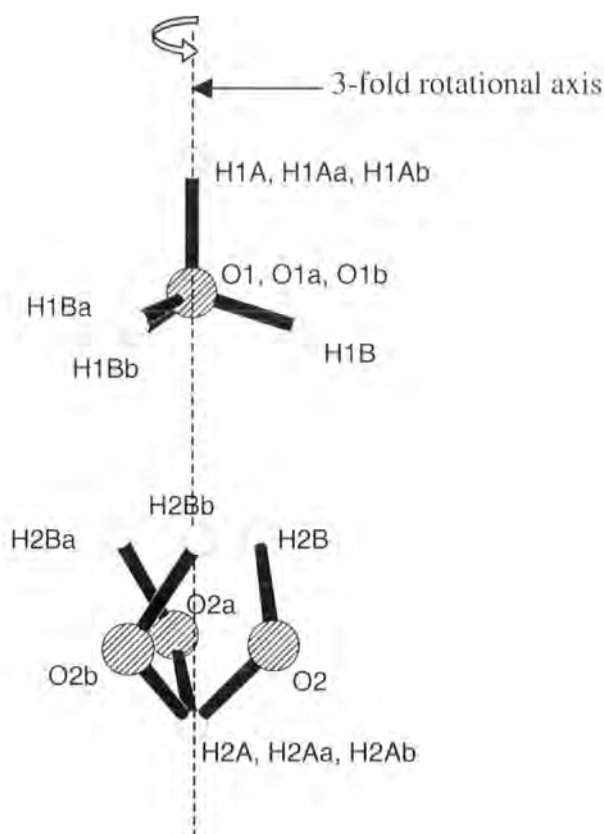


Figure 18.2: The disordered water molecules.

For the rest of the structure analysis the disordered water has been ignored and is not included in any of the following diagrams.

Each molecule is involved in many different motifs, the structure consists of two different types of dimeric interaction, two different types of helices, and two different types of six membered rings, making six different motifs altogether. As there is only one molecule in the asymmetric unit, each molecule is simultaneously involved in all six motifs.

The dimers:

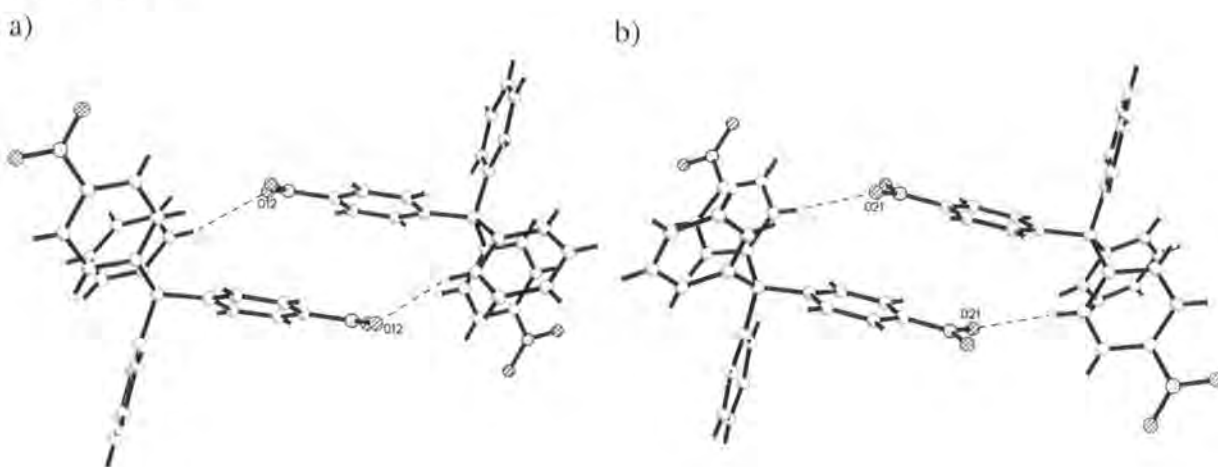


Figure 18.3: Dimers of 4,4'-dinitrophenyl methane a) dimer 1, b) dimer 2.

There is an interaction between O₁₂ and H₃₂ which results in a dimer, and another interaction of O₂₁ and O₂₂ with H₁₂ which results in a second dimer. Each molecule is involved in both dimers resulting in chains of alternating dimers running through the structure. For clarity the dimers have been drawn separately in Figure 18.3.

The helices:

The two helices both run parallel to the c axis. Both helices are propagated by C-H...O interactions. In the first helix these interactions are between C₃₄-H₃₄...O₁₂, and in the second helix these interactions are between C₄₅-H₄₅...O₁₁.

Helix 1:

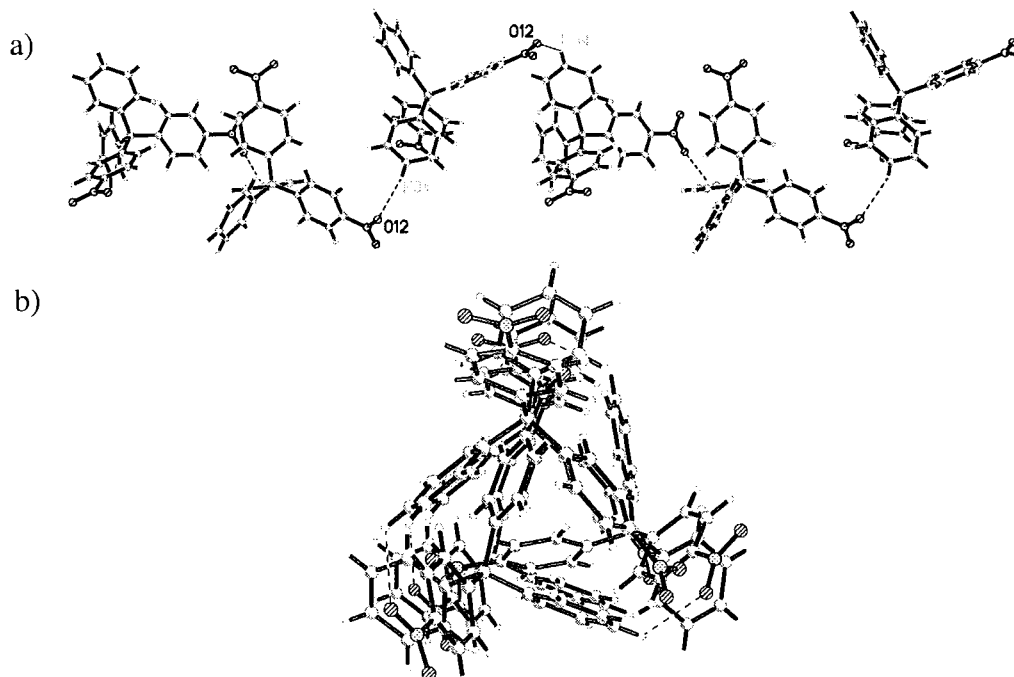


Figure 18.4: Helix of 4,4'-dinitrophenyl methane molecules (helix 1), a) viewed perpendicular to helix axis, b) viewed down axis of helix.

Helix 2:

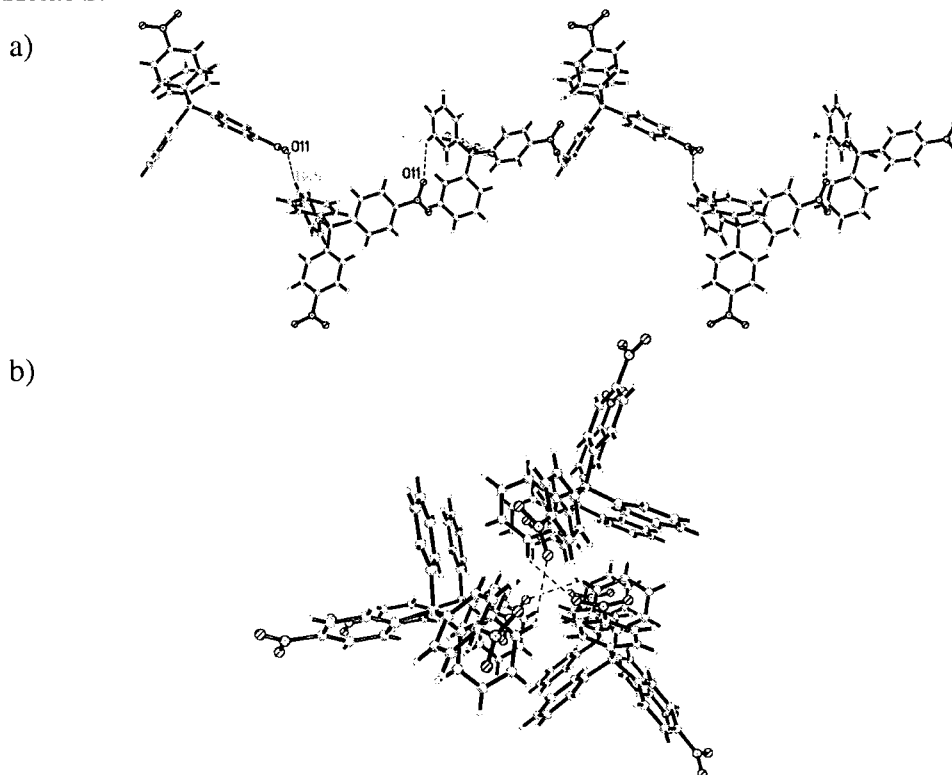


Figure 18.5: Helix of 4,4'-dinitrophenyl methane molecules (helix 2), a) viewed perpendicular to helix axis, b) viewed down axis of helix.

The 6-membered rings:

Both the six-membered rings lie in the *ab* plane, i.e. perpendicular to the *c* axis. The first ring is made of C-H...O interactions ($C_{35}-H_{35}\dots O_{22}$). The second ring is generated by two different C-H... π interactions where π is the two phenyl rings without nitro groups attached. The ring is formed from an inner ring of $C_{33}-H_{33}\dots\pi_{(C31-C36)}$ and an outer ring of $C_{23}-H_{23}\dots\pi_{(C41-C46)}$.

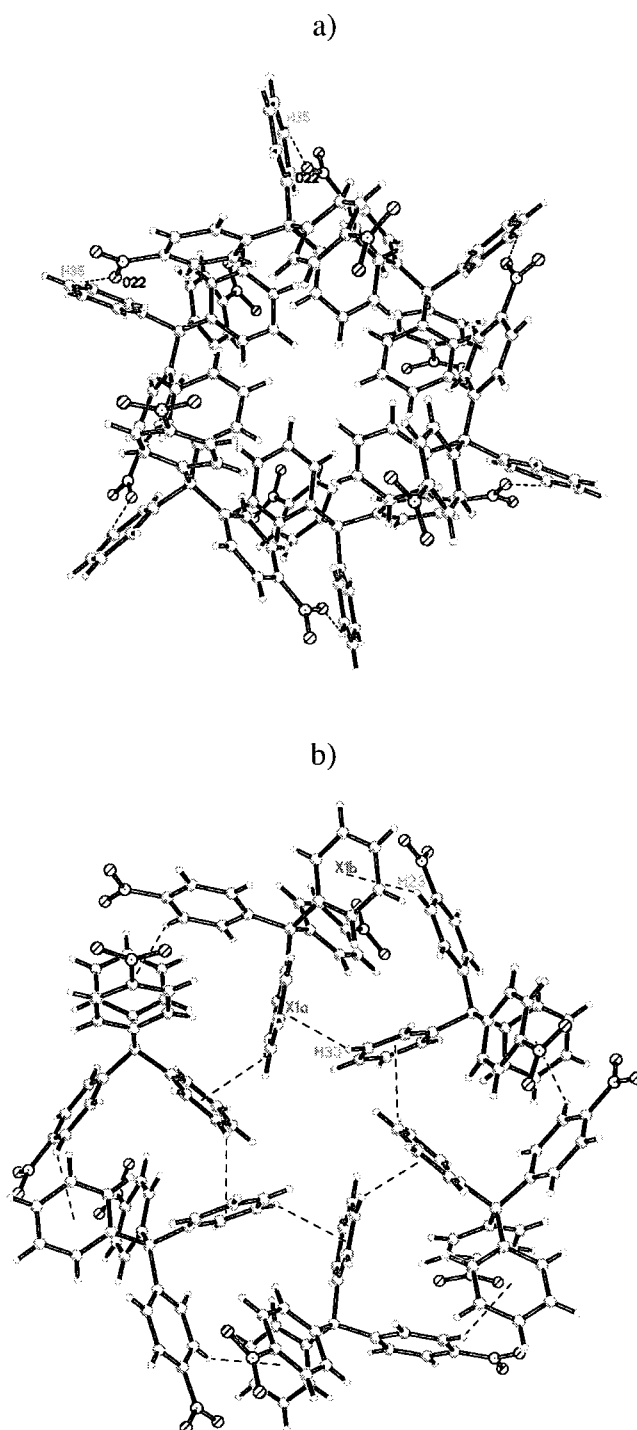


Figure 18.6: Six-membered rings of 4,4'-dinitrophenyl methane molecules a) ring propagated by C-H...O hydrogen bonds b) ring propagated by C-H... π hydrogen bonds.

Overall these interaction motifs fit together to give the packing shown below. With so many motifs occurring simultaneously it is hard to pick each motif out from the final packing diagram. The voids or channels that are filled by the solvent water are clearly seen running parallel to the c axis, a channel at each corner of the cell face, and two channels in the middle of the cell.

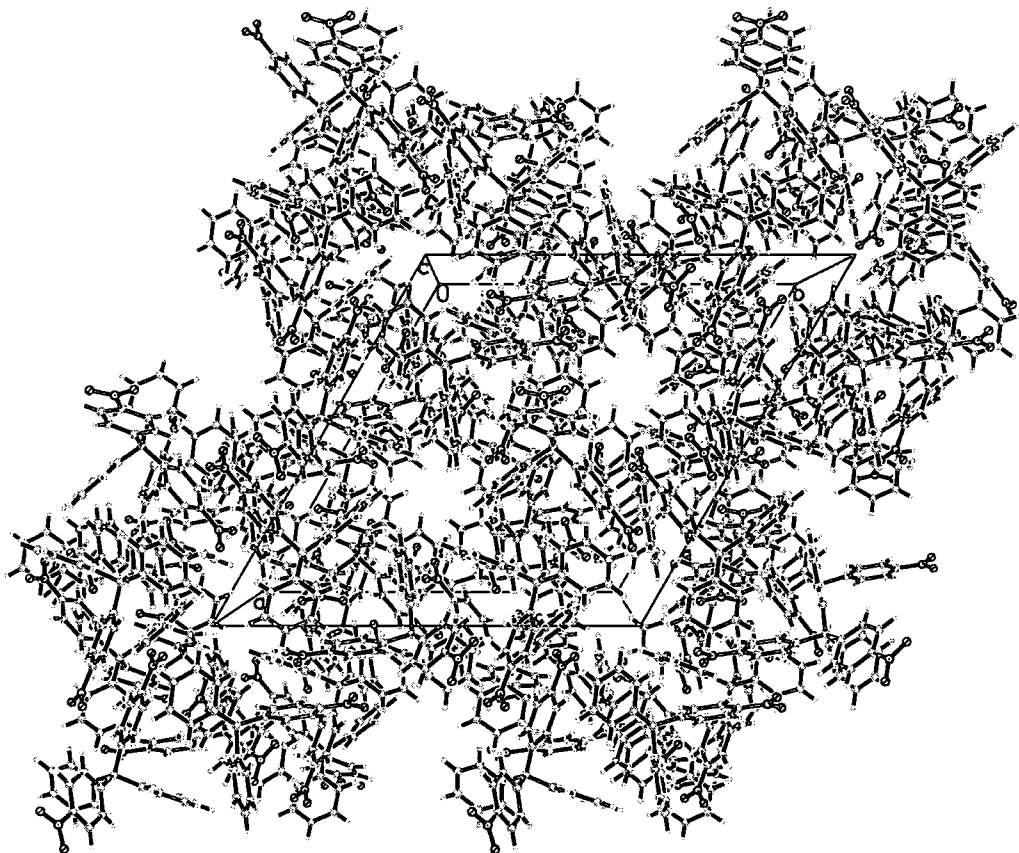


Figure 18.7: The packing of 4,4'-dinitrotetraphenyl methane in the three dimensional structure.

Motif	C-H...A	Distance H...A /Å	Distance C...A /Å	Angle CHA /°
Dimer 1	O ₁₂ ...H ₃₂ -C ₃₂	2.65	3.392(3)	135
Dimer 2	O ₂₁ ...H ₁₂ -C ₁₂	2.62	3.564(3)	175
Helix 1	O ₁₂ ...H ₃₄ -C ₃₄	2.71	3.371(4)	127
Helix 2	O ₁₁ ...H ₄₅ -C ₄₅	2.68	3.339(3)	127
Ring 1	O ₂₂ ...H ₃₅ -C ₃₅	2.58	3.318(4)	134
Ring 2	X1a...H ₃₃ -C ₃₃	2.87	3.661	141
Ring 2	X1b...H ₂₃ -C ₂₃	2.90	3.748	149

Table 18.2: Hydrogen bonding interactions in compound 8.

18.3 Conclusions

Looking at the interactions described above it can be seen that each possible hydrogen bond acceptor is utilised in the structure.

As was discussed in the introduction the crystals of compound **8**, 4,4'-dinitrotetraphenyl methane, have been found to exhibit non-linear optical properties and therefore must have a non-centro symmetric symmetry. However, as has been seen, the 4,4'-dinitrotetraphenyl methane molecule fits the centro-symmetric R-3 structure, and it is only the water molecules that break the centro-symmetric symmetry. It is interesting that such a small break in the symmetry, that would routinely be described as disorder in a crystal structure determination, can lead to such an important physical property as second harmonic generation. This result is especially interesting in view of the possibilities of crystal engineering such materials; structure prediction is hard enough without the added complications of solvent inclusion and disorder completely altering the structure's physical properties.

It would be interesting to try to grow crystals from a solvent that could fit the three-fold symmetry of the solvent channels, or alternatively to try and remove the water from these channels without causing the destruction of the crystal. Would the removal of the part of the structure that breaks the symmetry, result in the disappearance of the nonlinear optical properties?

It can be seen that the interaction motifs mirror the symmetry elements in the crystal, with the dimers forming around the inversion centres, the helices about the three-fold screw axis, and the rings about the three-fold axis with the solvent channels running down the centre of the rings.

Chapter 19 : 2,3-dichloro-1,4-diethynyl-1,4-dihydroxy-napthalene

19.1 Introduction

Compound **9**, 2,3-dichloro-1,4-diethynyl-1,4-dihydroxy-napthalene, is a *gem*-alkynol: it contains a hydroxyl group and an ethyne group bound to the same carbon. *Gem*-alkynols have been proposed for use as crystal engineering building blocks, and used to study hydrogen bonding^{5,20,21}, since they contain two very different hydrogen bonding groups, the hydroxyl and the ethyne groups. The interplay of these hydroxyl and ethyne groups, in terms of hydrogen bonding potential and structure motif determining features, is of great interest²². There are four possible hydrogen bond interactions between two *gem*-alkynols:

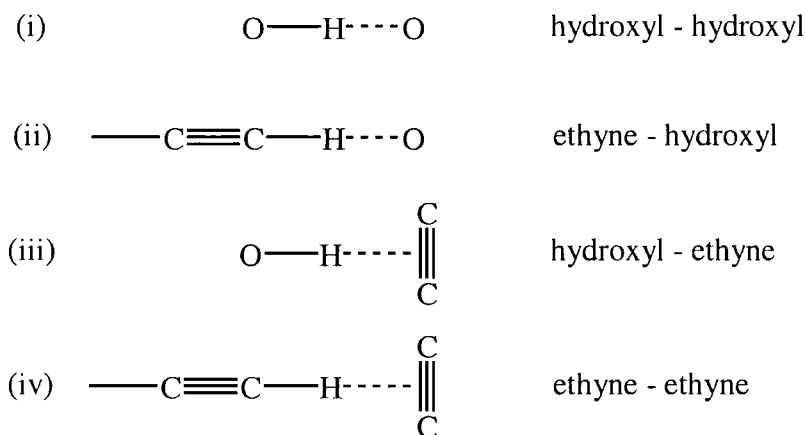


Figure 19.1: Possible hydrogen bond interactions between two *gem*-alkynol groups.

These four interactions are interesting since they are built up of the combination of a strong and a weaker hydrogen bond donor, and a strong and a weaker hydrogen bond acceptor. Within a *gem*-alkynol crystal structure there is the possibility for any one of these interactions to occur, or for a combination of the interactions, or for the *gem*-alkynol to interact with other parts of the molecule rather than another *gem*-alkynol. A

study* of the frequency with which each of these interactions occur within the *gem*-alkynol structures in the Cambridge Structural Database⁶ shows that while, as might be expected, the ‘strong – strong’ O-H...O interaction occurs most frequently, all of the interactions do occur in some cases, and the differences between the frequencies with which they are found are not great.

Interaction:		No. of structures (refcodes)	No. of occurrences of each interaction
i	O-H...O	30	46
ii	C-H...O	29	35
iii	O-H... π	10	15
iv	C-H... π	16	21
None of the above interactions		41	

Table 19.1: Frequencies of occurrence of the four *gem*-alkynol - *gem*-alkynol interactions.

It is interesting to note that the ‘strong’ donor – ‘weak’ acceptor interaction, O-H... π , occurs less frequently than the ‘weak’ donor – ‘weak’ acceptor interaction, C-H... π . A more detailed analysis of the situation is given in Table 19.2 below.

* The CSD⁶ search was carried out on the October 2001 release (245392 entries), using the Conquest 1.3 software package. Hydrogen bond limits of the sum of the van der Waals radii were taken: 2.72Å for H...O and 3.05 for H... π (C \equiv C centroid)²³, hydrogen atom positions were normalised to neutron distances, and only structures with R factors < 0.1, no errors, and not polymeric were accepted. Data includes cases with more than one *gem*-alkynol group per molecule and/or more than one molecule per asymmetric unit.

No. of types of interaction per crystal structure	Interaction type	Number of structures
One type	i	13
	ii	18
	iii	1
	iv	4
Two types	i & ii	1
	i & iii	1
	i & iv	7
	ii & iii	1
	ii & iv	1
	iii & iv	0
Three types	i & ii & iii	4
	i & ii & iv	1
	i & iii & iv	0
	ii & iii & iv	0
All four types	i & ii & iii & iv	3

Table 19.2: Frequencies of occurrence of the possible combinations of the four gem-alkynol - gem-alkynol interactions.

Although the data sample is not really big enough to draw any definite conclusions, a few patterns can be inferred. Firstly, that interaction (i) is often found in combination with other interactions, especially with interaction (iv). Interaction (iii) is rarely found. The preferred combinations are interactions (i) & (iv), interactions (i) & (ii) & (iii), and all four interactions, however, just interaction (i) or interaction (ii) without any further gem-alkynol - gem-alkynol interactions is much more likely than any combination of interactions.

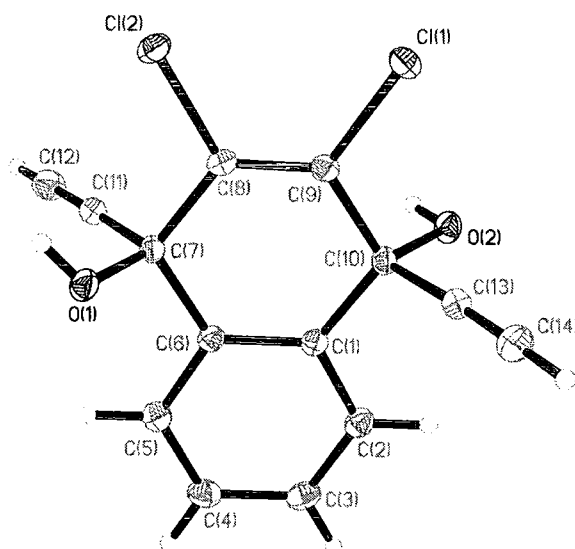


Figure 19.2: 2,3-dichloro-1,4-diethynyl-1,4-dihydroxy-naphthalene, thermal ellipsoids plotted at 50% probability.

In 2,3-dichloro-1,4-diethynyl-1,4-dihydroxy-naphthalene there are many possible and competing interactions. Not only are there the four possible *gem*-alkynol - *gem*-alkynol interactions discussed above, there is also the possibility for chlorine – chlorine type interactions (such as have been discussed in Chapter 16 and which have been shown to have a strong influence on structure given the right conditions), and the potential for chlorine atoms and the phenyl ring to act as hydrogen bond acceptors and C-H as hydrogen bond donors. With such a wealth of interactions to choose from, the combination of interactions utilised in the crystal structure will be very informative.

19.2 Crystal Data

Code	9
Radiation type	X-ray
Instrument	Smart-CCD ⁹
Instrument type	Area detector
Wavelength / Å	0.71073
Formula	C ₁₄ H ₈ Cl ₂ O ₂
Formula weight	279.10
Temp / K	120(2)
Crystal system	Monoclinic
Space group	P2 ₁ /c
Colour	Colourless
Habit	Block
Size / mm	0.45x0.35.x0.20
a / Å	7.4454(5)
b / Å	23.3125(17)
c / Å	7.5606(5)
$\alpha = \gamma$ / °	90
β / °	110.578(3)
Z	4
Mu / mm ⁻¹	0.517
Absorption correction type	None
R(int)	0.0318
Data/restraints/parameters	2815 / 0 / 179
GooF	1.062
R1	0.0301
wR2	0.0739

Table 19.3: Crystal data for compound 9, 2,3-dichloro-1,4-diethynyl-1,4-dihydroxy-naphthalene.

19.3 Crystal Structure and Results

Of the four possible *gem*-alkynol – *gem*-alkynol interactions, three (types (i), (ii), and (iii)) are seen in the crystal structure of compound **9**. Only the ‘weak-weak’ interaction, (iv) ($\text{C}\equiv\text{C}-\text{H}\dots\pi$) is not seen. Interactions (i) and (ii) link the molecules into chains and dimers respectively, overall this results in the formation of ladders.

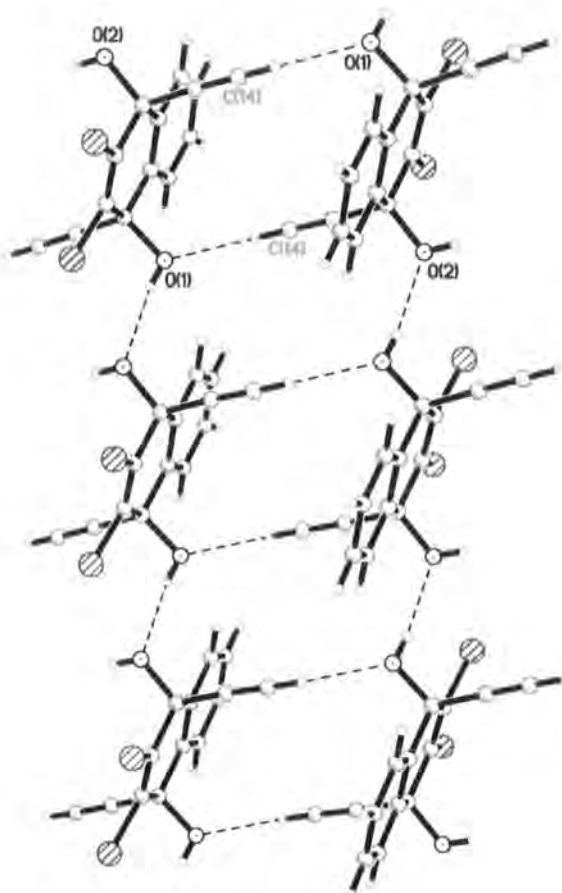
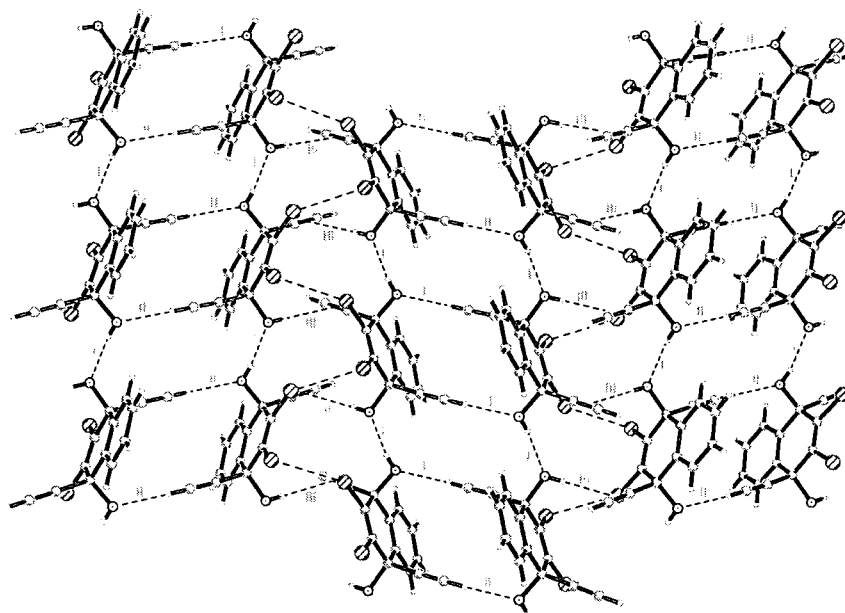


Figure 19.3: Ladder built up from *gem*-alkynol – *gem*-alkynol interactions (i) and (ii).

These chains are joined into zig-zag sheets by the *gem*-alkynol – *gem*-alkynol interaction type (iii), and by chlorine – chlorine interactions. These chlorine – chlorine interactions are type II halogen – halogen interactions (i.e. one $\text{C}-\text{Cl}\dots\text{Cl}$ angle of approximately 90° and the other of approximately 180°) such as occur within the co-crystal of 2,4,6-*tris*-(4-chlorophenoxy)-1,3,5-triazine and tribromobenzene (co-crystal **6**) discussed in Chapter 16.

a)



b)

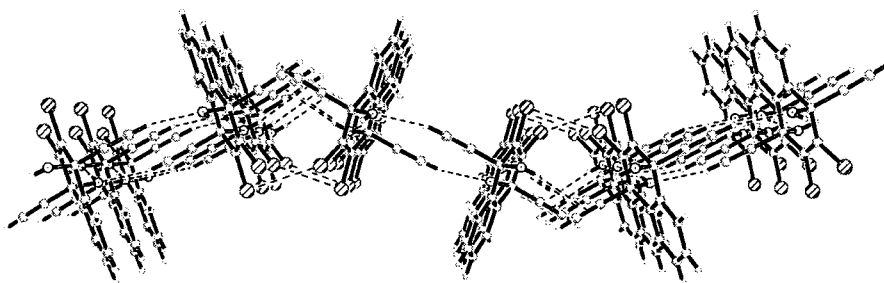
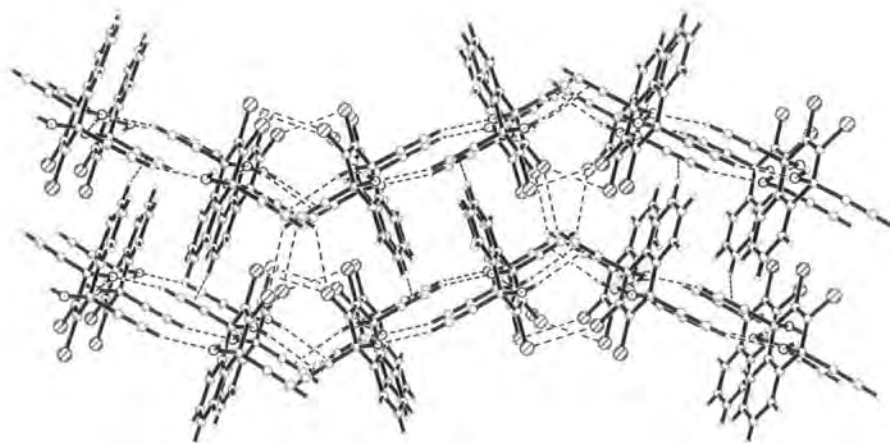


Figure 19.4: Zig-zag sheets of compound **9** showing the various *gem*-alkynol interactions and the chlorine - chlorine interaction, a) viewed from above with interactions (i), (ii), and (iii) labelled in grey, b) side view.

If the two *gem*-alkynol groups per molecule are considered as consisting of four donor hydrogen atoms (two hydroxyl and two ethyne hydrogen atoms) and four acceptor groups (two oxygen atoms and two ethyne bonds), then the three *gem*-alkynol – *gem*-alkynol interactions leave one ethyne donor hydrogen atom, and one ethyne acceptor group unused. This donor and acceptor do form interactions, but with other groups in the molecule; a chlorine atom and a phenyl hydrogen respectively.

It is of note that it is the weaker type of donor and the weaker type of acceptor that are not involved in the *gem*-alkynol – *gem*-alkynol interactions that form the sheets. The *gem*-alkynol – *gem*-alkynol interactions are involved in the formation of the sheets only, and it is the interactions between the *gem*-alkynol groups and other parts of the molecule that hold the sheets together, building the three dimensional lattice.

a)



b)

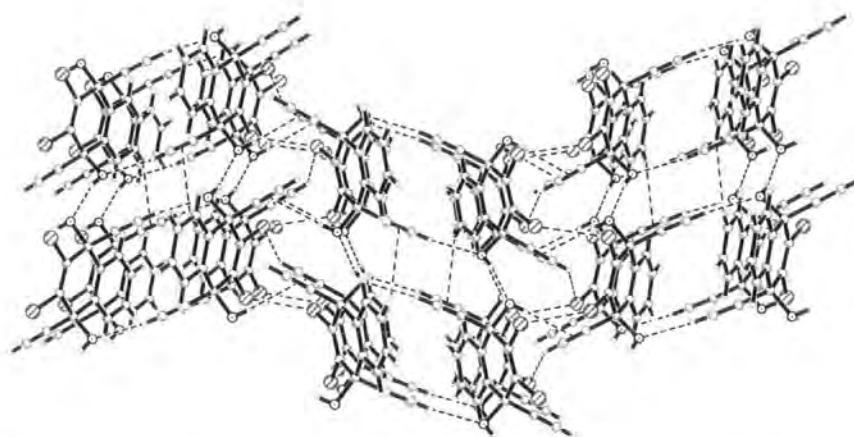


Figure 19.5: Zig-zag sheets of compound 9 showing all the various interactions, a) side view, b) looking down on a sheet with interactions within and between sheets shown.

Gem-alkynol – gem-alkynol interactions				
type	Hydrogen bond D-H...A	H...A / Å	D...A / Å	DHA /°
i	O ₁ -H ₁ ...O ₂	2.06(2)	2.794(2)	165(2)
ii	C ₁₄ -H ₁₄ ...O ₁	2.35(2)	3.282(2)	166(2)
iii	O ₂ -H ₂ ...π _A	2.72	3.516	172
Interactions between the gem-alkynol groups and other parts of the molecule				
	Hydrogen bond D-H...A	H...A / Å	D...A / Å	DHA /°
	C ₁₂ -H ₁₂ ...Cl ₂	2.98(2)	3.703(2)	135(2)
	C ₄ -H ₄ ...π ₂	3.04	3.744	131
Halogen – halogen interaction				
	Halogen bond Cl...Cl	Cl...Cl / Å	C-Cl...Cl /°	Cl...Cl-C /°
	C ₉ -Cl ₁ ...Cl ₂ -C ₈	3.2987(6)	91.39(5)	144.25(5)

Table 19.4: Interactions within the 2,3-dichloro-1,4-diethynyl-1,4-dihydroxy-naphthalene crystal structure.

19.4 Conclusions

This structure is very interesting due to the sheer diversity of the intermolecular interactions. Of the possible hydrogen bond, and halogen – halogen bond, donor and acceptor groups discussed at the beginning of the chapter, most are utilised in the structure.

The gem-alkynol – gem-alkynol interactions show a close correlation between the lengthening of the hydrogen bond and the weakening of the donor and acceptor groups. There are three interactions running in different directions within the plane of the sheet. The longest and, therefore, probably the weakest of these interactions is reinforced by the chlorine – chlorine interactions. In comparison to the interactions within the sheet, the interactions between two sheets are fewer, longer and less linear.

The combination of gem-alkynol – gem-alkynol interactions found in compound **9** (interactions (i) & (ii) & (iii)) appears to be one of the more common interaction combinations.

Chapter 20 : 4,4-diphenyl-2,5-cyclohexadienone

20.1 Introduction

Compound **10**, 4,4-diphenyl-2,5-cyclohexadienone is interesting because it exists in many different structural forms or polymorphs. In fact it appears to form different polymorphs exceptionally easily.

Polymorphism is a very intriguing phenomenon. It has been suggested by McCrone (1965) that 'the number of forms known for a given compound is proportional to the time spent in research on that compound'²⁴, that said, the discovery of a new polymorphic system is still of great interest. From a crystal engineering aspect, polymorphism can be both a help and a hindrance. When trying to understand the various influences of several inter- and intra-molecular interactions, the existence of a compound in more than one crystal packing arrangement gives a set of systems where the only variable is the crystal structure. However, the ultimate aim of crystal engineering is to predict the crystal structure of a given compound and here the occurrence of polymorphism makes accurate prediction even harder than it already is.

The polymorphic forms of 4,4-diphenyl-2,5-cyclohexadienone are especially interesting because at least three polymorphs form concomitantly^{3,25}, that is to say, they form under completely identical conditions - to the extent of being found in the same re-crystallisation flask. The first two forms (**1** and **2**) were identified during routine analysis, form **3** was obtained when larger crystals were grown under similar, but not identical, conditions for a neutron experiment (pending). Re-examination of the sample that was known to contain forms **1** and **2** identified another form (**4**). Since then systematic attempts to obtain further polymorphs have been carried out at the University of Hyderabad, India*, and here in Durham†, these studies have resulted in the

* Study being carried out by Dr A. Nangia's laboratory, University of Hyderabad, India.

† Study being carried out by Mr. R. Mondal, University of Durham, U.K.

20.2 Crystal Data

Code	10 (form 3)
Radiation type	X-ray
Instrument	Smart-CCD ⁹
Instrument type	Area detector
Wavelength / Å	0.71073
Formula	C ₁₈ H ₁₄ O ₁
Formula weight	246.29
Temp / K	100(2)
Crystal system	Orthorhombic
Space group	Pbca
Colour	Colourless
Habit	Block
Melting Point / °C	124-126
Size / mm	0.55x0.40x0.30
a / Å	10.7921(6)
b / Å	17.475(1)
c / Å	27.934(2)
$\alpha (= \beta = \gamma) / ^\circ$	90
Z	16
Z'	2
Mu / mm ⁻¹	0.075
Absorption correction type	Psi-scan
R(int)	0.0742
Data/restraints/parameters	6538 / 0 / 371
GooF	1.061
R1	0.0589
wR2	0.1243
Density (calculated) Mg/m ³	1.242
Solvent of re-crystallisation	Hexane/EtOAc/DMC

Table 20.2: Crystal data for compound 10, 4,4-diphenyl-2,5-cyclohexadienone, form 3.

Code	10 (form 1) ^{1,3}	10 (form 2) ^{1,3}	10 (form 3)
Formula	C ₁₈ H ₁₄ O ₁	C ₁₈ H ₁₄ O ₁	C ₁₈ H ₁₄ O ₁
Formula weight	246.29	246.29	246.29
Temp / K	160	150	100(2)
Crystal system	Monoclinic	Triclinic	Orthorhombic
Space group	P2 ₁	P-1	Pbca
Colour	Colourless	Colourless	Colourless
Habit	Triangular	Sphere	Block
Melting point / °C	120-122	120-122	124-126
a / Å	7.9170(6)	10.0939(2)	10.7921(6)
b / Å	8.4455(6)	16.2592(3)	17.475(1)
c / Å	10.3086(9)	16.2921(3)	27.934(2)
α / °	90	88.257(1)	90
β / °	105.758(8)	85.338(1)	90
γ / °	90	83.645(1)	90
Z	2	8	16
Z'	1	4	2
Mu / mm ⁻¹	0.075	0.075	0.075
R1	0.050	0.0684	0.0589
wR2	0.1149	0.1567	0.1243
Density (calculated) Mg/m ³	1.233	1.236	1.242
Solvent of re- crystallisation	Hexane/EtOAc	Hexane/EtOAc	Hexane/EtOAc /DMC

Table 20.3: Comparison of forms 1, 2, and 3 of compound 10.

20.3 Crystal Structure and Results

Both the overall molecular packing and the hydrogen bond motifs that give rise to this packing are very different between the three polymorphs:

Polymorph 1

(Data taken from CSD⁶ – Code HEYHOU¹)

The structure of polymorph **1** is based on helical chains of O...H-C hydrogen bonds that are bi-furcated at the oxygen acceptor atom, and where the C-H hydrogen bond donor is part of the phenyl groups rather than the more acidic quinoid group. The angle between the bi-furcated hydrogen bonds is 125°.

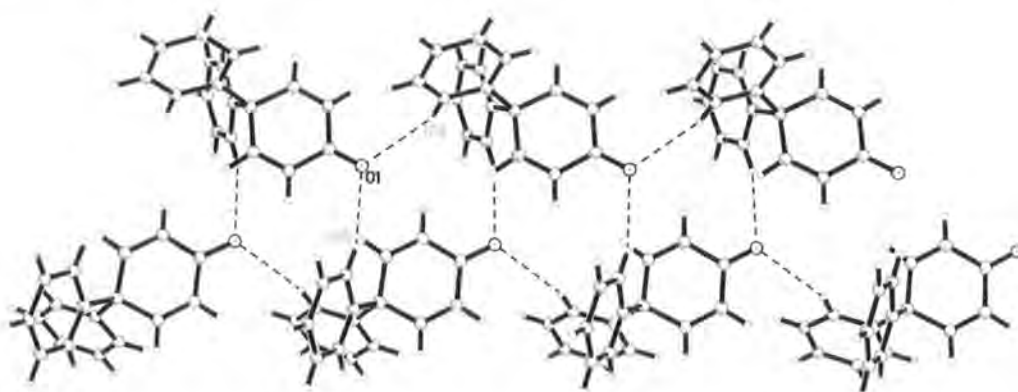


Figure 20.2: Helical chains mediated by O...H-C hydrogen bonds.

These chains are linked to each other by C-H... π bonds between a hydrogen atom of the quinoid and a phenyl ring centroid thereby creating sheets.

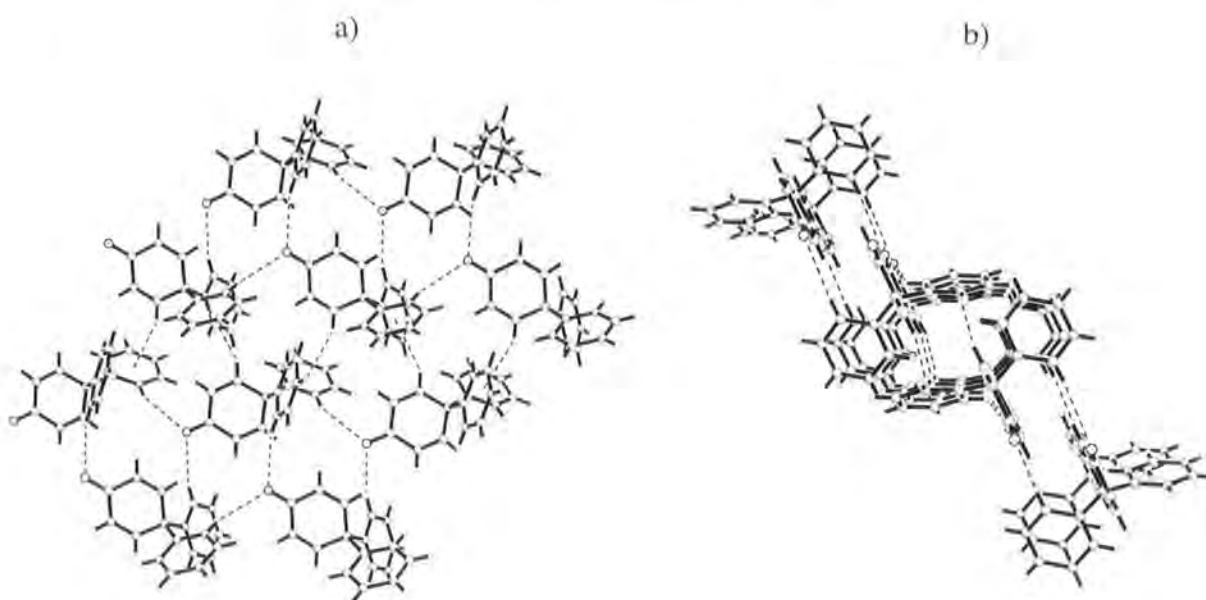


Figure 20.3: Sheets of C-H... π linked chains, a) top view of sheet, b) side view of sheet.

Adjacent sheets are also linked by C-H... π hydrogen bonds, but this time between the hydrogen of a phenyl ring and one of the double bonds of the quinoid group, to give a three-dimensional network of hydrogen bonds.

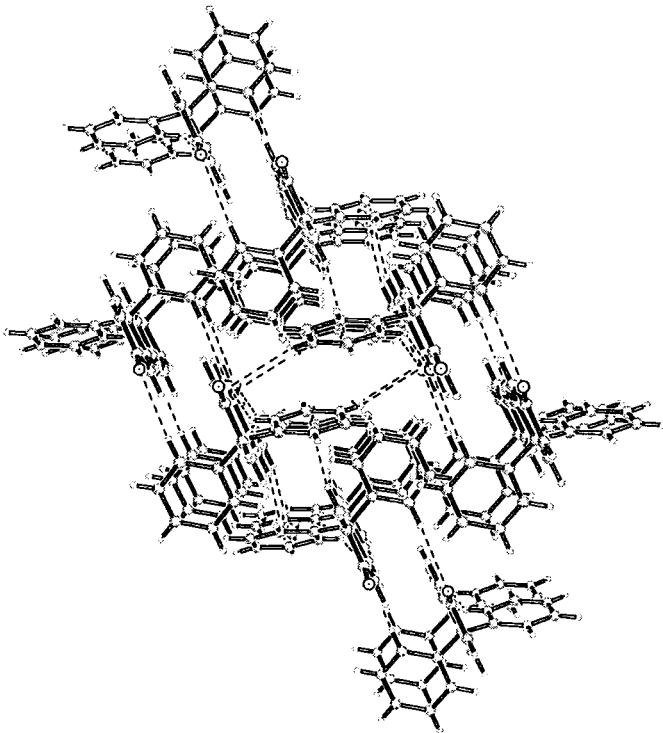


Figure 20.4: Hydrogen bonding within and between two sheets of polymorph **1**, viewed edge on to the sheets.

C-H...A	Distance H...A /Å	Distance C...A /Å	Angle CHA /°
C ₁₄ -H ₁₀ ...O ₁	2.692	3.401	132
C ₁₅ -H ₁₁ ...O ₁	2.682	3.605	164
C ₇ -H ₅ ... $\pi_{\text{(phenyl)}}$	2.821	3.712	157
C ₈ -H ₆ ... $\pi_{\text{(quinoid)}}$	3.000	3.875	154

Table 20.4: Hydrogen bonds occurring in polymorph **1**.

Polymorph 2

(Data taken from CSD⁶ – Code HEYHOU01¹)

Polymorph 2 is a much more complicated structure to follow since it contains four independent molecules of 4,4-diphenyl-2,5-cyclohexadienone in the asymmetric unit. To aid clarity in the following diagrams the molecule containing the atom O₁ has been coloured green, that containing O₂ has been coloured blue, that containing O₃ coloured red, and that containing O₄ coloured yellow. These colours are constant in all the following diagrams and the molecules are distinguished by the colour they are drawn with in the text as well.

Overall the crystal structure is very different to that seen for polymorph 1. Within the structure the hydrogen bonding pattern around one molecule in the asymmetric unit is very different to that around the next.

The molecules coloured red and those molecules coloured blue both form dimers with themselves, i.e. red-red and blue-blue. These dimers are formed in a manner analogous to carboxylic acid dimers: by two O...H-C hydrogen bonds where the hydrogen is a quinodial hydrogen from a position adjacent to the ketone oxygen.

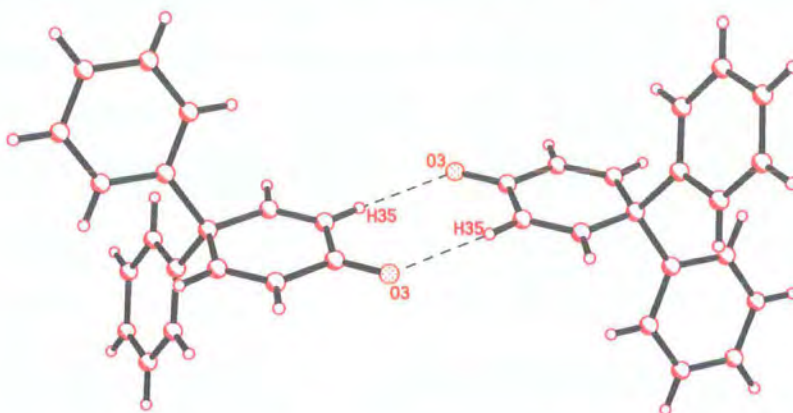


Figure 20.5: Red-red dimer in polymorph 2 structure, the blue-blue dimer is similar.

The red and blue coloured molecule dimers combine to form ladders with adjacent dimers, linked by C-H...O hydrogen bonds where the hydrogen atom is part of the phenyl ring on the red molecule, and by C-H... π bonds where the hydrogen atom is from a phenyl ring on the blue molecule and the π group is a quinodial double bond on the red coloured molecule.

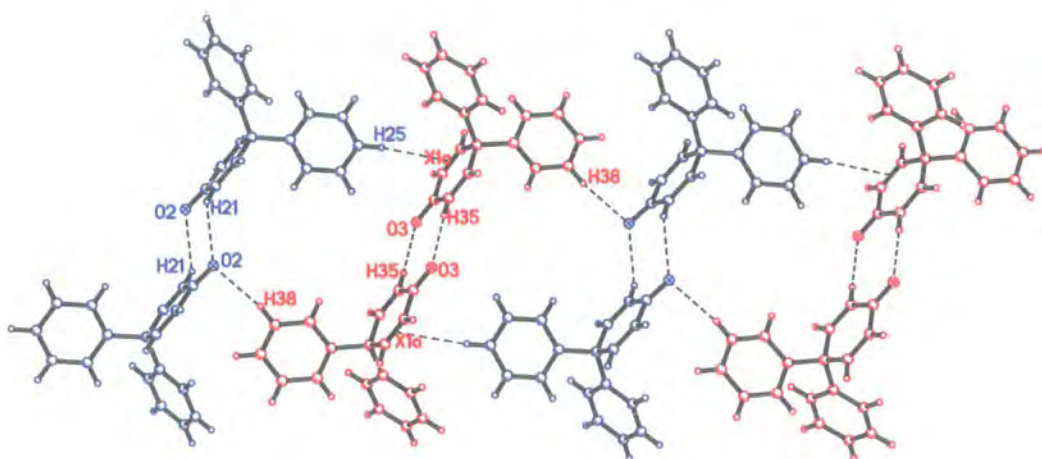


Figure 20.6: Ladder of red-red and blue-blue dimers.

The yellow coloured molecules also form dimers, but these dimers are different from the red-red and the blue-blue dimers with the C-H...O hydrogen bonds being between a hydrogen atom in the para position in the phenyl group and the oxygen atom.

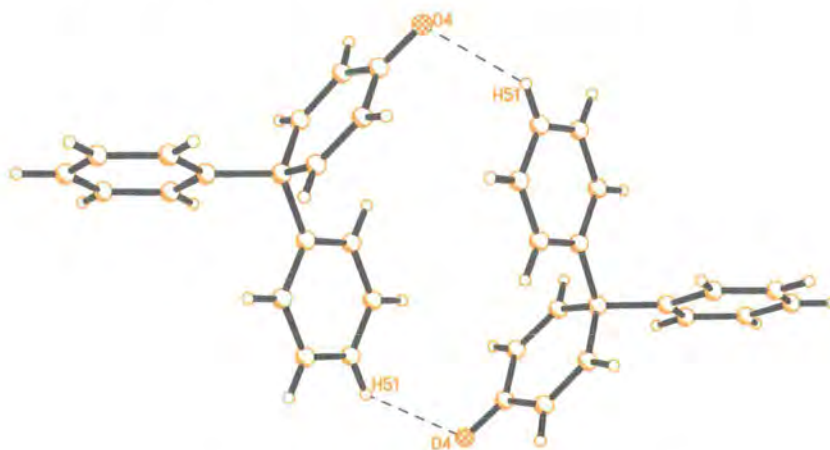


Figure 20.7: Yellow-yellow dimers in the polymorph 2 structure.

The ladders consisting of the red-red and the blue-blue dimers lie parallel to each other, with a strip of alternating yellow-yellow dimers and two green coloured molecules in the gap between adjacent ladders.

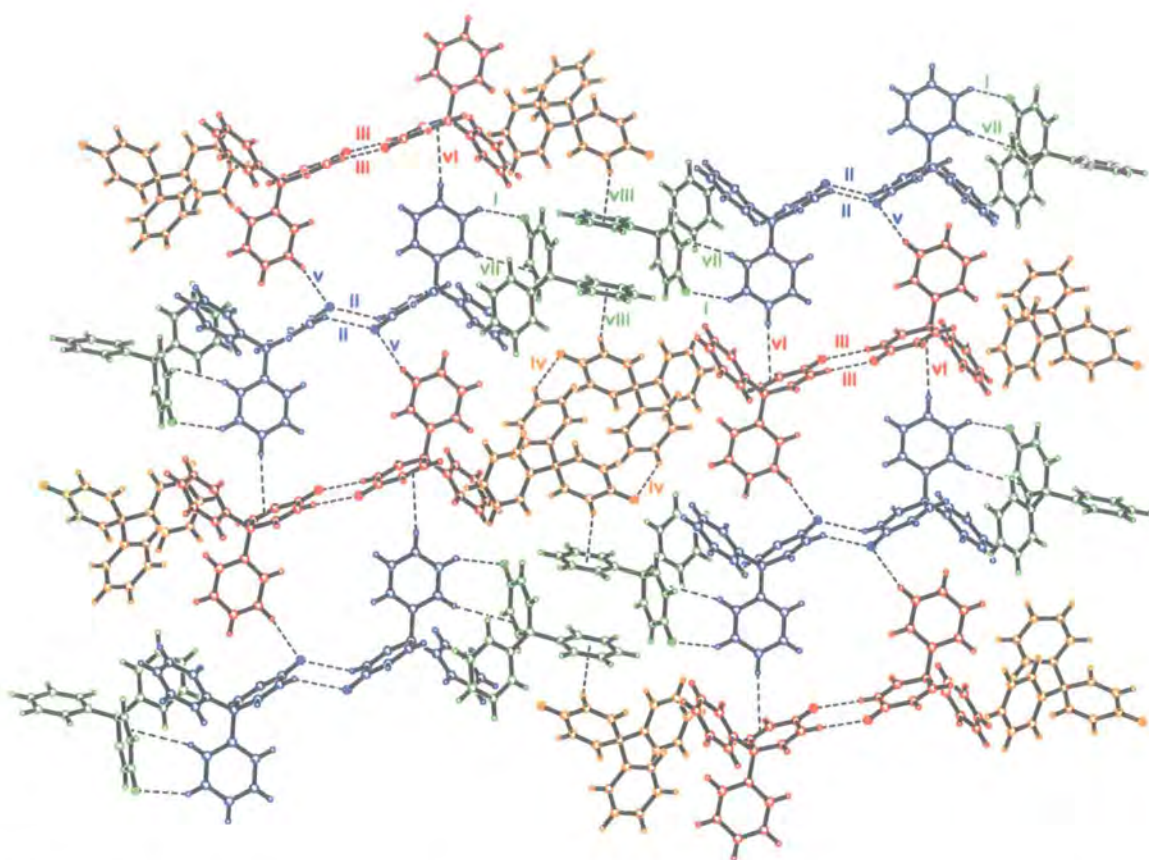


Figure 20.8: All the interactions within one sheet of the polymorph 2 structure. Each type of interaction has been given a different number.

Adjacent sheets are connected to each other by C-H... π interactions to the phenyl rings of the red and blue coloured molecules. The interaction at the phenyl ring of the blue coloured molecule is a 'double faced' C-H... π interaction with an angle of 174.2° between the two hydrogen bonds.

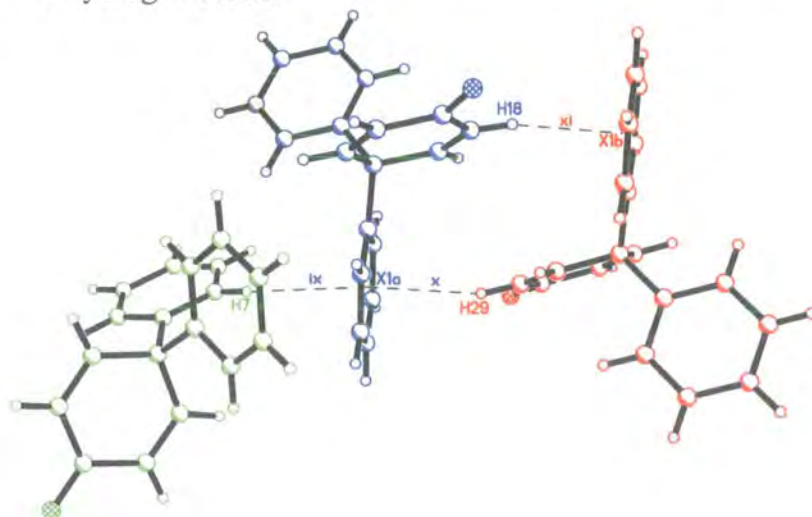


Figure 20.9: The C-H... π interactions that occur between sheets, note the double faced C-H... π hydrogen bond across the phenyl ring of the blue coloured molecule.

Label	D-H...A	H...A / Å	D...A / Å	DHA / °
i	C ₃₂ -H ₂₄ ...O ₁	2.58	3.295	132
ii	C ₂₈ -H ₂₁ ...O ₂	2.57	3.224	126
iii	C ₄₇ -H ₃₅ ...O ₃	2.47	3.405	170
iv	C ₆₆ -H ₅₁ ...O ₄	2.74	3.525	140
v	C ₅₀ -H ₃₈ ...O ₂	2.50	3.426	164
vi	C ₃₃ -H ₂₅ ... $\pi_{\text{(quinoid)}}$	3.03	3.976	171
vii	C ₂₄ -H ₁₇ ... $\pi_{\text{(quinoid)}}$	3.10	3.976	155
viii	C ₆₇ -H ₅₂ ... $\pi_{\text{(phenyl)}}$	2.69	3.557	152
ix	C ₁₁ -H ₇ ... $\pi_{\text{(phenyl)}}$	2.80	3.646	149
x	C ₃₉ -H ₂₉ ... $\pi_{\text{(phenyl)}}$	2.66	3.569	161
xi	C ₂₅ -H ₁₈ ... $\pi_{\text{(phenyl)}}$	2.64	3.547	161

Table 20.5: Hydrogen bonds occurring in polymorphs 2.

From the table above it can be seen that the hydrogen bonds to a quinoid π group (interactions (vi) and (vii)) tend to be notably longer than those to the phenyl π groups.

Polymorph 3

There are two independent molecules in the asymmetric unit of polymorph **3**, as in polymorph **2** the independent molecules have been coloured to distinguish them from each other. The first molecule containing the atom O₁ is coloured purple, and that containing the atom O₂ is coloured cyan.

The structure of polymorph **3** exhibits features of both the previous polymorph structures; as in polymorph **1** it has C-H...O hydrogen bonds that are bi-furcated at the donor oxygen atom, as in polymorph **2** there are C-H...O dimers and double faced C-H... π bonds.

The first type of molecule, coloured purple, forms C-H...O hydrogen bonds that are bi-furcated at the donor oxygen atom like those seen in polymorph **1**, however unlike polymorph **1** these hydrogen bonds form sheets rather than chains. The angle between the bi-furcated hydrogen bonds is 96°. This is further from the idealised angle between the two oxygen lone pairs (the hydrogen bond acceptor points) than is seen for the polymorph **1** bi-furcated bond.

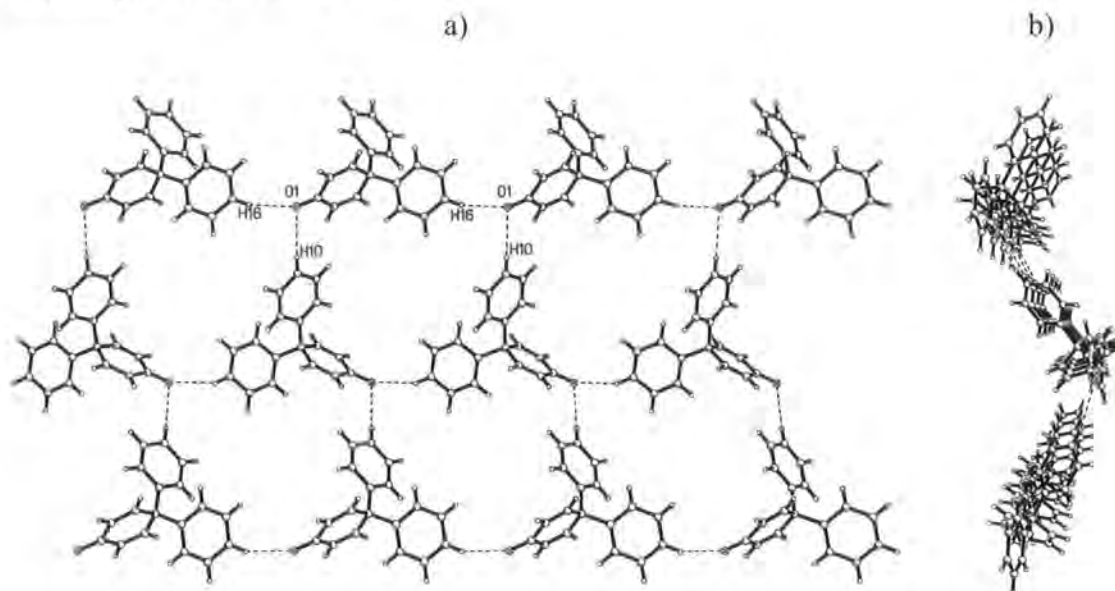


Figure 20.10: The packing of the first type of molecule into sheets in polymorph **3**, a) viewed from above and b) viewed from the side.

Each sheet is very puckered, but in the 3-dimensional crystal structure two sheets are interlaced to give a thicker, flatter, double sheet.

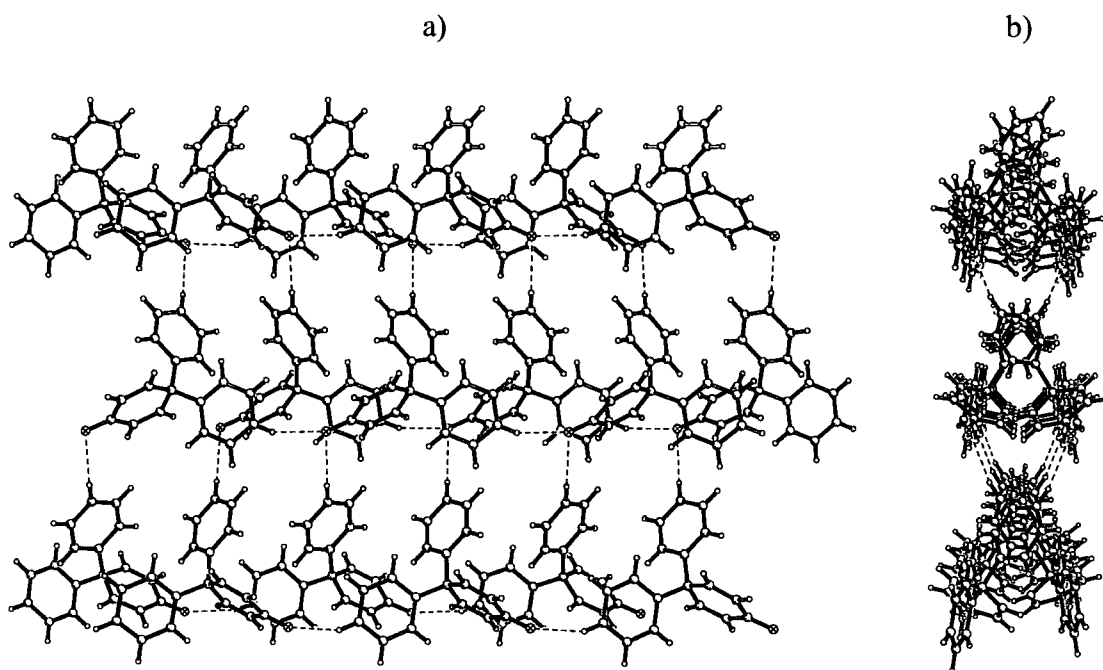


Figure 20.11: The interweaving of two of the sheets shown in Figure 20.10, a) viewed from above and b) viewed from the side.

The second type of molecule, coloured cyan, forms dimers similar to the yellow-yellow dimer seen in polymorph **2**, although in polymorph **3** the hydrogen bond is from the hydrogen atoms in the meta position on the phenyl ring, not the para position. A second C-H...O hydrogen bond from the same oxygen (i.e. again bi-furcated at the oxygen atom) forms to a purple coloured molecule. The angle between the bi-furcated hydrogen bonds is 143° .

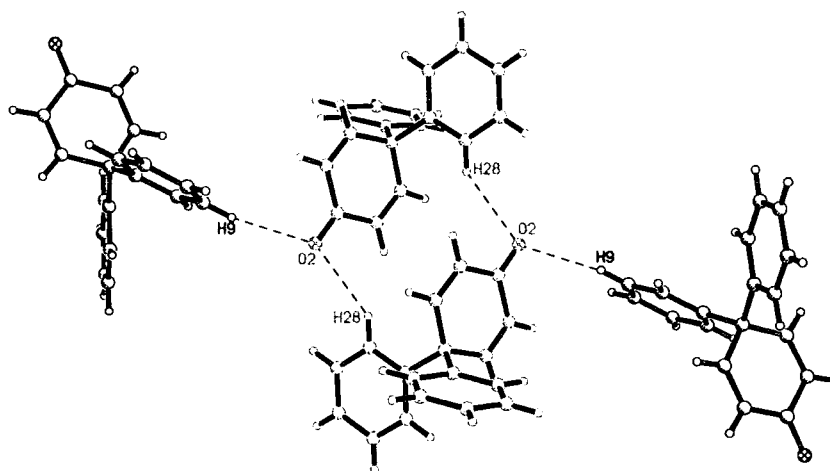
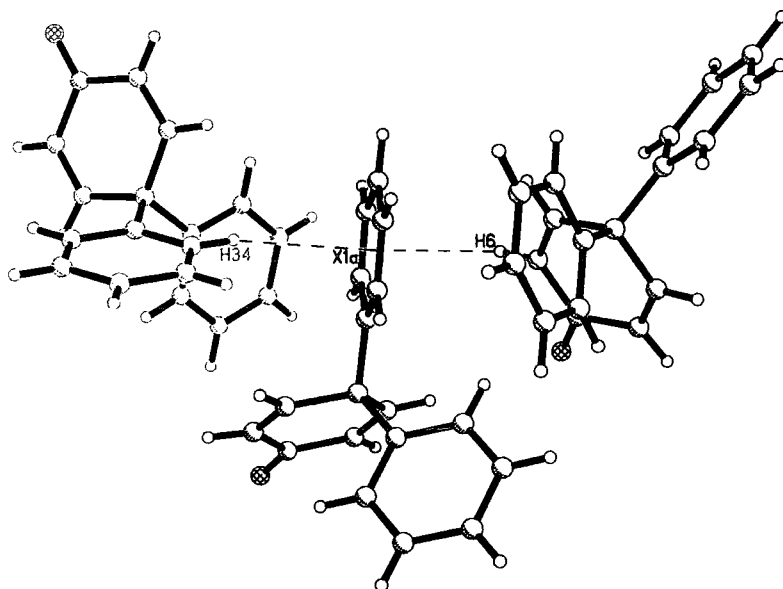


Figure 20.12: Dimers of the cyan coloured molecule.

The structure of polymorph **3** also exhibits the same type of 'double-faced' C-H... π hydrogen bonds seen in polymorph **2**. The angle between the two hydrogen bonds is 153° .



*Figure 20.13: The 'double faced' hydrogen bond in polymorph **3**.*

When all these elements of the structure of polymorph **3** are put together, the structure is seen to consist of alternate layers of purple and cyan coloured molecules. The double sheets of the purple coloured molecules are separated by layers made of the cyan coloured dimers.

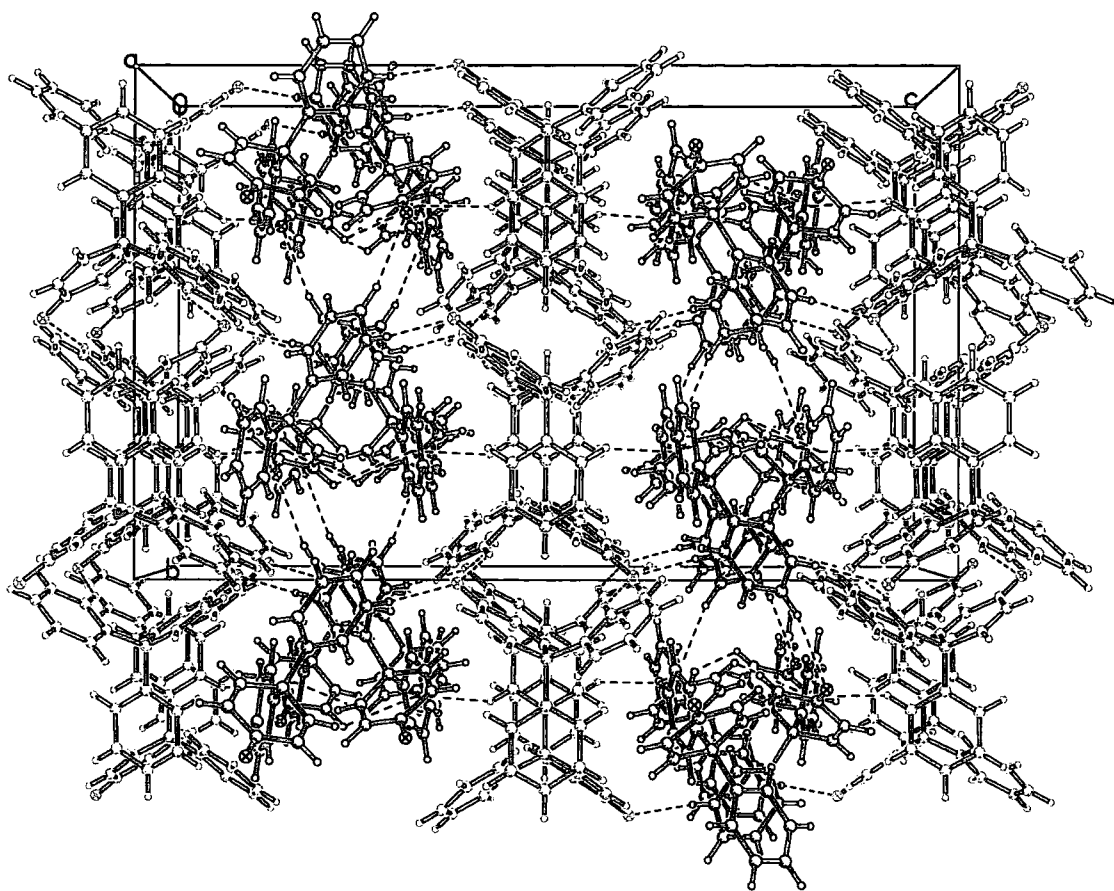


Figure 20.14: The overall structure of polymorph 3.

D-H...A	H...A /Å	D...A /Å	DHA /°
C ₁₀ -H ₁₀ ...O ₁	2.68	3.613(3)	168
C ₁₆ -H ₁₆ ...O ₁	2.46	3.247(2)	140
C ₁₁ -H ₁₁ ...O ₁	1.58	2.219(2)	121
C ₉ -H ₉ ...O ₁	2.60	3.531(2)	166
C ₆ -H ₆ ...π _(phenyl)	2.95	3.482	116
C ₁₁ -H ₁₁ ...π _(phenyl)	2.81	3.646	148

Table 20.6: Hydrogen bonds occurring in polymorph 3.

20.4 Conclusions

Polymorphism is perhaps encouraged (or at least not hindered) by the fact that there are ten essentially identical hydrogen atom donors giving the possibility to form hydrogen bonds in very different directions, as well as four slightly more acidic H-donors also all pointing in different directions. Add to this the fact that the overall molecular shape is not designed to fit together in one greatly preferred orientation, and could even be considered as pseudo-spherical, it is not surprising that there are many similar energy packing motifs, i.e. many polymorphs.

The hydrogen bond motifs of dimers, C-H...O bonds bi-furcated at the oxygen, and C-H... π bond are seen in various combinations in all the polymorphs, though not all the motifs are seen in each polymorph. However, it is the effect of having chemically identical, but crystallographically different molecules, that allows the variation of structure polymorphs to be found. The crystallographically independent molecules differ slightly in their molecular geometry, but the main difference is in the crystallographic environment.

Why does this compound choose to form structures that rely on having molecules on crystallographically independent sites? Or perhaps that question should be; how do most crystal structures form with only one crystallographically independent molecule?

20.5 References for Part 3

- 1) A.Anthony, G.R.Desiraju, R.K.R.Jetti, S.S.Kuduva, N.N.L.Madhavi, A.Nangia, R.Thaimattam, V.R.Thalladi. *Mat. Res. Bull.*, 1998, **SS**, 1-18.
- 2) P.K.Thallapally, K.Chakraborty, H.L.Carrell, S.Kotha, G.R.Desiraju. *Tetrahedron*, 2000, **36**, 6721-6728.
- 3) V.S.Senthil, A.Addlagatta, A.Nangia, W.T.Robinson, C.K.Broder, R.Mondal, I.R.Evans, J.A.K.Howard. *Conformational Polymorphism, Conformational Isomorphism and Concomitant Polymorphism in 4,4-Diphenyl-2,5-cyclohexadienone*. paper submitted 2002.
- 4) V.R.Thalladi, R.Boese, S.Brasselet, I.Ledoux, J.Zyss, R.K.R.Jetti, G.R.Desiraju, *Chem. Commun.*, 1999, 1639-1640.
- 5) Bilton, Clair. *Hydrogen bonding in organic systems. A study using X-ray and neutron diffraction and database analysis*. Ph.D. thesis, University of Durham 1999.
- 6) F.H.Allen, O.Kennard. *Chem. Des.Autom. News*, 1993, **8**, 30-37.
- 7) V.R.Thalladi, S.Brasselet, H-C. Weiss, D.Blaser, A.K.Katz, H.L.Carrell, J.Zyss, A.Nangia, G.R.Desiraju, *J. Am. Chem. Soc.*, 1998, **120**, 2563-2577.
- 8) A.S.Jessiman, D.D.MacNicol, P.R.Mallinson, I.Vallance. *Chem. Commun.*, 1990, 1619-1621.
- 9) G.M.Sheldrick,. (1997). SHELX-97, Structure determination software, G.M. Sheldrick, University of Göttingen, Germany, 1997.
- 10) C.C.Wilson,. in *Neutron Scattering Data Analysis*, ed. M.W.Johnson, pp.145-163, IoP Conference Series, **107**, Bristol: Adam Hilger, 1990.
- 11) C.C.Wilson, *J. Mol. Struct.*, 1997, **405**, 207-217.
- 12) V.R.Pedireddi, D.S.Reddy, B.S.Goud, D.C.Craig, A.D.Rae, G.R.Desiraju. *J. Chem. Soc. Perkin Trans. 2*, 1994, 2353-2360.
- 13) G.R.Desiraju, R.Parthasurathy. *J. Am. Chem. Soc.*, 1989, **111**, 8725-8726.
- 14) R.K.R.Jetti, P.K.Thallapally, F.Xue, T.C.W.Mak, A.Nangia. *Tetrahedron*, 2000, **36**, 6707-6719.
- 15) C.K.Broder, J.A.K.Howard, D.A.Keen, C.C.Wilson, F.H.Allen, R.K.R.Jetti, A.Nangia, G.R.Desiraju. *Acta Cryst.*, 2000, **B56**, 1080-1084.
- 16) R.K.R.Jetti, A.Nangia, F.Xeu, T.C.W.Mak, *Chem. Commun.*, 2001, 919-920.
- 17) O.Konig, H-B.Burgi, T.Armbruster, J.Hulliger, T.Weber. *J. Am. Chem. Soc.*, 1997, **119**, 10633-10640.
- 18) P. van der. Sluis, A.L. Spek. *Acta Cryst.* 1990, **A46**, 194-201

- 19) Platon99: A.L.Spek, *Acta Cryst.*, 1990, **A46**, C-34
- 20) N.N.L.Madhavi, G.R.Desiraju, C.Bilton, J.A.K.Howard, F.H.Allen. *Acta. Cryst.*, 2000, **B56**, 1063-1070.
- 21) N.N.L.Madhavi, C.Bilton, J.A.K.Howard, F.H.Allen, A.Nangia, G.R.Desiraju. *New J. Chem.* 2000, **24**, 1-4.
- 22) C.Bilton, J.A.K.Howard, N.N.L.Madhavi, A.Nangia, G.R.Desiraju, F.H.Allen, C.C.Wilson, *Chem. Commun.*, 1999, 1675,-1676.
- 23) CRC Handbook of Chemistry and Physics, 53rd ed. CRC Press., Cleveland, 1973.
Mark Winter, University of Sheffield, *Chemistry: Web elements* [online], 1993-2002, available from <http://www.webelements.com>.
- 24) W.C.McCrone in '*Physics and Chemistry of the Organic Solid State Vol 2*'. Ed: D.Fox, M.M.Labes, New York: A.Weissberger Interscience, 1965, p725
- 25) J.Bernstein, R.Davey, J.-O.Henck, *Angew. Chem. Int. Ed. Eng.*, 1999, **38**, 3440-3461.

Chapter 21 : Conclusions

A study of a wide range of compounds, as has been seen in Parts 2 and 3, really emphasised the variety seen in crystal structures, with each structure containing different patterns arising from both the different shapes of the molecule that the structure is built from and the different interaction motifs.

It can be seen just how difficult it will be to fully predict the crystal structure of a given molecule. So many factors influence the structure, from the molecular shape through to the interplay of the various intermolecular interactions. Despite the fact that the only types of interactions that have been considered here are the types that are described as 'directional' interactions, a quick glance at any of the tables listing the interaction lengths and angles will show that there is a large amount of leeway in this 'directionality'. However, I hope that this thesis shows that we can, on the whole, understand in retrospect the factors that influence a crystal structure, and that from the study of groups of similar compounds (such as has been carried out in Part 2 and in some cases in Part 3) it is possible to predict the structures to a degree.

The more I look at crystal structures, the more I wonder at the way such tiny building blocks as molecules can pack together with such precision and constancy to give such beautiful patterns and structures - both on a molecular scale of lattices, sheets and chains, helices and stacks and voids, ever repeating, and on a macromolecular scale of the crystals themselves.



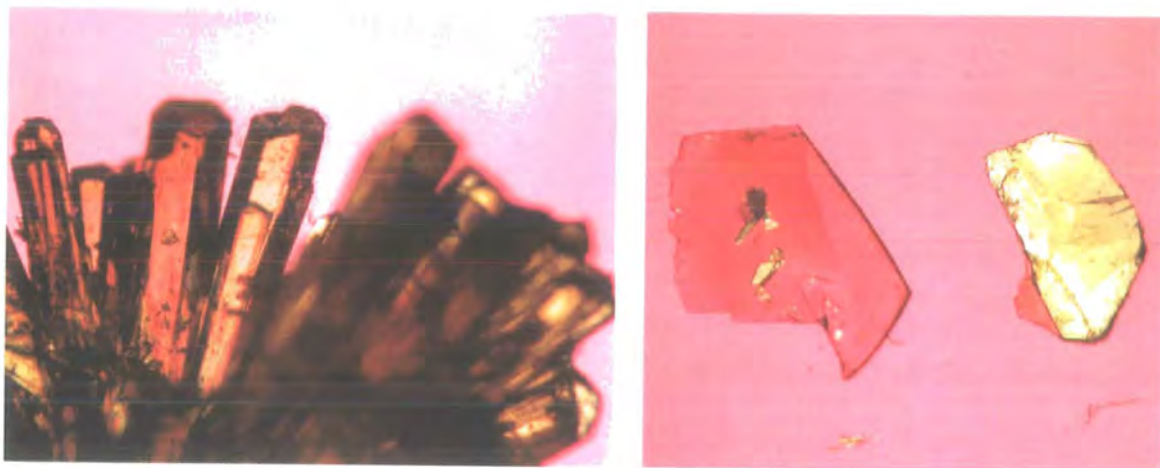


Figure 21.1: Crystals of 4,4'-Dinitrotetraphenylmethane (**8**) and 4-amino-4'-hydroxydiphenylpropane (**3a**) (left and right of previous page respectively). A 'hedgehog' of needle crystals of thiodianiline and thiodiphenol (on going work), and thin plates of 4-amino-4'-hydroxydiphenylpropane (**3a**) (left and right of current page respectively).

Appendix

Appendix A: Melting Points of Meta and Para Disubstituted Benzenes

Report of work carried out during visit to Prof. Desiraju's laboratory, University of Hyderabad, India. January 2001.

Ongoing Project.

This report is a record of this preliminary / feasibility study. It was meant, primarily, as a detailed account of the experimental work that has been carried out, for whichever student is to continue the project.

21.1 Introduction

It is a well known observation that, in the majority of cases, the melting point of para disubstituted benzenes is significantly higher than that of meta disubstituted benzenes. This observation has been attributed to shape considerations¹, a 'rule of thumb'² states that 'symmetrical molecules pack in a 3-D periodic lattice more easily than less symmetric ones, hence forming more stable, higher melting and less soluble crystals'¹. Given that para-disubstituted benzenes are more 'symmetric' (even if only 'symmetric' in general terms of bulk and shape not in actual true molecular symmetry) this can be said to go some of the way towards explaining the melting point variation, but is not a full explanation.

Here pairs of meta and para disubstituted benzenes have been studied with the aim of increasing the understanding, in terms of both structural and thermodynamical considerations, why the para isomer (nearly) always melts at a higher temperature than the meta.

In going from meta to para disubstituted benzenes, we have a system where there is no change in functional groups, only a variation in the shape of the molecule and the relative orientation of the functional groups. Within a meta/para pair the possible structural synthons are (usually) the same, but the changes in shape and orientation alter

the way in which these synthons can be used, and therefore must result in different crystal structures.

21.2 Experimental

Structures of 107* pairs of meta/para disubstituted benzenes were obtained from the Cambridge Structural Database³ (April 2000 release - version 5.19 215403 entries).

Melting points were obtained for both isomers of 43 pairs, and for 19 single isomers (where the melting point of other isomer is not yet obtained)[†]. Melting points were obtained from a variety of sources:

- Cambridge Structural Database data files
- Acros catalog (1997 edition)
- Original papers referenced in Cambridge Structural Database hit
- Other literature on the compound

Of the 43 pairs for which both melting points are known, there are only 2 examples of cases where the para isomer melts at a lower temperature than the meta isomer. In one the difference in temperatures $\Delta T = -2$ (where $\Delta T =$ melting point of the para isomer - melting point of the meta isomer) with the meta compound undergoing decomposition rather than melting. The second has a $\Delta T = -37$, if calculated using the value for melting point given in the Cambridge Structural Database data files. However the original paper⁴ lists the melting point of the meta and para compounds the other way round resulting in a $\Delta T = +37$. The crystallographic parameters in the paper are also inverted with the meta isomer cell listed as the para and vice versa. The correct order of the melting points for this compound is uncertain without further work.

10 pairs of compounds were chosen for further study with the selection made on the basis of greatest ΔT . The pair of compounds with $\Delta T = -37$ (or $+37$) was also included. Where there are multiple determinations of the same compound in the Cambridge Structural Database one structure was chosen, based firstly on which structure the melting point refers to (in cases where the melting point was obtained from the

* originally 109, 2 structure pairs were rejected, due to not being true meta/para pairs; in one the para isomer is a salt of the meta isomer (No. 102), in the other the 'meta isomer' is the Me derivative while the 'para isomer' is the Et derivative (No. 3).

[†] More recent work carried out with Miss Ashley Smith using the Beilstein Database⁵ has increased the numbers of pairs for which both melting points are known to 58 and the total number of known melting points to 141 isomers out of a possible total of 214 isomers.

Cambridge Structural Database) and secondly by the best data and structural refinement. In the case of 1,4-dihydroxybenzene (3 polymorphs) the 2 polymorphs with well determined structures were chosen.

The 10 pairs are:

No.	Meta refcode	Para refcode	$\Delta T / ^\circ$
49	MCBZAC	CLBZAP03	99
46	MNBZAC01	NBZOAC03	97
20	DNBENZ10	DNITBZ02	85
43	LAVBOZ	LAVBUF	74
60	NOGKAV	HIBCOK	73
37	JICVIA10	JICVEW10	72
45	MAMPOL	AMPHOL01	64
69	RESORA13	HYQUIN, HYQUIN05	63
85	TEWXOI	TEWWUN	62
106	ZONKAO	ZONJOB	-37 (+37)

A detailed analysis of the crystal structure was carried out for each of these compounds. The structures were defined in terms of chains, sheets and 3-D nets constructed from hydrogen bonds, weak hydrogen bonds and other intermolecular interactions such as Cl...Cl and π - π interactions. The analysis was carried out using the Cambridge Structural Database program 'PLUTO' with all hydrogen positions normalized to standard neutron positions.

From the 10 pairs for which a structural analysis was carried out 2 pairs were chosen for a more detailed analysis in terms of energy and the thermodynamics of the systems. One pair with similar packing in the 3-D structure for both the meta and para structures, and one pair with very different packing were chosen:

similar packing MCBZAC / CLBZAP
different packing MAMPOL / AMPHOL01

Initially the energy calculations were attempted on the 'different structure' pair DNBENZ10 / DNITBZ02, however sensible, or even consistent, results for this pair were not obtained, so the MAMPOL / AMPHOL01 pair was chosen instead.

The concept behind the study is that, for the pair with similar packing, ΔH_f for each structure would be similar and the difference in melting point dependent on ΔS_f (entropic considerations). However if the structures are very different then the difference in melting point is dependent on ΔH_f (as well as ΔS_f)

Given that $T_f = \Delta H_f / \Delta S_f$

where T_f = Temperature of fusion

ΔH_f = Enthalpy of fusion

ΔS_f = Entropy of fusion

the melting point will increase with increasing ΔH_f

or with decreasing ΔS_f

ΔS_f decreases with increasing freedom of motion in the crystal pre-melting, i.e. if the entropy increase can be incorporated into the crystal structure, and not result in a change of state, then ΔS_f decreases.

Energy calculations were carried out on all 4 molecules (2 pairs) to determine the packing energy per molecule and the relative contributions from Van de Waals, electrostatics, and H-bond interactions.

The calculations were performed using the Cerius² program⁶ using the following procedure:

1. The structure was read from Cambridge Structural Database DAT file.
2. The crystal was 'un-built' to give a single molecule.
3. The bonds were identified on the diagram as single, double or resonance bonds, and the structure 'cleaned'.
4. The molecular structure was optimised by a quantum mechanical simulation using the semi-empirical procedure AM1 in the MOPAC program.
5. The crystal was rebuilt, and any H-bond interactions calculated (H-bond defined as $<2.5\text{\AA}$ and angles $>90^\circ$).
6. Open Force Field (OFF) was set up using Dreiding 2.21 force field and the Evald setting for Van der Waals and Colombic interactions.
7. OFF expression set up.
8. Minimization run using OFF methods.
9. Output recorded and all values divided by the number of molecules per unit cell, to obtain energies per molecule.

NIPMAT⁷⁻⁹ crystal packing diagrams were also calculated for the similar and different packing pairs MCBZAC / CLBZAP and MAMPOL / AMPHOL01. NIPMAT⁷

diagrams are a graphical representation of the nearest neighbour distances between all atoms in a crystallographical asymmetric unit. The atom atom contacts are plotted on a square grid, with the atom atom distance indicated by the degree of shading. NIPMAT⁷ plots are useful for a rapid visual comparison of structures.

21.3 Results

No	m/p	refcode	melting point /°C	ΔT /°	volume /Å ³	density /g cm ⁻³	Vol (mol) /Å ³	T (exp) /K	S.G.	Z (Z')
46	meta	MCBZAC	155-7 ^a	99	688	1.510	172.085	295	P21/c	4
46	para	CLBZAP03	240-2 ^a	99	327	1.591	163.345	110	P-1	2
49	meta	MNBZAC01	142 ^a	97	1485	1.494	185.637	295	P21/n	8 (z' 2)
49	para	NBZOAC03	237-9 ^c	97	1378	1.611	172.229	295	A2/a	8
20	meta	DNBENZ10	88-90 ^a	85	709	1.569	177.202	295	Pbn21	4
20	para	DNITBZ02	173-5 ^a	85	345	1.617	172.513	295	P21/n	2 (z' 0.5)
43	meta	LAVBOZ	99-101 ^c	74	1855	1.211	463.686	295	P21/c	4
43	para	LAVBUF	173-5 ^c	74	916	1.227	457.937	295	P-1	2
60	meta	NOGKAV	185-190 ^c	73	552	1.577	276.150	295	P-1	2
60	para	HIBCOK	258-9 ^c	73	1135	1.535	283.645	295	Ama2	4
37	meta	JICVIA10	198-200 ^c	72	1222	1.333	611.021	295	P-1	2
37	para	JICVEW10	270-7 ^c	72	2553	1.276	638.161	263	P21/n	4
45	meta	MAMPOL	124-6 ^a	64	567	1.277	141.808	295	Pca21	4
45	para	AMPHOL01	188-190 ^a	64	558	1.299	139.431	295	Pna21	4
69	meta	RESORA13	109-110 ^d	63	562	1.301	140.491	295	Pna21	4
69	para	HYQUIN, HYQUIN05	172-5 ^a	63	530, 1309	1.380, 1.258	132.430 145.391	295, 295	P21/c, R-3	4, 9
85	meta	TEWXOI	109-111 ^c	62	978	1.478	489.183	295	P21	2
85	para	TEWWUN	171-3 ^c	62	485	1.490	485.216	123	P1	1
106	meta	ZONKAO	153-5 ^c (116-7 ^b)	-37 (+37)	1490	1.348	372.456	295	P21/a	4
106	para	ZONJOB	116-7 ^c (153-5 ^b)	-37 (+37)	1537	1.306	384.269	295	P21/c	4

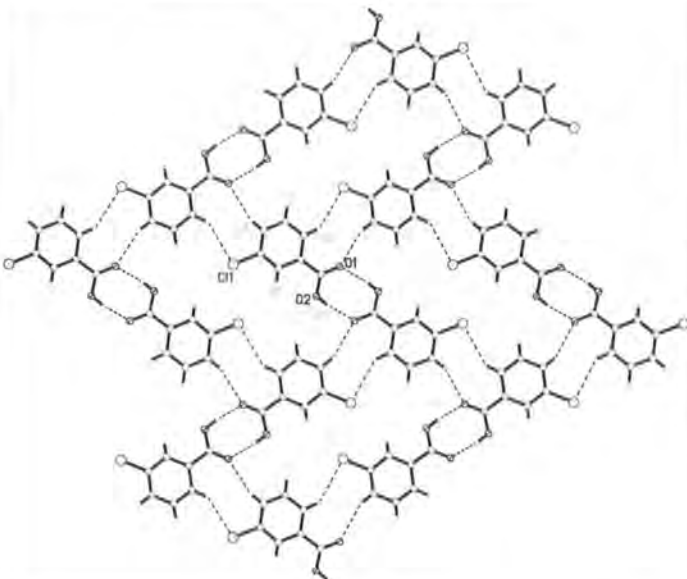
Source for melting points:

- a) Acros catalogue (1997)
- b) Original paper describing structure
- c) Cambridge Structural Database data files

Analysis of crystal packing of 'similar' compounds MCBZAC and CLBZAP03

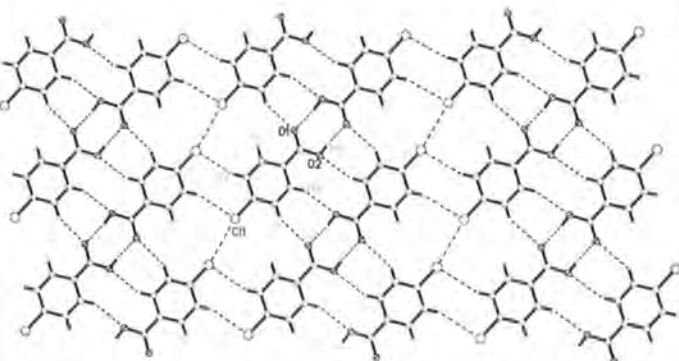
MACZAC:

The structure consists of sheets, with interactions running in one plane only – there are no strong interactions between the planes

				
	D...H-A	D...H /Å	D...A /Å	DHA /°
	O ₁ ...H ₅ -O ₂	1.76	2.663	171
	O ₁ ...H ₄ -C ₆	2.57	3.432	151
	Cl ₁ ...H ₂ -C ₄	2.92	3.778	143
	(Angle C ₁ -Cl ₁ ...H ₂ = 97°)			

CLBZAP03:

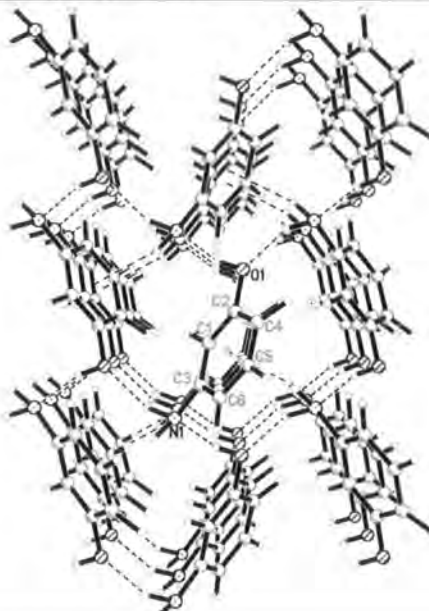
The structure consists of sheets, with interactions running in one plane only – there are no strong interactions between the planes

				
	D...H-A	D...H /Å	D...A /Å	DHA /°
	O ₁ ...H ₅ -O ₂	1.72	2.612	173
	O ₁ ...H ₃ -C ₅	2.56	3.430	146
	O ₂ ...H ₄ -C ₆	2.498	3.396	152
	Cl ₁ ...H ₂ -C ₃	3.02	3.887	151
	(Angle C ₁ -Cl ₁ ...H ₂ = 101°)			
	Cl ₁ ...Cl ₁	Cl...Cl /Å	C-Cl...Cl /°	C-Cl...Cl /°
Cl ₁ ...Cl ₁ (Type I interaction)		3.396	167	167

Analysis of crystal packing of 'different' compounds MAMPOL and AMPHOL01

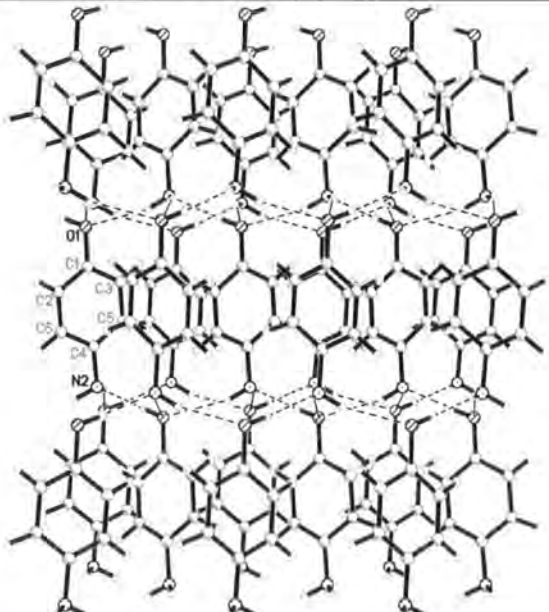
MAMPOL:

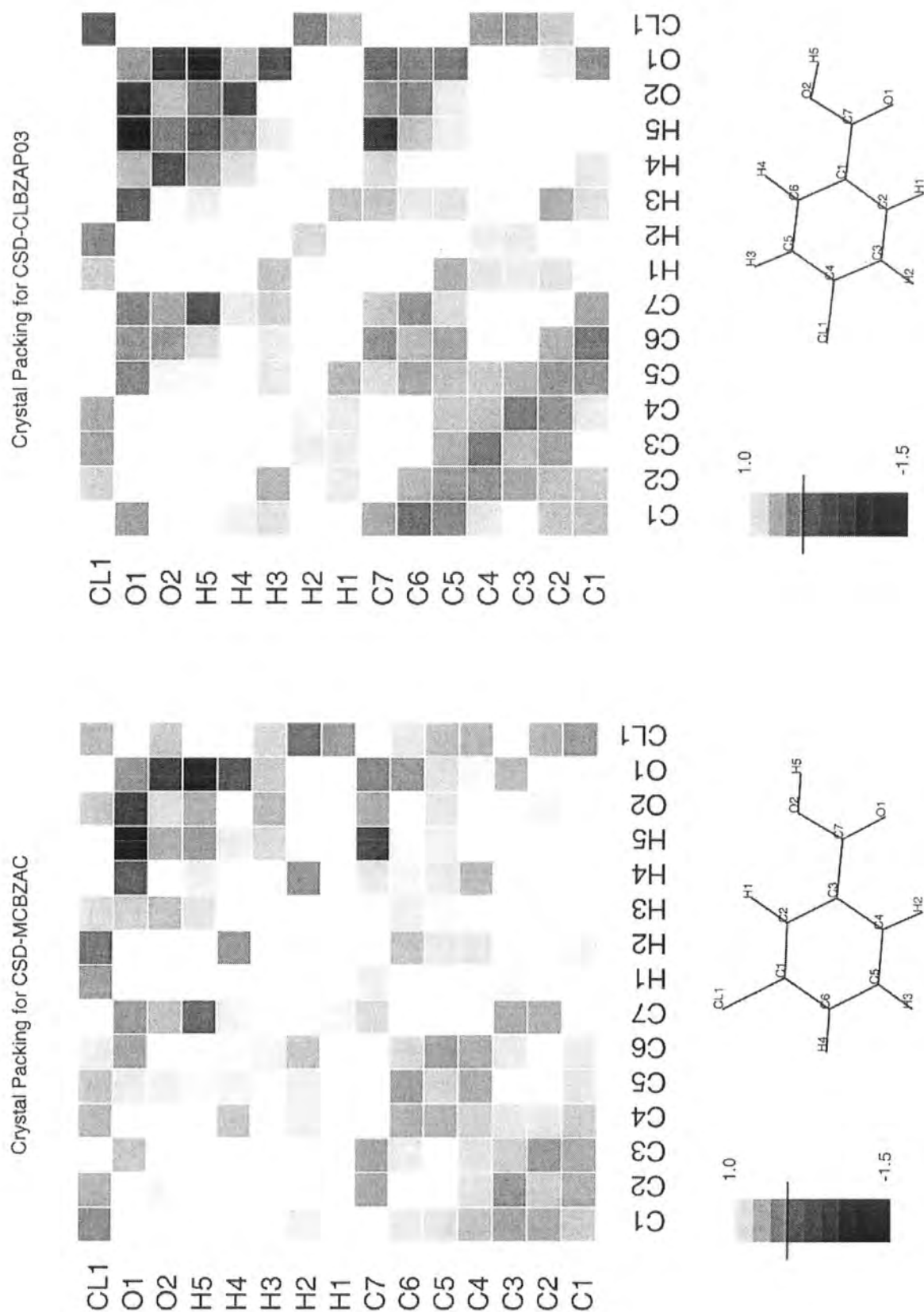
The structure sheets constructed from chains of O-H...N-H...O-H interactions, there are also N-H... π interactions.

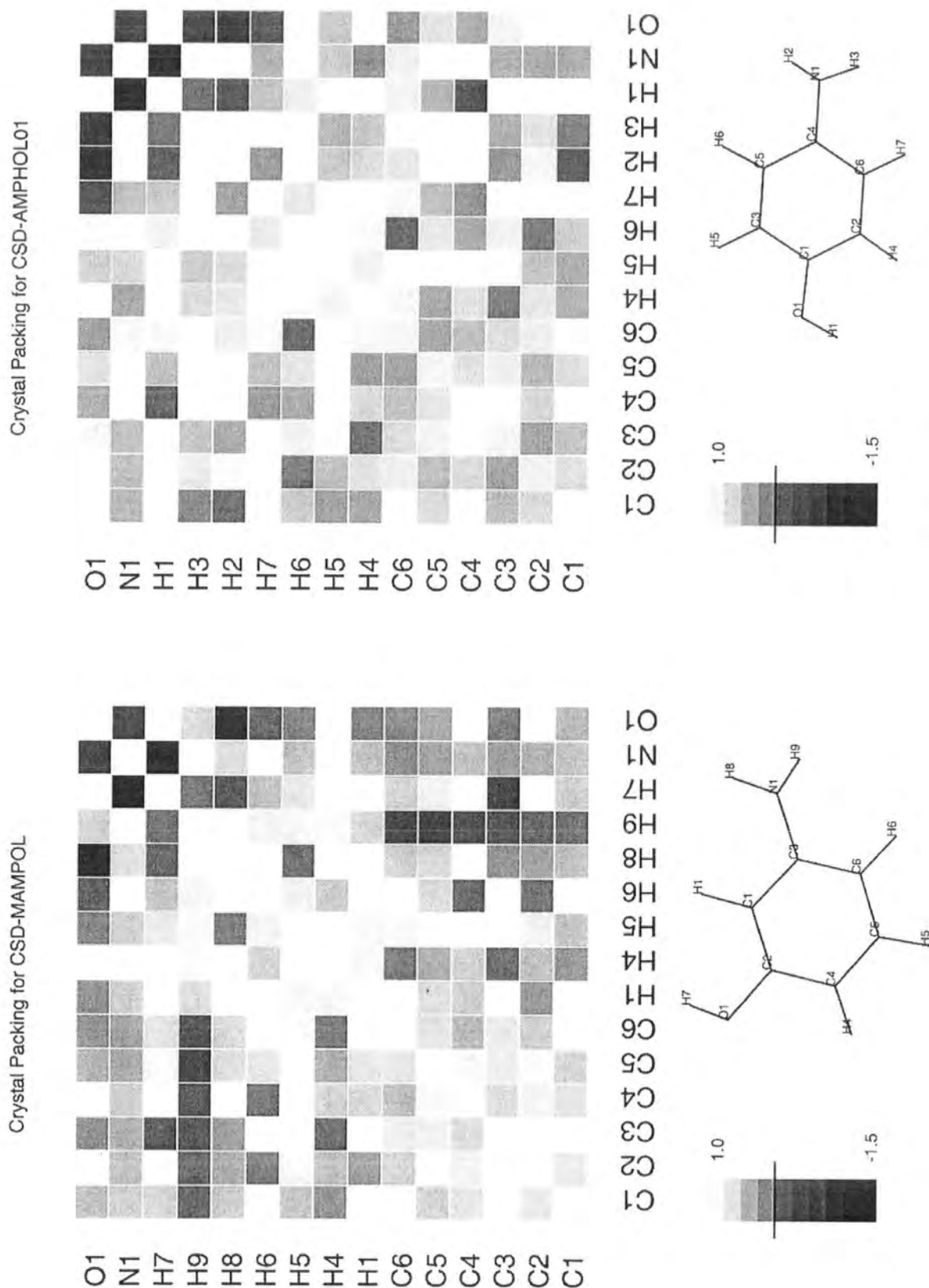
				
	D...H-A	D...H /Å	D...A /Å	DHA /°
	O ₁ ...H ₈ -N ₁	1.94	3.011	153
	O ₁ -H ₇ ...N ₁	1.88	2.753	161
	N ₁ -H ₉ ... π	2.41	3.341	161

AMPHOL01:

The structure consists of β -As sheets (see part 2), creating a 3-D network, there are also π - π face to edge interactions.

				
	D...H-A	D...H /Å	D...A /Å	DHA /°
	O ₁ ...H ₂ -N ₁	2.22	3.142	161
	O ₁ ...H ₃ -N ₁	2.38	3.258	164
	O ₁ -H ₁ -N ₁	1.91	2.776	175

Figure A.1: NIPMAT⁷ diagrams of MCBZAC and CLBZAP03

Figure A.2: NIPMAT⁷ diagram of MAMPOL and AMPHOL01

Even at first glance it can be seen that the NIPMAT^{#319} diagrams for the 'similar' pair are indeed similar and the intermolecular interactions are comparable, however the 'different' pair shows distinct differences in intermolecular contacts.

For the similar structural pair, MCBZAC / CLBZAP03, the strongest interaction is the carboxylic acid dimer especially the O-H...O hydrogen bond (indicated by the dark square for O₁ H₅ in both cases), there are also some close contacts between adjacent benzene rings (indicated by the shading in the bottom left corner of the diagram) which appears to be more dominant in the para isomer.

For the different structural pair, MAMPOL / AMPHOL01, the same O-H...N interaction is seen (top right corner), however while there are 2 strong N-H...O interactions in the AMPHOL01 structure, in MAMPOL there is only one, with the second N-H (H₉) interacting strongly with the carbons of the benzene ring.

This NIPMAT analysis confirms the patterns seen in the standard structure analysis carried out using PLUTO.

Energy Minimization Calculations:

	Similar Structures		Different Structures	
Energy contribution per molecule / kcal mol ⁻¹	MCBZAC	CLPZAP03	MAMPOL	DNITBZ02
	meta	para	meta	para
Van der Waals	-1.57817	-1.67257	4.14893	1.87976
Electrostatic	-18.05950	-20.28475	-58.51525	-22.93280
H-Bond	-3.21920	-3.45982	-5.32103	-5.37178
Bonds	1.55076	1.51862	0.79591	0.90954
Angles	0.94784	0.85749	0.03540	0.06532
Torsion	0.13720	0.06502	0.15144	0.41539
Inversion	0.01779	0.21614	0.05930	0.17715
Total E (related to ΔH_f)	-20.4033	-22.9739	-58.6453	-24.8574

It can be seen that in the case where the structures are very similar (MCBZAC / CLPZIP03) the total energy of each compound is also very similar. This agrees with

the assumption that in this case the ΔH_f for each structure would be similar, and the change in melting point dependent on ΔS_f .

For the case where the structures are quite different (MAMPOL / AMPHOL01) the total energies are also quite different (as would be expected for such different structures). Also the higher melting point corresponds to the higher total energy value, i.e. the higher ΔH_f value. While the contribution from ΔS_f is unknown, the change in melting point can be accounted for (in part) by the change in ΔH_f .

$$T_f = \Delta H_f / \Delta S_f$$

21.4 References for Appendix A

- 1) A. Gavezzotti, *J. Chem. Soc. Perkin Trans. 2*, 1995, 1399 - 1404.
- 2) W. Huckel, *Theoretische Grundlagen der Organischen Chemie*, Lipzig: Akademische Verlagsgesellschaft, 1931, vol. II, pp. 185-186.
- 3) F.H.Allen, O.Kennard. *Chem. Des. Autom. News*, 1993, **8**, 30-37.
- 4) Y. Mazaki, K. Mutai, *Bull. Chem. Soc. Jpn.*, 1995, **68**, 3247 - 3254.
- 5) Beilstein Commander 2000, Version 5.0. 1995-2000 MDL Information Systems GmbH.
- 6) Cerius², Accelrys, 9685 Scranton Road, San Diego, CA92121-3752, U.S.A. and 240/250 The Quorum, Barnwell Road, Cambridge CB5 8RE, U.K.
- 7) NIPMAT Non-bonded Interaction Pattern Matrix. R.S. Rowland. Am. Cryst. Assoc. Abstr., 23, 63 1995 (Abstract 2a.5.B, Montreal Meeting.)
- 8) V.J.Hoy, Weak Intermolecular Interactions in Organic Systems : a Concerted Study Involving X-ray and Neutron Diffraction and Database Analysis, Ph.D thesis, University of Durham, 1996.
- 9) G.R.Desiraju, T.Steiner, *The Weak Hydrogen Bond in Structural Chemistry and Biology*. New York, Oxford: Oxford University Press, 1999.

Appendix B: Publications

Halogen trimer synthons in crystal engineering: low temperature X-ray and neutron diffraction study of the 1:1 complex of 2,4,6-tris(4-chloro-phenoxy)-1,3,5-triazene with tribromobenzene.

C.K.Broder, J.A.K.Howard, D.A.Keen, C.C.Wilson, F.H.Allen, R.K.R.Jetti, A.Nangia, G.R.Desiraju. *Acta Cryst B*, 2000, **B56**, 1080-1084.

A highly functionalised ferrocenyl-pyrazolo[2,3-*a*]pyridine.

S.Sarkhel, P.Srivastava, V.J.Ram, P.R.Maulik, C.K.Broder, J.A.K.Howard. *Acta Cryst. C*. 2000, **C56**, e88-e89.

Insertion and cleavage reactions of [*closo*-3,1,2-Ta(NMe₂)₃-(C₂B₉H₁₁)] with nitriles, phenols and thiols; structural characterisation of *N,N*-dimethylamidinate ligands.

C.K.Broder, A.E.Goeta, J.A.K.Howard, A.K.Hughes, A.L.Johnson, J.M.Malget, K.Wade. *J. Chem. Soc., Dalton. Trans.* 2000, 3526-3533.

(*Z*)-3-Acetonilidene-2,3-dihydro-1*H*-isoindolin-1-one.

K.Chowdhury, R.Mukhopadhyay, M.Mukherjee, C.K.Broder, N.G.Kundu. *Acta Cryst. E*, 2001, **E57**, o421-o423.

2-*p*-Toluoylquinoxaline

K.Chowdhury, R.Mukhopadhyay, M.Mukherjee, C.K.Broder, N.G.Kundu. *Acta Cryst. E*, 2001, **E57**, o794-o795.

¹H NMR and X-ray crystallographic analysis of 1,2-bis(4,6-diethylthio-1*H*-pyrazolo[3,4-*d*]pyrimidin-1-yl)ethane and its 'propylene linker' -analog: molecular recognition versus crystal engineering.

K.Avasthi, D.S.Rawat, P.R.Maulik, S.Sarkhel, C.K.Broder, J.A.K.Howard. *Tetrahedron Lett.* 2001, **42**, 7115-7117.

Cinnamoyl shikonin.

S.Sarkhel, Shefali, V.T.Mathad, K.Raj, A.P.Bhaduri, P.R.Maulik, C.K.Broder, J.A.K.Howard. *Acta Cryst. C*, 2001, **C57**, 1199-1200.

Synthesis, structure and reactivity of 1-(α -C, α' -halo-*o*-xylyl)-2-trialkylsilyl-1,2-dicarboranes.

A.S.Batsanov, C.K.Broder, A.E.Goeta, J.A.K.Howard, A.K.Hughes, J.M.Malget. *J. Chem. Soc., Dalton Trans.* 2002, 14-18.

In Preparation:

On the reliability of C-H...O interactions in crystal engineering: synthesis and structures of two hydrogen bonded phosphonium bis(aryloxide) salts.

C.K.Broder, M.G.Davidson, V.T.Forsyth, J.A.K.Howard, S.Lamb, S.A.Mason. *Crystal Growth and Design*. (Accepted Feb 2002).

Conformational polymorphism, conformational isomorphism and concomitant polymorphism in 4,4-diphenyl-2,5-cyclohexadione.

V.S.S.Kumar, A.Addlagatta, A.Nangia, XXXX, W.T.Robinson, C.K.Broder, R.Mondal, I.R.Evans, J.A.K.Howard, F.H.Allen. *Angew. Chem. Int. Ed. Engl.*

Appendix C: Cif Files

1a) 4-amino-4'-hydroxydiphenylmethane

Synthesis: Venugopal Vangala, University of Hyderabad, India.

Table 1. Crystal data and structure refinement for **1a**.

Identification code	1a	
Empirical formula	C ₁₃ H ₁₃ N O	
Formula weight	199.25	
Temperature	12(2) K	
Wavelength	0.5-5.0 Å	
Crystal system	Monoclinic	
Space group	P2(1)/n	
Unit cell dimensions	a = 5.9180(12) Å	$\alpha = 90^\circ$,
	b = 19.213(4) Å	$\beta = 101.25(3)^\circ$,
	c = 9.6510(19) Å	$\gamma = 90^\circ$,
Volume	1076.3(4) Å ³	
Z	4	
Density (calculated)	1.230 Mg/m ³	
Absorption coefficient	1.870, at 1 Angstrom mm ⁻¹	
F(000)	21.27	
Crystal size	1.5 x 1.5 x 1.3 mm ³	
Theta range for data collection	1.56 to 24.72°	
Index ranges	0 ≤ h ≤ 17, 0 ≤ k ≤ 51, -29 ≤ l ≤ 24	
Reflections collected	6172	
Independent reflections	2403 [R(int) = 0.064]	
Completeness to theta = 24.72°	5.7 %	
Absorption correction	Empirical	
Max. and min. transmission	0.82 and 0.62	
Refinement method	Full-matrix least-squares on F ²	
Data / restraints / parameters	2403 / 0 / 253	
Goodness-of-fit on F ²	1.081	
Final R indices [I > 2sigma(I)]	R1 = 0.0791, wR2 = 0.2230	
R indices (all data)	R1 = 0.0793, wR2 = 0.2231	
Extinction coefficient	0.044	
Largest diff. peak and hole	3.387 and -2.930 e.Å ⁻³	

Table 2. Atomic coordinates ($\times 10^4$) and equivalent isotropic displacement parameters ($\text{\AA}^2 \times 10^3$) for **1a**. $U(\text{eq})$ is defined as one third of the trace of the orthogonalized U_{ij} tensor.

	x	y	z	$U(\text{eq})$
O(1)	12754(8)	518(3)	633(4)	10(1)
C(1)	11360(5)	830(2)	1393(3)	7(1)
C(2)	10112(6)	463(2)	2240(3)	7(1)
C(3)	8633(6)	821(2)	2950(3)	7(1)
C(4)	8409(6)	1544(2)	2864(3)	7(1)
C(5)	9693(6)	1901(2)	2039(3)	7(1)
C(6)	11166(6)	1550(2)	1310(3)	7(1)
C(7)	6759(6)	1922(2)	3592(3)	8(1)
C(8)	6615(5)	1650(2)	5028(3)	5(1)
C(9)	4641(5)	1328(2)	5286(3)	6(1)
C(10)	4514(5)	1080(2)	6620(3)	6(1)
C(11)	6393(5)	1149(2)	7737(3)	6(1)
C(12)	8386(5)	1469(2)	7476(3)	6(1)
C(13)	8488(5)	1712(2)	6148(3)	6(1)
N(1)	6331(4)	869(2)	9071(2)	9(1)

Table 3. Bond lengths [Å] and angles [°] for **1a**.

O(1)-C(1)	1.347(5)	C(2)-C(3)-H(3)	118.4(8)
O(1)-H(1)	0.969(15)	C(4)-C(3)-H(3)	120.0(7)
C(1)-C(6)	1.388(6)	C(5)-C(4)-C(3)	118.0(3)
C(1)-C(2)	1.395(5)	C(5)-C(4)-C(7)	120.8(4)
C(2)-C(3)	1.394(5)	C(3)-C(4)-C(7)	121.2(3)
C(2)-H(2)	1.060(12)	C(4)-C(5)-C(6)	121.2(4)
C(3)-C(4)	1.396(6)	C(4)-C(5)-H(5)	120.6(6)
C(3)-H(3)	1.078(9)	C(6)-C(5)-H(5)	118.2(6)
C(4)-C(5)	1.385(5)	C(1)-C(6)-C(5)	120.3(3)
C(4)-C(7)	1.497(5)	C(1)-C(6)-H(6)	119.5(7)
C(5)-C(6)	1.396(5)	C(5)-C(6)-H(6)	120.3(7)
C(5)-H(5)	1.081(14)	C(4)-C(7)-C(8)	115.2(3)
C(6)-H(6)	1.080(9)	C(4)-C(7)-H(7A)	107.5(5)
C(7)-C(8)	1.499(4)	C(8)-C(7)-H(7A)	109.4(6)
C(7)-H(7A)	1.115(13)	C(4)-C(7)-H(7B)	110.4(6)
C(7)-H(7B)	1.087(9)	C(8)-C(7)-H(7B)	108.8(5)
C(8)-C(9)	1.387(5)	H(7A)-C(7)-H(7B)	105.2(10)
C(8)-C(13)	1.394(4)	C(9)-C(8)-C(13)	117.9(3)
C(9)-C(10)	1.388(4)	C(9)-C(8)-C(7)	121.6(3)
C(9)-H(9)	1.075(9)	C(13)-C(8)-C(7)	120.5(3)
C(10)-C(11)	1.396(5)	C(8)-C(9)-C(10)	121.3(3)
C(10)-H(10)	1.079(10)	C(8)-C(9)-H(9)	119.3(6)
C(11)-C(12)	1.396(5)	C(10)-C(9)-H(9)	119.4(6)
C(11)-N(1)	1.403(4)	C(9)-C(10)-C(11)	120.3(3)
C(12)-C(13)	1.376(4)	C(9)-C(10)-H(10)	120.5(6)
C(12)-H(12)	1.073(8)	C(11)-C(10)-H(10)	119.2(6)
C(13)-H(13)	1.070(9)	C(10)-C(11)-C(12)	118.4(3)
N(1)-H(1A)	1.009(8)	C(10)-C(11)-N(1)	120.9(3)
N(1)-H(1B)	1.001(10)	C(12)-C(11)-N(1)	120.6(3)
		C(13)-C(12)-C(11)	120.6(3)
		C(13)-C(12)-H(12)	121.0(6)
		C(11)-C(12)-H(12)	118.3(6)
		C(12)-C(13)-C(8)	121.4(3)
C(1)-O(1)-H(1)	113.0(7)	C(12)-C(13)-H(13)	119.6(6)
O(1)-C(1)-C(6)	117.7(4)	C(8)-C(13)-H(13)	119.0(6)
O(1)-C(1)-C(2)	122.9(4)	C(11)-N(1)-H(1A)	116.1(6)
C(6)-C(1)-C(2)	119.4(3)	C(11)-N(1)-H(1B)	113.0(6)
C(3)-C(2)-C(1)	119.6(4)	H(1A)-N(1)-H(1B)	109.1(9)
C(3)-C(2)-H(2)	120.4(6)		
C(1)-C(2)-H(2)	120.0(6)		
C(2)-C(3)-C(4)	121.6(3)		

Symmetry transformations used to generate equivalent atoms:

Table 4. Anisotropic displacement parameters ($\text{\AA}^2 \times 10^3$) for **1a**. The anisotropic displacement factor exponent takes the form: $-2\pi^2 [h^2 a^{*2} U^{11} + \dots + 2 h k a^* b^* U^{12}]$

	U ¹¹	U ²²	U ³³	U ²³	U ¹³	U ¹²
O(1)	12(2)	8(2)	12(1)	1(2)	8(1)	0(2)
H(1)	20(4)	24(5)	26(4)	-2(4)	9(3)	-2(4)
C(1)	6(1)	8(2)	6(1)	0(1)	2(1)	0(1)
C(2)	11(1)	5(1)	7(1)	0(1)	4(1)	0(1)
C(3)	8(1)	7(2)	8(1)	1(1)	4(1)	0(1)
C(4)	7(1)	9(2)	5(1)	0(1)	2(1)	1(1)
C(5)	10(1)	4(1)	6(1)	2(1)	3(1)	0(1)
C(6)	9(1)	7(2)	6(1)	-1(1)	3(1)	-1(1)
H(2)	34(5)	11(4)	31(4)	-3(4)	17(4)	7(4)
H(3)	27(4)	19(5)	27(4)	0(4)	16(3)	-10(4)
H(5)	31(5)	16(5)	33(4)	-2(4)	13(4)	6(4)
H(6)	28(4)	20(5)	20(3)	2(4)	13(3)	-8(4)
C(7)	7(1)	10(2)	6(1)	-1(1)	2(1)	2(1)
H(7A)	29(4)	15(4)	25(3)	1(4)	14(3)	0(4)
H(7B)	16(3)	30(6)	15(2)	4(4)	1(2)	4(4)
C(8)	5(1)	6(1)	4(1)	-1(1)	0(1)	-1(1)
C(9)	5(1)	7(2)	5(1)	1(1)	0(1)	-1(1)
C(10)	4(1)	8(2)	7(1)	0(1)	1(1)	-1(1)
C(11)	6(1)	8(2)	6(1)	-3(1)	2(1)	-3(1)
C(12)	5(1)	8(2)	6(1)	2(1)	1(1)	0(1)
C(13)	6(1)	5(1)	5(1)	2(1)	1(1)	0(1)
H(9)	15(3)	39(8)	15(2)	3(4)	-2(2)	-8(4)
H(10)	14(3)	37(6)	21(3)	7(4)	4(2)	-7(4)
H(12)	18(3)	36(6)	13(2)	5(4)	-7(2)	-11(4)
H(13)	9(3)	35(7)	32(4)	16(5)	6(3)	-4(3)
N(1)	7(1)	12(1)	7(1)	2(1)	3(1)	2(1)
H(1A)	16(3)	24(5)	24(3)	9(4)	9(2)	3(4)
H(1B)	26(4)	36(7)	14(2)	3(4)	0(2)	-17(5)

Table 5. Hydrogen coordinates ($\times 10^4$) and isotropic displacement parameters ($\text{\AA}^2 \times 10^3$) for **1a**.

	x	y	z	U(eq)
H(1)	12905(17)	22(7)	806(11)	23(2)
H(2)	10260(20)	-86(6)	2316(12)	24(2)
H(3)	7683(17)	528(6)	3598(10)	23(2)
H(5)	9590(20)	2461(7)	1954(12)	26(2)
H(6)	12169(18)	1836(6)	679(9)	21(2)
H(7A)	7290(18)	2479(6)	3677(10)	22(2)
H(7B)	5043(15)	1921(7)	2937(8)	21(2)
H(9)	3185(15)	1266(7)	4435(9)	24(2)
H(10)	2981(15)	820(7)	6801(9)	24(2)
H(12)	9839(15)	1514(7)	8332(8)	24(2)
H(13)	10031(14)	1955(7)	5967(11)	25(2)
H(1A)	4764(15)	839(7)	9332(10)	21(2)
H(1B)	7425(17)	1104(7)	9854(9)	26(2)

1b) Methylenedianiline and thiodiphenyl

Synthesis: Venugopal Vangala, University of Hyderabad, India.

Table 1. Crystal data and structure refinement for **1b**.

Identification code	1b	
Empirical formula	C ₂₅ H ₂₄ N ₂ O ₂ S	
Formula weight	416.52	
Temperature	100(2) K	
Wavelength	0.71073 Å	
Crystal system	Monoclinic	
Space group	P2(1)/n	
Unit cell dimensions	a = 11.2547(11) Å	$\alpha = 90^\circ$.
	b = 10.1129(9) Å	$\beta = 103.654(5)^\circ$.
	c = 19.9982(17) Å	$\gamma = 90^\circ$.
Volume	2211.8(3) Å ³	
Z	4	
Density (calculated)	1.251 Mg/m ³	
Absorption coefficient	0.170 mm ⁻¹	
F(000)	880	
Crystal size	0.50 x 0.15 x 0.05 mm ³	
Theta range for data collection	1.91 to 27.48°.	
Index ranges	-14 ≤ h ≤ 14, -13 ≤ k ≤ 13, -25 ≤ l ≤ 25	
Reflections collected	15070	
Independent reflections	5052 [R(int) = 0.1065]	
Completeness to theta = 27.48°	99.7 %	
Absorption correction	Psi-scan	
Max. and min. transmission	0.98259 and 0.83120	
Refinement method	Full-matrix least-squares on F ²	
Data / restraints / parameters	5052 / 0 / 295	
Goodness-of-fit on F ²	0.987	
Final R indices [I > 2σ(I)]	R1 = 0.0571, wR2 = 0.1162	
R indices (all data)	R1 = 0.1215, wR2 = 0.1397	
Extinction coefficient	not refined	
Largest diff. peak and hole	0.261 and -0.440 e.Å ⁻³	

Table 2. Atomic coordinates ($\times 10^4$) and equivalent isotropic displacement parameters ($\text{\AA}^2 \times 10^3$) for **1b**. $U(\text{eq})$ is defined as one third of the trace of the orthogonalized U^{ij} tensor.

	x	y	z	$U(\text{eq})$
O(1)	6751(2)	189(2)	411(1)	29(1)
C(1)	7280(2)	1265(2)	786(1)	20(1)
C(2)	7656(2)	1113(3)	1496(1)	20(1)
C(3)	8195(2)	2157(3)	1905(1)	20(1)
C(4)	8351(2)	3380(2)	1612(1)	19(1)
C(5)	7977(2)	3525(2)	898(1)	19(1)
C(6)	7443(2)	2476(2)	486(1)	19(1)
S(1)	8926(1)	4685(1)	2191(1)	32(1)
C(7)	9471(2)	5856(2)	1682(1)	21(1)
C(8)	10433(2)	5553(3)	1368(1)	26(1)
C(9)	10910(2)	6514(3)	1017(1)	25(1)
C(10)	10475(2)	7809(3)	989(1)	21(1)
C(11)	9510(2)	8115(3)	1283(1)	21(1)
C(12)	9003(2)	7136(2)	1620(1)	22(1)
O(2)	11009(2)	8723(2)	648(1)	29(1)
N(21)	10446(2)	11321(2)	863(2)	25(1)
C(21)	11593(2)	11992(2)	1049(1)	20(1)
C(22)	12195(3)	12114(3)	1729(1)	29(1)
C(23)	13340(3)	12731(3)	1919(1)	29(1)
C(24)	13905(2)	13231(3)	1429(1)	21(1)
C(25)	13295(3)	13077(3)	741(1)	32(1)
C(26)	12160(3)	12471(3)	548(1)	30(1)
C(20)	15106(2)	13973(3)	1618(1)	24(1)
C(27)	14963(2)	15446(3)	1466(1)	20(1)
C(28)	15691(2)	16109(3)	1105(1)	27(1)
C(29)	15542(2)	17465(3)	964(1)	26(1)
C(30)	14649(2)	18175(3)	1179(1)	21(1)
C(31)	13920(2)	17523(3)	1548(1)	25(1)
C(32)	14074(2)	16182(3)	1686(1)	24(1)
N(22)	14421(2)	19521(2)	979(1)	26(1)

Table 3. Bond lengths [\AA] and angles [$^\circ$] for **1b**.

O(1)-C(1)	1.375(3)	C(23)-H(23)	0.9500
O(1)-H(1A)	0.84(3)	C(24)-C(25)	1.394(4)
C(1)-C(2)	1.390(3)	C(24)-C(20)	1.514(4)
C(1)-C(6)	1.395(3)	C(25)-C(26)	1.387(4)
C(2)-C(3)	1.385(3)	C(25)-H(25)	0.9500
C(2)-H(2)	0.9500	C(26)-H(26)	0.9500
C(3)-C(4)	1.397(3)	C(20)-C(27)	1.521(3)
C(3)-H(3)	0.9500	C(20)-H(20A)	0.9900
C(4)-C(5)	1.397(3)	C(20)-H(20B)	0.9900
C(4)-S(1)	1.774(3)	C(27)-C(28)	1.387(4)
C(5)-C(6)	1.391(3)	C(27)-C(32)	1.398(4)
C(5)-H(5)	0.9500	C(28)-C(29)	1.402(4)
C(6)-H(6)	0.9500	C(28)-H(28)	0.9500
S(1)-C(7)	1.763(3)	C(29)-C(30)	1.384(4)
C(7)-C(12)	1.392(4)	C(29)-H(29)	0.9500
C(7)-C(8)	1.407(4)	C(30)-C(31)	1.392(4)
C(8)-C(9)	1.380(4)	C(30)-N(22)	1.424(3)
C(8)-H(8)	0.9500	C(31)-C(32)	1.386(4)
C(9)-C(10)	1.395(4)	C(31)-H(31)	0.9500
C(9)-H(9)	0.9500	C(32)-H(32)	0.9500
C(10)-O(2)	1.368(3)	N(22)-H(22A)	0.85(3)
C(10)-C(11)	1.387(4)	N(22)-H(22B)	0.88(3)
C(11)-C(12)	1.394(4)	C(1)-O(1)-H(1A)	114(2)
C(11)-H(11)	0.9500	O(1)-C(1)-C(2)	117.2(2)
C(12)-H(12)	0.9500	O(1)-C(1)-C(6)	122.9(2)
O(2)-H(2A)	0.88(4)	C(2)-C(1)-C(6)	119.9(2)
N(21)-C(21)	1.428(3)	C(3)-C(2)-C(1)	120.2(2)
N(21)-H(21A)	0.87(3)	C(3)-C(2)-H(2)	119.9
N(21)-H(21B)	0.86(3)	C(1)-C(2)-H(2)	119.9
C(21)-C(22)	1.374(4)	C(2)-C(3)-C(4)	120.6(2)
C(21)-C(26)	1.395(4)	C(2)-C(3)-H(3)	119.7
C(22)-C(23)	1.401(4)	C(4)-C(3)-H(3)	119.7
C(22)-H(22)	0.9500	C(5)-C(4)-C(3)	118.9(2)
C(23)-C(24)	1.384(4)	C(5)-C(4)-S(1)	124.4(2)
		C(3)-C(4)-S(1)	116.58(19)
		C(6)-C(5)-C(4)	120.7(2)

C(6)-C(5)-H(5)	119.7	C(23)-C(24)-C(20)	122.5(2)
C(4)-C(5)-H(5)	119.7	C(25)-C(24)-C(20)	120.3(2)
C(5)-C(6)-C(1)	119.7(2)	C(26)-C(25)-C(24)	122.1(3)
C(5)-C(6)-H(6)	120.1	C(26)-C(25)-H(25)	119.0
C(1)-C(6)-H(6)	120.1	C(24)-C(25)-H(25)	119.0
C(7)-S(1)-C(4)	104.20(12)	C(25)-C(26)-C(21)	120.0(2)
C(12)-C(7)-C(8)	118.5(2)	C(25)-C(26)-H(26)	120.0
C(12)-C(7)-S(1)	120.0(2)	C(21)-C(26)-H(26)	120.0
C(8)-C(7)-S(1)	121.4(2)	C(24)-C(20)-C(27)	112.9(2)
C(9)-C(8)-C(7)	120.4(2)	C(24)-C(20)-H(20A)	109.0
C(9)-C(8)-H(8)	119.8	C(27)-C(20)-H(20A)	109.0
C(7)-C(8)-H(8)	119.8	C(24)-C(20)-H(20B)	109.0
C(8)-C(9)-C(10)	120.5(3)	C(27)-C(20)-H(20B)	109.0
C(8)-C(9)-H(9)	119.8	H(20A)-C(20)-H(20B)	107.8
C(10)-C(9)-H(9)	119.8	C(28)-C(27)-C(32)	117.4(2)
O(2)-C(10)-C(11)	122.7(2)	C(28)-C(27)-C(20)	122.0(2)
O(2)-C(10)-C(9)	117.6(2)	C(32)-C(27)-C(20)	120.6(2)
C(11)-C(10)-C(9)	119.7(2)	C(27)-C(28)-C(29)	121.4(3)
C(10)-C(11)-C(12)	119.9(2)	C(27)-C(28)-H(28)	119.3
C(10)-C(11)-H(11)	120.1	C(29)-C(28)-H(28)	119.3
C(12)-C(11)-H(11)	120.1	C(30)-C(29)-C(28)	120.4(3)
C(7)-C(12)-C(11)	120.9(2)	C(30)-C(29)-H(29)	119.8
C(7)-C(12)-H(12)	119.5	C(28)-C(29)-H(29)	119.8
C(11)-C(12)-H(12)	119.5	C(29)-C(30)-C(31)	118.7(2)
C(10)-O(2)-H(2A)	113(3)	C(29)-C(30)-N(22)	120.3(2)
C(21)-N(21)-H(21A)	111(2)	C(31)-C(30)-N(22)	120.8(3)
C(21)-N(21)-H(21B)	110.7(18)	C(32)-C(31)-C(30)	120.5(3)
H(21A)-N(21)-H(21B)	114(3)	C(32)-C(31)-H(31)	119.7
C(22)-C(21)-C(26)	118.5(2)	C(30)-C(31)-H(31)	119.7
C(22)-C(21)-N(21)	120.3(3)	C(31)-C(32)-C(27)	121.6(3)
C(26)-C(21)-N(21)	121.1(2)	C(31)-C(32)-H(32)	119.2
C(21)-C(22)-C(23)	121.0(3)	C(27)-C(32)-H(32)	119.2
C(21)-C(22)-H(22)	119.5	C(30)-N(22)-H(22A)	112(2)
C(23)-C(22)-H(22)	119.5	C(30)-N(22)-H(22B)	116.1(19)
C(24)-C(23)-C(22)	121.2(2)	H(22A)-N(22)-H(22B)	111(3)
C(24)-C(23)-H(23)	119.4		
C(22)-C(23)-H(23)	119.4		
C(23)-C(24)-C(25)	117.2(2)		

Symmetry transformations used to generate equivalent atoms:

Table 4. Anisotropic displacement parameters ($\text{\AA}^2 \times 10^3$) for **1b**. The anisotropic displacement factor exponent takes the form: $-2\pi^2 [h^2 a^{*2} U^{11} + \dots + 2 h k a^* b^* U^{12}]$

	U ¹¹	U ²²	U ³³	U ²³	U ¹³	U ¹²
O(1)	34(1)	22(1)	28(1)	1(1)	3(1)	-9(1)
C(1)	16(1)	16(1)	29(2)	0(1)	7(1)	-1(1)
C(2)	18(1)	17(1)	27(1)	5(1)	7(1)	-1(1)
C(3)	15(1)	24(1)	22(1)	5(1)	5(1)	2(1)
C(4)	15(1)	22(1)	22(1)	-1(1)	6(1)	0(1)
C(5)	18(1)	16(1)	24(1)	3(1)	8(1)	-1(1)
C(6)	16(1)	21(1)	21(1)	1(1)	7(1)	1(1)
S(1)	47(1)	25(1)	24(1)	-2(1)	10(1)	-8(1)
C(7)	22(1)	19(1)	19(1)	-2(1)	2(1)	-4(1)
C(8)	23(1)	18(1)	34(2)	-1(1)	2(1)	1(1)
C(9)	20(1)	22(1)	33(2)	-5(1)	9(1)	-1(1)
C(10)	20(1)	20(1)	24(1)	-3(1)	3(1)	-2(1)
C(11)	21(1)	14(1)	26(1)	0(1)	2(1)	1(1)
C(12)	19(1)	25(1)	21(1)	-7(1)	5(1)	-1(1)
O(2)	32(1)	19(1)	39(1)	2(1)	15(1)	-1(1)
N(21)	18(1)	24(1)	32(2)	-1(1)	6(1)	-3(1)
C(21)	18(1)	12(1)	31(2)	-3(1)	5(1)	-1(1)
C(22)	29(2)	33(2)	26(2)	6(1)	10(1)	-8(1)
C(23)	31(2)	34(2)	20(1)	8(1)	0(1)	-7(1)
C(24)	21(1)	16(1)	26(1)	2(1)	5(1)	1(1)
C(25)	34(2)	39(2)	24(2)	-2(1)	12(1)	-12(1)
C(26)	31(2)	39(2)	19(1)	-5(1)	3(1)	-12(1)
C(20)	22(1)	20(1)	30(2)	5(1)	4(1)	-2(1)
C(27)	15(1)	23(1)	20(1)	1(1)	-1(1)	-6(1)
C(28)	22(1)	27(2)	32(2)	-1(1)	8(1)	1(1)
C(29)	25(2)	25(1)	29(2)	3(1)	12(1)	-6(1)
C(30)	21(1)	20(1)	18(1)	-2(1)	-1(1)	-4(1)
C(31)	24(1)	24(1)	28(2)	-3(1)	9(1)	-2(1)
C(32)	23(1)	27(2)	24(1)	1(1)	10(1)	-6(1)
N(22)	25(1)	20(1)	33(1)	-2(1)	7(1)	-5(1)

Table 5. Hydrogen coordinates ($\times 10^4$) and isotropic displacement parameters ($\text{\AA}^2 \times 10^3$) for **1b**.

	x	y	z	U(eq)
H(1A)	6550(30)	330(30)	-13(18)	53(11)
H(2)	7543	289	1701	24
H(3)	8461	2041	2388	24
H(5)	8089	4348	693	22
H(6)	7190	2583	1	23
H(8)	10755	4681	1398	31
H(9)	11540	6292	794	29
H(11)	9195	8990	1254	25
H(12)	8329	7346	1811	26
H(2A)	10780(30)	9540(40)	706(19)	72(13)
H(21A)	10030(30)	11450(30)	1169(16)	48(10)
H(21B)	10060(20)	11530(30)	450(14)	21(8)
H(22)	11829	11775	2075	35
H(23)	13736	12807	2393	35
H(25)	13668	13398	393	38
H(26)	11768	12382	74	36
H(20A)	15673	13594	1358	29
H(20B)	15476	13847	2114	29
H(28)	16304	15635	951	32
H(29)	16057	17899	719	31
H(31)	13313	18000	1707	30
H(32)	13564	15754	1935	29
H(22A)	14070(30)	19940(30)	1251(16)	45(10)
H(22B)	15050(30)	19970(30)	905(15)	34(9)

2a) 4-amino-4'-hydroxydiphenylethane

Synthesis: Venugopal Vangala, University of Hyderabad, India.

Table 1. Crystal data and structure refinement for **2a**.

Identification code	2a	
Empirical formula	C ₁₄ H ₁₅ N O	
Formula weight	213.27	
Temperature	100(2) K	
Wavelength	0.71073 Å	
Crystal system	Monoclinic	
Space group	Pc	
Unit cell dimensions	a = 13.682(3) Å	$\alpha = 90^\circ$.
	b = 5.2619(11) Å	$\beta = 107.28(3)^\circ$.
	c = 8.1916(16) Å	$\gamma = 90^\circ$.
Volume	563.1(2) Å ³	
Z	2	
Density (calculated)	1.258 Mg/m ³	
Absorption coefficient	0.079 mm ⁻¹	
F(000)	228	
Crystal size	0.50 x 0.35 x 0.10 mm ³	
Theta range for data collection	1.56 to 30.32°.	
Index ranges	-18 ≤ h ≤ 15, -7 ≤ k ≤ 7, -10 ≤ l ≤ 11	
Reflections collected	6709	
Independent reflections	2509 [R(int) = 0.0322]	
Completeness to theta = 30.32°	92.1 %	
Absorption correction	None	
Refinement method	Full-matrix least-squares on F ²	
Data / restraints / parameters	2509 / 2 / 205	
Goodness-of-fit on F ²	1.034	
Final R indices [I > 2σ(I)]	R1 = 0.0405, wR2 = 0.1087	
R indices (all data)	R1 = 0.0448, wR2 = 0.1137	
Absolute structure parameter	-0.7(13)	
Extinction coefficient	not refined	
Largest diff. peak and hole	0.370 and -0.186 e.Å ⁻³	

Table 2. Atomic coordinates ($\times 10^4$) and equivalent isotropic displacement parameters ($\text{\AA}^2 \times 10^3$) for **2a**. $U(\text{eq})$ is defined as one third of the trace of the orthogonalized U_{ij} tensor.

	x	y	z	$U(\text{eq})$
O(1)	8204(1)	1649(2)	14343(2)	22(1)
C(1)	7180(1)	2022(3)	13471(2)	17(1)
C(2)	6686(1)	4128(3)	13910(2)	19(1)
C(3)	5653(1)	4556(3)	13057(2)	19(1)
C(4)	5096(1)	2910(3)	11762(2)	17(1)
C(5)	5610(1)	825(3)	11345(2)	19(1)
C(6)	6637(1)	382(3)	12179(2)	18(1)
C(7)	3971(1)	3340(3)	10895(2)	19(1)
C(8)	3288(1)	1866(3)	11771(2)	20(1)
C(9)	2156(1)	2150(3)	10851(2)	17(1)
C(10)	1580(1)	4136(3)	11234(2)	19(1)
C(11)	537(1)	4398(3)	10362(2)	18(1)
C(12)	52(1)	2658(3)	9084(2)	17(1)
C(13)	622(1)	674(3)	8690(2)	19(1)
C(14)	1658(1)	441(3)	9564(2)	19(1)
N(1)	-1025(1)	2801(3)	8266(2)	20(1)

Table 3. Bond lengths [\AA] and angles [$^\circ$] for **2a**.

O(1)-C(1)	1.385(2)	O(1)-C(1)-C(2)	118.14(15)
O(1)-H(1)	0.80(3)	C(6)-C(1)-C(2)	119.68(15)
C(1)-C(6)	1.396(2)	C(3)-C(2)-C(1)	119.56(15)
C(1)-C(2)	1.399(2)	C(3)-C(2)-H(2)	120.7(13)
C(2)-C(3)	1.396(3)	C(1)-C(2)-H(2)	119.7(13)
C(2)-H(2)	1.00(2)	C(2)-C(3)-C(4)	121.32(16)
C(3)-C(4)	1.405(2)	C(2)-C(3)-H(3)	120.0(16)
C(3)-H(3)	0.96(2)	C(4)-C(3)-H(3)	118.7(16)
C(4)-C(5)	1.400(2)	C(5)-C(4)-C(3)	117.90(15)
C(4)-C(7)	1.508(2)	C(5)-C(4)-C(7)	121.27(15)
C(5)-C(6)	1.387(2)	C(3)-C(4)-C(7)	120.80(16)
C(5)-H(5)	1.01(3)	C(6)-C(5)-C(4)	121.37(16)
C(6)-H(6)	0.97(2)	C(6)-C(5)-H(5)	121.7(15)
C(7)-C(8)	1.5452(19)	C(4)-C(5)-H(5)	116.9(15)
C(7)-H(8A)	0.99(3)	C(5)-C(6)-C(1)	120.17(15)
C(7)-H(8B)	1.01(2)	C(5)-C(6)-H(6)	120.9(16)
C(8)-C(9)	1.516(2)	C(1)-C(6)-H(6)	118.9(16)
C(8)-H(7A)	1.00(2)	C(4)-C(7)-C(8)	112.31(12)
C(8)-H(7B)	0.97(3)	C(4)-C(7)-H(8A)	111.4(15)
C(9)-C(10)	1.399(2)	C(8)-C(7)-H(8A)	109.4(14)
C(9)-C(14)	1.399(2)	C(4)-C(7)-H(8B)	108.7(14)
C(10)-C(11)	1.400(2)	C(8)-C(7)-H(8B)	105.5(13)
C(10)-H(10)	0.97(2)	H(8A)-C(7)-H(8B)	109(2)
C(11)-C(12)	1.401(2)	C(9)-C(8)-C(7)	112.93(12)
C(11)-H(11)	0.99(2)	C(9)-C(8)-H(7A)	111.6(12)
C(12)-C(13)	1.397(2)	C(7)-C(8)-H(7A)	106.2(12)
C(12)-N(1)	1.428(2)	C(9)-C(8)-H(7B)	110.8(15)
C(13)-C(14)	1.390(3)	C(7)-C(8)-H(7B)	110.2(15)
C(13)-H(13)	0.98(3)	H(7A)-C(8)-H(7B)	105(2)
C(14)-H(14)	0.99(3)	C(10)-C(9)-C(14)	117.92(15)
N(1)-H(1A)	0.97(3)	C(10)-C(9)-C(8)	121.52(15)
N(1)-H(1B)	0.91(2)	C(14)-C(9)-C(8)	120.56(15)
		C(9)-C(10)-C(11)	121.05(15)
		C(9)-C(10)-H(10)	122.1(15)
		C(11)-C(10)-H(10)	116.9(15)
		C(10)-C(11)-C(12)	120.13(15)
C(1)-O(1)-H(1)	111(2)	C(10)-C(11)-H(11)	120.7(14)
O(1)-C(1)-C(6)	122.17(15)	C(12)-C(11)-H(11)	119.1(14)

C(13)-C(12)-C(11)	119.19(15)	C(9)-C(14)-H(14)	119.3(15)
C(13)-C(12)-N(1)	120.01(15)	C(12)-N(1)-H(1A)	108.2(19)
C(11)-C(12)-N(1)	120.68(15)	C(12)-N(1)-H(1B)	111.6(17)
C(14)-C(13)-C(12)	120.06(15)	H(1A)-N(1)-H(1B)	114(3)
C(14)-C(13)-H(13)	119.4(16)	<hr/> Symmetry transformations used to generate equivalent atom: <hr/>	
C(12)-C(13)-H(13)	120.5(16)		
C(13)-C(14)-C(9)	121.66(16)		
C(13)-C(14)-H(14)	119.0(15)		

Table 4. Anisotropic displacement parameters ($\text{\AA}^2 \times 10^3$) for **2a**. The anisotropic displacement factor exponent takes the form: $-2\pi^2 [h^2 a^{*2} U^{11} + \dots + 2 h k a^* b^* U^{12}]$

	U ¹¹	U ²²	U ³³	U ²³	U ¹³	U ¹²
O(1)	15(1)	24(1)	23(1)	-5(1)	1(1)	0(1)
C(1)	16(1)	19(1)	15(1)	3(1)	5(1)	0(1)
C(2)	18(1)	20(1)	16(1)	-2(1)	3(1)	-2(1)
C(3)	19(1)	17(1)	21(1)	0(1)	8(1)	2(1)
C(4)	15(1)	20(1)	17(1)	2(1)	4(1)	-1(1)
C(5)	18(1)	20(1)	17(1)	0(1)	4(1)	0(1)
C(6)	19(1)	18(1)	17(1)	-1(1)	5(1)	0(1)
C(7)	15(1)	23(1)	19(1)	6(1)	4(1)	3(1)
C(8)	16(1)	24(1)	20(1)	3(1)	4(1)	0(1)
C(9)	16(1)	19(1)	17(1)	3(1)	6(1)	0(1)
C(10)	18(1)	18(1)	19(1)	-2(1)	2(1)	-2(1)
C(11)	16(1)	19(1)	21(1)	0(1)	5(1)	2(1)
C(12)	15(1)	19(1)	15(1)	1(1)	3(1)	-2(1)
C(13)	19(1)	20(1)	19(1)	-3(1)	6(1)	-1(1)
C(14)	18(1)	20(1)	19(1)	-2(1)	6(1)	2(1)
N(1)	14(1)	25(1)	21(1)	0(1)	3(1)	1(1)

Table 5. Hydrogen coordinates ($\times 10^4$) and isotropic displacement parameters ($\text{\AA}^2 \times 10^3$) for **2a**.

	x	y	z	U(eq)
H(1)	8410(20)	320(50)	14090(40)	31(7)
H(2)	7083(18)	5350(40)	14800(30)	22(6)
H(3)	5317(19)	6040(40)	13320(30)	23(6)
H(5)	5200(20)	-330(50)	10400(30)	31(6)
H(6)	6980(20)	-1100(50)	11920(30)	30(6)
H(7A)	3465(16)	2520(40)	12970(30)	20(5)
H(7B)	3482(19)	90(50)	11890(30)	30(6)
H(8A)	3781(19)	2870(40)	9670(30)	27(6)
H(8B)	3811(19)	5190(50)	11000(30)	26(6)
H(10)	1878(19)	5390(40)	12110(30)	26(6)
H(11)	137(19)	5850(40)	10610(30)	34(7)
H(13)	300(20)	-530(40)	7770(30)	32(6)
H(14)	2050(20)	-1010(50)	9290(40)	35(7)
H(1A)	-1270(20)	4400(50)	8590(40)	46(8)
H(1B)	-1180(20)	2570(50)	7120(30)	39(6)

2b) 4-amino-4'-hydroxydiphenylmethysulphide

Synthesis: Venugopal Vangala, University of Hyderabad, India.

Table 1. Crystal data and structure refinement for **2b**.

Identification code	2b	
Empirical formula	C13 H13 N O S	
Formula weight	231.30	
Temperature	100(2) K	
Wavelength	1.54178 Å	
Crystal system	Monoclinic	
Space group	Pc	
Unit cell dimensions	a = 13.844(3) Å	$\alpha = 90^\circ$.
	b = 5.1626(10) Å	$\beta = 107.22(3)^\circ$.
	c = 8.2485(16) Å	$\gamma = 90^\circ$.
Volume	563.07(19) Å ³	
Z	2	
Density (calculated)	1.364 Mg/m ³	
Absorption coefficient	0.235 mm ⁻¹	
F(000)	244	
Crystal size	0.45 x 0.15 x 0.05 mm ³	
Theta range for data collection	3.34 to 74.96°.	
Index ranges	-17<= <i>h</i> <=17, -6<= <i>k</i> <=6, -6<= <i>l</i> <=10	
Reflections collected	3842	
Independent reflections	1935 [R(int) = 0.0449]	
Completeness to theta = 74.96°	89.4 %	
Absorption correction	None	
Refinement method	Full-matrix least-squares on F ²	
Data / restraints / parameters	1935 / 2 / 158	
Goodness-of-fit on F ²	1.095	
Final R indices [I>2sigma(I)]	R1 = 0.0435, wR2 = 0.1170	
R indices (all data)	R1 = 0.0497, wR2 = 0.1259	
Absolute structure parameter	-0.02(3)	
Extinction coefficient	0.0069(11)	
Largest diff. peak and hole	0.312 and -0.318 e.Å ⁻³	

Table 2. Atomic coordinates ($\times 10^4$) and equivalent isotropic displacement parameters ($\text{\AA}^2 \times 10^3$) for **2b**. $U(\text{eq})$ is defined as one third of the trace of the orthogonalized U_{ij} tensor.

	x	y	z	$U(\text{eq})$
S(1)	5064(1)	1351(2)	4410(1)	29(1)
N(1)	9998(2)	2184(7)	6593(5)	28(1)
O(1)	784(2)	3402(5)	505(3)	28(1)
C(1)	1773(3)	2984(7)	1412(5)	22(1)
C(2)	2273(3)	867(7)	1014(5)	24(1)
C(3)	3274(3)	392(7)	1913(5)	25(1)
C(4)	3800(3)	2018(7)	3225(5)	23(1)
C(5)	3288(3)	4130(7)	3632(5)	24(1)
C(6)	2287(3)	4636(7)	2737(5)	24(1)
C(7)	5749(3)	3265(7)	3247(5)	26(1)
C(8)	6862(3)	2931(7)	4119(4)	22(1)
C(9)	7419(3)	916(7)	3719(5)	25(1)
C(11)	8932(3)	2362(7)	5807(5)	22(1)
C(12)	8387(3)	4365(7)	6239(5)	26(1)
C(10)	8434(3)	623(7)	4541(5)	23(1)
C(13)	7371(3)	4648(7)	5402(5)	24(1)

Table 3. Bond lengths [\AA] and angles [$^\circ$] for **2b**.

S(1)-C(4)	1.768(4)	C(1)-O(1)-H(1)	112(4)
S(1)-C(7)	1.827(4)	O(1)-C(1)-C(2)	118.9(3)
N(1)-C(11)	1.429(4)	O(1)-C(1)-C(6)	121.6(3)
N(1)-H(1B)	0.92(5)	C(2)-C(1)-C(6)	119.4(3)
N(1)-H(1A)	0.85(5)	C(1)-C(2)-C(3)	120.2(3)
O(1)-C(1)	1.370(4)	C(1)-C(2)-H(2A)	119.9
O(1)-H(1)	0.98(7)	C(3)-C(2)-H(2A)	119.9
C(1)-C(2)	1.384(5)	C(2)-C(3)-C(4)	121.2(3)
C(1)-C(6)	1.402(5)	C(2)-C(3)-H(3A)	119.4
C(2)-C(3)	1.386(5)	C(4)-C(3)-H(3A)	119.4
C(2)-H(2A)	0.9500	C(3)-C(4)-C(5)	118.2(3)
C(3)-C(4)	1.392(5)	C(3)-C(4)-S(1)	121.1(3)
C(3)-H(3A)	0.9500	C(5)-C(4)-S(1)	120.6(3)
C(4)-C(5)	1.394(5)	C(6)-C(5)-C(4)	121.2(3)
C(5)-C(6)	1.388(5)	C(6)-C(5)-H(5A)	119.4
C(5)-H(5A)	0.9500	C(4)-C(5)-H(5A)	119.4
C(6)-H(6A)	0.9500	C(5)-C(6)-C(1)	119.7(4)
C(7)-C(8)	1.504(5)	C(5)-C(6)-H(6A)	120.1
C(7)-H(7A)	0.9900	C(1)-C(6)-H(6A)	120.1
C(7)-H(7B)	0.9900	C(8)-C(7)-S(1)	107.7(3)
C(8)-C(9)	1.391(5)	C(8)-C(7)-H(7A)	110.2
C(8)-C(13)	1.400(5)	S(1)-C(7)-H(7A)	110.2
C(9)-C(10)	1.376(5)	C(8)-C(7)-H(7B)	110.2
C(9)-H(9A)	0.9500	S(1)-C(7)-H(7B)	110.2
C(11)-C(12)	1.387(5)	H(7A)-C(7)-H(7B)	108.5
C(11)-C(10)	1.395(5)	C(9)-C(8)-C(13)	117.5(3)
C(12)-C(13)	1.379(5)	C(9)-C(8)-C(7)	122.2(3)
C(12)-H(12A)	0.9500	C(13)-C(8)-C(7)	120.3(3)
C(10)-H(10A)	0.9500	C(10)-C(9)-C(8)	121.5(3)
C(13)-H(13A)	0.9500	C(10)-C(9)-H(9A)	119.2
		C(8)-C(9)-H(9A)	119.2
C(4)-S(1)-C(7)	100.80(17)	C(12)-C(11)-C(10)	119.1(3)
C(11)-N(1)-H(1B)	112(3)	C(12)-C(11)-N(1)	119.9(3)
C(11)-N(1)-H(1A)	110(3)	C(10)-C(11)-N(1)	120.9(3)
H(1B)-N(1)-H(1A)	108(4)	C(13)-C(12)-C(11)	120.2(3)
		C(13)-C(12)-H(12A)	119.9
		C(11)-C(12)-H(12A)	119.9
		C(9)-C(10)-C(11)	120.3(3)

C(9)-C(10)-H(10A)	119.9	C(8)-C(13)-H(13A)	119.3
C(11)-C(10)-H(10A)	119.9		
C(12)-C(13)-C(8)	121.5(4)	Symmetry transformations used to	
C(12)-C(13)-H(13A)	119.3	generate equivalent atoms:	

Table 4. Anisotropic displacement parameters ($\text{\AA}^2 \times 10^3$) for **2b**. The anisotropic displacement factor exponent takes the form: $-2\pi^2 [h^2 a^{*2} U^{11} + \dots + 2 h k a^* b^* U^{12}]$

	U ¹¹	U ²²	U ³³	U ²³	U ¹³	U ¹²
S(1)	24(1)	32(1)	28(1)	9(1)	5(1)	3(1)
N(1)	28(2)	27(2)	26(2)	0(1)	3(1)	1(1)
O(1)	24(1)	30(1)	26(2)	-4(1)	3(1)	2(1)
C(1)	19(2)	24(2)	21(2)	1(1)	5(1)	0(1)
C(2)	21(2)	26(2)	25(2)	-2(2)	7(2)	-2(2)
C(3)	34(2)	24(2)	21(2)	3(2)	16(2)	6(2)
C(4)	24(2)	28(2)	20(2)	8(2)	7(2)	-1(2)
C(5)	24(2)	24(2)	20(2)	0(2)	2(2)	2(2)
C(6)	28(2)	23(2)	20(2)	0(2)	3(2)	-1(2)
C(7)	29(2)	28(2)	20(2)	4(2)	7(2)	-3(2)
C(8)	23(2)	23(2)	20(2)	2(1)	5(2)	-4(1)
C(9)	27(2)	22(2)	24(2)	-2(1)	4(2)	-4(1)
C(11)	18(2)	23(2)	22(2)	2(1)	2(1)	-3(1)
C(12)	29(2)	23(2)	23(2)	-4(2)	0(2)	-1(2)
C(10)	26(2)	20(2)	24(2)	-2(1)	8(2)	1(1)
C(13)	24(2)	23(2)	23(2)	-2(2)	5(2)	-1(2)

Table 5. Hydrogen coordinates ($\times 10^4$) and isotropic displacement parameters ($\text{\AA}^2 \times 10^3$) for **2b**.

	x	y	z	U(eq)
H(1B)	10170(30)	2480(90)	7740(60)	34(12)
H(1A)	10210(40)	680(100)	6440(60)	42(14)
H(1)	520(50)	4970(140)	880(80)	73(18)
H(2A)	1929	-264	122	28
H(3A)	3608	-1070	1629	30
H(5A)	3631	5242	4537	29
H(6A)	1952	6095	3021	29
H(7A)	5581	2661	2057	31
H(7B)	5560	5115	3244	31
H(9A)	7091	-284	2860	30
H(12A)	8714	5544	7113	32
H(10A)	8797	-770	4244	28
H(13A)	7009	6039	5702	28

2c) 4-amino-4'-hydroxydiphenyldisulphide

Synthesis: Venugopal Vangala, University of Hyderabad, India.

Table 1. Crystal data and structure refinement for **2c**.

Identification code	2c	
Empirical formula	C ₁₂ H ₁₁ N O S ₂	
Formula weight	249.34	
Temperature	100(2) K	
Wavelength	0.71073 Å	
Crystal system	Monoclinic	
Space group	P2(1)/c	
Unit cell dimensions	a = 10.4321(12) Å	$\alpha = 90^\circ$.
	b = 8.1179(11) Å	$\beta = 109.633(6)^\circ$.
	c = 14.791(2) Å	$\gamma = 90^\circ$.
Volume	1179.8(3) Å ³	
Z	4	
Density (calculated)	1.404 Mg/m ³	
Absorption coefficient	0.428 mm ⁻¹	
F(000)	520	
Crystal size	0.55 x 0.50 x 0.10 mm ³	
Theta range for data collection	2.07 to 28.32°.	
Index ranges	-12 ≤ h ≤ 13, -7 ≤ k ≤ 10, -19 ≤ l ≤ 19	
Reflections collected	8343	
Independent reflections	2926 [R(int) = 0.0278]	
Completeness to theta = 28.32°	99.6 %	
Absorption correction	Psi-scan	
Max. and min. transmission	0.90251 and 0.76269	
Refinement method	Full-matrix least-squares on F ²	
Data / restraints / parameters	2926 / 0 / 157	
Goodness-of-fit on F ²	1.078	
Final R indices [I > 2σ(I)]	R1 = 0.0348, wR2 = 0.0836	
R indices (all data)	R1 = 0.0417, wR2 = 0.0871	
Extinction coefficient	not refined	
Largest diff. peak and hole	0.381 and -0.221 e.Å ⁻³	

Table 2. Atomic coordinates ($\times 10^4$) and equivalent isotropic displacement parameters ($\text{\AA}^2 \times 10^3$) for **2c**. $U(\text{eq})$ is defined as one third of the trace of the orthogonalized U_{ij} tensor.

	x	y	z	$U(\text{eq})$
O(1)	681(1)	-5936(1)	-1851(1)	27(1)
C(1)	1004(2)	-4928(2)	-1068(1)	21(1)
C(2)	2213(2)	-5240(2)	-304(1)	25(1)
C(3)	2566(2)	-4276(2)	520(1)	25(1)
C(4)	1724(2)	-2978(2)	596(1)	22(1)
C(5)	507(2)	-2685(2)	-162(1)	21(1)
C(6)	149(1)	-3641(2)	-991(1)	21(1)
S(1)	2155(1)	-1739(1)	1653(1)	28(1)
S(2)	2842(1)	410(1)	1242(1)	27(1)
N(1)	8715(1)	-411(2)	1572(1)	23(1)
C(11)	7318(2)	-264(2)	1485(1)	21(1)
C(12)	6577(2)	1139(2)	1068(1)	23(1)
C(13)	5220(2)	1294(2)	1003(1)	24(1)
C(14)	4592(2)	69(2)	1375(1)	21(1)
C(15)	5337(2)	-1320(2)	1808(1)	23(1)
C(16)	6691(2)	-1488(2)	1854(1)	23(1)

Table 3. Bond lengths [\AA] and angles [$^\circ$] for **2c**.

O(1)-C(1)	1.3651(19)	C(3)-C(2)-H(2)	119.8
O(1)-H(1)	0.85(2)	C(1)-C(2)-H(2)	119.8
C(1)-C(6)	1.403(2)	C(2)-C(3)-C(4)	120.35(14)
C(1)-C(2)	1.405(2)	C(2)-C(3)-H(3)	119.8
C(2)-C(3)	1.390(2)	C(4)-C(3)-H(3)	119.8
C(2)-H(2)	0.9500	C(3)-C(4)-C(5)	119.08(14)
C(3)-C(4)	1.401(2)	C(3)-C(4)-S(1)	120.95(12)
C(3)-H(3)	0.9500	C(5)-C(4)-S(1)	119.94(12)
C(4)-C(5)	1.403(2)	C(6)-C(5)-C(4)	120.88(14)
C(4)-S(1)	1.7845(16)	C(6)-C(5)-H(5)	119.6
C(5)-C(6)	1.391(2)	C(4)-C(5)-H(5)	119.6
C(5)-H(5)	0.9500	C(5)-C(6)-C(1)	119.80(13)
C(6)-H(6)	0.9500	C(5)-C(6)-H(6)	120.1
S(1)-S(2)	2.0540(6)	C(1)-C(6)-H(6)	120.1
S(2)-C(14)	1.7910(15)	C(4)-S(1)-S(2)	103.30(5)
N(1)-C(11)	1.4242(19)	C(14)-S(2)-S(1)	106.28(5)
N(1)-H(1A)	0.82(2)	C(11)-N(1)-H(1A)	109.7(17)
N(1)-H(1B)	0.80(2)	C(11)-N(1)-H(1B)	111.5(15)
C(11)-C(16)	1.398(2)	H(1A)-N(1)-H(1B)	112(2)
C(11)-C(12)	1.398(2)	C(16)-C(11)-C(12)	119.28(14)
C(12)-C(13)	1.392(2)	C(16)-C(11)-N(1)	120.31(14)
C(12)-H(12)	0.9500	C(12)-C(11)-N(1)	120.34(14)
C(13)-C(14)	1.401(2)	C(13)-C(12)-C(11)	120.21(14)
C(13)-H(13)	0.9500	C(13)-C(12)-H(12)	119.9
C(14)-C(15)	1.397(2)	C(11)-C(12)-H(12)	119.9
C(15)-C(16)	1.398(2)	C(12)-C(13)-C(14)	120.48(14)
C(15)-H(15)	0.9500	C(12)-C(13)-H(13)	119.8
C(16)-H(16A)	0.9500	C(14)-C(13)-H(13)	119.8
		C(15)-C(14)-C(13)	119.48(14)
		C(15)-C(14)-S(2)	124.34(12)
		C(13)-C(14)-S(2)	116.17(12)
		C(14)-C(15)-C(16)	119.86(14)
C(1)-O(1)-H(1)	110.8(14)	C(14)-C(15)-H(15)	120.1
O(1)-C(1)-C(6)	122.24(13)	C(16)-C(15)-H(15)	120.1
O(1)-C(1)-C(2)	118.26(14)	C(15)-C(16)-C(11)	120.66(14)
C(6)-C(1)-C(2)	119.46(14)	C(15)-C(16)-H(16A)	119.7
C(3)-C(2)-C(1)	120.41(14)	C(11)-C(16)-H(16A)	119.7

Table 4. Anisotropic displacement parameters ($\text{\AA}^2 \times 10^3$) for **2c**. The anisotropic displacement factor exponent takes the form: $-2\pi^2 [h^2 a^{*2} U^{11} + \dots + 2 h k a^* b^* U^{12}]$

	U ¹¹	U ²²	U ³³	U ²³	U ¹³	U ¹²
O(1)	26(1)	21(1)	29(1)	-1(1)	3(1)	5(1)
C(1)	21(1)	17(1)	26(1)	3(1)	8(1)	-2(1)
C(2)	21(1)	21(1)	33(1)	4(1)	7(1)	4(1)
C(3)	18(1)	27(1)	27(1)	7(1)	4(1)	0(1)
C(4)	18(1)	26(1)	23(1)	1(1)	8(1)	-4(1)
C(5)	18(1)	22(1)	26(1)	3(1)	9(1)	1(1)
C(6)	17(1)	21(1)	25(1)	4(1)	5(1)	0(1)
S(1)	21(1)	43(1)	22(1)	-4(1)	9(1)	-4(1)
S(2)	19(1)	28(1)	32(1)	-8(1)	6(1)	2(1)
N(1)	19(1)	25(1)	25(1)	4(1)	8(1)	-1(1)
C(11)	19(1)	23(1)	18(1)	-2(1)	5(1)	-3(1)
C(12)	26(1)	19(1)	23(1)	1(1)	7(1)	-4(1)
C(13)	26(1)	20(1)	24(1)	0(1)	4(1)	2(1)
C(14)	18(1)	24(1)	19(1)	-4(1)	4(1)	0(1)
C(15)	21(1)	25(1)	23(1)	3(1)	7(1)	-3(1)
C(16)	20(1)	22(1)	24(1)	5(1)	5(1)	1(1)

Table 5. Hydrogen coordinates ($\times 10^4$) and isotropic displacement parameters ($\text{\AA}^2 \times 10^3$) for **2c**.

	x	y	z	U(eq)
H(1)	60(20)	-5510(30)	-2322(16)	36(6)
H(2)	2792	-6114	-351	30
H(3)	3383	-4499	1034	30
H(5)	-80	-1824	-109	26
H(6)	-672	-3422	-1503	25
H(1A)	8850(20)	80(30)	1130(17)	48(7)
H(1B)	8940(20)	-1350(30)	1591(14)	28(5)
H(12)	7000	1989	829	28
H(13)	4716	2238	704	29
H(15)	4924	-2150	2071	28
H(16A)	7190	-2443	2140	27

3a) 4-amino-4'-hydroxydiphenylpropane

Synthesis: Venugopal Vangala, University of Hyderabad, India.

Table 1. Crystal data and structure refinement for **3a**.

Identification code	3a	
Empirical formula	C ₁₅ H ₁₇ N O	
Formula weight	227.30	
Temperature	100(2) K	
Wavelength	0.71073 Å	
Crystal system	Orthorhombic	
Space group	Pca2(1)	
Unit cell dimensions	a = 23.9370(7) Å	$\alpha = 90^\circ$.
	b = 6.2160(2) Å	$\beta = 90^\circ$.
	c = 8.3970(3) Å	$\gamma = 90^\circ$.
Volume	1249.41(7) Å ³	
Z	4	
Density (calculated)	1.208 Mg/m ³	
Absorption coefficient	0.075 mm ⁻¹	
F(000)	488	
Crystal size	0.52 x 0.25 x 0.07 mm ³	
Theta range for data collection	1.70 to 28.27°.	
Index ranges	-31 ≤ h ≤ 31, -5 ≤ k ≤ 8, -11 ≤ l ≤ 10	
Reflections collected	8492	
Independent reflections	3069 [R(int) = 0.0365]	
Completeness to theta = 28.27°	100.0 %	
Absorption correction	None	
Refinement method	Full-matrix least-squares on F ²	
Data / restraints / parameters	3069 / 1 / 223	
Goodness-of-fit on F ²	1.016	
Final R indices [I > 2σ(I)]	R1 = 0.0389, wR2 = 0.0856	
R indices (all data)	R1 = 0.0510, wR2 = 0.0918	
Absolute structure parameter	0.3(15)	
Extinction coefficient	not refined	
Largest diff. peak and hole	0.205 and -0.159 e.Å ⁻³	

Table 2. Atomic coordinates ($\times 10^4$) and equivalent isotropic displacement parameters ($\text{\AA}^2 \times 10^3$) for **3a**. $U(\text{eq})$ is defined as one third of the trace of the orthogonalized U_{ij} tensor.

	x	y	z	U(eq)
O(1)	3091(1)	6252(2)	8976(2)	30(1)
C(1)	3602(1)	5501(3)	8474(2)	25(1)
C(2)	3776(1)	3403(3)	8759(2)	26(1)
C(3)	4287(1)	2707(3)	8160(2)	25(1)
C(4)	4634(1)	4049(3)	7282(2)	23(1)
C(5)	4457(1)	6161(3)	7039(2)	25(1)
C(6)	3942(1)	6890(3)	7620(2)	26(1)
C(7)	5171(1)	3205(3)	6551(2)	27(1)
C(8)	5562(1)	2066(3)	7723(2)	24(1)
C(9)	6078(1)	1120(3)	6910(2)	32(1)
C(10)	6451(1)	-143(3)	8018(2)	26(1)
C(11)	6298(1)	-2195(3)	8552(2)	27(1)
C(12)	6636(1)	-3346(3)	9589(2)	26(1)
C(13)	7136(1)	-2478(3)	10137(2)	24(1)
C(14)	7295(1)	-434(3)	9621(2)	26(1)
C(15)	6952(1)	704(3)	8573(2)	28(1)
N(1)	7502(1)	-3713(3)	11117(2)	27(1)

Table 3. Bond lengths [\AA] and angles [$^\circ$] for **3a**.

		N(1)-H(1B)	0.90(2)
		C(1)-O(1)-H(1)	112.4(14)
O(1)-C(1)	1.3756(19)	O(1)-C(1)-C(6)	118.05(15)
O(1)-H(1)	0.91(2)	O(1)-C(1)-C(2)	122.21(15)
C(1)-C(6)	1.387(2)	C(6)-C(1)-C(2)	119.72(15)
C(1)-C(2)	1.390(2)	C(3)-C(2)-C(1)	119.59(16)
C(2)-C(3)	1.390(2)	C(3)-C(2)-H(2)	119.6(11)
C(2)-H(2)	0.943(19)	C(1)-C(2)-H(2)	120.8(11)
C(3)-C(4)	1.390(2)	C(4)-C(3)-C(2)	122.12(16)
C(3)-H(3)	0.93(2)	C(4)-C(3)-H(3)	120.4(13)
C(4)-C(5)	1.396(2)	C(2)-C(3)-H(3)	117.4(13)
C(4)-C(7)	1.516(2)	C(3)-C(4)-C(5)	117.34(15)
C(5)-C(6)	1.399(2)	C(3)-C(4)-C(7)	120.95(15)
C(5)-H(5)	0.95(2)	C(5)-C(4)-C(7)	121.64(15)
C(6)-H(6)	0.960(18)	C(4)-C(5)-C(6)	121.47(15)
C(7)-C(8)	1.532(2)	C(4)-C(5)-H(5)	118.0(12)
C(7)-H(7A)	0.97(2)	C(6)-C(5)-H(5)	120.5(12)
C(7)-H(7B)	0.98(2)	C(1)-C(6)-C(5)	119.73(15)
C(8)-C(9)	1.529(2)	C(1)-C(6)-H(6)	120.2(11)
C(8)-H(8A)	0.95(2)	C(5)-C(6)-H(6)	120.0(11)
C(8)-H(8B)	0.99(2)	C(4)-C(7)-C(8)	114.63(14)
C(9)-C(10)	1.510(2)	C(4)-C(7)-H(7A)	109.0(13)
C(9)-H(9A)	0.98(2)	C(8)-C(7)-H(7A)	109.5(13)
C(9)-H(9B)	0.99(3)	C(4)-C(7)-H(7B)	108.2(13)
C(10)-C(15)	1.391(2)	C(8)-C(7)-H(7B)	109.3(12)
C(10)-C(11)	1.400(2)	H(7A)-C(7)-H(7B)	105.9(18)
C(11)-C(12)	1.387(2)	C(9)-C(8)-C(7)	112.60(14)
C(11)-H(11)	0.942(19)	C(9)-C(8)-H(8A)	110.3(11)
C(12)-C(13)	1.393(2)	C(7)-C(8)-H(8A)	110.0(12)
C(12)-H(12)	0.96(2)	C(9)-C(8)-H(8B)	112.0(12)
C(13)-C(14)	1.395(2)	C(7)-C(8)-H(8B)	108.4(12)
C(13)-N(1)	1.425(2)	H(8A)-C(8)-H(8B)	103.2(16)
C(14)-C(15)	1.395(3)	C(10)-C(9)-C(8)	113.74(14)
C(14)-H(14)	0.96(2)	C(10)-C(9)-H(9A)	110.1(13)
C(15)-H(15)	0.95(2)	C(8)-C(9)-H(9A)	109.2(13)
N(1)-H(1A)	0.85(2)	C(10)-C(9)-H(9B)	111.4(14)

C(8)-C(9)-H(9B)	107.0(14)	C(14)-C(13)-N(1)	120.21(15)
H(9A)-C(9)-H(9B)	105(2)	C(13)-C(14)-C(15)	119.92(16)
C(15)-C(10)-C(11)	117.58(15)	C(13)-C(14)-H(14)	120.1(13)
C(15)-C(10)-C(9)	121.31(16)	C(15)-C(14)-H(14)	120.0(13)
C(11)-C(10)-C(9)	121.10(16)	C(10)-C(15)-C(14)	121.72(16)
C(12)-C(11)-C(10)	121.27(15)	C(10)-C(15)-H(15)	119.6(11)
C(12)-C(11)-H(11)	120.2(12)	C(14)-C(15)-H(15)	118.7(11)
C(10)-C(11)-H(11)	118.4(12)	C(13)-N(1)-H(1A)	111.8(16)
C(11)-C(12)-C(13)	120.61(16)	C(13)-N(1)-H(1B)	111.3(12)
C(11)-C(12)-H(12)	119.8(11)	H(1A)-N(1)-H(1B)	113(2)
C(13)-C(12)-H(12)	119.4(11)		
C(12)-C(13)-C(14)	118.91(15)	Symmetry transformations used to generate equivalent atoms:	
C(12)-C(13)-N(1)	120.72(16)		

Table 4. Anisotropic displacement parameters ($\text{\AA}^2 \times 10^3$) for **3a**. The anisotropic displacement factor exponent takes the form: $-2\pi^2 [h^2 a^{*2} U^{11} + \dots + 2 h k a^* b^* U^{12}]$

	U ¹¹	U ²²	U ³³	U ²³	U ¹³	U ¹²
O(1)	23(1)	31(1)	38(1)	-2(1)	2(1)	4(1)
C(1)	21(1)	28(1)	24(1)	-5(1)	-4(1)	0(1)
C(2)	23(1)	27(1)	29(1)	-1(1)	0(1)	-2(1)
C(3)	24(1)	21(1)	30(1)	0(1)	1(1)	0(1)
C(4)	21(1)	27(1)	21(1)	-1(1)	-2(1)	1(1)
C(5)	26(1)	28(1)	22(1)	0(1)	-5(1)	-3(1)
C(6)	29(1)	21(1)	28(1)	-2(1)	-8(1)	3(1)
C(7)	24(1)	33(1)	23(1)	3(1)	3(1)	4(1)
C(8)	23(1)	29(1)	21(1)	0(1)	1(1)	1(1)
C(9)	29(1)	43(1)	23(1)	4(1)	4(1)	8(1)
C(10)	24(1)	34(1)	21(1)	1(1)	5(1)	5(1)
C(11)	19(1)	37(1)	25(1)	-2(1)	2(1)	-4(1)
C(12)	24(1)	27(1)	25(1)	3(1)	4(1)	-4(1)
C(13)	22(1)	30(1)	21(1)	-1(1)	4(1)	2(1)
C(14)	21(1)	29(1)	29(1)	0(1)	0(1)	-4(1)
C(15)	28(1)	25(1)	30(1)	2(1)	6(1)	-1(1)
N(1)	23(1)	33(1)	25(1)	6(1)	-1(1)	-2(1)

Table 5. Hydrogen coordinates ($\times 10^4$) and isotropic displacement parameters ($\text{\AA}^2 \times 10^3$) for **3a**.

	x	y	z	U(eq)
H(1)	2923(9)	5350(40)	9670(30)	40(6)
H(2)	3551(8)	2440(30)	9340(20)	26(5)
H(3)	4383(8)	1270(30)	8330(30)	35(5)
H(5)	4698(8)	7110(30)	6480(20)	27(5)
H(6)	3824(8)	8340(30)	7420(20)	27(5)
H(7A)	5367(9)	4390(40)	6050(30)	41(6)
H(7B)	5072(9)	2210(30)	5690(30)	35(5)
H(8A)	5670(8)	3030(30)	8550(20)	29(5)
H(8B)	5345(8)	960(30)	8300(20)	37(6)
H(9A)	6290(9)	2280(40)	6400(30)	47(6)
H(9B)	5943(10)	220(40)	6020(30)	54(7)
H(11)	5949(8)	-2750(30)	8240(20)	32(5)
H(12)	6513(8)	-4720(30)	9990(20)	28(5)
H(14)	7643(9)	170(30)	9960(30)	36(6)
H(15)	7066(7)	2090(30)	8240(20)	28(5)
H(1A)	7706(9)	-2920(40)	11690(30)	46(7)
H(1B)	7314(8)	-4710(30)	11670(20)	29(5)

3b) 4-amino-4'-hydroxyphenylethylsulphide

Synthesis: Venugopal Vangala, University of Hyderabad, India.

Table 1. Crystal data and structure refinement for **3b**.

Identification code	3b	
Empirical formula	C ₁₄ H ₁₅ N O S	
Formula weight	245.33	
Temperature	100(2) K	
Wavelength	0.71073 Å	
Crystal system	Monoclinic	
Space group	Pc	
Unit cell dimensions	a = 12.6341(9) Å	α = 90°.
	b = 5.8636(4) Å	β = 90.351(3)°.
	c = 8.5671(5) Å	γ = 90°.
Volume	634.65(7) Å ³	
Z	2	
Density (calculated)	1.284 Mg/m ³	
Absorption coefficient	0.238 mm ⁻¹	
F(000)	260	
Crystal size	0.35 x 0.25 x 0.20 mm ³	
Theta range for data collection	1.61 to 30.08°.	
Index ranges	-17<=h<=17, -6<=k<=7, -11<=l<=11	
Reflections collected	4751	
Independent reflections	3138 [R(int) = 0.0256]	
Completeness to theta = 30.08°	92.6 %	
Absorption correction	Psi-scan	
Max. and min. transmission	0.93286 and 0.88891	
Refinement method	Full-matrix least-squares on F ²	
Data / restraints / parameters	3138 / 2 / 166	
Goodness-of-fit on F ²	1.055	
Final R indices [I>2sigma(I)]	R1 = 0.0322, wR2 = 0.0822	
R indices (all data)	R1 = 0.0337, wR2 = 0.0835	
Absolute structure parameter	0.04(6)	
Extinction coefficient	not refined	
Largest diff. peak and hole	0.304 and -0.177 e.Å ⁻³	

Table 2. Atomic coordinates ($\times 10^4$) and equivalent isotropic displacement parameters ($\text{\AA}^2 \times 10^3$) for **3b**. $U(\text{eq})$ is defined as one third of the trace of the orthogonalized U_{ij} tensor.

	x	y	z	$U(\text{eq})$
O(1)	8085(1)	7481(2)	1880(2)	24(1)
C(1)	7044(1)	7568(3)	2291(2)	19(1)
C(2)	6345(1)	9240(3)	1732(2)	20(1)
C(3)	5301(1)	9265(3)	2265(2)	21(1)
C(4)	4946(1)	7645(3)	3339(2)	18(1)
C(5)	5650(1)	5968(3)	3871(2)	22(1)
C(6)	6691(1)	5930(3)	3354(2)	23(1)
S(1)	3635(1)	7765(1)	4081(1)	19(1)
C(7)	2959(1)	5733(4)	2813(2)	28(1)
C(8)	1893(1)	5115(3)	3513(2)	22(1)
C(9)	1192(1)	3671(3)	2470(2)	16(1)
C(10)	200(1)	4484(3)	1989(2)	17(1)
C(11)	-465(1)	3211(3)	1018(2)	17(1)
C(12)	-142(1)	1062(3)	489(2)	16(1)
C(13)	839(1)	201(3)	974(2)	16(1)
C(14)	1496(1)	1493(3)	1954(2)	17(1)
N(1)	-844(1)	-267(3)	-449(2)	19(1)

Table 3. Bond lengths [\AA] and angles [$^\circ$] for **3b**.

O(1)-C(1)	1.365(2)	O(1)-C(1)-C(6)	117.01(15)
O(1)-H(1)	0.85(3)	O(1)-C(1)-C(2)	122.96(15)
C(1)-C(6)	1.399(2)	C(6)-C(1)-C(2)	120.01(16)
C(1)-C(2)	1.402(2)	C(3)-C(2)-C(1)	119.28(15)
C(2)-C(3)	1.398(2)	C(3)-C(2)-H(2A)	120.4
C(2)-H(2A)	0.9500	C(1)-C(2)-H(2A)	120.4
C(3)-C(4)	1.398(2)	C(2)-C(3)-C(4)	121.02(15)
C(3)-H(3A)	0.9500	C(2)-C(3)-H(3A)	119.5
C(4)-C(5)	1.401(2)	C(4)-C(3)-H(3A)	119.5
C(4)-S(1)	1.7787(17)	C(3)-C(4)-C(5)	118.98(16)
C(5)-C(6)	1.390(2)	C(3)-C(4)-S(1)	120.79(13)
C(5)-H(5A)	0.9500	C(5)-C(4)-S(1)	120.18(13)
C(6)-H(6A)	0.9500	C(6)-C(5)-C(4)	120.56(15)
S(1)-C(7)	1.8218(18)	C(6)-C(5)-H(5A)	119.7
C(7)-C(8)	1.521(2)	C(4)-C(5)-H(5A)	119.7
C(7)-H(7A)	0.9900	C(5)-C(6)-C(1)	120.14(16)
C(7)-H(7B)	0.9900	C(5)-C(6)-H(6A)	119.9
C(8)-C(9)	1.514(2)	C(1)-C(6)-H(6A)	119.9
C(8)-H(8A)	0.9900	C(4)-S(1)-C(7)	101.26(8)
C(8)-H(8B)	0.9900	C(8)-C(7)-S(1)	109.47(12)
C(9)-C(10)	1.400(2)	C(8)-C(7)-H(7A)	109.8
C(9)-C(14)	1.405(2)	S(1)-C(7)-H(7A)	109.8
C(10)-C(11)	1.395(2)	C(8)-C(7)-H(7B)	109.8
C(10)-H(10A)	0.9500	S(1)-C(7)-H(7B)	109.8
C(11)-C(12)	1.401(2)	H(7A)-C(7)-H(7B)	108.2
C(11)-H(11A)	0.9500	C(9)-C(8)-C(7)	114.62(13)
C(12)-C(13)	1.400(2)	C(9)-C(8)-H(8A)	108.6
C(12)-N(1)	1.425(2)	C(7)-C(8)-H(8A)	108.6
C(13)-C(14)	1.400(2)	C(9)-C(8)-H(8B)	108.6
C(13)-H(13A)	0.9500	C(7)-C(8)-H(8B)	108.6
C(14)-H(14A)	0.9500	H(8A)-C(8)-H(8B)	107.6
N(1)-H(1A)	0.82(3)	C(10)-C(9)-C(14)	117.58(14)
N(1)-H(1B)	0.90(3)	C(10)-C(9)-C(8)	120.17(14)
		C(14)-C(9)-C(8)	122.25(15)
		C(11)-C(10)-C(9)	121.82(14)
		C(11)-C(10)-H(10A)	119.1
		C(9)-C(10)-H(10A)	119.1
C(1)-O(1)-H(1)	111(2)	C(10)-C(11)-C(12)	119.96(15)

C(10)-C(11)-H(11A)	120.0	C(13)-C(14)-H(14A)	119.4
C(12)-C(11)-H(11A)	120.0	C(9)-C(14)-H(14A)	119.4
C(13)-C(12)-C(11)	119.15(14)	C(12)-N(1)-H(1A)	111.0(16)
C(13)-C(12)-N(1)	121.16(14)	C(12)-N(1)-H(1B)	114.7(16)
C(11)-C(12)-N(1)	119.56(14)	H(1A)-N(1)-H(1B)	105(2)
C(14)-C(13)-C(12)	120.23(14)	Symmetry transformations used to generate equivalent atoms:	
C(14)-C(13)-H(13A)	119.9		
C(12)-C(13)-H(13A)	119.9		
C(13)-C(14)-C(9)	121.23(14)		

Table 4. Anisotropic displacement parameters ($\text{\AA}^2 \times 10^3$) for **3b**. The anisotropic displacement factor exponent takes the form: $-2\pi^2 [h^2 a^{*2} U^{11} + \dots + 2 h k a^* b^* U^{12}]$

	U ¹¹	U ²²	U ³³	U ²³	U ¹³	U ¹²
O(1)	15(1)	26(1)	30(1)	4(1)	4(1)	2(1)
C(1)	16(1)	19(1)	21(1)	-2(1)	1(1)	-1(1)
C(2)	16(1)	21(1)	24(1)	5(1)	2(1)	1(1)
C(3)	16(1)	25(1)	22(1)	4(1)	0(1)	3(1)
C(4)	13(1)	23(1)	19(1)	-1(1)	-1(1)	-3(1)
C(5)	21(1)	23(1)	23(1)	6(1)	1(1)	-3(1)
C(6)	17(1)	21(1)	32(1)	5(1)	0(1)	2(1)
S(1)	13(1)	25(1)	18(1)	-4(1)	1(1)	-4(1)
C(7)	15(1)	42(1)	26(1)	-16(1)	6(1)	-11(1)
C(8)	20(1)	29(1)	16(1)	-5(1)	2(1)	-8(1)
C(9)	16(1)	19(1)	12(1)	-1(1)	2(1)	-5(1)
C(10)	19(1)	15(1)	18(1)	-1(1)	4(1)	-1(1)
C(11)	16(1)	19(1)	17(1)	2(1)	2(1)	1(1)
C(12)	17(1)	17(1)	13(1)	0(1)	2(1)	-2(1)
C(13)	18(1)	15(1)	16(1)	-1(1)	3(1)	0(1)
C(14)	14(1)	20(1)	16(1)	3(1)	2(1)	2(1)
N(1)	18(1)	24(1)	17(1)	-5(1)	-1(1)	-1(1)

Table 5. Hydrogen coordinates ($\times 10^4$) and isotropic displacement parameters ($\text{\AA}^2 \times 10^3$) for **3b**.

	x	y	z	U(eq)
H(1)	8200(30)	8350(60)	1110(40)	53(8)
H(2A)	6578	10343	998	24
H(3A)	4827	10401	1893	25
H(5A)	5415	4848	4591	26
H(6A)	7164	4788	3724	28
H(7A)	2852	6411	1765	33
H(7B)	3395	4342	2697	33
H(8A)	2018	4282	4503	26
H(8B)	1512	6540	3769	26
H(10A)	-26	5944	2334	21
H(11A)	-1135	3801	716	20
H(13A)	1061	-1266	637	19
H(14A)	2159	887	2277	20
H(1A)	-1145(18)	530(40)	-1110(30)	24(6)
H(1B)	-531(19)	-1380(40)	-1000(30)	31(6)

4a) 4-amino-4'-hydroxydiphenylbutane

Synthesis: Venugopal Vangala, University of Hyderabad, India.

Table 1. Crystal data and structure refinement for **4a**.

Identification code	4a	
Empirical formula	C ₁₆ H ₁₉ N O	
Formula weight	241.32	
Temperature	105(2) K	
Wavelength	0.71073 Å	
Crystal system	Monoclinic	
Space group	Pc	
Unit cell dimensions	a = 15.7888(16) Å	$\alpha = 90^\circ$.
	b = 5.2088(6) Å	$\beta = 100.912(5)^\circ$.
	c = 8.3399(8) Å	$\gamma = 90^\circ$.
Volume	673.48(12) Å ³	
Z	2	
Density (calculated)	1.190 Mg/m ³	
Absorption coefficient	0.074 mm ⁻¹	
F(000)	260	
Crystal size	0.40 x 0.20 x 0.20 mm ³	
Theta range for data collection	2.63 to 27.54°.	
Index ranges	-20 ≤ h ≤ 19, -6 ≤ k ≤ 5, -10 ≤ l ≤ 10	
Reflections collected	4048	
Independent reflections	2816 [R(int) = 0.0546]	
Completeness to theta = 27.54°	99.7 %	
Absorption correction	None	
Refinement method	Full-matrix least-squares on F ²	
Data / restraints / parameters	2816 / 2 / 176	
Goodness-of-fit on F ²	1.026	
Final R indices [I > 2σ(I)]	R ₁ = 0.0429, wR ₂ = 0.0960	
R indices (all data)	R ₁ = 0.0626, wR ₂ = 0.1081	
Absolute structure parameter	0.1(19)	
Extinction coefficient	not refined	
Largest diff. peak and hole	0.200 and -0.174 e.Å ⁻³	

Table 2. Atomic coordinates ($\times 10^4$) and equivalent isotropic displacement parameters ($\text{\AA}^2 \times 10^3$) for **4a**. $U(\text{eq})$ is defined as one third of the trace of the orthogonalized U_{ij} tensor.

	x	y	z	$U(\text{eq})$
N(1)	2503(1)	2901(4)	3233(3)	26(1)
O(1)	11862(1)	1551(4)	6492(2)	27(1)
C(1)	10995(2)	1973(4)	6491(3)	21(1)
C(2)	10517(2)	375(5)	7323(3)	22(1)
C(3)	9651(2)	872(5)	7282(3)	23(1)
C(4)	9237(2)	2981(5)	6438(3)	22(1)
C(5)	9729(2)	4571(5)	5609(3)	25(1)
C(6)	10598(2)	4083(5)	5633(3)	23(1)
C(7)	8283(2)	3513(5)	6368(3)	26(1)
C(8)	7692(2)	2196(5)	4925(4)	24(1)
C(9)	6740(2)	2944(5)	4784(4)	25(1)
C(10)	6150(2)	1658(5)	3316(4)	26(1)
C(11)	3419(2)	2711(5)	3312(3)	20(1)
C(12)	3883(2)	704(5)	4189(3)	24(1)
C(13)	4753(2)	415(5)	4168(3)	23(1)
C(14)	5193(2)	2069(4)	3296(3)	22(1)
C(15)	4727(2)	4080(5)	2429(3)	23(1)
C(16)	3844(2)	4408(4)	2439(3)	23(1)

Table 3. Bond lengths [\AA] and angles [$^\circ$] for **4a**.

		C(13)-H(13)	0.9500
		C(14)-C(15)	1.400(4)
		C(15)-C(16)	1.407(4)
		C(15)-H(15)	0.9500
		C(16)-H(16)	0.9500
N(1)-C(11)	1.439(3)	C(11)-N(1)-H(1A)	110.8(17)
N(1)-H(1A)	0.98(3)	C(11)-N(1)-H(1B)	111.7(16)
N(1)-H(1B)	0.91(2)	H(1A)-N(1)-H(1B)	114(2)
O(1)-C(1)	1.385(3)	C(1)-O(1)-H(1)	105(3)
O(1)-H(1)	0.85(5)	O(1)-C(1)-C(6)	118.3(2)
C(1)-C(6)	1.394(3)	O(1)-C(1)-C(2)	122.2(2)
C(1)-C(2)	1.395(4)	C(6)-C(1)-C(2)	119.5(2)
C(2)-C(3)	1.386(4)	C(3)-C(2)-C(1)	120.1(2)
C(2)-H(2)	0.9500	C(3)-C(2)-H(2)	120.0
C(3)-C(4)	1.398(3)	C(1)-C(2)-H(2)	120.0
C(3)-H(3)	0.9500	C(2)-C(3)-C(4)	121.6(2)
C(4)-C(5)	1.405(4)	C(2)-C(3)-H(3)	119.2
C(4)-C(7)	1.521(4)	C(4)-C(3)-H(3)	119.2
C(5)-C(6)	1.391(4)	C(3)-C(4)-C(5)	117.5(2)
C(5)-H(5)	0.9500	C(3)-C(4)-C(7)	121.8(2)
C(6)-H(6)	0.9500	C(5)-C(4)-C(7)	120.7(2)
C(7)-C(8)	1.538(4)	C(6)-C(5)-C(4)	121.4(3)
C(7)-H(7A)	0.9900	C(6)-C(5)-H(5)	119.3
C(7)-H(7B)	0.9900	C(4)-C(5)-H(5)	119.3
C(8)-C(9)	1.535(2)	C(5)-C(6)-C(1)	119.9(3)
C(8)-H(8A)	0.9900	C(5)-C(6)-H(6)	120.0
C(8)-H(8B)	0.9900	C(1)-C(6)-H(6)	120.0
C(9)-C(10)	1.544(4)	C(4)-C(7)-C(8)	113.5(2)
C(9)-H(9A)	0.9900	C(4)-C(7)-H(7A)	108.9
C(9)-H(9B)	0.9900	C(8)-C(7)-H(7A)	108.9
C(10)-C(14)	1.523(4)	C(4)-C(7)-H(7B)	108.9
C(10)-H(10A)	0.9900	C(8)-C(7)-H(7B)	108.9
C(10)-H(10B)	0.9900	H(7A)-C(7)-H(7B)	107.7
C(11)-C(16)	1.395(4)	C(9)-C(8)-C(7)	112.80(18)
C(11)-C(12)	1.400(3)	C(9)-C(8)-H(8A)	109.0
C(12)-C(13)	1.385(4)	C(7)-C(8)-H(8A)	109.0
C(12)-H(12)	0.9500		
C(13)-C(14)	1.396(4)		

C(9)-C(8)-H(8B)	109.0	C(13)-C(12)-H(12)	120.1
C(7)-C(8)-H(8B)	109.0	C(11)-C(12)-H(12)	120.1
H(8A)-C(8)-H(8B)	107.8	C(12)-C(13)-C(14)	122.2(2)
C(8)-C(9)-C(10)	112.70(18)	C(12)-C(13)-H(13)	118.9
C(8)-C(9)-H(9A)	109.1	C(14)-C(13)-H(13)	118.9
C(10)-C(9)-H(9A)	109.1	C(13)-C(14)-C(15)	117.8(2)
C(8)-C(9)-H(9B)	109.1	C(13)-C(14)-C(10)	119.9(2)
C(10)-C(9)-H(9B)	109.1	C(15)-C(14)-C(10)	122.3(3)
H(9A)-C(9)-H(9B)	107.8	C(14)-C(15)-C(16)	120.9(2)
C(14)-C(10)-C(9)	113.4(2)	C(14)-C(15)-H(15)	119.6
C(14)-C(10)-H(10A)	108.9	C(16)-C(15)-H(15)	119.6
C(9)-C(10)-H(10A)	108.9	C(11)-C(16)-C(15)	120.1(2)
C(14)-C(10)-H(10B)	108.9	C(11)-C(16)-H(16)	120.0
C(9)-C(10)-H(10B)	108.9	C(15)-C(16)-H(16)	120.0
H(10A)-C(10)-H(10B)	107.7		
C(16)-C(11)-C(12)	119.4(2)	Symmetry transformations used to generate equivalent atoms:	
C(16)-C(11)-N(1)	120.7(2)		
C(12)-C(11)-N(1)	119.8(2)		
C(13)-C(12)-C(11)	119.8(2)		

Table 4. Anisotropic displacement parameters ($\text{\AA}^2 \times 10^3$) for **4a**. The anisotropic displacement factor exponent takes the form: $-2\pi^2 [h^2 a^{*2} U^{11} + \dots + 2 h k a^* b^* U^{12}]$

	U ¹¹	U ²²	U ³³	U ²³	U ¹³	U ¹²
N(1)	15(1)	33(1)	29(1)	1(1)	4(1)	1(1)
O(1)	18(1)	32(1)	32(1)	4(1)	5(1)	-1(1)
C(1)	17(1)	26(1)	19(1)	-3(1)	0(1)	1(1)
C(2)	22(1)	23(1)	19(1)	4(1)	2(1)	-1(1)
C(3)	20(1)	26(1)	25(2)	1(1)	6(1)	-2(1)
C(4)	17(1)	27(1)	20(2)	-5(1)	1(1)	0(1)
C(5)	25(2)	25(1)	22(1)	-2(1)	1(1)	3(1)
C(6)	23(1)	25(1)	20(1)	0(1)	5(1)	-3(1)
C(7)	21(1)	31(1)	25(2)	-6(1)	4(1)	4(1)
C(8)	20(1)	26(1)	25(2)	-1(1)	4(1)	2(1)
C(9)	17(1)	31(1)	25(2)	0(1)	4(1)	1(1)
C(10)	17(1)	34(1)	27(2)	-4(1)	3(1)	1(1)
C(11)	16(1)	25(1)	19(1)	-5(1)	4(1)	-4(1)
C(12)	23(1)	24(1)	23(1)	2(1)	4(1)	-1(1)
C(13)	21(1)	26(1)	19(1)	2(1)	-1(1)	3(1)
C(14)	18(1)	26(1)	22(2)	-6(1)	2(1)	0(1)
C(15)	24(1)	24(1)	22(1)	-1(1)	4(1)	-4(1)
C(16)	18(1)	25(1)	25(1)	-2(1)	1(1)	3(1)

Table 5. Hydrogen coordinates ($\times 10^4$) and isotropic displacement parameters ($\text{\AA}^2 \times 10^3$) for **4a**.

	x	y	z	U(eq)
H(1A)	2283(18)	4540(60)	2760(30)	28(7)
H(1B)	2358(16)	2570(50)	4210(30)	34(7)
H(1)	11980(30)	110(90)	6970(60)	99(16)
H(2)	10785	-1056	7919	26
H(3)	9330	-248	7841	28
H(5)	9464	6011	5019	30
H(6)	10919	5186	5066	27
H(7A)	8185	5389	6287	31
H(7B)	8123	2920	7399	31
H(8A)	7883	2665	3900	28
H(8B)	7748	312	5059	28
H(9A)	6685	4831	4672	29
H(9B)	6545	2445	5801	29
H(10A)	6291	2353	2294	32
H(10B)	6270	-208	3342	32
H(12)	3602	-455	4796	28
H(13)	5060	-956	4768	27
H(15)	5011	5238	1827	28
H(16)	3536	5786	1851	27

5a) 4-amino-4'-hydroxydiphenylpentane

Synthesis: Venugopal Vangala, University of Hyderabad, India.

Table 1. Crystal data and structure refinement for **5a**.

Identification code	5a	
Empirical formula	C ₁₇ H ₂₁ N O	
Formula weight	255.35	
Temperature	100(2) K	
Wavelength	0.71073 Å	
Crystal system	Monoclinic	
Space group	Pc	
Unit cell dimensions	a = 14.9554(9) Å	$\alpha = 90^\circ$.
	b = 11.2370(8) Å	$\beta = 90.893(3)^\circ$.
	c = 8.6841(6) Å	$\gamma = 90^\circ$.
Volume	1459.22(17) Å ³	
Z	4	
Density (calculated)	1.162 Mg/m ³	
Absorption coefficient	0.071 mm ⁻¹	
F(000)	552	
Crystal size	0.60 x 0.55 x 0.30 mm ³	
Theta range for data collection	2.27 to 27.55°.	
Index ranges	-19 ≤ h ≤ 19, -11 ≤ k ≤ 14, -11 ≤ l ≤ 11	
Reflections collected	9991	
Independent reflections	5476 [R(int) = 0.0215]	
Completeness to theta = 27.55°	99.6 %	
Absorption correction	Psi-scan	
Max. and min. transmission	0.99477 and 0.89622	
Refinement method	Full-matrix least-squares on F ²	
Data / restraints / parameters	5476 / 2 / 367	
Goodness-of-fit on F ²	1.033	
Final R indices [I > 2σ(I)]	R1 = 0.0355, wR2 = 0.0885	
R indices (all data)	R1 = 0.0418, wR2 = 0.0938	
Absolute structure parameter	-0.2(11)	
Extinction coefficient	not refined	
Largest diff. peak and hole	0.252 and -0.160 e.Å ⁻³	

Table 2. Atomic coordinates ($\times 10^4$) and equivalent isotropic displacement parameters ($\text{\AA}^2 \times 10^3$) for **5a**. $U(\text{eq})$ is defined as one third of the trace of the orthogonalized U_{ij} tensor.

	x	y	z	$U(\text{eq})$
O(1)	18714(1)	6720(1)	636(2)	38(1)
C(1)	17914(1)	6397(2)	-47(2)	30(1)
C(2)	17506(1)	5312(2)	257(2)	29(1)
C(3)	16713(1)	5019(2)	-500(2)	30(1)
C(4)	16299(1)	5791(2)	-1547(2)	30(1)
C(5)	16721(1)	6871(2)	-1837(2)	37(1)
C(6)	17522(1)	7174(2)	-1107(2)	36(1)
C(7)	15441(1)	5428(2)	-2362(2)	35(1)
C(8)	14582(1)	5618(2)	-1442(2)	31(1)
C(9)	14380(1)	6928(2)	-1123(2)	28(1)
C(10)	13428(1)	7113(2)	-545(2)	27(1)
C(11)	13162(1)	8426(2)	-443(2)	26(1)
C(12)	12212(1)	8621(1)	90(2)	24(1)
C(13)	11499(1)	7944(2)	-504(2)	28(1)
C(14)	10630(1)	8094(2)	28(2)	29(1)
C(15)	10452(1)	8917(1)	1171(2)	26(1)
C(16)	11146(1)	9633(2)	1735(2)	29(1)
C(17)	12011(1)	9476(1)	1189(2)	28(1)
N(1)	9560(1)	9069(1)	1715(2)	32(1)
O(21)	28910(1)	1044(1)	181(2)	37(1)
C(21)	28013(1)	1060(2)	-189(2)	29(1)
C(22)	27414(1)	219(2)	371(2)	31(1)
C(23)	26524(1)	257(2)	-101(2)	33(1)
C(24)	26206(1)	1121(2)	-1127(2)	29(1)
C(25)	26814(1)	1964(2)	-1646(2)	33(1)
C(26)	27703(1)	1945(2)	-1177(2)	33(1)
C(27)	25235(1)	1162(2)	-1624(2)	35(1)
C(28)	24639(1)	1813(2)	-486(2)	30(1)
C(29)	23683(1)	1956(2)	-1076(2)	33(1)
C(30)	23051(1)	2622(2)	-14(2)	28(1)
C(31)	22137(1)	2800(2)	-777(2)	44(1)
C(32)	21444(1)	3419(2)	188(2)	30(1)

C(33)	20646(1)	2855(2)	556(2)	31(1)
C(34)	20000(1)	3415(2)	1428(2)	29(1)
C(35)	20143(1)	4564(2)	1972(2)	26(1)
C(36)	20930(1)	5153(2)	1584(2)	29(1)
C(37)	21568(1)	4583(2)	715(2)	31(1)
N(21)	19474(1)	5186(2)	2814(2)	34(1)

Table 3. Bond lengths [\AA] and angles [$^\circ$] for **5a**.

		C(11)-C(12)	1.517(2)
		C(11)-H(11A)	0.9900
		C(11)-H(11B)	0.9900
O(1)-C(1)	1.375(2)	C(12)-C(17)	1.390(2)
O(1)-H(1)	0.85(3)	C(12)-C(13)	1.402(2)
C(1)-C(2)	1.391(2)	C(13)-C(14)	1.395(2)
C(1)-C(6)	1.392(3)	C(13)-H(13)	0.9500
C(2)-C(3)	1.386(3)	C(14)-C(15)	1.386(2)
C(2)-H(2)	0.9500	C(14)-H(14)	0.9500
C(3)-C(4)	1.396(3)	C(15)-C(16)	1.395(2)
C(3)-H(3)	0.9500	C(15)-N(1)	1.432(2)
C(4)-C(5)	1.392(3)	C(16)-C(17)	1.397(2)
C(4)-C(7)	1.512(3)	C(16)-H(16)	0.9500
C(5)-C(6)	1.388(3)	C(17)-H(17)	0.9500
C(5)-H(5)	0.9500	N(1)-H(1B)	0.92(3)
C(6)-H(6)	0.9500	N(1)-H(1A)	0.90(3)
C(7)-C(8)	1.539(3)	O(21)-C(21)	1.374(2)
C(7)-H(7A)	0.9900	O(21)-H(21)	0.89(3)
C(7)-H(7B)	0.9900	C(21)-C(26)	1.389(3)
C(8)-C(9)	1.529(2)	C(21)-C(22)	1.395(2)
C(8)-H(8A)	0.9900	C(22)-C(23)	1.388(3)
C(8)-H(8B)	0.9900	C(22)-H(22)	0.9500
C(9)-C(10)	1.530(2)	C(23)-C(24)	1.396(3)
C(9)-H(9A)	0.9900	C(23)-H(23)	0.9500
C(9)-H(9B)	0.9900	C(24)-C(25)	1.393(3)
C(10)-C(11)	1.532(2)	C(24)-C(27)	1.509(2)
C(10)-H(10A)	0.9900	C(25)-C(26)	1.385(3)
C(10)-H(10B)	0.9900	C(25)-H(25)	0.9500

C(26)-H(26)	0.9500	C(2)-C(3)-H(3)	119.0
C(27)-C(28)	1.527(2)	C(4)-C(3)-H(3)	119.0
C(27)-H(27A)	0.9900	C(5)-C(4)-C(3)	117.50(17)
C(27)-H(27B)	0.9900	C(5)-C(4)-C(7)	122.36(17)
C(28)-C(29)	1.520(2)	C(3)-C(4)-C(7)	120.11(17)
C(28)-H(28A)	0.9900	C(6)-C(5)-C(4)	121.47(17)
C(28)-H(28B)	0.9900	C(6)-C(5)-H(5)	119.3
C(29)-C(30)	1.527(2)	C(4)-C(5)-H(5)	119.3
C(29)-H(29A)	0.9900	C(5)-C(6)-C(1)	119.96(17)
C(29)-H(29B)	0.9900	C(5)-C(6)-H(6)	120.0
C(30)-C(31)	1.523(3)	C(1)-C(6)-H(6)	120.0
C(30)-H(30A)	0.9900	C(4)-C(7)-C(8)	115.39(15)
C(30)-H(30B)	0.9900	C(4)-C(7)-H(7A)	108.4
C(31)-C(32)	1.512(3)	C(8)-C(7)-H(7A)	108.4
C(31)-H(31A)	0.9900	C(4)-C(7)-H(7B)	108.4
C(31)-H(31B)	0.9900	C(8)-C(7)-H(7B)	108.4
C(32)-C(33)	1.392(3)	H(7A)-C(7)-H(7B)	107.5
C(32)-C(37)	1.397(3)	C(9)-C(8)-C(7)	113.38(15)
C(33)-C(34)	1.388(3)	C(9)-C(8)-H(8A)	108.9
C(33)-H(33)	0.9500	C(7)-C(8)-H(8A)	108.9
C(34)-C(35)	1.390(2)	C(9)-C(8)-H(8B)	108.9
C(34)-H(34)	0.9500	C(7)-C(8)-H(8B)	108.9
C(35)-C(36)	1.397(2)	H(8A)-C(8)-H(8B)	107.7
C(35)-N(21)	1.430(2)	C(8)-C(9)-C(10)	112.19(14)
C(36)-C(37)	1.383(3)	C(8)-C(9)-H(9A)	109.2
C(36)-H(36)	0.9500	C(10)-C(9)-H(9A)	109.2
C(37)-H(37)	0.9500	C(8)-C(9)-H(9B)	109.2
N(21)-H(21A)	0.90(3)	C(10)-C(9)-H(9B)	109.2
N(21)-H(21B)	0.86(3)	H(9A)-C(9)-H(9B)	107.9
		C(9)-C(10)-C(11)	113.20(14)
C(1)-O(1)-H(1)	111.9(19)	C(9)-C(10)-H(10A)	108.9
O(1)-C(1)-C(2)	122.08(16)	C(11)-C(10)-H(10A)	108.9
O(1)-C(1)-C(6)	118.31(17)	C(9)-C(10)-H(10B)	108.9
C(2)-C(1)-C(6)	119.58(17)	C(11)-C(10)-H(10B)	108.9
C(3)-C(2)-C(1)	119.57(16)	H(10A)-C(10)-H(10B)	107.8
C(3)-C(2)-H(2)	120.2	C(12)-C(11)-C(10)	113.73(13)
C(1)-C(2)-H(2)	120.2	C(12)-C(11)-H(11A)	108.8
C(2)-C(3)-C(4)	121.91(17)	C(10)-C(11)-H(11A)	108.8

C(12)-C(11)-H(11B)	108.8	C(26)-C(25)-H(25)	119.2
C(10)-C(11)-H(11B)	108.8	C(24)-C(25)-H(25)	119.2
H(11A)-C(11)-H(11B)	107.7	C(25)-C(26)-C(21)	120.14(17)
C(17)-C(12)-C(13)	117.18(16)	C(25)-C(26)-H(26)	119.9
C(17)-C(12)-C(11)	121.48(15)	C(21)-C(26)-H(26)	119.9
C(13)-C(12)-C(11)	121.34(15)	C(24)-C(27)-C(28)	113.48(15)
C(14)-C(13)-C(12)	121.29(16)	C(24)-C(27)-H(27A)	108.9
C(14)-C(13)-H(13)	119.4	C(28)-C(27)-H(27A)	108.9
C(12)-C(13)-H(13)	119.4	C(24)-C(27)-H(27B)	108.9
C(15)-C(14)-C(13)	120.51(15)	C(28)-C(27)-H(27B)	108.9
C(15)-C(14)-H(14)	119.7	H(27A)-C(27)-H(27B)	107.7
C(13)-C(14)-H(14)	119.7	C(29)-C(28)-C(27)	112.82(14)
C(14)-C(15)-C(16)	119.11(16)	C(29)-C(28)-H(28A)	109.0
C(14)-C(15)-N(1)	120.41(15)	C(27)-C(28)-H(28A)	109.0
C(16)-C(15)-N(1)	120.41(16)	C(29)-C(28)-H(28B)	109.0
C(15)-C(16)-C(17)	119.70(15)	C(27)-C(28)-H(28B)	109.0
C(15)-C(16)-H(16)	120.1	H(28A)-C(28)-H(28B)	107.8
C(17)-C(16)-H(16)	120.1	C(28)-C(29)-C(30)	115.87(14)
C(12)-C(17)-C(16)	122.09(15)	C(28)-C(29)-H(29A)	108.3
C(12)-C(17)-H(17)	119.0	C(30)-C(29)-H(29A)	108.3
C(16)-C(17)-H(17)	119.0	C(28)-C(29)-H(29B)	108.3
C(15)-N(1)-H(1B)	111.5(16)	C(30)-C(29)-H(29B)	108.3
C(15)-N(1)-H(1A)	113.1(17)	H(29A)-C(29)-H(29B)	107.4
H(1B)-N(1)-H(1A)	110(2)	C(31)-C(30)-C(29)	111.20(15)
C(21)-O(21)-H(21)	109.6(19)	C(31)-C(30)-H(30A)	109.4
O(21)-C(21)-C(26)	117.94(16)	C(29)-C(30)-H(30A)	109.4
O(21)-C(21)-C(22)	122.66(16)	C(31)-C(30)-H(30B)	109.4
C(26)-C(21)-C(22)	119.40(17)	C(29)-C(30)-H(30B)	109.4
C(23)-C(22)-C(21)	119.65(16)	H(30A)-C(30)-H(30B)	108.0
C(23)-C(22)-H(22)	120.2	C(32)-C(31)-C(30)	115.96(16)
C(21)-C(22)-H(22)	120.2	C(32)-C(31)-H(31A)	108.3
C(22)-C(23)-C(24)	121.68(17)	C(30)-C(31)-H(31A)	108.3
C(22)-C(23)-H(23)	119.2	C(32)-C(31)-H(31B)	108.3
C(24)-C(23)-H(23)	119.2	C(30)-C(31)-H(31B)	108.3
C(25)-C(24)-C(23)	117.51(17)	H(31A)-C(31)-H(31B)	107.4
C(25)-C(24)-C(27)	121.14(17)	C(33)-C(32)-C(37)	117.40(17)
C(23)-C(24)-C(27)	121.33(17)	C(33)-C(32)-C(31)	121.04(18)
C(26)-C(25)-C(24)	121.57(17)	C(37)-C(32)-C(31)	121.55(19)

C(34)-C(33)-C(32)	121.72(17)	C(35)-C(36)-H(36)	119.9
C(34)-C(33)-H(33)	119.1	C(36)-C(37)-C(32)	121.57(17)
C(32)-C(33)-H(33)	119.1	C(36)-C(37)-H(37)	119.2
C(33)-C(34)-C(35)	120.14(17)	C(32)-C(37)-H(37)	119.2
C(33)-C(34)-H(34)	119.9	C(35)-N(21)-H(21A)	111.1(16)
C(35)-C(34)-H(34)	119.9	C(35)-N(21)-H(21B)	105.0(18)
C(34)-C(35)-C(36)	118.89(16)	H(21A)-N(21)-H(21B)	110(2)
C(34)-C(35)-N(21)	121.56(16)	<hr/>	
C(36)-C(35)-N(21)	119.37(16)	Symmetry transformations used to	
C(37)-C(36)-C(35)	120.24(16)	generate equivalent atoms:	
C(37)-C(36)-H(36)	119.9		

Table 4. Anisotropic displacement parameters ($\text{\AA}^2 \times 10^3$) for **5a**. The anisotropic displacement factor exponent takes the form: $-2\pi^2 [h^2 a^{*2} U^{11} + \dots + 2 h k a^* b^* U^{12}]$

	U ¹¹	U ²²	U ³³	U ²³	U ¹³	U ¹²
O(1)	24(1)	36(1)	52(1)	-1(1)	-1(1)	-3(1)
C(1)	22(1)	31(1)	36(1)	-6(1)	6(1)	4(1)
C(2)	24(1)	32(1)	32(1)	3(1)	4(1)	4(1)
C(3)	25(1)	32(1)	33(1)	-1(1)	6(1)	0(1)
C(4)	26(1)	37(1)	27(1)	-6(1)	3(1)	5(1)
C(5)	41(1)	32(1)	36(1)	0(1)	0(1)	9(1)
C(6)	35(1)	28(1)	44(1)	1(1)	5(1)	0(1)
C(7)	31(1)	41(1)	33(1)	-8(1)	-3(1)	7(1)
C(8)	27(1)	36(1)	31(1)	-1(1)	-4(1)	3(1)
C(9)	24(1)	33(1)	27(1)	3(1)	0(1)	3(1)
C(10)	23(1)	31(1)	26(1)	2(1)	0(1)	1(1)
C(11)	23(1)	30(1)	26(1)	2(1)	-1(1)	-1(1)
C(12)	23(1)	25(1)	24(1)	3(1)	-3(1)	0(1)
C(13)	27(1)	28(1)	28(1)	-4(1)	-2(1)	-1(1)
C(14)	23(1)	30(1)	34(1)	-3(1)	-4(1)	-4(1)
C(15)	22(1)	26(1)	30(1)	5(1)	-1(1)	2(1)
C(16)	28(1)	25(1)	33(1)	-6(1)	-5(1)	4(1)
C(17)	23(1)	25(1)	34(1)	-1(1)	-7(1)	-1(1)
N(1)	23(1)	34(1)	40(1)	-3(1)	1(1)	2(1)
O(21)	22(1)	33(1)	56(1)	6(1)	0(1)	-3(1)
C(21)	22(1)	27(1)	38(1)	-3(1)	4(1)	2(1)
C(22)	24(1)	29(1)	40(1)	6(1)	0(1)	2(1)
C(23)	24(1)	35(1)	40(1)	4(1)	3(1)	-2(1)
C(24)	24(1)	34(1)	30(1)	-6(1)	2(1)	8(1)
C(25)	35(1)	30(1)	34(1)	3(1)	5(1)	9(1)
C(26)	32(1)	25(1)	44(1)	4(1)	9(1)	1(1)
C(27)	28(1)	47(1)	31(1)	-8(1)	-2(1)	9(1)
C(28)	23(1)	38(1)	29(1)	-4(1)	-2(1)	7(1)
C(29)	27(1)	42(1)	29(1)	-5(1)	-5(1)	10(1)
C(30)	23(1)	34(1)	29(1)	-1(1)	-3(1)	5(1)
C(31)	31(1)	64(1)	36(1)	-14(1)	-10(1)	19(1)
C(32)	25(1)	40(1)	26(1)	-5(1)	-6(1)	8(1)
C(33)	31(1)	26(1)	35(1)	-2(1)	-11(1)	3(1)

C(34)	25(1)	32(1)	29(1)	5(1)	-3(1)	-5(1)
C(35)	22(1)	34(1)	21(1)	2(1)	-1(1)	-1(1)
C(36)	27(1)	29(1)	30(1)	-3(1)	-2(1)	-4(1)
C(37)	21(1)	39(1)	34(1)	0(1)	1(1)	-5(1)
N(21)	27(1)	47(1)	28(1)	-6(1)	5(1)	-3(1)

Table 5. Hydrogen coordinates ($\times 10^4$) and isotropic displacement parameters ($\text{\AA}^2 \times 10^3$) for **5a**.

	x	y	z	U(eq)
H(1)	18880(19)	6220(20)	1320(30)	59(8)
H(2)	17769	4775	978	35
H(3)	16444	4270	-299	36
H(5)	16456	7411	-2551	44
H(6)	17801	7912	-1330	43
H(7A)	15484	4574	-2634	42
H(7B)	15388	5882	-3336	42
H(8A)	14072	5265	-2022	37
H(8B)	14639	5190	-449	37
H(9A)	14459	7392	-2080	34
H(9B)	14811	7232	-343	34
H(10A)	13378	6746	486	32
H(10B)	13004	6698	-1248	32
H(11A)	13578	8835	280	31
H(11B)	13229	8797	-1469	31
H(13)	11609	7371	-1283	33
H(14)	10157	7628	-398	35
H(16)	11029	10224	2487	35
H(17)	12478	9970	1581	33
H(1B)	9215(18)	8400(20)	1530(30)	51(7)
H(1A)	9542(17)	9270(20)	2720(30)	44(6)
H(21)	29030(19)	430(20)	790(30)	56(8)
H(22)	27615	-377	1072	37
H(23)	26120	-320	284	39

H(25)	26614	2565	-2339	40
H(26)	28102	2540	-1531	40
H(27A)	25012	338	-1753	42
H(27B)	25187	1562	-2638	42
H(28A)	24635	1366	496	36
H(28B)	24895	2610	-274	36
H(29A)	23432	1154	-1274	39
H(29B)	23697	2380	-2074	39
H(30A)	22982	2166	952	34
H(30B)	23312	3406	252	34
H(31A)	22218	3268	-1731	53
H(31B)	21900	2011	-1082	53
H(33)	20542	2067	201	37
H(34)	19459	3012	1653	35
H(36)	21027	5948	1917	35
H(37)	22103	4992	471	38
H(21A)	19722(17)	5620(20)	3580(30)	45(6)
H(21B)	19140(20)	4640(20)	3190(30)	55(8)

6_x) 2,4,6-tris-(4-chlorophenoxy)-1,3,5-triazene and tribromobenzene

Synthesis: J. Ramakoteswara Rao, University of Hyderabad, India.

Table 1. Crystal data and structure refinement for **6_x**.

Identification code	6_x	
Empirical formula	C ₂₇ H ₁₅ Br ₃ Cl ₃ N ₃ O ₃	
Formula weight	775.50	
Temperature	150(2) K	
Wavelength	0.71073 Å	
Crystal system	Hexagonal	
Space group	P6(3)	
Unit cell dimensions	a = 15.250(2) Å	α = 90°.
	b = 15.250(2) Å	β = 90°.
	c = 6.8149(14) Å	γ = 120°.
Volume	1372.6(4) Å ³	
Z	2	
Density (calculated)	1.876 Mg/m ³	
Absorption coefficient	4.737 mm ⁻¹	
F(000)	756	
Crystal size	0.35 x 0.27 x 0.27 mm ³	
Theta range for data collection	1.54 to 30.45°.	
Index ranges	-20 ≤ h ≤ 20, -21 ≤ k ≤ 21, -9 ≤ l ≤ 9	
Reflections collected	17004	
Independent reflections	2568 [R(int) = 0.0301]	
Completeness to theta = 30.45°	94.1 %	
Absorption correction	Multiscan	
Max. and min. transmission	0.379004 and 0.298932	
Refinement method	Full-matrix least-squares on F ²	
Data / restraints / parameters	2568 / 1 / 122	
Goodness-of-fit on F ²	1.037	
Final R indices [I > 2σ(I)]	R1 = 0.0267, wR2 = 0.0623	
R indices (all data)	R1 = 0.0328, wR2 = 0.0642	
Absolute structure parameter	0.015(8)	
Extinction coefficient	not refined	
Largest diff. peak and hole	0.400 and -0.899 e.Å ⁻³	

Table 2. Atomic coordinates ($\times 10^4$) and equivalent isotropic displacement parameters ($\text{\AA}^2 \times 10^3$) for **6x**. $U(\text{eq})$ is defined as one third of the trace of the orthogonalized U^{ij} tensor.

	x	y	z	$U(\text{eq})$
Cl(1)	2825(1)	5176(1)	6511(1)	26(1)
C(1)	3389(1)	4420(1)	6510(4)	20(1)
C(2)	3961(2)	4458(2)	8120(3)	22(1)
C(3)	4430(2)	3869(2)	8123(3)	22(1)
C(4)	4299(1)	3262(1)	6503(4)	18(1)
C(5)	3720(1)	3215(1)	4900(4)	22(1)
C(6)	3256(1)	3808(1)	4893(4)	23(1)
O(1)	4704(1)	2604(1)	6491(2)	19(1)
C(7)	5716(1)	3010(1)	6516(3)	17(1)
N(1)	5996(1)	2304(1)	6523(3)	18(1)
Br(1)	7809(1)	9894(1)	10068(1)	47(1)
C(8)	9085(2)	9957(2)	10167(5)	29(1)
C(9)	9956(2)	10900(2)	10164(5)	29(1)

Table 3. Bond lengths [\AA] and angles [$^\circ$] for **6x**.

Cl(1)-C(1)	1.7501(18)	C(4)-C(5)-C(6)	119.0(2)
C(1)-C(2)	1.385(3)	C(4)-C(5)-H(5)	120.5
C(1)-C(6)	1.392(3)	C(6)-C(5)-H(5)	120.5
C(2)-C(3)	1.399(3)	C(1)-C(6)-C(5)	118.7(2)
C(2)-H(2)	0.9300	C(1)-C(6)-H(6)	120.7
C(3)-C(4)	1.390(3)	C(5)-C(6)-H(6)	120.7
C(3)-H(3)	0.9300	C(7)-O(1)-C(4)	118.67(13)
C(4)-C(5)	1.384(3)	N(1)#1-C(7)-N(1)	127.70(16)
C(4)-O(1)	1.416(2)	N(1)#1-C(7)-O(1)	119.79(15)
C(5)-C(6)	1.399(3)	N(1)-C(7)-O(1)	112.50(14)
C(5)-H(5)	0.9300	C(7)#2-N(1)-C(7)	112.29(16)
C(6)-H(6)	0.9300	C(9)#3-C(8)-C(9)	123.1(2)
O(1)-C(7)	1.346(2)	C(9)#3-C(8)-Br(1)	118.31(16)
C(7)-N(1)#1	1.320(2)	C(9)-C(8)-Br(1)	118.55(16)
C(7)-N(1)	1.343(2)	C(8)#4-C(9)-C(8)	116.9(2)
N(1)-C(7)#2	1.320(2)	C(8)#4-C(9)-H(9)	121.5
Br(1)-C(8)	1.901(2)	C(8)-C(9)-H(9)	121.5
C(8)-C(9)#3	1.386(3)	Symmetry transformations used to generate equivalent atoms: #1 -x+y+1,-x+1,z #2 -y+1,x-y,z #3 -y+2,x-y+1,z #4 -x+y+1,-x+2,z	
C(8)-C(9)	1.387(3)		
C(9)-C(8)#4	1.386(3)		
C(9)-H(9)	0.9300		
C(2)-C(1)-C(6)	122.22(17)		
C(2)-C(1)-Cl(1)	118.61(17)		
C(6)-C(1)-Cl(1)	119.17(16)		
C(1)-C(2)-C(3)	119.16(19)		
C(1)-C(2)-H(2)	120.4		
C(3)-C(2)-H(2)	120.4		
C(4)-C(3)-C(2)	118.50(19)		
C(4)-C(3)-H(3)	120.8		
C(2)-C(3)-H(3)	120.8		
C(5)-C(4)-C(3)	122.45(17)		
C(5)-C(4)-O(1)	116.85(18)		
C(3)-C(4)-O(1)	120.56(19)		

Table 4. Anisotropic displacement parameters ($\text{\AA}^2 \times 10^3$) for **6x**. The anisotropic displacement factor exponent takes the form: $-2\pi^2 [h^2 a^{*2} U^{11} + \dots + 2 h k a^* b^* U^{12}]$

	U11	U22	U33	U23	U13	U12
Cl(1)	28(1)	26(1)	31(1)	0(1)	0(1)	19(1)
C(1)	17(1)	18(1)	27(1)	2(1)	2(1)	10(1)
C(2)	22(1)	21(1)	24(1)	-3(1)	-1(1)	10(1)
C(3)	19(1)	23(1)	24(1)	0(1)	-3(1)	11(1)
C(4)	13(1)	15(1)	25(1)	1(1)	3(1)	6(1)
C(5)	22(1)	20(1)	24(1)	-3(1)	-2(1)	12(1)
C(6)	22(1)	26(1)	26(1)	0(1)	-3(1)	15(1)
O(1)	14(1)	16(1)	29(1)	-1(1)	-2(1)	8(1)
C(7)	15(1)	18(1)	16(1)	0(1)	-1(1)	7(1)
N(1)	16(1)	16(1)	21(1)	0(1)	1(1)	8(1)
Br(1)	37(1)	72(1)	42(1)	-1(1)	0(1)	35(1)
C(8)	29(1)	40(1)	20(1)	0(1)	1(1)	19(1)
C(9)	40(1)	32(1)	18(1)	0(1)	1(1)	19(1)

Table 5. Hydrogen coordinates ($\times 10^4$) and isotropic displacement parameters ($\text{\AA}^2 \times 10^3$) for **6x**.

	x	y	z	U(eq)
H(2)	4033	4869	9186	30(7)
H(3)	4820	3884	9185	24(6)
H(5)	3641	2796	3842	26
H(6)	2866	3793	3830	23(6)
H(9)	9927	11495	10160	47(8)

6_N) 2,4,6-tris-(4-chlorophenoxy)-1,3,5-triazene and tribromobenzene

Synthesis: J. Ramakoteswara Rao, University of Hyderabad, India.

Table 1. Crystal data and structure refinement for 6_N.

Identification code	6_N	
Empirical formula	C ₂₇ H ₁₅ Br ₃ Cl ₃ N ₃ O ₃	
Formula weight	771.00	
Temperature	100(5) K	
Wavelength	0.5-5.0 Å	
Crystal system	Hexagonal	
Space group	P6(3)	
Unit cell dimensions	a = 15.166(6) Å	α = 90°.
	b = 15.166(6) Å	β = 90°.
	c = 6.743(2) Å	γ = 120°.
Volume	1343(1) Å ³	
Z	2	
Density (calculated)	1.906 Mg/m ³	
Absorption coefficient	1.080, at 1 Angstrom mm ⁻¹	
F(000)	43.57	
Crystal size	6.0 x 1.5 x 1.0 mm ³	
Theta range for data collection	1.42 to 16.92°.	
Index ranges	0 ≤ h ≤ 30, 0 ≤ k ≤ 30, 0 ≤ l ≤ 15	
Reflections collected	30681	
Independent reflections	3102 [R(int) = 0.071]	
Completeness to theta = 16.92°	49.9 %	
Absorption correction	Empirical	
Max. and min. transmission	0.91 and 0.30	
Refinement method	Full-matrix least-squares on F ²	
Data / restraints / parameters	3102 / 1 / 163	
Goodness-of-fit on F ²	1.230	
Final R indices [I > 2σ(I)]	R1 = 0.0834, wR2 = 0.2121	
R indices (all data)	R1 = 0.0834, wR2 = 0.2121	
Extinction coefficient	0.560	
Largest diff. peak and hole	3.229 and -3.980 e.Å ⁻³	

Table 2. Atomic coordinates ($\times 10^4$) and equivalent isotropic displacement parameters ($\text{\AA}^2 \times 10^3$) for **6_N**. $U(\text{eq})$ is defined as one third of the trace of the orthogonalized U^{ij} tensor.

	x	y	z	$U(\text{eq})$
Cl(1)	7182(1)	4823(1)	3485(4)	13(1)
C(1)	6620(2)	5579(2)	3485(6)	11(1)
C(2)	6032(2)	5536(2)	1864(4)	12(1)
C(3)	5574(2)	6132(2)	1865(4)	12(1)
C(4)	5703(1)	6746(2)	3491(5)	9(1)
C(5)	6292(2)	6793(2)	5107(4)	11(1)
C(6)	6756(2)	6198(2)	5114(4)	12(1)
O(1)	5298(2)	7398(2)	3508(7)	10(1)
C(7)	4289(1)	6995(2)	3479(5)	8(1)
N(1)	4004(1)	7698(1)	3469(4)	9(1)
Br(1)	2209(3)	124(4)	-57(7)	25(1)
C(8)	928(3)	49(3)	-148(4)	16(1)
C(9)	52(3)	-898(3)	-150(5)	17(1)

Table 3. Bond lengths [\AA] and angles [$^\circ$] for **6N**.

Cl(1)-C(1)	1.737(2)	C(4)-C(5)-C(6)	119.3(2)
C(1)-C(2)	1.392(4)	C(4)-C(5)-H(5)	119.4(5)
C(1)-C(6)	1.392(4)	C(6)-C(5)-H(5)	121.3(5)
C(2)-C(3)	1.388(3)	C(1)-C(6)-C(5)	118.8(2)
C(2)-H(2)	1.080(8)	C(1)-C(6)-H(6)	119.6(5)
C(3)-C(4)	1.388(4)	C(5)-C(6)-H(6)	121.6(6)
C(3)-H(3)	1.083(8)	C(7)-O(1)-C(4)	119.0(2)
C(4)-C(5)	1.388(4)	N(1)#1-C(7)-O(1)	119.64(19)
C(4)-O(1)	1.400(3)	N(1)#1-C(7)-N(1)	127.38(17)
C(5)-C(6)	1.395(3)	O(1)-C(7)-N(1)	112.98(18)
C(5)-H(5)	1.089(8)	C(7)#2-N(1)-C(7)	112.61(17)
C(6)-H(6)	1.085(9)	C(9)-C(8)-C(9)#3	122.3(3)
O(1)-C(7)	1.334(3)	C(9)-C(8)-Br(1)	119.1(3)
C(7)-N(1)#1	1.320(2)	C(9)#3-C(8)-Br(1)	118.6(3)
C(7)-N(1)	1.335(2)	C(8)-C(9)-C(8)#4	117.7(3)
N(1)-C(7)#2	1.320(2)	C(8)-C(9)-H(9)	121.1(7)
Br(1)-C(8)	1.890(5)	C(8)#4-C(9)-H(9)	121.2(7)
C(8)-C(9)	1.386(5)	Symmetry transformations used to generate equivalent atoms: #1 -x+y,-x+1,z #2 -y+1,x-y+1,z #3 -y,x-y,z #4 -x+y,-x,z	
C(8)-C(9)#3	1.389(5)		
C(9)-C(8)#4	1.389(5)		
C(9)-H(9)	1.083(9)		
C(2)-C(1)-C(6)	121.8(2)		
C(2)-C(1)-Cl(1)	118.9(2)		
C(6)-C(1)-Cl(1)	119.3(2)		
C(3)-C(2)-C(1)	119.1(2)		
C(3)-C(2)-H(2)	121.0(6)		
C(1)-C(2)-H(2)	119.8(6)		
C(4)-C(3)-C(2)	119.3(3)		
C(4)-C(3)-H(3)	120.0(5)		
C(2)-C(3)-H(3)	120.7(6)		
C(3)-C(4)-C(5)	121.7(2)		
C(3)-C(4)-O(1)	121.1(3)		
C(5)-C(4)-O(1)	117.1(3)		

Table 4. Anisotropic displacement parameters ($\text{\AA}^2 \times 10^3$) for **6_N**. The anisotropic displacement factor exponent takes the form: $-2\pi^2 [h^2 a^{*2} U^{11} + \dots + 2 h k a^* b^* U^{12}]$

	U11	U22	U33	U23	U13	U12
Cl(1)	15(1)	13(1)	15(1)	0(1)	0(1)	10(1)
C(1)	10(1)	12(1)	12(1)	-1(1)	0(1)	7(1)
C(2)	12(1)	12(1)	13(1)	-4(1)	-2(1)	7(1)
C(3)	11(1)	12(1)	13(1)	-2(1)	-3(1)	7(1)
C(4)	7(1)	8(1)	12(1)	0(1)	1(1)	4(1)
C(5)	12(1)	13(1)	11(1)	-3(1)	-3(1)	8(1)
C(6)	15(1)	15(1)	11(1)	-3(1)	-4(1)	11(1)
O(1)	6(1)	9(1)	16(1)	-1(1)	-1(1)	3(1)
C(7)	7(1)	8(1)	10(1)	0(1)	0(1)	4(1)
N(1)	8(1)	8(1)	13(1)	-1(1)	0(1)	4(1)
Br(1)	21(1)	40(2)	22(1)	-1(2)	-1(1)	21(1)
C(8)	19(1)	23(1)	9(1)	1(1)	0(1)	13(1)
C(9)	21(1)	19(1)	11(1)	0(1)	0(1)	11(1)
H(2)	34(3)	33(3)	26(3)	-15(3)	-7(3)	21(3)
H(3)	37(4)	43(4)	23(3)	-8(3)	-13(3)	27(4)
H(6)	34(4)	41(4)	25(3)	-6(3)	-11(3)	26(3)
H(5)	40(4)	35(4)	23(3)	-12(3)	-11(3)	26(3)
H(9)	41(4)	32(4)	44(5)	-2(4)	-1(4)	25(4)

Table 5. Hydrogen coordinates ($\times 10^4$) and isotropic displacement parameters ($\text{\AA}^2 \times 10^3$) for **6_N**.

	x	y	z	U(eq)
H(2)	5946(7)	5050(7)	621(14)	29(2)
H(3)	5116(8)	6117(8)	620(14)	31(2)
H(6)	7213(8)	6203(8)	6358(14)	30(2)
H(5)	6375(8)	7286(8)	6353(14)	30(2)
H(9)	92(9)	-1591(8)	-160(20)	36(2)

7_x) Triphenylisocyanurate, trinitrobenzene and benzene

Synthesis: Praveen K. Thallapally, University of Hyderabad, India.

Table 1. Crystal data and structure refinement for 7_x.

Identification code	7 _x	
Empirical formula	C30 H21 N6 O9	
Formula weight	609.53	
Temperature	100(2) K	
Wavelength	0.71073 Å	
Crystal system	Triclinic	
Space group	P-1	
Unit cell dimensions	a = 11.3825(3) Å	α = 69.866(1)°.
	b = 11.5495(3) Å	β = 63.497(1)°.
	c = 12.5513(3) Å	γ = 86.397(1)°.
Volume	1378.27(6) Å ³	
Z	2	
Density (calculated)	1.469 Mg/m ³	
Absorption coefficient	0.111 mm ⁻¹	
F(000)	630	
Crystal size	1.2 x 0.6 x 0.25 mm ³	
Theta range for data collection	1.89 to 30.33°.	
Index ranges	-15<=h<=16, -16<=k<=13, -17<=l<=17	
Reflections collected	11166	
Independent reflections	7227 [R(int) = 0.0327]	
Completeness to theta = 30.33°	87.1 %	
Absorption correction	None	
Refinement method	Full-matrix least-squares on F ²	
Data / restraints / parameters	7227 / 0 / 406	
Goodness-of-fit on F ²	1.034	
Final R indices [I>2sigma(I)]	R1 = 0.0392, wR2 = 0.1001	
R indices (all data)	R1 = 0.0460, wR2 = 0.1066	
Extinction coefficient	not refined	
Largest diff. peak and hole	0.355 and -0.258 e.Å ⁻³	

Table 2. Atomic coordinates ($\times 10^4$) and equivalent isotropic displacement parameters ($\text{\AA}^2 \times 10^3$) for $7_{\mathbf{x}}$. $U(\text{eq})$ is defined as one third of the trace of the orthogonalized U_{ij} tensor.

	x	y	z	$U(\text{eq})$
O(10)	6615(1)	2112(1)	4176(1)	23(1)
C(10)	6872(1)	2036(1)	5036(1)	18(1)
N(10)	8160(1)	2109(1)	4869(1)	18(1)
C(11)	9194(1)	2261(1)	3598(1)	19(1)
C(12)	9528(1)	3431(1)	2664(1)	25(1)
C(13)	10424(1)	3563(1)	1413(1)	30(1)
C(14)	10974(1)	2536(1)	1127(1)	31(1)
C(15)	10656(1)	1377(1)	2088(1)	29(1)
C(16)	9758(1)	1228(1)	3338(1)	23(1)
O(20)	9638(1)	1874(1)	5679(1)	23(1)
C(20)	8509(1)	1947(1)	5837(1)	18(1)
N(20)	7460(1)	1902(1)	6998(1)	19(1)
C(21)	7766(1)	1817(1)	8029(1)	19(1)
C(22)	8569(1)	2780(1)	7880(1)	22(1)
C(23)	8861(1)	2688(1)	8871(1)	26(1)
C(24)	8364(1)	1653(1)	9982(1)	28(1)
C(25)	7549(1)	702(1)	10122(1)	27(1)
C(26)	7240(1)	783(1)	9142(1)	23(1)
O(30)	5253(1)	1820(1)	8286(1)	27(1)
C(30)	6130(1)	1857(1)	7268(1)	20(1)
N(30)	5888(1)	1855(1)	6267(1)	18(1)
C(31)	4527(1)	1668(1)	6520(1)	18(1)
C(32)	3637(1)	2476(1)	6956(1)	24(1)
C(33)	2320(1)	2263(1)	7236(1)	26(1)
C(34)	1901(1)	1259(1)	7070(1)	25(1)
C(35)	2803(1)	458(1)	6629(1)	23(1)
C(36)	4118(1)	658(1)	6357(1)	20(1)
N(1)	2425(1)	4552(1)	4782(1)	35(1)
O(1)	1253(1)	4302(1)	5155(1)	52(1)
O(2)	2892(1)	5321(1)	5009(1)	48(1)
C(1)	3366(1)	3891(1)	3993(1)	25(1)
C(2)	2888(1)	2873(1)	3896(1)	24(1)

N(2)	3391(1)	1238(1)	2960(1)	23(1)
O(3)	2318(1)	663(1)	3784(1)	32(1)
O(4)	4134(1)	958(1)	2038(1)	31(1)
C(3)	3828(1)	2328(1)	3100(1)	20(1)
C(4)	5162(1)	2754(1)	2413(1)	19(1)
N(3)	6966(1)	4257(1)	1868(1)	21(1)
O(5)	7720(1)	3745(1)	1159(1)	26(1)
O(6)	7292(1)	5164(1)	2013(1)	30(1)
C(5)	5558(1)	3764(1)	2578(1)	20(1)
C(6)	4689(1)	4344(1)	3366(1)	25(1)
C(1X)	6363(1)	5075(1)	-713(1)	27(1)
C(2X)	5553(1)	4108(1)	-543(1)	28(1)
C(3X)	4188(1)	4034(1)	169(1)	27(1)

Table 3. Bond lengths [\AA] and angles [$^\circ$] for **7_x**.

O(10)-C(10)	1.2132(14)	C(1)-C(2)	1.3894(17)
C(10)-N(10)	1.3886(14)	C(2)-C(3)	1.3902(16)
C(10)-N(30)	1.3953(13)	N(2)-O(3)	1.2263(13)
N(10)-C(20)	1.3904(14)	N(2)-O(4)	1.2286(14)
N(10)-C(11)	1.4552(13)	N(2)-C(3)	1.4741(15)
C(11)-C(12)	1.3861(16)	C(3)-C(4)	1.3877(15)
C(11)-C(16)	1.3873(16)	C(4)-C(5)	1.3853(16)
C(12)-C(13)	1.3973(17)	N(3)-O(5)	1.2227(13)
C(13)-C(14)	1.388(2)	N(3)-O(6)	1.2291(13)
C(14)-C(15)	1.392(2)	N(3)-C(5)	1.4759(14)
C(15)-C(16)	1.3931(16)	C(5)-C(6)	1.3807(16)
O(20)-C(20)	1.2123(13)	C(1X)-C(2X)	1.3893(19)
C(20)-N(20)	1.3986(13)	C(1X)-C(3X)#1	1.3938(19)
N(20)-C(30)	1.3960(14)	C(2X)-C(3X)	1.3939(18)
N(20)-C(21)	1.4548(14)	C(3X)-C(1X)#1	1.3938(19)
C(21)-C(26)	1.3894(16)	O(10)-C(10)-N(10)	122.46(10)
C(21)-C(22)	1.3920(16)	O(10)-C(10)-N(30)	122.02(10)
C(22)-C(23)	1.3942(16)	N(10)-C(10)-N(30)	115.51(9)
C(23)-C(24)	1.3877(19)	C(10)-N(10)-C(20)	124.79(9)
C(24)-C(25)	1.3963(19)	C(10)-N(10)-C(11)	115.98(9)
C(25)-C(26)	1.3942(17)	C(20)-N(10)-C(11)	119.01(9)
O(30)-C(30)	1.2075(14)	C(12)-C(11)-C(16)	122.03(10)
C(30)-N(30)	1.4025(14)	C(12)-C(11)-N(10)	118.41(10)
N(30)-C(31)	1.4508(13)	C(16)-C(11)-N(10)	119.45(10)
C(31)-C(32)	1.3908(15)	C(11)-C(12)-C(13)	118.82(12)
C(31)-C(36)	1.3915(15)	C(14)-C(13)-C(12)	120.01(12)
C(32)-C(33)	1.3951(16)	C(13)-C(14)-C(15)	120.17(11)
C(33)-C(34)	1.3927(18)	C(14)-C(15)-C(16)	120.47(12)
C(34)-C(35)	1.3933(17)	C(11)-C(16)-C(15)	118.45(11)
C(35)-C(36)	1.3940(15)	O(20)-C(20)-N(10)	122.58(10)
N(1)-O(1)	1.2172(17)	O(20)-C(20)-N(20)	122.64(10)
N(1)-O(2)	1.2332(17)	N(10)-C(20)-N(20)	114.77(9)
N(1)-C(1)	1.4773(15)	C(30)-N(20)-C(20)	124.85(9)
C(1)-C(6)	1.3853(17)	C(30)-N(20)-C(21)	117.27(9)
		C(20)-N(20)-C(21)	117.75(9)
		C(26)-C(21)-C(22)	121.64(10)

C(26)-C(21)-N(20)	119.24(10)	C(6)-C(5)-C(4)	122.94(11)
C(22)-C(21)-N(20)	119.12(10)	C(6)-C(5)-N(3)	118.21(10)
C(21)-C(22)-C(23)	118.73(11)	C(4)-C(5)-N(3)	118.84(10)
C(24)-C(23)-C(22)	120.50(11)	C(5)-C(6)-C(1)	117.26(11)
C(23)-C(24)-C(25)	120.05(11)	C(2X)-C(1X)-C(3X)#1	120.02(11)
C(26)-C(25)-C(24)	120.15(12)	C(1X)-C(2X)-C(3X)	119.99(12)
C(21)-C(26)-C(25)	118.93(11)	C(1X)#1-C(3X)-C(2X)	119.99(12)
O(30)-C(30)-N(20)	122.75(10)		
O(30)-C(30)-N(30)	122.44(10)	Symmetry transformations used to generate equivalent atoms:	
N(20)-C(30)-N(30)	114.81(9)		
C(10)-N(30)-C(30)	124.23(9)	#1 -x+1,-y+1,-z	
C(10)-N(30)-C(31)	117.75(9)		
C(30)-N(30)-C(31)	118.02(9)		
C(32)-C(31)-C(36)	120.70(10)		
C(32)-C(31)-N(30)	119.84(10)		
C(36)-C(31)-N(30)	119.43(10)		
C(31)-C(32)-C(33)	119.31(11)		
C(34)-C(33)-C(32)	120.50(11)		
C(33)-C(34)-C(35)	119.65(11)		
C(34)-C(35)-C(36)	120.24(11)		
C(31)-C(36)-C(35)	119.59(10)		
O(1)-N(1)-O(2)	124.93(12)		
O(1)-N(1)-C(1)	117.84(12)		
O(2)-N(1)-C(1)	117.23(12)		
C(6)-C(1)-C(2)	123.54(11)		
C(6)-C(1)-N(1)	117.38(11)		
C(2)-C(1)-N(1)	119.07(11)		
C(1)-C(2)-C(3)	115.64(10)		
O(3)-N(2)-O(4)	124.59(11)		
O(3)-N(2)-C(3)	117.58(10)		
O(4)-N(2)-C(3)	117.82(10)		
C(4)-C(3)-C(2)	124.00(11)		
C(4)-C(3)-N(2)	117.47(10)		
C(2)-C(3)-N(2)	118.53(10)		
C(5)-C(4)-C(3)	116.58(10)		
O(5)-N(3)-O(6)	124.71(10)		
O(5)-N(3)-C(5)	117.48(9)		
O(6)-N(3)-C(5)	117.80(10)		

Table 4. Anisotropic displacement parameters ($\text{\AA}^2 \times 10^3$) for $7\mathbf{x}$. The anisotropic displacement factor exponent takes the form: $-2\pi^2 [h^2 a^{*2} U^{11} + \dots + 2 h k a^* b^* U^{12}]$

	U ¹¹	U ²²	U ³³	U ²³	U ¹³	U ¹²
O(10)	20(1)	30(1)	19(1)	-8(1)	-9(1)	3(1)
C(10)	16(1)	18(1)	18(1)	-6(1)	-6(1)	2(1)
N(10)	14(1)	20(1)	16(1)	-7(1)	-5(1)	2(1)
C(11)	14(1)	25(1)	17(1)	-9(1)	-6(1)	0(1)
C(12)	21(1)	26(1)	23(1)	-6(1)	-7(1)	0(1)
C(13)	23(1)	37(1)	21(1)	-2(1)	-7(1)	-6(1)
C(14)	19(1)	50(1)	20(1)	-14(1)	-3(1)	-5(1)
C(15)	20(1)	39(1)	29(1)	-20(1)	-6(1)	3(1)
C(16)	19(1)	25(1)	24(1)	-11(1)	-7(1)	2(1)
O(20)	16(1)	32(1)	23(1)	-13(1)	-8(1)	3(1)
C(20)	17(1)	18(1)	19(1)	-8(1)	-7(1)	1(1)
N(20)	16(1)	24(1)	18(1)	-10(1)	-7(1)	2(1)
C(21)	16(1)	25(1)	19(1)	-13(1)	-7(1)	4(1)
C(22)	18(1)	26(1)	23(1)	-13(1)	-7(1)	3(1)
C(23)	20(1)	34(1)	30(1)	-20(1)	-11(1)	4(1)
C(24)	28(1)	39(1)	26(1)	-20(1)	-15(1)	9(1)
C(25)	29(1)	31(1)	20(1)	-10(1)	-10(1)	5(1)
C(26)	22(1)	25(1)	22(1)	-12(1)	-8(1)	2(1)
O(30)	18(1)	41(1)	24(1)	-19(1)	-7(1)	4(1)
C(30)	17(1)	23(1)	21(1)	-10(1)	-7(1)	1(1)
N(30)	13(1)	23(1)	19(1)	-9(1)	-6(1)	1(1)
C(31)	14(1)	21(1)	18(1)	-6(1)	-6(1)	1(1)
C(32)	18(1)	22(1)	30(1)	-11(1)	-8(1)	2(1)
C(33)	17(1)	28(1)	31(1)	-12(1)	-9(1)	5(1)
C(34)	17(1)	32(1)	25(1)	-8(1)	-10(1)	0(1)
C(35)	23(1)	27(1)	23(1)	-9(1)	-11(1)	-2(1)
C(36)	20(1)	23(1)	19(1)	-9(1)	-9(1)	3(1)
N(1)	32(1)	21(1)	31(1)	-8(1)	2(1)	2(1)
O(1)	28(1)	42(1)	62(1)	-24(1)	4(1)	5(1)
O(2)	49(1)	30(1)	48(1)	-24(1)	1(1)	0(1)
C(1)	25(1)	20(1)	22(1)	-7(1)	-3(1)	3(1)
C(2)	21(1)	20(1)	21(1)	-2(1)	-6(1)	1(1)
N(2)	24(1)	20(1)	24(1)	-5(1)	-13(1)	0(1)

O(3)	27(1)	29(1)	34(1)	-7(1)	-9(1)	-8(1)
O(4)	33(1)	30(1)	32(1)	-16(1)	-11(1)	0(1)
C(3)	22(1)	17(1)	19(1)	-3(1)	-10(1)	0(1)
C(4)	21(1)	18(1)	17(1)	-5(1)	-9(1)	3(1)
N(3)	21(1)	21(1)	21(1)	-6(1)	-9(1)	0(1)
O(5)	22(1)	31(1)	23(1)	-12(1)	-7(1)	2(1)
O(6)	28(1)	25(1)	38(1)	-14(1)	-13(1)	-2(1)
C(5)	20(1)	19(1)	17(1)	-3(1)	-7(1)	0(1)
C(6)	27(1)	18(1)	23(1)	-7(1)	-6(1)	-1(1)
C(1X)	21(1)	36(1)	22(1)	-6(1)	-10(1)	6(1)
C(2X)	31(1)	32(1)	25(1)	-12(1)	-17(1)	11(1)
C(3X)	28(1)	29(1)	26(1)	-5(1)	-16(1)	1(1)

Table 5. Hydrogen coordinates ($\times 10^4$) and isotropic displacement parameters ($\text{\AA}^2 \times 10^3$) for **7_X**.

	x	y	z	U(eq)
H(12)	9154	4130	2869	30
H(13)	10657	4356	759	36
H(14)	11569	2624	274	37
H(15)	11055	682	1891	35
H(16)	9536	439	3996	27
H(22)	8911	3486	7118	26
H(23)	9406	3338	8785	31
H(24)	8577	1592	10648	33
H(25)	7204	-3	10885	33
H(26)	6680	142	9235	28
H(32)	3922	3165	7062	28
H(33)	1706	2806	7542	32
H(34)	1004	1121	7257	30
H(35)	2520	-226	6513	28
H(36)	4730	108	6062	24
H(2)	1978	2570	4343	28
H(4)	5774	2373	1859	22
H(6)	4986	5026	3475	30
H(1X)	7292	5127	-1201	41
H(2X)	5929	3499	-912	33
H(3X)	3634	3375	282	41

7_N) Triphenylisocyanurate, trinitrobenzene and benzene

Synthesis: Praveen K. Thallapally, University of Hyderabad, India.

Table 1. Crystal data and structure refinement for 7_N.

Identification code	7 _N	
Empirical formula	C30 H21 N6 O9	
Formula weight	609.00	
Temperature	25(1) K	
Wavelength	0.5-5.0 Å	
Crystal system	Triclinic	
Space group	P-1	
Unit cell dimensions	a = 11.320(4) Å	α = 70.48(2)°.
	b = 11.558(5) Å	β = 63.43(3)°.
	c = 12.455(5) Å	γ = 86.93(3)°.
Volume	1364.8(9) Å ³	
Z	2	
Density (calculated)	1.482 Mg/m ³	
Absorption coefficient	1.230, at 1 Angstrom mm ⁻¹	
F(000)	45.80	
Crystal size	2.0 x 2.0 x 1.0 mm ³	
Theta/lambda range for data collection	0.088 to 0.90°/Å.	
Index ranges	0<=h<=18, -19<=k<=19, -17<=l<=20	
Reflections collected	20712	
Independent reflections	6069 [R(int) = 0.066]	
Completeness to theta = 12.02°	45.9 %	
Absorption correction	Empirical	
Max. and min. transmission	0.90 and 0.65	
Refinement method	Full-matrix least-squares on F ²	
Data / restraints / parameters	6069 / 0 / 595	
Goodness-of-fit on F ²	1.057	
Final R indices [I>2sigma(I)]	R1 = 0.0799, wR2 = 0.2013	
R indices (all data)	R1 = 0.0799, wR2 = 0.2013	
Extinction coefficient	0.160	
Largest diff. peak and hole	1.900 and -1.993 e.Å ⁻³	

Table 2. Atomic coordinates ($\times 10^4$) and equivalent isotropic displacement parameters ($\text{\AA}^2 \times 10^3$) for 7_N . $U(\text{eq})$ is defined as one third of the trace of the orthogonalized U_{ij} tensor.

	x	y	z	$U(\text{eq})$
O(10)	6612(3)	2110(3)	4180(3)	14(1)
C(10)	6864(3)	2036(2)	5037(2)	8(1)
N(10)	8156(2)	2103(2)	4867(2)	8(1)
C(11)	9185(3)	2260(2)	3603(2)	8(1)
C(12)	9521(3)	3422(3)	2667(3)	15(1)
C(13)	10412(4)	3556(4)	1416(3)	22(1)
C(14)	10976(4)	2532(4)	1123(3)	24(1)
C(15)	10661(3)	1377(4)	2084(3)	21(1)
C(16)	9761(3)	1229(3)	3340(3)	13(1)
O(20)	9617(3)	1871(3)	5681(3)	13(1)
C(20)	8501(3)	1942(2)	5838(2)	8(1)
N(20)	7453(2)	1897(2)	7000(2)	9(1)
C(21)	7760(3)	1815(2)	8025(2)	10(1)
C(22)	8563(3)	2777(3)	7878(3)	12(1)
C(23)	8858(3)	2689(3)	8873(3)	16(1)
C(24)	8363(4)	1650(4)	9987(3)	21(1)
C(25)	7540(4)	698(3)	10124(3)	18(1)
C(26)	7236(3)	790(3)	9137(3)	13(1)
O(30)	5266(3)	1817(4)	8278(3)	17(1)
C(30)	6130(3)	1856(3)	7264(2)	9(1)
N(30)	5889(2)	1852(2)	6268(2)	9(1)
C(31)	4529(3)	1670(2)	6520(2)	8(1)
C(32)	3651(3)	2480(3)	6951(3)	14(1)
C(33)	2333(3)	2264(3)	7240(3)	17(1)
C(34)	1905(3)	1256(3)	7070(3)	15(1)
C(35)	2799(3)	453(3)	6632(3)	13(1)
C(36)	4115(3)	658(3)	6359(3)	10(1)
N(1)	2423(3)	4554(2)	4775(3)	29(1)
O(1)	1261(6)	4297(6)	5162(7)	50(2)
O(2)	2886(7)	5321(5)	5004(6)	43(2)
C(1)	3364(3)	3898(2)	3988(3)	16(1)
C(2)	2888(3)	2875(3)	3898(3)	15(1)

N(2)	3399(2)	1240(2)	2962(2)	14(1)
O(3)	2341(5)	667(4)	3776(4)	24(1)
O(4)	4138(5)	957(4)	2046(4)	25(1)
C(3)	3832(3)	2325(2)	3102(2)	10(1)
C(4)	5164(3)	2755(2)	2412(2)	9(1)
N(3)	6959(2)	4256(2)	1872(2)	13(1)
O(5)	7709(4)	3759(4)	1157(3)	18(1)
O(6)	7288(4)	5162(4)	2013(4)	23(1)
C(5)	5562(3)	3765(2)	2576(2)	9(1)
C(6)	4690(3)	4345(3)	3365(3)	17(1)
C(1X)	6369(3)	5080(4)	-718(3)	20(1)
C(2X)	5555(4)	4109(3)	-547(3)	21(1)
C(3X)	4190(4)	4033(3)	175(3)	20(1)

Table 3. Bond lengths [\AA] and angles [$^\circ$] for **7_N**.

O(10)-C(10)	1.199(4)	C(31)-C(32)	1.383(4)
C(10)-N(30)	1.382(3)	C(31)-C(36)	1.390(4)
C(10)-N(10)	1.383(3)	C(32)-C(33)	1.384(4)
N(10)-C(20)	1.383(3)	C(32)-H(32)	1.085(8)
N(10)-C(11)	1.435(3)	C(33)-C(34)	1.399(5)
C(11)-C(12)	1.386(4)	C(33)-H(33)	1.087(9)
C(11)-C(16)	1.392(4)	C(34)-C(35)	1.388(5)
C(12)-C(13)	1.384(4)	C(34)-H(34)	1.083(8)
C(12)-H(12)	1.077(9)	C(35)-C(36)	1.386(4)
C(13)-C(14)	1.393(6)	C(35)-H(35)	1.077(8)
C(13)-H(13)	1.082(10)	C(36)-H(36)	1.071(7)
C(14)-C(15)	1.394(6)	N(1)-O(1)	1.196(8)
C(14)-H(14)	1.075(8)	N(1)-O(2)	1.222(7)
C(15)-C(16)	1.389(4)	N(1)-C(1)	1.464(4)
C(15)-H(15)	1.089(10)	C(1)-C(6)	1.377(5)
C(16)-H(16)	1.087(8)	C(1)-C(2)	1.383(4)
O(20)-C(20)	1.192(4)	C(2)-C(3)	1.389(4)
C(20)-N(20)	1.387(3)	C(2)-H(2)	1.076(9)
N(20)-C(30)	1.382(3)	N(2)-O(3)	1.204(4)
N(20)-C(21)	1.440(3)	N(2)-O(4)	1.215(5)
C(21)-C(26)	1.385(4)	N(2)-C(3)	1.460(3)
C(21)-C(22)	1.385(4)	C(3)-C(4)	1.377(4)
C(22)-C(23)	1.393(4)	C(4)-C(5)	1.380(4)
C(22)-H(22)	1.081(8)	C(4)-H(4)	1.086(7)
C(23)-C(24)	1.394(5)	N(3)-O(5)	1.207(4)
C(23)-H(23)	1.081(9)	N(3)-O(6)	1.220(4)
C(24)-C(25)	1.396(5)	N(3)-C(5)	1.454(3)
C(24)-H(24)	1.082(8)	C(5)-C(6)	1.376(4)
C(25)-C(26)	1.388(4)	C(6)-H(6)	1.072(8)
C(25)-H(25)	1.075(10)	C(1X)-C(3X)#1	1.384(5)
C(26)-H(26)	1.089(8)	C(1X)-C(2X)	1.389(6)
O(30)-C(30)	1.189(4)	C(1X)-H(1X)	1.066(10)
C(30)-N(30)	1.386(3)	C(2X)-C(3X)	1.386(6)
N(30)-C(31)	1.439(3)	C(2X)-H(2X)	1.084(9)
		C(3X)-C(1X)#1	1.384(5)
		C(3X)-H(3X)	1.067(10)

O(10)-C(10)-N(30)	122.5(3)	C(24)-C(23)-H(23)	120.7(6)
O(10)-C(10)-N(10)	122.2(3)	C(23)-C(24)-C(25)	120.0(3)
N(30)-C(10)-N(10)	115.2(2)	C(23)-C(24)-H(24)	120.5(7)
C(20)-N(10)-C(10)	124.55(19)	C(25)-C(24)-H(24)	119.5(7)
C(20)-N(10)-C(11)	119.1(2)	C(26)-C(25)-C(24)	119.5(3)
C(10)-N(10)-C(11)	116.2(2)	C(26)-C(25)-H(25)	119.2(7)
C(12)-C(11)-C(16)	122.2(2)	C(24)-C(25)-H(25)	121.3(6)
C(12)-C(11)-N(10)	118.8(2)	C(21)-C(26)-C(25)	119.8(3)
C(16)-C(11)-N(10)	119.0(2)	C(21)-C(26)-H(26)	120.9(5)
C(13)-C(12)-C(11)	119.1(3)	C(25)-C(26)-H(26)	119.3(5)
C(13)-C(12)-H(12)	120.6(5)	O(30)-C(30)-N(20)	122.2(3)
C(11)-C(12)-H(12)	120.3(5)	O(30)-C(30)-N(30)	122.8(3)
C(12)-C(13)-C(14)	119.8(3)	N(20)-C(30)-N(30)	115.1(2)
C(12)-C(13)-H(13)	120.0(7)	C(10)-N(30)-C(30)	124.5(2)
C(14)-C(13)-H(13)	120.2(7)	C(10)-N(30)-C(31)	117.4(2)
C(13)-C(14)-C(15)	120.4(3)	C(30)-N(30)-C(31)	118.05(19)
C(13)-C(14)-H(14)	120.2(8)	C(32)-C(31)-C(36)	121.1(2)
C(15)-C(14)-H(14)	119.4(8)	C(32)-C(31)-N(30)	119.8(2)
C(16)-C(15)-C(14)	120.3(3)	C(36)-C(31)-N(30)	119.1(2)
C(16)-C(15)-H(15)	119.5(7)	C(31)-C(32)-C(33)	119.1(3)
C(14)-C(15)-H(15)	120.1(7)	C(31)-C(32)-H(32)	120.7(6)
C(15)-C(16)-C(11)	118.2(3)	C(33)-C(32)-H(32)	120.0(6)
C(15)-C(16)-H(16)	120.8(5)	C(32)-C(33)-C(34)	120.3(3)
C(11)-C(16)-H(16)	121.0(5)	C(32)-C(33)-H(33)	118.8(6)
O(20)-C(20)-N(10)	122.5(3)	C(34)-C(33)-H(33)	120.9(6)
O(20)-C(20)-N(20)	122.6(3)	C(35)-C(34)-C(33)	119.9(3)
N(10)-C(20)-N(20)	114.9(2)	C(35)-C(34)-H(34)	120.5(6)
C(30)-N(20)-C(20)	124.7(2)	C(33)-C(34)-H(34)	119.5(6)
C(30)-N(20)-C(21)	117.65(19)	C(36)-C(35)-C(34)	119.8(3)
C(20)-N(20)-C(21)	117.6(2)	C(36)-C(35)-H(35)	118.4(6)
C(26)-C(21)-C(22)	121.6(3)	C(34)-C(35)-H(35)	121.7(6)
C(26)-C(21)-N(20)	119.6(2)	C(35)-C(36)-C(31)	119.7(3)
C(22)-C(21)-N(20)	118.9(2)	C(35)-C(36)-H(36)	119.2(5)
C(21)-C(22)-C(23)	118.5(3)	C(31)-C(36)-H(36)	121.1(5)
C(21)-C(22)-H(22)	120.3(5)	O(1)-N(1)-O(2)	124.5(4)
C(23)-C(22)-H(22)	121.2(5)	O(1)-N(1)-C(1)	118.2(4)
C(22)-C(23)-C(24)	120.6(3)	O(2)-N(1)-C(1)	117.3(4)
C(22)-C(23)-H(23)	118.7(6)	C(6)-C(1)-C(2)	123.2(3)

C(6)-C(1)-N(1)	117.6(3)
C(2)-C(1)-N(1)	119.1(3)
C(1)-C(2)-C(3)	115.9(3)
C(1)-C(2)-H(2)	122.7(5)
C(3)-C(2)-H(2)	121.4(5)
O(3)-N(2)-O(4)	124.0(3)
O(3)-N(2)-C(3)	117.9(3)
O(4)-N(2)-C(3)	118.1(3)
C(4)-C(3)-C(2)	123.8(3)
C(4)-C(3)-N(2)	117.4(2)
C(2)-C(3)-N(2)	118.8(3)
C(3)-C(4)-C(5)	116.7(2)
C(3)-C(4)-H(4)	122.5(4)
C(5)-C(4)-H(4)	120.8(5)
O(5)-N(3)-O(6)	124.4(3)
O(5)-N(3)-C(5)	117.5(2)
O(6)-N(3)-C(5)	118.0(3)
C(6)-C(5)-C(4)	122.8(3)
C(6)-C(5)-N(3)	118.2(2)
C(4)-C(5)-N(3)	119.0(2)
C(5)-C(6)-C(1)	117.5(3)
C(5)-C(6)-H(6)	121.6(6)
C(1)-C(6)-H(6)	120.9(6)
C(3X)#1-C(1X)-C(2X)	119.8(3)
C(3X)#1-C(1X)-H(1X)	121.1(8)
C(2X)-C(1X)-H(1X)	119.1(7)
C(3X)-C(2X)-C(1X)	119.5(3)
C(3X)-C(2X)-H(2X)	119.5(8)
C(1X)-C(2X)-H(2X)	121.0(8)
C(1X)#1-C(3X)-C(2X)	120.7(3)
C(1X)#1-C(3X)-H(3X)	120.6(8)
C(2X)-C(3X)-H(3X)	118.7(8)

Symmetry transformations used to
generate equivalent atoms:

#1 -x+1,-y+1,-z

Table 4. Anisotropic displacement parameters ($\text{\AA}^2 \times 10^3$) for 7_N . The anisotropic displacement factor exponent takes the form: $-2\pi^2 [h^2 a^{*2} U^{11} + \dots + 2 h k a^* b^* U^{12}]$

	U ¹¹	U ²²	U ³³	U ²³	U ¹³	U ¹²
O(10)	12(1)	21(2)	7(1)	-3(1)	-5(1)	4(1)
C(10)	8(1)	9(1)	7(1)	-2(1)	-4(1)	1(1)
N(10)	6(1)	9(1)	7(1)	-3(1)	-2(1)	1(1)
C(11)	7(1)	9(1)	7(1)	-3(1)	-2(1)	2(1)
C(12)	14(1)	13(1)	10(1)	1(1)	-2(1)	-1(1)
C(13)	19(1)	27(2)	9(1)	2(1)	-2(1)	-5(1)
C(14)	19(1)	38(2)	7(1)	-8(1)	2(1)	-7(1)
C(15)	17(1)	30(2)	15(1)	-16(1)	-1(1)	2(1)
C(16)	13(1)	12(1)	13(1)	-7(1)	-3(1)	3(1)
O(20)	4(1)	24(2)	12(1)	-8(1)	-3(1)	3(1)
C(20)	7(1)	11(1)	8(1)	-4(1)	-3(1)	1(1)
N(20)	7(1)	14(1)	8(1)	-6(1)	-3(1)	1(1)
C(21)	9(1)	12(1)	8(1)	-4(1)	-3(1)	1(1)
C(22)	10(1)	14(1)	15(1)	-8(1)	-5(1)	1(1)
C(23)	17(1)	21(1)	18(1)	-13(1)	-9(1)	3(1)
C(24)	28(2)	27(2)	17(1)	-14(1)	-14(1)	7(1)
C(25)	28(2)	18(1)	10(1)	-6(1)	-8(1)	4(1)
C(26)	17(1)	13(1)	10(1)	-5(1)	-6(1)	4(1)
O(30)	9(1)	32(2)	14(1)	-16(1)	-3(1)	4(1)
C(30)	7(1)	14(1)	8(1)	-8(1)	-3(1)	2(1)
N(30)	8(1)	11(1)	9(1)	-5(1)	-3(1)	1(1)
C(31)	7(1)	7(1)	9(1)	-3(1)	-3(1)	1(1)
C(32)	8(1)	12(1)	23(1)	-9(1)	-6(1)	3(1)
C(33)	9(1)	17(1)	26(1)	-11(1)	-6(1)	6(1)
C(34)	10(1)	17(1)	19(1)	-5(1)	-8(1)	2(1)
C(35)	13(1)	16(1)	14(1)	-6(1)	-9(1)	-1(1)
C(36)	10(1)	12(1)	12(1)	-6(1)	-7(1)	2(1)
N(1)	35(1)	8(1)	22(1)	-5(1)	6(1)	5(1)
O(1)	32(3)	30(2)	57(4)	-25(3)	11(2)	6(2)
O(2)	49(3)	23(2)	38(3)	-21(2)	5(2)	1(2)
C(1)	18(1)	4(1)	13(1)	-2(1)	1(1)	1(1)
C(2)	14(1)	9(1)	13(1)	-1(1)	-2(1)	2(1)
N(2)	19(1)	8(1)	15(1)	-2(1)	-9(1)	0(1)

O(3)	25(2)	17(2)	24(2)	-4(1)	-6(2)	-9(1)
O(4)	33(2)	17(2)	23(2)	-11(1)	-8(2)	-4(2)
C(3)	14(1)	5(1)	9(1)	1(1)	-5(1)	1(1)
C(4)	12(1)	6(1)	7(1)	-1(1)	-4(1)	2(1)
N(3)	16(1)	9(1)	11(1)	-2(1)	-5(1)	-2(1)
O(5)	15(1)	21(2)	14(1)	-7(1)	-2(1)	-2(1)
O(6)	24(2)	15(1)	28(2)	-10(1)	-9(2)	-3(1)
C(5)	12(1)	5(1)	8(1)	-1(1)	-4(1)	0(1)
C(6)	21(1)	8(1)	13(1)	-4(1)	-1(1)	-2(1)
C(1X)	18(1)	25(2)	16(1)	-6(1)	-9(1)	8(1)
C(2X)	31(2)	19(1)	17(1)	-8(1)	-14(1)	12(1)
C(3X)	25(2)	18(1)	19(1)	-3(1)	-13(1)	1(1)
H(4)	28(3)	17(2)	26(3)	-13(2)	-7(2)	5(2)
H(36)	28(3)	28(3)	41(4)	-26(3)	-18(3)	16(3)
H(6)	53(5)	20(3)	35(4)	-14(3)	-8(3)	-7(3)
H(2)	25(3)	32(4)	32(3)	-9(3)	-3(3)	-1(3)
H(16)	43(4)	14(2)	29(3)	-2(2)	-5(3)	6(3)
H(35)	37(4)	34(4)	47(4)	-25(3)	-24(4)	2(3)
H(26)	37(4)	23(3)	27(3)	-3(2)	-15(3)	-8(3)
H(22)	38(4)	23(3)	27(3)	0(2)	-16(3)	-8(3)
H(33)	31(4)	38(4)	66(6)	-32(4)	-17(4)	19(3)
H(13)	48(5)	42(5)	23(3)	10(3)	-4(3)	-3(4)
H(23)	42(4)	36(4)	40(4)	-19(3)	-23(4)	-1(3)
H(34)	22(3)	42(4)	51(5)	-20(4)	-22(3)	5(3)
H(24)	65(6)	53(5)	31(4)	-19(4)	-34(4)	6(5)
H(25)	68(7)	40(4)	22(3)	-6(3)	-22(4)	4(4)
H(32)	32(4)	29(4)	67(6)	-33(4)	-18(4)	5(3)
H(12)	46(5)	17(3)	35(4)	-3(3)	-7(3)	14(3)
H(15)	40(5)	52(6)	45(5)	-37(5)	-4(4)	11(4)
H(2X)	78(8)	40(5)	54(6)	-36(5)	-37(6)	33(5)
H(14)	46(5)	62(6)	17(3)	-18(3)	0(3)	-3(4)
H(3X)	60(6)	34(4)	56(6)	-9(4)	-38(5)	-7(4)
H(1X)	25(4)	56(6)	41(4)	-15(4)	-9(3)	14(4)

Table 5. Hydrogen coordinates ($\times 10^4$) and isotropic displacement parameters ($\text{\AA}^2 \times 10^3$) for 7_N .

	x	y	z	U(eq)
H(4)	5884(7)	2313(6)	1791(7)	24(1)
H(36)	4797(8)	35(7)	6018(8)	28(1)
H(6)	5019(10)	5133(7)	3473(8)	38(2)
H(2)	1851(8)	2525(8)	4398(8)	34(2)
H(16)	9496(9)	328(6)	4092(8)	35(2)
H(35)	2496(9)	-343(8)	6510(9)	34(2)
H(26)	6591(9)	47(7)	9248(7)	30(2)
H(22)	8960(9)	3569(7)	7002(7)	30(2)
H(33)	1640(9)	2886(10)	7610(12)	43(2)
H(13)	10670(11)	4453(10)	671(8)	48(3)
H(23)	9482(10)	3440(8)	8761(9)	36(2)
H(34)	873(8)	1103(9)	7292(10)	35(2)
H(24)	8595(12)	1583(10)	10759(9)	43(2)
H(25)	7119(13)	-96(10)	10986(8)	44(2)
H(32)	3966(9)	3232(8)	7137(11)	40(2)
H(12)	9053(10)	4200(7)	2901(9)	39(2)
H(15)	11101(10)	579(11)	1849(10)	47(2)
H(2X)	5973(14)	3399(10)	-954(11)	50(3)
H(14)	11665(11)	2629(11)	153(8)	46(2)
H(3X)	3578(13)	3280(9)	302(11)	47(2)
H(1X)	7418(9)	5127(11)	-1265(10)	44(2)

8) 4,4'-dinitrotetraphenylmethane

Synthesis: Basavoju Srinivas, University of Hyderabad, India.

Table 1. Crystal data and structure refinement for **8**.

Identification code	8	
Empirical formula	C ₂₅ H _{19.08} N ₂ O _{4.54}	
Formula weight	420.18	
Temperature	30(2) K	
Wavelength	0.71073 Å	
Crystal system	Rhombohedral	
Space group	R-3	
Unit cell dimensions	a = 20.759(3) Å	$\alpha = 90^\circ$.
	b = 20.759(3) Å	$\beta = 90^\circ$.
	c = 25.142(5) Å	$\gamma = 120^\circ$.
Volume	9383(3) Å ³	
Z	18	
Density (calculated)	1.338 Mg/m ³	
Absorption coefficient	0.093 mm ⁻¹	
F(000)	3950	
Crystal size	0.30 x 0.26 x 0.20 mm ³	
Theta range for data collection	2.41 to 27.50°.	
Index ranges	-26 ≤ h ≤ 24, -26 ≤ k ≤ 26, -20 ≤ l ≤ 31	
Reflections collected	19194	
Independent reflections	4654 [R(int) = 0.0604]	
Completeness to theta = 27.50°	97.2 %	
Absorption correction	None	
Refinement method	Full-matrix least-squares on F ²	
Data / restraints / parameters	4654 / 6 / 300	
Goodness-of-fit on F ²	1.044	
Final R indices [I > 2σ(I)]	R1 = 0.0618, wR2 = 0.1397	
R indices (all data)	R1 = 0.1018, wR2 = 0.1636	
Extinction coefficient	not refined	
Largest diff. peak and hole	0.945 and -0.828 e.Å ⁻³	

Table 2. Atomic coordinates ($\times 10^4$) and equivalent isotropic displacement parameters ($\text{\AA}^2 \times 10^3$) for **8**. $U(\text{eq})$ is defined as one third of the trace of the orthogonalized U_{ij} tensor.

	x	y	z	$U(\text{eq})$
C(1)	5182(1)	5613(1)	-1934(1)	21(1)
N(1)	3799(1)	4661(1)	138(1)	32(1)
O(12)	3650(1)	5078(1)	390(1)	41(1)
O(11)	3663(1)	4044(1)	299(1)	39(1)
C(11)	4850(1)	5382(1)	-1368(1)	22(1)
C(12)	4755(2)	5869(2)	-1037(1)	37(1)
C(13)	4405(2)	5636(2)	-545(1)	42(1)
C(14)	4158(2)	4907(2)	-387(1)	28(1)
C(15)	4230(1)	4405(1)	-709(1)	23(1)
C(16)	4565(1)	4647(1)	-1201(1)	22(1)
N(2)	7561(1)	8635(1)	-2261(1)	32(1)
O(22)	7600(1)	8931(1)	-2696(1)	46(1)
O(21)	8019(1)	8941(1)	-1902(1)	40(1)
C(21)	5762(1)	6449(1)	-1994(1)	21(1)
C(22)	6290(2)	6833(1)	-1596(1)	27(1)
C(23)	6875(2)	7551(1)	-1681(1)	27(1)
C(24)	6934(2)	7884(1)	-2171(1)	24(1)
C(25)	6424(2)	7522(1)	-2575(1)	25(1)
C(26)	5841(1)	6806(1)	-2482(1)	23(1)
C(31)	5653(1)	5247(1)	-2084(1)	22(1)
C(32)	6074(1)	5148(1)	-1690(1)	25(1)
C(33)	6549(1)	4885(2)	-1814(1)	30(1)
C(34)	6617(2)	4710(2)	-2336(1)	33(1)
C(35)	6212(2)	4813(2)	-2733(1)	31(1)
C(36)	5742(1)	5092(1)	-2609(1)	25(1)
C(41)	4487(1)	5370(1)	-2285(1)	21(1)
C(42)	4163(2)	5822(2)	-2317(1)	27(1)
C(43)	3509(2)	5593(2)	-2601(1)	30(1)
C(44)	3154(1)	4910(2)	-2853(1)	28(1)
C(45)	3457(1)	4446(2)	-2812(1)	25(1)
C(46)	4115(1)	4674(1)	-2529(1)	22(1)
O(1)	3333	6667	-171(2)	32(2)

O(2)	9632(3)	9767(3)	-2054(2)	11(2)
------	---------	---------	----------	-------

Table 3. Bond lengths [\AA] and angles [$^\circ$] for **8**.

C(1)-C(41)	1.544(3)	C(41)-C(42)	1.404(4)
C(1)-C(21)	1.548(3)	C(42)-C(43)	1.391(4)
C(1)-C(11)	1.549(3)	C(43)-C(44)	1.381(4)
C(1)-C(31)	1.555(3)	C(44)-C(45)	1.394(4)
N(1)-O(12)	1.232(3)	C(45)-C(46)	1.397(3)
N(1)-O(11)	1.235(3)	O(2)-O(2)#1	1.160(9)
N(1)-C(14)	1.474(3)	O(2)-O(2)#2	1.160(9)
C(11)-C(16)	1.397(3)	C(41)-C(1)-C(21)	112.7(2)
C(11)-C(12)	1.398(4)	C(41)-C(1)-C(11)	102.99(19)
C(12)-C(13)	1.392(4)	C(21)-C(1)-C(11)	114.3(2)
C(13)-C(14)	1.389(4)	C(41)-C(1)-C(31)	114.5(2)
C(14)-C(15)	1.386(4)	C(21)-C(1)-C(31)	101.45(19)
C(15)-C(16)	1.384(4)	C(11)-C(1)-C(31)	111.3(2)
N(2)-O(21)	1.231(3)	O(12)-N(1)-O(11)	123.5(2)
N(2)-O(22)	1.237(3)	O(12)-N(1)-C(14)	118.6(2)
N(2)-C(24)	1.465(3)	O(11)-N(1)-C(14)	117.9(2)
C(21)-C(26)	1.400(3)	C(16)-C(11)-C(12)	118.4(2)
C(21)-C(22)	1.401(4)	C(16)-C(11)-C(1)	119.6(2)
C(22)-C(23)	1.390(4)	C(12)-C(11)-C(1)	121.7(2)
C(23)-C(24)	1.389(4)	C(13)-C(12)-C(11)	120.9(3)
C(24)-C(25)	1.384(4)	C(14)-C(13)-C(12)	118.6(3)
C(25)-C(26)	1.389(4)	C(15)-C(14)-C(13)	122.0(2)
C(31)-C(36)	1.393(4)	C(15)-C(14)-N(1)	119.2(2)
C(31)-C(32)	1.401(4)	C(13)-C(14)-N(1)	118.8(3)
C(32)-C(33)	1.381(4)	C(16)-C(15)-C(14)	118.3(2)
C(33)-C(34)	1.388(4)	C(15)-C(16)-C(11)	121.7(2)
C(34)-C(35)	1.390(4)	O(21)-N(2)-O(22)	123.3(2)
C(35)-C(36)	1.398(4)	O(21)-N(2)-C(24)	118.8(2)
C(41)-C(46)	1.394(4)	O(22)-N(2)-C(24)	117.9(2)
		C(26)-C(21)-C(22)	118.2(2)
		C(26)-C(21)-C(1)	119.9(2)

C(22)-C(21)-C(1)	121.1(2)
C(23)-C(22)-C(21)	121.0(2)
C(24)-C(23)-C(22)	118.8(2)
C(25)-C(24)-C(23)	121.9(2)
C(25)-C(24)-N(2)	119.7(2)
C(23)-C(24)-N(2)	118.4(2)
C(24)-C(25)-C(26)	118.5(2)
C(25)-C(26)-C(21)	121.5(2)
C(36)-C(31)-C(32)	118.2(2)
C(36)-C(31)-C(1)	122.0(2)
C(32)-C(31)-C(1)	119.4(2)
C(33)-C(32)-C(31)	121.4(3)
C(32)-C(33)-C(34)	120.2(3)
C(33)-C(34)-C(35)	119.4(3)
C(34)-C(35)-C(36)	120.4(3)
C(31)-C(36)-C(35)	120.5(2)
C(46)-C(41)-C(42)	117.7(2)
C(46)-C(41)-C(1)	122.2(2)
C(42)-C(41)-C(1)	119.8(2)
C(43)-C(42)-C(41)	120.9(2)
C(44)-C(43)-C(42)	121.0(2)
C(43)-C(44)-C(45)	118.9(2)
C(44)-C(45)-C(46)	120.3(2)
C(41)-C(46)-C(45)	121.2(2)
O(2)#1-O(2)-O(2)#2	60.000(2)

Symmetry transformations used to
generate equivalent atoms:

#1 -x+y+1,-x+2,z #2 -y+2,x-y+1,z

Table 4. Anisotropic displacement parameters ($\text{\AA}^2 \times 10^3$) for **8**. The anisotropic displacement factor exponent takes the form: $-2\pi^2 [h^2 a^{*2} U^{11} + \dots + 2 h k a^* b^* U^{12}]$

	U ¹¹	U ²²	U ³³	U ²³	U ¹³	U ¹²
C(1)	26(1)	19(1)	17(1)	0(1)	-1(1)	10(1)
N(1)	30(1)	30(1)	21(1)	2(1)	-2(1)	2(1)
O(12)	50(1)	38(1)	22(1)	-5(1)	7(1)	13(1)
O(11)	43(1)	32(1)	28(1)	10(1)	4(1)	9(1)
C(11)	27(1)	20(1)	17(1)	0(1)	-3(1)	10(1)
C(12)	58(2)	17(1)	25(2)	2(1)	10(1)	10(1)
C(13)	60(2)	24(1)	26(2)	-3(1)	11(1)	10(1)
C(14)	29(1)	25(1)	18(1)	1(1)	-1(1)	5(1)
C(15)	21(1)	21(1)	25(1)	4(1)	-4(1)	8(1)
C(16)	22(1)	20(1)	23(1)	-1(1)	-3(1)	10(1)
N(2)	39(1)	21(1)	29(1)	1(1)	-2(1)	9(1)
O(22)	65(2)	26(1)	26(1)	7(1)	-2(1)	6(1)
O(21)	45(1)	23(1)	37(1)	1(1)	-13(1)	5(1)
C(21)	26(1)	19(1)	20(1)	1(1)	1(1)	11(1)
C(22)	37(2)	21(1)	20(1)	2(1)	-4(1)	12(1)
C(23)	36(2)	18(1)	24(1)	-3(1)	-8(1)	11(1)
C(24)	29(1)	17(1)	25(1)	0(1)	2(1)	10(1)
C(25)	32(1)	23(1)	20(1)	2(1)	1(1)	15(1)
C(26)	26(1)	24(1)	20(1)	0(1)	-2(1)	12(1)
C(31)	20(1)	15(1)	25(1)	1(1)	1(1)	4(1)
C(32)	21(1)	22(1)	26(1)	4(1)	0(1)	5(1)
C(33)	19(1)	29(1)	38(2)	12(1)	1(1)	9(1)
C(34)	24(1)	30(2)	45(2)	7(1)	8(1)	15(1)
C(35)	25(1)	30(2)	32(2)	-2(1)	5(1)	11(1)
C(36)	21(1)	23(1)	27(1)	0(1)	-1(1)	9(1)
C(41)	22(1)	25(1)	14(1)	4(1)	2(1)	11(1)
C(42)	29(1)	23(1)	27(1)	3(1)	3(1)	12(1)
C(43)	29(1)	34(2)	33(2)	9(1)	5(1)	20(1)
C(44)	22(1)	35(2)	26(1)	8(1)	3(1)	13(1)
C(45)	25(1)	30(1)	16(1)	2(1)	4(1)	12(1)
C(46)	25(1)	26(1)	17(1)	2(1)	1(1)	14(1)

Table 5. Hydrogen coordinates ($\times 10^4$) and isotropic displacement parameters ($\text{\AA}^2 \times 10^3$) for **8**.

	x	y	z	U(eq)
H(12)	4931	6367	-1149	45
H(13)	4338	5967	-323	50
H(15)	4053	3908	-596	28
H(16)	4602	4304	-1431	26
H(22)	6248	6598	-1263	32
H(23)	7229	7810	-1408	33
H(25)	6473	7758	-2908	29
H(26)	5488	6553	-2755	28
H(32)	6031	5265	-1331	31
H(33)	6830	4824	-1541	36
H(34)	6938	4522	-2421	39
H(35)	6256	4693	-3091	37
H(36)	5480	5177	-2885	30
H(42)	4393	6290	-2142	32
H(43)	3303	5910	-2622	36
H(44)	2711	4760	-3051	33
H(45)	3215	3971	-2978	30
H(46)	4313	4350	-2502	26
H(1A)	3333	6667	238(8)	0(11)
H(1B)	3300(40)	6210(20)	-290(20)	0(19)
H(2A)	9820(30)	9630(30)	-2392(15)	0(18)
H(2B)	10000	10000	-1793(10)	12(12)

9) 2,3-dichloro-1,4-diethynyl-1,4-dihydroxy-naphthalene

Synthesis: Rahul Banerjee, University of Hyderabad, India.

Table 1. Crystal data and structure refinement for **9**.

Identification code	9	
Empirical formula	C ₁₄ H ₈ Cl ₂ O ₂	
Formula weight	279.10	
Temperature	120(2) K	
Wavelength	0.71073 Å	
Crystal system	Monoclinic	
Space group	P2(1)/c	
Unit cell dimensions	a = 7.4454(5) Å	$\alpha = 90^\circ$.
	b = 23.3125(17) Å	$\beta = 110.578(3)^\circ$.
	c = 7.5606(5) Å	$\gamma = 90^\circ$.
Volume	1228.57(15) Å ³	
Z	4	
Density (calculated)	1.509 Mg/m ³	
Absorption coefficient	0.517 mm ⁻¹	
F(000)	568	
Crystal size	0.45 x 0.35 x 0.20 mm ³	
Theta range for data collection	1.75 to 27.48°.	
Index ranges	-9 ≤ h ≤ 9, -29 ≤ k ≤ 30, -9 ≤ l ≤ 9	
Reflections collected	8666	
Independent reflections	2815 [R(int) = 0.0318]	
Completeness to theta = 27.48°	99.9 %	
Absorption correction	None	
Refinement method	Full-matrix least-squares on F ²	
Data / restraints / parameters	2815 / 0 / 179	
Goodness-of-fit on F ²	1.062	
Final R indices [I > 2σ(I)]	R1 = 0.0301, wR2 = 0.0739	
R indices (all data)	R1 = 0.0335, wR2 = 0.0759	
Extinction coefficient	not refined	
Largest diff. peak and hole	0.358 and -0.257 e.Å ⁻³	

Table 2. Atomic coordinates ($\times 10^4$) and equivalent isotropic displacement parameters ($\text{\AA}^2 \times 10^3$) for **9**. $U(\text{eq})$ is defined as one third of the trace of the orthogonalized U_{ij} tensor.

	x	y	z	$U(\text{eq})$
C(1)	7996(2)	3938(1)	10060(2)	14(1)
C(2)	9258(2)	4204(1)	9306(2)	18(1)
C(3)	11078(2)	4368(1)	10475(2)	20(1)
C(4)	11655(2)	4275(1)	12416(2)	21(1)
C(5)	10427(2)	4008(1)	13170(2)	19(1)
C(6)	8591(2)	3833(1)	11994(2)	15(1)
C(7)	7338(2)	3528(1)	12916(2)	14(1)
O(1)	7075(2)	3921(1)	14260(2)	18(1)
C(11)	8345(2)	2999(1)	13878(2)	17(1)
C(12)	9187(2)	2584(1)	14651(2)	22(1)
C(8)	5393(2)	3359(1)	11492(2)	14(1)
Cl(1)	2504(1)	3303(1)	8156(1)	17(1)
C(9)	4778(2)	3486(1)	9660(2)	14(1)
Cl(2)	3979(1)	2986(1)	12486(1)	20(1)
C(10)	5987(2)	3791(1)	8693(2)	15(1)
O(2)	6099(2)	3432(1)	7174(2)	18(1)
C(13)	4999(2)	4326(1)	7799(2)	17(1)
C(14)	4233(2)	4765(1)	7175(2)	23(1)

Table 3. Bond lengths [\AA] and angles [$^\circ$] for **9**.

C(1)-C(6)	1.393(2)	C(2)-C(3)-C(4)	119.95(14)
C(1)-C(2)	1.403(2)	C(2)-C(3)-H(3A)	120.0
C(1)-C(10)	1.528(2)	C(4)-C(3)-H(3A)	120.0
C(2)-C(3)	1.386(2)	C(5)-C(4)-C(3)	119.98(14)
C(2)-H(2A)	0.9500	C(5)-C(4)-H(4A)	120.0
C(3)-C(4)	1.393(2)	C(3)-C(4)-H(4A)	120.0
C(3)-H(3A)	0.9500	C(4)-C(5)-C(6)	120.50(14)
C(4)-C(5)	1.383(2)	C(4)-C(5)-H(5A)	119.7
C(4)-H(4A)	0.9500	C(6)-C(5)-H(5A)	119.7
C(5)-C(6)	1.404(2)	C(1)-C(6)-C(5)	119.54(13)
C(5)-H(5A)	0.9500	C(1)-C(6)-C(7)	122.88(13)
C(6)-C(7)	1.5229(19)	C(5)-C(6)-C(7)	117.58(13)
C(7)-O(1)	1.4321(17)	O(1)-C(7)-C(11)	110.70(12)
C(7)-C(11)	1.492(2)	O(1)-C(7)-C(8)	109.50(12)
C(7)-C(8)	1.522(2)	C(11)-C(7)-C(8)	108.77(12)
O(1)-H(1)	0.75(2)	O(1)-C(7)-C(6)	106.54(12)
C(11)-C(12)	1.189(2)	C(11)-C(7)-C(6)	108.96(12)
C(12)-H(12)	0.93(2)	C(8)-C(7)-C(6)	112.37(12)
C(8)-C(9)	1.330(2)	C(7)-O(1)-H(1)	108.3(17)
C(8)-Cl(2)	1.7276(14)	C(12)-C(11)-C(7)	178.48(16)
Cl(1)-C(9)	1.7292(15)	C(11)-C(12)-H(12)	178.6(14)
C(9)-C(10)	1.521(2)	C(9)-C(8)-C(7)	124.93(13)
C(10)-O(2)	1.4474(17)	C(9)-C(8)-Cl(2)	121.75(12)
C(10)-C(13)	1.485(2)	C(7)-C(8)-Cl(2)	113.31(10)
O(2)-H(2)	0.80(2)	C(8)-C(9)-C(10)	124.04(13)
C(13)-C(14)	1.185(2)	C(8)-C(9)-Cl(1)	121.90(11)
C(14)-H(14)	0.95(2)	C(10)-C(9)-Cl(1)	114.05(10)
		O(2)-C(10)-C(13)	106.39(12)
		O(2)-C(10)-C(9)	108.68(12)
		C(13)-C(10)-C(9)	109.24(12)
		O(2)-C(10)-C(1)	110.50(12)
C(6)-C(1)-C(2)	119.53(14)	C(13)-C(10)-C(1)	109.28(12)
C(6)-C(1)-C(10)	123.02(13)	C(9)-C(10)-C(1)	112.56(12)
C(2)-C(1)-C(10)	117.43(13)	C(10)-O(2)-H(2)	108.3(15)
C(3)-C(2)-C(1)	120.47(14)	C(14)-C(13)-C(10)	176.64(16)
C(3)-C(2)-H(2A)	119.8	C(13)-C(14)-H(14)	178.6(14)
C(1)-C(2)-H(2A)	119.8		

Table 4. Anisotropic displacement parameters ($\text{\AA}^2 \times 10^3$) for **9**. The anisotropic displacement factor exponent takes the form: $-2\pi^2 [h^2 a^{*2} U^{11} + \dots + 2 h k a^* b^* U^{12}]$

	U ¹¹	U ²²	U ³³	U ²³	U ¹³	U ¹²
C(1)	15(1)	12(1)	15(1)	-1(1)	6(1)	1(1)
C(2)	22(1)	16(1)	18(1)	0(1)	10(1)	1(1)
C(3)	19(1)	17(1)	26(1)	1(1)	12(1)	-1(1)
C(4)	16(1)	20(1)	25(1)	-1(1)	5(1)	-3(1)
C(5)	18(1)	21(1)	17(1)	1(1)	3(1)	-1(1)
C(6)	16(1)	13(1)	16(1)	0(1)	6(1)	0(1)
C(7)	16(1)	14(1)	12(1)	0(1)	4(1)	0(1)
O(1)	26(1)	16(1)	15(1)	-1(1)	10(1)	-2(1)
C(11)	16(1)	19(1)	15(1)	-2(1)	5(1)	-4(1)
C(12)	20(1)	18(1)	23(1)	2(1)	2(1)	0(1)
C(8)	15(1)	13(1)	17(1)	1(1)	8(1)	-1(1)
Cl(1)	15(1)	18(1)	17(1)	-1(1)	2(1)	-1(1)
C(9)	14(1)	13(1)	16(1)	-2(1)	4(1)	0(1)
Cl(2)	18(1)	23(1)	20(1)	6(1)	7(1)	-4(1)
C(10)	18(1)	14(1)	12(1)	0(1)	5(1)	0(1)
O(2)	25(1)	15(1)	13(1)	-2(1)	8(1)	1(1)
C(13)	18(1)	18(1)	14(1)	-1(1)	4(1)	-2(1)
C(14)	24(1)	19(1)	23(1)	3(1)	6(1)	0(1)

Table 5. Hydrogen coordinates ($\times 10^4$) and isotropic displacement parameters ($\text{\AA}^2 \times 10^3$) for **9**.

	x	y	z	U(eq)
H(2A)	8863	4272	7985	21
H(3A)	11932	4543	9954	24
H(4A)	12891	4395	13222	25
H(5A)	10829	3943	14493	23
H(1)	6680(30)	3757(10)	14900(30)	32(6)
H(12)	9870(30)	2260(10)	15240(30)	37(6)
H(2)	6600(30)	3137(10)	7620(30)	25(5)
H(14)	3650(30)	5120(10)	6680(30)	39(6)

10) 4,4-diphenyl-2,5-cyclohexadienone

Synthesis: V.S.Senthil Kumar, University of Hyderabad, India.

Table 1. Crystal data and structure refinement for **10**.

Identification code	10	
Empirical formula	C ₁₈ H ₁₄ O	
Formula weight	246.29	
Temperature	100(2) K	
Wavelength	0.71073 Å	
Crystal system	Orthorhombic	
Space group	Pbca	
Unit cell dimensions	a = 10.7921(6) Å	$\alpha = 90^\circ$.
	b = 17.4749(12) Å	$\beta = 90^\circ$.
	c = 27.9344(19) Å	$\gamma = 90^\circ$.
Volume	5268.2(6) Å ³	
Z	16	
Density (calculated)	1.242 Mg/m ³	
Absorption coefficient	0.075 mm ⁻¹	
F(000)	2080	
Crystal size	0.55 x 0.40 x 0.30 mm ³	
Theta range for data collection	1.46 to 28.28°.	
Index ranges	-13 ≤ h ≤ 14, -16 ≤ k ≤ 23, -37 ≤ l ≤ 37	
Reflections collected	37963	
Independent reflections	6538 [R(int) = 0.0742]	
Completeness to theta = 28.28°	100.0 %	
Absorption correction	Psi-scan	
Max. and min. transmission	0.98281 and 0.89816	
Refinement method	Full-matrix least-squares on F ²	
Data / restraints / parameters	6538 / 0 / 371	
Goodness-of-fit on F ²	1.061	
Final R indices [I > 2σ(I)]	R1 = 0.0589, wR2 = 0.1243	
R indices (all data)	R1 = 0.0855, wR2 = 0.1360	
Largest diff. peak and hole	0.349 and -0.259 e.Å ⁻³	

Table 2. Atomic coordinates ($\times 10^4$) and equivalent isotropic displacement parameters ($\text{\AA}^2 \times 10^3$) for **10**. $U(\text{eq})$ is defined as one third of the trace of the orthogonalized U^{ij} tensor.

	x	y	z	$U(\text{eq})$
O(1)	6715(1)	2963(1)	1660(1)	31(1)
C(1)	5688(2)	2676(1)	1734(1)	22(1)
C(2)	5089(2)	2166(1)	1383(1)	21(1)
C(3)	4015(2)	1815(1)	1477(1)	19(1)
C(4)	3289(2)	1923(1)	1936(1)	17(1)
C(5)	3903(2)	2496(1)	2267(1)	19(1)
C(6)	4998(2)	2822(1)	2180(1)	22(1)
C(7)	3240(2)	1168(1)	2228(1)	19(1)
C(8)	2405(2)	1086(1)	2608(1)	24(1)
C(9)	2407(2)	422(1)	2888(1)	27(1)
C(10)	3253(2)	-161(1)	2797(1)	28(1)
C(11)	4092(2)	-76(1)	2424(1)	29(1)
C(12)	4084(2)	581(1)	2140(1)	23(1)
C(13)	1989(2)	2218(1)	1786(1)	18(1)
C(14)	999(2)	1715(1)	1704(1)	22(1)
C(15)	-150(2)	1998(1)	1557(1)	25(1)
C(16)	-325(2)	2780(1)	1488(1)	26(1)
C(17)	664(2)	3279(1)	1557(1)	24(1)
C(18)	1812(2)	2998(1)	1705(1)	21(1)
O(2)	5694(1)	51(1)	1060(1)	29(1)
C(21)	6166(2)	463(1)	753(1)	20(1)
C(22)	5427(2)	809(1)	364(1)	20(1)
C(23)	5945(2)	1225(1)	17(1)	19(1)
C(24)	7313(2)	1422(1)	-7(1)	17(1)
C(25)	8016(2)	1085(1)	414(1)	20(1)
C(26)	7506(2)	644(1)	751(1)	21(1)
C(27)	7929(2)	1089(1)	-464(1)	18(1)
C(28)	7303(2)	583(1)	-764(1)	20(1)
C(29)	7900(2)	266(1)	-1161(1)	24(1)
C(30)	9128(2)	446(1)	-1258(1)	26(1)
C(31)	9760(2)	953(1)	-960(1)	25(1)
C(32)	9166(2)	1277(1)	-568(1)	23(1)

C(33)	7364(2)	2310(1)	-6(1)	18(1)
C(34)	6956(2)	2711(1)	-409(1)	21(1)
C(35)	6884(2)	3507(1)	-402(1)	23(1)
C(36)	7231(2)	3910(1)	8(1)	24(1)
C(37)	7655(2)	3516(1)	407(1)	24(1)
C(38)	7710(2)	2716(1)	402(1)	22(1)

Table 3. Bond lengths [\AA] and angles [$^\circ$] for **10**.

		C(13)-C(14)	1.402(3)
		C(14)-C(15)	1.396(3)
		C(14)-H(14)	0.9500
O(1)-C(1)	1.234(2)	C(15)-C(16)	1.393(3)
C(1)-C(6)	1.474(3)	C(15)-H(15)	0.9500
C(1)-C(2)	1.474(3)	C(16)-C(17)	1.392(3)
C(2)-C(3)	1.337(3)	C(16)-H(16)	0.9500
C(2)-H(2)	0.9500	C(17)-C(18)	1.395(3)
C(3)-C(4)	1.516(2)	C(17)-H(17)	0.9500
C(3)-H(3)	0.9500	C(18)-H(18)	0.9500
C(4)-C(5)	1.515(2)	O(2)-C(21)	1.231(2)
C(4)-C(7)	1.551(2)	C(21)-C(22)	1.477(3)
C(4)-C(13)	1.552(2)	C(21)-C(26)	1.480(3)
C(5)-C(6)	1.335(3)	C(22)-C(23)	1.335(3)
C(5)-H(5)	0.9500	C(22)-H(22)	0.9500
C(6)-H(6)	0.9500	C(23)-C(24)	1.517(2)
C(7)-C(12)	1.394(3)	C(23)-H(23)	0.9500
C(7)-C(8)	1.401(3)	C(24)-C(25)	1.519(2)
C(8)-C(9)	1.399(3)	C(24)-C(27)	1.551(2)
C(8)-H(8)	0.9500	C(24)-C(33)	1.552(2)
C(9)-C(10)	1.392(3)	C(25)-C(26)	1.335(3)
C(9)-H(9)	0.9500	C(25)-H(25)	0.9500
C(10)-C(11)	1.387(3)	C(26)-H(26)	0.9500
C(10)-H(10)	0.9500	C(27)-C(28)	1.395(2)
C(11)-C(12)	1.395(3)	C(27)-C(32)	1.405(3)
C(11)-H(11)	0.9500	C(28)-C(29)	1.397(3)
C(12)-H(12)	0.9500	C(28)-H(28)	0.9500
C(13)-C(18)	1.396(3)	C(29)-C(30)	1.390(3)

C(29)-H(29)	0.9500	C(1)-C(6)-H(6)	119.1
C(30)-C(31)	1.394(3)	C(12)-C(7)-C(8)	118.56(17)
C(30)-H(30)	0.9500	C(12)-C(7)-C(4)	120.83(16)
C(31)-C(32)	1.389(3)	C(8)-C(7)-C(4)	120.44(16)
C(31)-H(31)	0.9500	C(9)-C(8)-C(7)	120.50(18)
C(32)-H(32)	0.9500	C(9)-C(8)-H(8)	119.7
C(33)-C(38)	1.395(3)	C(7)-C(8)-H(8)	119.7
C(33)-C(34)	1.397(3)	C(10)-C(9)-C(8)	120.38(18)
C(34)-C(35)	1.394(3)	C(10)-C(9)-H(9)	119.8
C(34)-H(34)	0.9500	C(8)-C(9)-H(9)	119.8
C(35)-C(36)	1.395(3)	C(11)-C(10)-C(9)	119.18(18)
C(35)-H(35)	0.9500	C(11)-C(10)-H(10)	120.4
C(36)-C(37)	1.388(3)	C(9)-C(10)-H(10)	120.4
C(36)-H(36)	0.9500	C(10)-C(11)-C(12)	120.65(18)
C(37)-C(38)	1.399(3)	C(10)-C(11)-H(11)	119.7
C(37)-H(37)	0.9500	C(12)-C(11)-H(11)	119.7
C(38)-H(38)	0.9500	C(7)-C(12)-C(11)	120.70(18)
		C(7)-C(12)-H(12)	119.6
O(1)-C(1)-C(6)	121.65(18)	C(11)-C(12)-H(12)	119.6
O(1)-C(1)-C(2)	121.86(18)	C(18)-C(13)-C(14)	118.71(17)
C(6)-C(1)-C(2)	116.49(16)	C(18)-C(13)-C(4)	119.49(16)
C(3)-C(2)-C(1)	121.76(17)	C(14)-C(13)-C(4)	121.71(16)
C(3)-C(2)-H(2)	119.1	C(15)-C(14)-C(13)	120.24(18)
C(1)-C(2)-H(2)	119.1	C(15)-C(14)-H(14)	119.9
C(2)-C(3)-C(4)	123.90(16)	C(13)-C(14)-H(14)	119.9
C(2)-C(3)-H(3)	118.0	C(16)-C(15)-C(14)	120.54(18)
C(4)-C(3)-H(3)	118.0	C(16)-C(15)-H(15)	119.7
C(5)-C(4)-C(3)	111.82(15)	C(14)-C(15)-H(15)	119.7
C(5)-C(4)-C(7)	104.93(14)	C(17)-C(16)-C(15)	119.44(18)
C(3)-C(4)-C(7)	110.85(14)	C(17)-C(16)-H(16)	120.3
C(5)-C(4)-C(13)	109.92(14)	C(15)-C(16)-H(16)	120.3
C(3)-C(4)-C(13)	106.25(14)	C(16)-C(17)-C(18)	120.11(18)
C(7)-C(4)-C(13)	113.19(14)	C(16)-C(17)-H(17)	119.9
C(6)-C(5)-C(4)	124.00(17)	C(18)-C(17)-H(17)	119.9
C(6)-C(5)-H(5)	118.0	C(17)-C(18)-C(13)	120.93(18)
C(4)-C(5)-H(5)	118.0	C(17)-C(18)-H(18)	119.5
C(5)-C(6)-C(1)	121.80(17)	C(13)-C(18)-H(18)	119.5
C(5)-C(6)-H(6)	119.1	O(2)-C(21)-C(22)	121.98(17)

O(2)-C(21)-C(26)	122.09(18)	C(29)-C(30)-H(30)	120.2
C(22)-C(21)-C(26)	115.94(16)	C(31)-C(30)-H(30)	120.2
C(23)-C(22)-C(21)	122.06(17)	C(32)-C(31)-C(30)	120.33(18)
C(23)-C(22)-H(22)	119.0	C(32)-C(31)-H(31)	119.8
C(21)-C(22)-H(22)	119.0	C(30)-C(31)-H(31)	119.8
C(22)-C(23)-C(24)	124.35(17)	C(31)-C(32)-C(27)	120.44(17)
C(22)-C(23)-H(23)	117.8	C(31)-C(32)-H(32)	119.8
C(24)-C(23)-H(23)	117.8	C(27)-C(32)-H(32)	119.8
C(23)-C(24)-C(25)	111.31(15)	C(38)-C(33)-C(34)	119.16(16)
C(23)-C(24)-C(27)	111.66(14)	C(38)-C(33)-C(24)	121.34(16)
C(25)-C(24)-C(27)	106.00(14)	C(34)-C(33)-C(24)	119.28(16)
C(23)-C(24)-C(33)	105.17(14)	C(35)-C(34)-C(33)	120.46(17)
C(25)-C(24)-C(33)	111.65(14)	C(35)-C(34)-H(34)	119.8
C(27)-C(24)-C(33)	111.18(14)	C(33)-C(34)-H(34)	119.8
C(26)-C(25)-C(24)	124.30(17)	C(34)-C(35)-C(36)	120.07(18)
C(26)-C(25)-H(25)	117.9	C(34)-C(35)-H(35)	120.0
C(24)-C(25)-H(25)	117.9	C(36)-C(35)-H(35)	120.0
C(25)-C(26)-C(21)	121.93(17)	C(37)-C(36)-C(35)	119.81(17)
C(25)-C(26)-H(26)	119.0	C(37)-C(36)-H(36)	120.1
C(21)-C(26)-H(26)	119.0	C(35)-C(36)-H(36)	120.1
C(28)-C(27)-C(32)	118.91(17)	C(36)-C(37)-C(38)	120.08(18)
C(28)-C(27)-C(24)	121.65(16)	C(36)-C(37)-H(37)	120.0
C(32)-C(27)-C(24)	119.40(16)	C(38)-C(37)-H(37)	120.0
C(27)-C(28)-C(29)	120.40(17)	C(33)-C(38)-C(37)	120.39(17)
C(27)-C(28)-H(28)	119.8	C(33)-C(38)-H(38)	119.8
C(29)-C(28)-H(28)	119.8	C(37)-C(38)-H(38)	119.8
C(30)-C(29)-C(28)	120.33(18)		
C(30)-C(29)-H(29)	119.8	Symmetry transformations used to generate equivalent atoms:	
C(28)-C(29)-H(29)	119.8		
C(29)-C(30)-C(31)	119.58(18)		

Table 4. Anisotropic displacement parameters ($\text{\AA}^2 \times 10^3$) for **10**. The anisotropic displacement factor exponent takes the form: $-2\pi^2 [h^2 a^{*2} U^{11} + \dots + 2 h k a^* b^* U^{12}]$

	U ¹¹	U ²²	U ³³	U ²³	U ¹³	U ¹²
O(1)	21(1)	34(1)	39(1)	1(1)	1(1)	-6(1)
C(1)	16(1)	19(1)	29(1)	3(1)	-3(1)	3(1)
C(2)	21(1)	23(1)	18(1)	1(1)	3(1)	4(1)
C(3)	22(1)	16(1)	18(1)	-2(1)	-3(1)	2(1)
C(4)	18(1)	16(1)	17(1)	-1(1)	0(1)	1(1)
C(5)	22(1)	18(1)	17(1)	-1(1)	-2(1)	4(1)
C(6)	23(1)	19(1)	23(1)	-2(1)	-7(1)	1(1)
C(7)	20(1)	18(1)	18(1)	0(1)	-4(1)	-1(1)
C(8)	22(1)	27(1)	22(1)	2(1)	2(1)	4(1)
C(9)	24(1)	34(1)	22(1)	6(1)	0(1)	-3(1)
C(10)	30(1)	26(1)	28(1)	7(1)	-4(1)	-2(1)
C(11)	32(1)	24(1)	30(1)	2(1)	-1(1)	8(1)
C(12)	23(1)	24(1)	24(1)	1(1)	1(1)	2(1)
C(13)	17(1)	23(1)	15(1)	-1(1)	2(1)	1(1)
C(14)	23(1)	23(1)	20(1)	-3(1)	1(1)	-1(1)
C(15)	19(1)	35(1)	21(1)	-4(1)	-1(1)	-5(1)
C(16)	19(1)	40(1)	17(1)	0(1)	0(1)	7(1)
C(17)	26(1)	26(1)	19(1)	3(1)	1(1)	5(1)
C(18)	23(1)	21(1)	20(1)	0(1)	1(1)	-1(1)
O(2)	34(1)	27(1)	25(1)	4(1)	3(1)	-8(1)
C(21)	26(1)	15(1)	19(1)	-5(1)	3(1)	-3(1)
C(22)	18(1)	18(1)	23(1)	-4(1)	1(1)	-2(1)
C(23)	19(1)	17(1)	21(1)	-3(1)	-3(1)	1(1)
C(24)	19(1)	15(1)	18(1)	0(1)	-1(1)	-1(1)
C(25)	17(1)	18(1)	23(1)	-4(1)	-2(1)	0(1)
C(26)	23(1)	18(1)	21(1)	-1(1)	-4(1)	2(1)
C(27)	21(1)	15(1)	19(1)	2(1)	-2(1)	2(1)
C(28)	22(1)	16(1)	23(1)	2(1)	-1(1)	-3(1)
C(29)	33(1)	17(1)	22(1)	-1(1)	-2(1)	-2(1)
C(30)	34(1)	21(1)	22(1)	-1(1)	4(1)	5(1)
C(31)	22(1)	24(1)	28(1)	3(1)	3(1)	1(1)
C(32)	22(1)	23(1)	23(1)	-2(1)	-4(1)	-3(1)
C(33)	16(1)	16(1)	22(1)	-2(1)	2(1)	-1(1)

C(34)	24(1)	19(1)	19(1)	-3(1)	1(1)	0(1)
C(35)	25(1)	20(1)	22(1)	4(1)	4(1)	1(1)
C(36)	26(1)	16(1)	28(1)	0(1)	7(1)	-2(1)
C(37)	27(1)	22(1)	24(1)	-6(1)	2(1)	-4(1)
C(38)	22(1)	24(1)	20(1)	2(1)	-1(1)	-3(1)

Table 5. Hydrogen coordinates ($\times 10^4$) and isotropic displacement parameters ($\text{\AA}^2 \times 10^3$) for **10**.

	x	y	z	U(eq)
H(2)	5476	2085	1082	29(6)
H(3)	3688	1478	1242	25(5)
H(5)	3482	2632	2553	21(5)
H(6)	5343	3158	2412	31(6)
H(8)	1833	1485	2677	29(6)
H(9)	1827	369	3142	31(6)
H(10)	3257	-611	2987	40(7)
H(11)	4678	-470	2362	39(7)
H(12)	4659	628	1885	24(5)
H(14)	1110	1181	1748	30(6)
H(15)	-819	1654	1505	27(6)
H(16)	-1112	2971	1393	32(6)
H(17)	557	3812	1505	37(6)
H(18)	2482	3343	1751	26(6)
H(22)	4555	734	361	15(5)
H(23)	5423	1410	-231	19(5)
H(25)	8876	1195	439	19(5)
H(26)	8018	440	996	25(5)
H(28)	6464	454	-699	22(5)
H(29)	7464	-75	-1366	23(5)
H(30)	9535	226	-1526	32(6)
H(31)	10600	1077	-1025	21(5)
H(32)	9600	1627	-369	24(5)
H(34)	6725	2439	-690	23(5)
H(35)	6598	3776	-676	30(6)
H(36)	7177	4453	14	29(6)
H(37)	7908	3790	684	20(5)
H(38)	7986	2449	678	25(6)

Appendix D: Conferences and Courses Attended

Meeting, Conferences and Courses:

Date	Title
12 th November 1997	BCA Autumn Meeting, University of Bristol. 'Disorder, Twinning and Incommensurate Structures.'
15 th November 1997	Scottish Protein Structure Group, University of Edinburgh.
5 th – 8 th April 1998	BCA Spring Meeting, University of St Andrews. Presented Poster - A Study of the Crystal Structure and Hydrogen Bonding Patterns of Nhmpa and Dicarba-Closo-Dodecarborane.
9 th April 1998 (last day only)	RSC Meeting, Durham
13 th May 1998	MSI (Life Sciences), MSI Cambridge
18 th Nov.1998	BCA Autumn Meeting, ISIS, Didcot. 'Neutrons for Structural Chemistry.'
7 th –14 th April 1999	BCA School, University of Durham. 'Seventh Intensive Course in X-Ray Structural Analysis.'
12 th -23 rd May 1999	Crystal Engineering school, Erice, Sicily. 'Crystal Engineering: From Molecules and Crystals to Materials.' Presented Poster - C-H... π Mediated Host-Guest Interactions in Organic Adducts.

4 th – 13 th August 1999	IUCr Congress, Glasgow. Presented Poster - Unusual C-H... π Hydrogen Bonding.
17 th November 1999	BCA Autumn Meeting, University of Manchester. 'Molecular Geometry using Methods Complementary to Crystallography'
27 th February – 6 th April 2000	Hercules Course, Grenoble, France. Higher European Research Course for Users of Large Experimental Systems, 10 th session, Neutron and Synchrotron Radiation for Physics and Chemistry of Condensed Matter.' Presented Poster - A neutron diffraction study of the 1:1 complex of 2,4,6-tris-(4-chlorophenoxy)-1,3,5-triazine with tribromobenzene.
6 th – 9 th April 2000	10 years of Hercules meeting, Grenoble, France.
11 th – 12 th May 2000	Metallo-Organic Workshop, CCDC, Cambridge.
15 th November 2000	BCA Autumn Meeting, Glaxo Smith-Kline, Harlow. 'Computational Methods'
28 th March 2001	CCDC Student Day, CCDC, Cambridge. Presented Talk - Bifurcation of Hydrogen Bonds in Organic Molecules.
7 th – 10 th April 2001	BCA Spring Meeting, Reading Presented Poster - Bifurcation of Hydrogen Bonds in Organic Molecules.
23 rd May – 3 rd June 2001	Crystal Engineering School, Erice, Sicily. 'Strength from Weakness.' Presented Poster - Bifurcation of Hydrogen Bonds in Organic Molecules.
14 th November 2001	BCA Autumn Meeting, University of Aston, Birmingham. 'Mesomolecular Crystallography'

Departmental Seminars:

Date	Title	Speaker
8 th October 1997	Advances in Control Of Architecture for Polyamides	Prof. E. Atkins
15 th October 1997	Studying Catalysts in Action	Dr. R.M.Ormerod
22 nd October 1997	Organoplatinum Chemistry and Catalysis	Prof. R.J. Puddephatt
23 rd October 1997	New Tetrathiafulvalene Derivatives in Molecular, Supramolecular and Macromolecular Chemistry	Prof. M.R.Bryce
27 th October 1997	Silyl Complexes of Ruthenium and Osmium	Prof. W.Roper
20 th November 1997	Polynuclear Metal Complexes	Dr. L. Spiccia
26 th November 1997	A Random Walk in Polymer Science	Prof. R.W.Richards
3 rd December 1997	Steroid-based frameworks for Supramolecular Chemistry	Prof. A.P.Davis
8 th January 1998	Control of Structure and Dimensionality in mixed organic-inorganic solids	Ian Williams
21 st January 1998	Aspects of Metal and Carbon Based Chemistry	Prof. D.Cardin
4 th February 1998	Classical and Non-Classical Fullerenes	Prof. P.Fowler
24 th February 1998	Synthesis and folding of Proteins	Prof. R.Ramage
18 th March 1998	Negative thermal expansion	Dr. J.Evans
20 th March 1998	Chemical Information Hidden in Charge Density	Dr. Paul Popelier
20 th March 1998	Buster Program	Dr. Pietro Roversi
15 th May 1998	Recrystallisation using gel methods	Dr. M. Leech
9 th October 1998	Carboranes exploitation of their unusual geometry and reactivities	Prof. M.F. Hawthorn
9 th October 1998	Carboranes, exploitation of there unusual geometry and reactivities.	Prof. M.F. Hawthorne
21 st October 1998	Dynamic Electrochemistry: Small is beautiful.	Prof. P.Unwin
26 th October 1998	Reactions of the Highly electrophilic Boranes $\text{HB}(\text{C}_6\text{F}_5)_2$ and $\text{B}(\text{C}_6\text{F}_5)_3$ with Zirconium and Tantalum based metallocenes.	Dr. W. Peirs
4 th November 1998	Computational adventures in d and f element chemistry.	Dr. N. Kaltsoyannis
12 th November 1998	From Macrocycles to Metallo-Supramolecular Chemistry.	Prof. S.Loeb
20 th January 1999	Luminescence of Large Molecules: From Conducting Polymers to Coral Reefs	Dr. A.Jones

27 th January 1999	NMR Characterisation of multi-phase fluid transport in porous solids	Prof. K.J.Packer
10 th March 1999	Designing model magnetic materials	Dr. A. Harrison
12 th October 1999	Chocolate for the Next Millennium	Dr. S. Beckett
20 th October 1999	Aspects of Complexation and Supramolecular Chemistry	Prof. S. Lincoln
3 rd November 1999	The Strengths of C-C and C-H bonds in Organic and Organometallic Molecules: Empirical, Semi-empirical and Ab Initio Calculations	Prof. D. W. Smith
24 th November 1999	Atomic and Molecular Control of Inorganic and Organic Semiconductor Thin Films	Prof. T. Jones
26 th November 1999	Fast Screening of Polymorphs	Dr. C. Lehmann
12 th January 2000	Atom Transfer Polymerisation – What is the Hype All About?	Prof. D. Haddleton
2 nd February 2000	Protons in Motion? Neutron Diffraction Studies of Hydrogen Atoms in Organic Crystal Structures	Dr. C. C. Wilson
16 th February 2000	Asymmetric Synthesis Using Planar Chiral TT-Allyl Cationic Complexes	Prof. Kocienski
11 th October 2000	Recent Developments on Organic LED Technology: Organolanthanide Phosphors	Dr. V. Christou
8 th November 2000	Cosmic: an unusual, DNA-Based Language for communicating with aliens and other intelligent lifeforms	Dr. J.P.L. Cox
22 nd November 2000	Synthesis of Novel Dendrimers and Hyper Branched Polymers	Dr. W. Hayes
2 nd May 2001	Escapades with Arenes and Transition Metals: From Lasers Spectroscopy to Synthetic Applications	Prof. R. Perutz
21 st February 2001	Liquid Crystals of all Shapes and Sizes	Prof. R. Richardson
28 th February 2001	Modelling Meso and Molecular Scale Interactions in Polymer Systems	Prof. A. Balazs
14 th March 2001	Probing Structural Disorder with Diffuse Neutron Scattering	Dr. D. Keen
6 th June 2001	The Melting Point Temperature Alternation of n-Alkenes and Derivatives	Prof. R. Boese

